MOLECULAR BASIS OF STRUCTURAL STUDIES, PHYTOCHEMICAL CHARACTERIZATION, AND NUTRITIONAL EVALUATION OF NEW MODIFIED ALFALFA DEVELOPED THROUGH DIFFERENT GENE TRANSFORMATION AND GENE MODIFICATION TECHNIQUES IN RUMINANT LIVESTOCK SYSTEMS

A Thesis Submitted to the

College of Graduate and Postdoctoral Studies

in Partial Fulfillment of the Requirements

for the Degree of Doctor of Philosophy

in the Department of Animal and Poultry Science

University of Saskatchewan

Saskatoon, SK

By

Yaogeng Lei

PERMISSION TO USE

In presenting this thesis in partial fulfillment of the requirements for a Postgraduate degree from the University of Saskatchewan, I agree that the Libraries of this University may make it freely available for inspection. I further agree that permission for copying of this thesis in any manner, in whole or in part, for scholarly purposes may be granted by the professor or professors who supervised my thesis work or, in their absence, by the Head of the Department or the Dean of the College in which my thesis work was done. It is understood that any copying or publication or use of this thesis or parts thereof for financial gain shall not be allowed without my written permission. It is also understood that due recognition shall be given to me and to the University of Saskatchewan in any scholarly use which may be made of any material in my thesis.

Requests for permission to copy or to make other uses of materials in this thesis in whole or part should be addressed to:

Head of the Department of Animal and Poultry Science, University of Saskatchewan, Saskatoon, Saskatchewan S7N 5A8

Canada

OR

Dean of College of Graduate and Postdoctoral Studies, University of Saskatchewan, 116 – 110 Science Place, Saskatoon, SK, S7N 5C9,

Canada

ABSTRACT

Alfalfa is one of the most important forage crops in the world due to its high nutritive value and good adaptability. However, alfalfa contains relatively high lignin that hinders its nutrients availability. Recently, genetic engineering has been used in alfalfa breeding and scientists from Agriculture Agri-Food Canada (AAFC) have developed several new genotypes of genetic-modified alfalfa. To reduce lignin content of alfalfa, transcriptional factor genes of *HB12* and *TT8* were silenced. In addition, overexpression of miR156 (miR156 OE) has been shown to delay flowering onset of alfalfa thereby increasing forage quality. Moreover, alfalfa with silenced miR156-targeting *SPL6* and *SPL13* (Squamosa promoter binding like protein, SPL) genes were generated to determine their roles in miR156 OE event. To date, little is known about the comprehensively nutritional values of these genetic modified alfalfa genotypes. This research combined conventional nutritional analysis with molecular structural analysis to assess nutritional profiles of genetic modified alfalfa and explored the relationship between spectral parameters and nutritional profiles of alfalfa.

Results showed that both *HB12*-silenced (HB12i) and *TT8*-silenced (TT8i) alfalfa had higher fiber and endogenous protein loss, but lower protein, dry matter (DM) degradation and microbial protein synthesis compared with wild type (WT). In addition, HB12i had higher lignin content, but lower energy, productions of gas, volatile fatty acids (VFA) and ammonia, protein effective degradation (EDCP), total available protein and feed milk value compared with other alfalfa genotypes. Molecular structure of HB12i and TT8i were different from WT in carbohydrate and lipid regions and all genotypes were different in amide region. As for miR156 OE and *SPL6/13*-silenced alfalfa, miR156 OE had lower fiber and endogenous protein loss, but higher insoluble true protein, energy, DM degradation and microbial protein synthesis compared with

other genotypes. In addition, overexpression of miR156 also improved protein degradation profiles of alfalfa. Molecular structures were similar between miR156 OE and *SPL6/13*-silenced alfalfa, which were different from WT in carbohydrates and lipid regions. Both projects found differences between transgenic alfalfa genotypes and WT in molecular structures and chemical localization of alfalfa leaves. Furthermore, significant correlations were found between molecular structures and nutritional profiles of alfalfa, providing good predictions of nutrient availability of alfalfa from spectral parameters.

In summary, TT8i provided equivalent energy and protein with improved nutrient balance compared with WT, making it a promising grazing variety. In addition, miR156 OE had improved forage quality that was more similar to SPL6 RNAi alfalfa, implying *SPL6* plays a more important role in miR156 OE event than *SPL13*. Meanwhile, there might be more *SPL* genes involved in miR156 OE event indicated by the nutritional differences between miR156 OE and *SPL6/13*-silenced alfalfa genotypes. Molecular structures of alfalfa forage were closely correlated with its nutritional profiles, which made it possible to predict alfalfa nutrient availability from its structural parameters with ATR-FTIR spectroscopy.

ACKNOWLEDGEMENTS

First of all, I would like to thank my supervisor, Dr. Peiqiang Yu, for giving me the opportunity to purse my PhD, to conduct researches in different labs, to attend international conferences and to publish my research papers. Thank you for providing me teaching assistant position, helping me applying scholarships, bringing me food when I was conducting experiments at Advance Light Source Berkeley lab, driving me to and pick me up from Lethbridge, inviting me to your Christmas potluck and giving me advice for my future. Thank you so much for all your kind help throughout my project. I would like to thank my Master supervisor, Yuxin Yang, for his support and encouragement.

I also would like to thank Dr. Abdelali Hannoufa for giving me the opportunity to learn how to do tissue culture for alfalfa and take care of plants in the greenhouse, collect samples, meet new people and experience life in London, Ontario. Thank you for revising my papers, sharing your knowledge and staying in my committee. I would also like to thank Dr. Yuxi Wang for giving me the opportunity to conduct experiments in his lab and giving me valuable advice for my project. Also, I would like to thank my dear committee members, Dr. David Christensen, Dr. John McKinnon, Dr. Bill Biligetu, Dr. Tim Mutsvanwa, and Dr. Ryan Brook for your kind help and encouragement.

I would like to thank Zhiyuan Niu for your technical assistance in the lab and for fixing my car. Thank you so much for driving me to Canadian tire and trying so many times in the cold Saskatoon winter. Thank you for inviting me to Charismas and New Year potluck. I would like to thank Zhongjun Xu for your technical help in the lab and providing accommodation during my stay in Lethbridge. Thank you for driving me to work daily and taking me to Waterton National park. Special thanks to Lisa Amyot (AAFC), Hans Bechtel (ALS-LBNL), Lisa Miller (NSLS-

BNL), Randy Smith (NSLS-BNL), Mana Croft for your technical help in my experiments. I would like to thank Trent Fehr, Luciana Prates, Nina Gao, Wei Chen, Jingjing Huang, Haitao Shi, Basim Refat and Na Liu for their help and friendship. I would like to acknowledge all faculty, staff, researchers and students of the Department of Animal and Poultry Science, Agriculture and Agri-Food Canada in London and Lethbridge and Advance Light Resources-LBNL and National Synchrotron Light Sources-BNL for their help and friendship.

I express my gratitude to Natural Sciences and Engineering Research Council of Canada, Saskatchewan Agriculture Strategic Research Program Fund, and China Scholarship Council (CSC) for the financial support of my project and my living in Saskatoon. I also appreciate scholarships of Purdy Postgraduate Scholarship; Graduate Student Teaching Fellowship, Kathleen and Norman Lean Post Graduate Scholarship and John Baerg Research Award.

Last but not least, I express my greatest gratitude to my parents, my brother and sister and my entire family. Thank you for your unconditional love, encouragement, support and care.

TABLE OF CONTENTS

LIST OF TABLES

LIST OF FIGURES

LIST OF ABBREVIATIONS

AA	Amide area
ABA	Abscisic acid
ADF	Acid detergent fiber
ADICP	Acid detergent insoluble protein
ADL	Acid detergent lignin
AIA	Amide I area
AIIA	Amide II area
AMCP	Absorbable MCP
AP	Average production of end products
APE	N^{15} enrichment
ARUP	Absorbable RUP
ASCC	Asymmetric and symmetric CH2 and CH3
ASCCA	ASCC area
ATR-FTIR	Attenuated total reflectance-Fourier transform infrared spectroscopy
bHLH	basic helix loop helix
CA4	Water soluble carbohydrate (sugar)
CB1	Starch
CB2	Soluble fiber
CB3	Digestible fiber
CC	Indigestible fiber
CCO	Carbonyl C=O
CCOA	CCO area
CEC	Cellulosic compounds
CECA	CEC area
CHO	Carbohydrate
CNCPS	Cornell net carbohydrate and protein system
CP	Crude protein
CWR	Cell wall residue
DE	Digestible energy

DM	Dry matter
DVE	Total truly absorbed protein
DW	Dry weight
ED	Effective degradation
EE	Ether extract
ENDP/ECP	Endogenous protein
FAMN	Firmly attached microbial nitrogen
FMV	Feed milk value
FOM	Fermentable OM
FTIR	Fourier transform infrared reflectance spectroscopy
HB12	Homeobox12
HB12i	HB12 RNAi
HCA	Hierarchical cluster analysis
IDRUP	Intestinal digestion of rumen undegradable protein
K_d	Degradation rate
K_p	Passage rate
LAMN	Loosely attached microbial nitrogen
LMN	Liquid associated microbial nitrogen
LSR	Leaf to stem ratio
MBW	MYB-bHLH-WD protein complex
MCP	Microbial protein
ME	Metabolizable energy
miR156 OE	miR156 overexpression
MN	Microbial nitrogen
MP	Metabolizable protein
NDF	Neutral detergent fiber
NDICP	Neutral detergent insoluble protein
NE_g	Net energy for weight gain
NE_L	Net energy for lactation
NE_m	Net energy for maintenance
NFC	Non-fiber carbohydrate

NPN	Non-protein nitrogen
OEB/DPB	Degraded protein balance
OM	Organic matter
PA2	Soluble true protein
PAs	Proanthocyanidins
PB1	Insoluble true protein
PB2	Fiber-bound protein
PC	Indigestible protein
PCA	Principle component analysis
RDCHO	Rumen degradable CHO
RDCP	Rumen degradable protein
RDP	Rumen degradable protein
RN	Residue nitrogen
RNAi	RNA interference
RSE	Residual standard error
RUCHO	Rumen undegradable CHO
RUCP	Rumen undegradable protein
RUP	Rumen undegradable protein
SCP	Soluble crude protein
SEM	Standard error for mean
SPL	Squamosa promoter binding protein like genes
SR-IMS	Synchrotron based FTIR microspectroscopy
STC	Structural carbohydrate
STCA	STC area
TC	Total carbohydrate
TCA	TC area
tdCP	Truly digestive CP
tdFA	Truly digestive fatty acids
TDN	Total digestible nutrients
tdNDF	Truly digestive NDF
tdNFC	Truly digestive NFC

TT8	Transparent Testa8
TT8i	TT8 RNAi
VFA	Volatile fatty acids
WT	Wild type

CHAPTER 1
GENERAL INTRODUCTION

Alfalfa (*Medicago sativa)* is one of the most widely cultivated forage crops around the world due to its high nutritive value and good adaptability (Russelle 2001; Lei et al. 2017). Alfalfa has a high content of protein and low content of fiber, and is widely used in ruminant rations (Berthiaume et al. 2010). In addition, the robust root system and symbiotic relationship with *Rhizobium* enables alfalfa to flourish in drought and barren lands (Radović et al. 2009; Zhang et al. 2016). According to Tesfaye et al. (2006), the global growing area of alfalfa is approximate 32 million hectares. Even though the growing area has declined to some extent in the United States (Mahanna 2015), alfalfa is still an important forage in the animal industry. To date, numerous studies have been conducted on alfalfa improvement with genetic engineering. Generally, studies on alfalfa improvement aim to either improve nutritive quality or increase biomass production.

Alfalfa contains relatively high lignin content compared with grass that hinders degradation of carbohydrates and other nutrients in the rumen (Lei et al. 2017). Research reported that expression levels of Transparent Testa8 (TT8) and Homeobox12 (HB12), which are two transcriptional factors in the phenylpropanoid pathway, might be positively related to lignin biosynthesis (Li et al. 2015). Downregulation of *TT8* and *HB12* genes might be beneficial to alfalfa quality, regarding their potential function in the phenylpropanoid pathway. Li et al. (2015) explored the effects of silencing *TT8* and *HB12* by RNAi technique on chemical profiles and carbohydrate structures in alfalfa. Results showed both RNAi silencing of *TT8* and *HB12* genes increased NDF content and digestibility but had negative influences on the digestibility of rapidly degradable carbohydrates (CHO) and total CHO in rumen. However, still little is known about the influences of silencing *TT8* and *HB12* genes in alfalfa on molecular structures and nutrient

availability in ruminant livestock systems. Therefore, the first project of this research aimed to explore the effects of silencing *TT8* and *HB12* genes on inherent molecular structures, chemical composition, CNCPS fractions, energy values, nutrients fermentation and degradations and protein availability of alfalfa.

MicroRNAs (miRNAs) are a class of small non-coding RNAs that control gene expression at both the transcriptional and post-transcriptional level (Spanudakis and Jackson 2014). Plant miRNAs predominantly regulate the expression of transcriptional factor genes, thereby regulating a variety of processes in plant development (Aung et al. 2015c). Among identified plant miRNAs, miR156 is highly conserved among flowering plants and is a master switch for plant phase transitions, including both the vegetative phase transition and the reproductive phase transition (Bhogale et al. 2014; Wang and Wang 2015; Aung et al. 2015c; Wang 2016). MiR156 regulates plant growth and development mainly by targeting *Squamosa promoter binding protein-like (SPL)* genes (Aung et al. 2015c). *SPLs* encode a family of heterologous transcriptional factors that contain a conserved 76-amino-acid domain, and target SPL proteins into the nucleus. SPL transcriptional factors are highly diverse in molecular structures and biological functions (Aung 2014; Wang and Wang 2015).

A previous study showed that overexpression of miR156 (miR156 OE) delayed the onset of flowering, enhanced shoot branching, and increased root length and biomass yield in alfalfa, and decreased expression of *SPL6*, *SPL12* and *SPL13* genes (Aung et al. 2015a). However, little is known about the effects of miR156 OE and silencing *SPL6* and *SPL13* genes individually on the nutritional value and inherent molecular structure of alfalfa. Therefore, the overall objectives of my second project were to explore the effects of miR156 OE on molecular structures, chemical

composition, CNCPS fractions, energy values, nutrients fermentation and degradations, and protein availability of alfalfa in comparison with silencing *SPL6* and *SPL13* genes.

Fourier transform infrared (FTIR) spectroscopy is a rapid and non-destructive analytical technique that has been used in several research fields to analyze inherent molecular structures (Stuart 2004; Bassbasi et al. 2014; Bekiaris et al. 2015; Chen et al. 2018). Researchers have implemented this technique in feed nutrition in recent years to explore internal molecular structures of feed ingredients in mid infrared (IR) range (Shi and Yu 2017; Prates and Yu 2017). Molecular structures of feedstuffs are closely correlated with their nutritional profiles and nutrient availability to the animal (Theodoridou and Yu 2013a; Peng et al. 2014; Xin et al. 2014; Prates et al. 2018a). However, correlations between spectral parameters and nutritional profiles are not consistent for different feed ingredients, implying unique correlation patterns for different feeds (Theodoridou and Yu 2013a; Xin and Yu 2013a). To date, there are few studies on relationships between molecular structures and nutritional profiles for alfalfa forage. Therefore, the objectives of the third project were to determine relationships between molecular spectral parameters and nutritional profiles of alfalfa.

CHAPTER 2
AGRONOMIC TRAITS OF ALFALFA AND GENETIC MODIFICATION TOWARDS ALFALFA IMPROVEMENT: A COMPREHENSIVE LITERATURE REVIEW

2.1 Alfalfa agronomy and nutritive value

Alfalfa (*Medicago sativa*), also known as the "Queen of Forage", is widely cultivated around the world due to its high biomass yield, good forage quality and palatability (Cash and Hu 2009). Alfalfa was firstly cultivated in central Eurasia 4000 years ago and was then spread to other places afterwards. Alfalfa can grow in a wide variety of landscapes and growing conditions thanks to its good adaptability. The extraordinary deep roots enable alfalfa to absorb water from the deep soil layer, which helps it flourish in arid and semi-arid areas (Radović et al. 2009). The symbiotic relationship with *Rhizobium*, a common feature of legume plants, provides nitrogen for the plant, enables alfalfa to grow in barren lands (Zhang et al. 2016). Good adaptability, high biomass yield and high nutritive value, make alfalfa one of the most widely cultivated forage crops around the world (Wang et al. 2015c). According to Tesfaye et al.(2006), the growing area of alfalfa is approximate 32 million hectares worldwide. The cultivated area of alfalfa in Canada was 4.5 million hectares in 2011 (Government of Canada 2016), double the value published before (Cash and Hu 2009). According to Agriculture and Agri-Food Canada, Canada is the first and the second largest exporter for alfalfa pellets and cubes, respectively (Government of Canada 2012). Around 75% of Canadian alfalfa production in area is grown in the prairie provinces and about 20% is grown in Ontario and Quebec (Government of Canada 2012).

A part of this chapter has been published previously. Lei, Y., Hannoufa, A., and Yu, P. 2017. The Use of Gene Modification and Advanced Molecular Structure Analyses towards Improving Alfalfa Forage. International Journal of Molecular Sciences 18: 298. doi:10.3390/ijms18020298.

Alfalfa has favorable nutritional profiles for ruminant rations in animal industry. Compared with grass forages, alfalfa contains high protein and energy contents and is also very palatable (Undersander et al. 2011). Yu et al. (2003b) compared chemical compositions of alfalfa and timothy and reported that at commercial harvest (late-bud for alfalfa and pre-bloom for timothy) alfalfa has 19% CP, 47% NDF and 29% ADF, while timothy had 10% CP, 70% NDF and 40% ADF. Studies reported that NDF contributes to rumen fill which negatively affects DM intake of animals (Allen and Piantoni 2013). As alfalfa contains low NDF content, it allows a high inclusion rate in ruminant rations. Nutritional values of alfalfa forage are affected by many factors, including variety, stage of maturity, management and environmental factors.

Fall dormancy is an important feature of alfalfa varieties which determines not only the suitable planting regions, but also the forage quality. Fall dormancy measures how much the alfalfa plant can regrow in September from a fresh cutting and is correlated with winterhardiness feature (Undersander et al. 2011). Alfalfa varieties with a low fall dormancy score (more dormant) and low winterhardiness provide high quality forages (Undersander et al. 2011). Putman et al. (2005) studied the effects of fall dormancy on forage quality and biomass yield and reported a linear negative correlation between fall dormancy and forage quality of alfalfa and a positive correlation between fall dormancy and biomass yield. Fall dormancy explained 93% variance of ADF content and 74% variance of biomass yield between alfalfa genotypes. More fall dormant alfalfa grows slower after each cutting and were at an earlier growth stage at harvest compared with compared with less-dormant variety (Putnam et al. 2005). However, variations in forage quality also exist between alfalfa varieties with similar fall dormancy. Hall et al. (2000) determined morphological development of two high quality alfalfa varieties against two control varieties with similar fall dormancy and found no significant differences between their morphological development stages.

High quality alfalfa had higher protein content and *in vitro* DM degradation and lower fiber content compared with those check varieties (Hall et al. 2000).

Stage of maturity at harvest is the most important factor in forage quality of alfalfa (Putnam and Orloff 2016). Previous studies discussed the tradeoff between forage quality and biomass yield of alfalfa (Orloff and Putnam 2004; Putnam et al. 2005). When alfalfa is approaching maturity, protein content and DM digestibility decrease, while fiber content and yield increase (Putnam et al. 2005). Yu et al. (2003b) and Yari et al. (2012a) explored the effects of stage of maturity on nutritional value of alfalfa and data from these two studies are shown in Table 2.1. As alfalfa grows from late-bud to early-flowering, its CP content decreases dramatically, whereas NDF and ADF contents increase. Interestingly, stage of maturity had more impact on alfalfa plants in Yari's study compared with those in Yu's study, indicating differences in response to maturity between alfalfa varieties and cultivation regions. Leaf to stem ratio (LSR) also declined as alfalfa grows from early bud to early flowering (Yari et al. 2012a), which is in line with Orloff and Putnam (2004). This dramatic decline of LSR results from the large increase of stem yield compared with leaf biomass (Figure 2.1). Generally, alfalfa leaves account for 50% of biomass at vegetative stage and production of leaves stops increasing at late-bud stage; however, stem production continues to increase until full flowering stage (Orloff and Putnam 2004). Alfalfa leaves are superior to stems with higher CP and lower fiber contents (Radović et al. 2009; Marković et al. 2012). Moreover, quality of alfalfa stems also decline with plant maturity and its decrease in CP content and DM degradability are higher than that for alfalfa leaves (Orloff and Putnam 2004; Radović et al. 2009). This is mainly because of the lignification in secondary cell walls of stems when plant approaches maturity (Putnam and Orloff 2016).

Table 2.1 Chemical composition of alfalfa at early-bud, late-bud and early-flower stage

Ref. [1]	(Yari et al. 2012a)			(Yu et al. 2003b)					
Variety	*cv.* Ranger			Pioneer			Beaver		
Stage [2]	S1	S2	S3	S1	S2	S3	S1	S2	S3
CP (%DM)	22.0	19.5	16.2	20.4	18.7	17.7	19.9	19.4	17.4
NDF (%DM)	45.3	46.5	51.4	49.8	47.1	54.3	48.8	46.9	49.6
ADF (%DM)	36.8	39.4	44.2	32.0	29.4	32.0	32.1	29.4	31.0

[1] Alfalfa plants were two-year-old grown at Mashhad, Iran in study of Yari et al. (2012a), and three-year-old grown in Western Canada in study of Yu et al. (2003b).
[2] S1, early bud stage; S2, late bud stage; S3, early flowering stage
[3] CP, crude protein; NDF, neutral detergent fiber; ADF, acid detergent fiber.

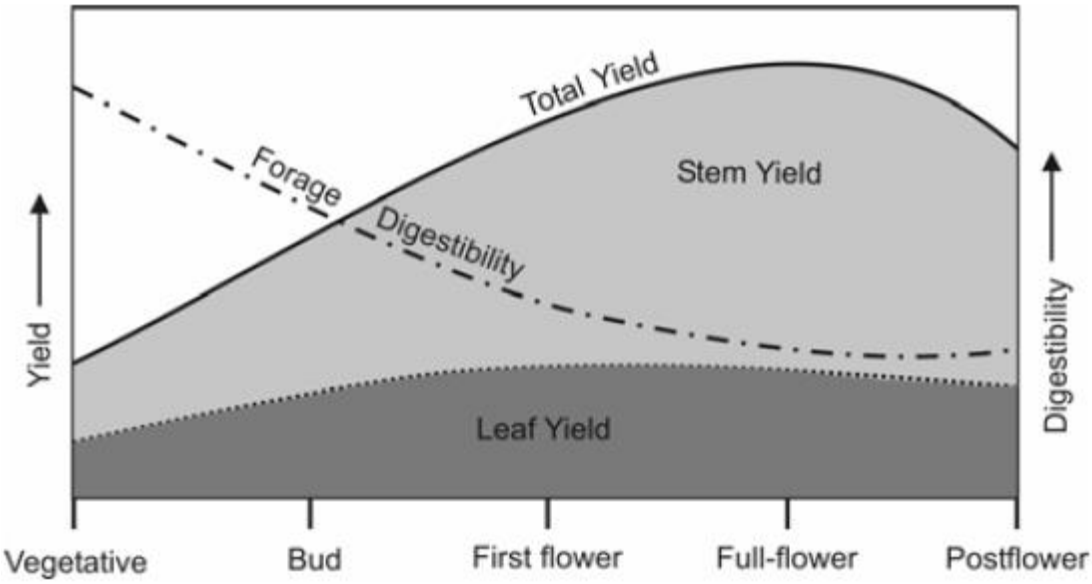

Figure 2.1 Relationship between biomass yield and forage quality for alfalfa from vegetative stage to post-flower stage (Orloff and Putnam 2004).

Environmental factors also play important roles in forage quality of alfalfa. As stage of maturity has negative impacts on forage quality of alfalfa, any environmental factors that promote plant growth also have negative influences on forage quality. Mueller and Orloff (1994) discussed the environmental factors that affect alfalfa forage quality, including season, soil type, fertility and moisture, pest and rain. Forage quality is higher in spring and autumn compared with summer

under same maturity due to higher leaf ratio and protein contents (Mueller and Orloff 1994). This seasonal effect is largely attributed to temperature as higher temperate in summer promotes plant growth, enhances lignification in cell wall and accelerate respiration rates (Putnam and Orloff 2016). Soil type, fertility and moisture affects forage quality through their influences on root growth, drought stress and nutrients uptake. Moderate water and mineral deficiencies could reduce growth rate, leading to a higher leaf to stem ratio and thereby increasing forage quality (Mueller and Orloff 1994). Pest pressure affects forage quality in different ways, which could lead to either increase or decrease in forage quality but all decrease forage yield. Moderate pressures that hinder alfalfa growth lead to higher forage quality, whereas severe pressures reduce forage quality, yield and even cause plant death (Mueller and Orloff 1994). Rainfall also affects alfalfa forage quality after forage harvest and could lead to losses of leaves and soluble nutrients and additional mechanical losses for reprocessing (Mueller and Orloff 1994).

Other factors, such as harvest management and time of day could also affect forage quality of alfalfa (Putnam and Orloff 2016). Processing of alfalfa after harvest could lead to leaf shatter during ranking and baling. Moreover, a longer processing period after harvest also could increase the risk of rain damage to alfalfa and thereby decreasing forage quality. The effect of harvest time of day on forage quality is largely attributed to respiration of alfalfa plants during the night (Putnam and Orloff 2016). Plants accumulate nutrients via photosynthesis during the day and utilize energy in the night. Therefore, harvest of alfalfa in the afternoon could lead to higher concentration of soluble carbohydrates, which increases energy values of alfalfa (Putnam and Orloff 2016). Yari et al. (2012a) compared the nutritional values of alfalfa harvested in the morning and afternoon and found that afternoon-harvest samples had higher LSR, soluble carbohydrates and protein contents, energy values and better rapidly degraded nitrogen to carbohydrate ratio.

2.2 Nutritional drawbacks of alfalfa

Despite its high quality, alfalfa protein is not utilized efficiently (Jonker et al. 2010). This drawback is mainly due to its high content of soluble crude protein, which can be rapidly degraded in the rumen resulting in waste of high-quality protein. In addition, the rapid degradation of alfalfa protein can increase the viscosity of ruminal fluid, posing a risk of frothy bloat to animals, especially under grazing condition (Wang et al. 2012). In contrast to alfalfa, some legume forages, such as sainfoin (*Onobrychis viciifolia*), birdsfoot trefoil (*Lotus corniculatus*) and big trefoil (*Lotus pedunculatus*), also have high content of protein but are bloat-free. This anti-bloat character is highly associated with their possession of proanthocyanidins (PAs), which are also known as condensed tannins (Foo et al. 1997; Jonker et al. 2010; Wang et al. 2015a). PAs could bind with protein in the rumen thereby decreasing its degradation, reducing the risk of rumen bloat and increasing the bypass protein as well (Xie et al. 2006a). A moderate amount of PAs in forages, about 2%-4% of dry matter (DM), can slow down protein degradation rate, increase rumen escape protein, and improve animal productivity (Aerts et al. 1999). However, there are only trace amounts of PAs in alfalfa, and they are restricted to the seed coat (Goplen et al. 1980; Jonker 2011).

Another drawback of alfalfa is its relatively high lignin content (Li et al. 2015). As the second most abundant component in secondary cell walls (Zhou et al. 2009), lignin is of great importance for plant growth, development and pathogen resistance (Tong et al. 2015). Many of the genetic modifications introduced to plants to reduce lignin content have resulted in dwarf phenotypes, which have led to the compromised biomass yield, limiting the benefits of reduced lignin (Bonawitz and Chapple 2013). However, lignin is very resistant to digestion and degradation and is merely useful to animals, even to ruminants. There are only a few microorganisms that are

able to degrade lignin, including some fungi and bacteria, by using extracellular enzymes like lignin peroxidase, manganese peroxidase and versatile peroxidase (Brown and Chang 2014; Zeng et al. 2014). However, this degradative process is an oxidative reaction requiring an aerobic environment. In the anaerobic environment of the rumen, the degradability of lignin is very limited and negligible compared to that of cellulose and hemicellulose (Susmel and Stefanon 1993). Moreover, lignin also hinders the degradation of other compounds by its inhibitory effects on cellulolytic enzymes and crosslinks with polysaccharides (Sewalt et al. 1997a, 1997b; Grabber 2005). In the production of biofuel, a thermochemical pretreatment is required to eliminate or delocalize lignin prior to the enzymatical hydrolysis of polysaccharides into fermentable sugars (Zeng et al. 2014).

2.3 Biosynthesis of proanthocyanins, anthocyanins and lignin

Attempts have been made to promote the accumulation of PAs in alfalfa. For that, studies were conducted to understand how PAs biosynthesis is regulated in plants (Schaart et al. 2013; Xu et al. 2015). PAs are a group of secondary metabolites derived from the phenylpropanoid pathway and are the final products of the flavonoid pathway. Three regulatory proteins have been reported to regulate the biosynthesis of PAs and anthocyanins; R/B-like basic helix-loop-helix (bHLH) protein, R2R3-MYB protein and WD40-repeated protein (Schaart et al. 2013). To exert their regulation functions, bHLH, MYB and WD proteins combine with each other forming a ternary complex (MBW). MBW controls the expression of late biosynthesis genes in phenylpropanoid pathway, thereby regulating the synthesis of PAs and anthocyanidins (Xu et al. 2015). The biosynthesis pathway of PAs and anthocyanidins is shown in Figure 2.2. Briefly, Phenylalanine is first deaminated and then converted into 4-coumaroyl-CoA, which can be either used for lignin synthesis or for flavonoid synthesis. In the PAs synthesis, 4-coumaroyl-CoA is transformed into

naringenin after two consecutive reactions. Naringenin can then be hydroxylated to form eriodictyol and 5' OH eriodictyol, which along with naringenin are hydroxylated and reduced into three forms of anthocyanidins, namely delphinidin, pelargonidin and cyanidin (Zabala et al. 2006). After that, these anthocyanidins can be converted to their corresponding anthocyanins through glycosylation (Zabala et al. 2006). Naringenin in this pathway can also be used to synthesize flavones and isoflavones following a series of reactions.

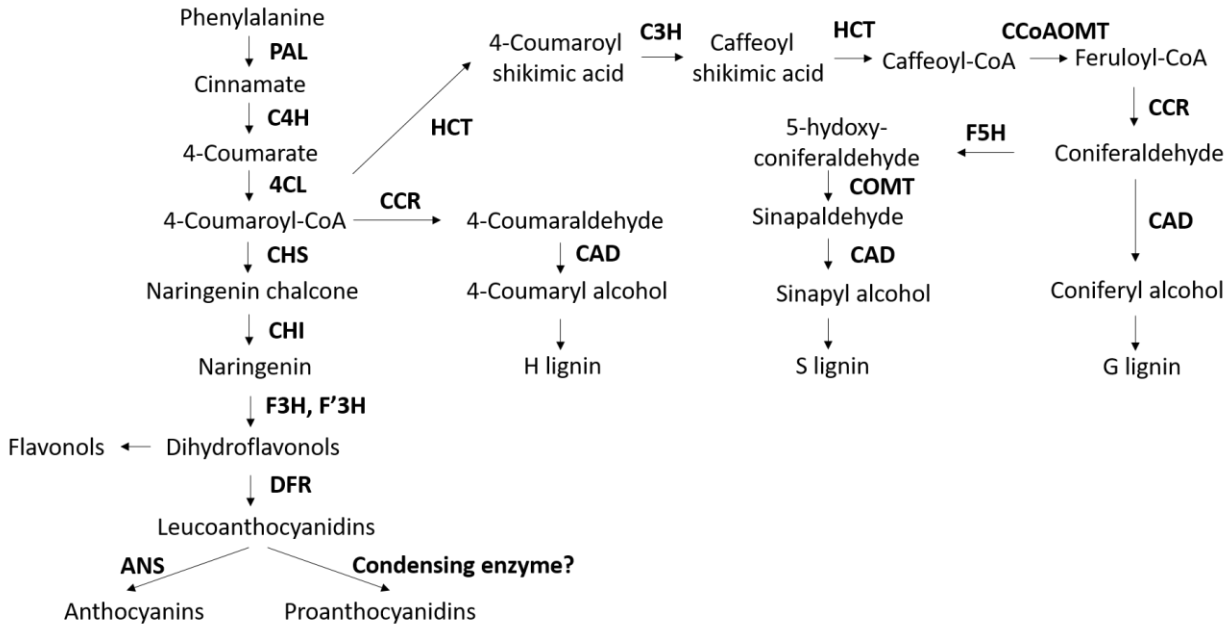

Figure 2.2 Biosynthesis of Proanthocyanidins/anthocyanins and lignin monolignols. This figure is adapted from Nesi et al. (2000), Vanholme et al. (2010) and Jonker (2011). Abbreviations means: PAL, L-phenylalanine ammonia-lyase; C4H, cinnamate 4-hydroxylase; 4CL, 4-coumarate coenzyme A ligase; CCR, cinnamoyl coenzyme A reductase; CAD, cinnamyl alcohol dehydrogenase; HCT, hydroxycinnamoyl-CoA : shikimate/quinate hydroxycinnamoyl transferase; C3H, coumarate 3-hydroxylase; CCoAOMT, caffeoyl CoA 3-O-methyltransferase; F5H, ferulate 5-hydroxylase; COMT, caffeic acid 3-O-methyltransferase; CHS, chalcone synthase; CHI, chalcone isomerase; F3H, flavanone 3-hydroxylase; DFR, dihydroflavanol 4-reductase;

Like anthocyanidins and PAs, lignin is also derived from the phenylpropanoid pathway (Figure 2.2). Lignin consists mainly of three monolignols: hydroxyphenyl (H lignin), guaiacyl (G lignin) and syringyl (S lignin). The major differences between these monolignols are the degree of

the hydroxylation and methylation. The proportion of these monolignols in lignification varies substantially among species and tissues. In angiosperm species, including alfalfa, lignin consists of mainly G and S monomers with only traces of H monomer, while in gymnosperms lignin possesses a large proportion of G monomer with low S monomer (Reddy et al. 2005). The proportion of monolignols composing lignin affects the digestive property of the resulting lignin. In paper production, wood containing high G monomer proportion is more resistant to chemical and physical treatments in lignin removal, and an increase in S/G ratio by genetic modification can improve pulping efficiency (Reddy et al. 2005). The biosynthesis of monolignols involves a series of hydroxylation and methylation reactions, which is displayed in Figures 2.2. The first three steps are shared with anthocyanidins and PA synthesis, from phenylalanine to 4-coumaroyl-CoA (Nesi et al. 2000). Downstream of 4-coumaroyl-CoA, the pathway splits into two branches, with one followed by direct reduction to synthesize 4-coumaroyl alcohol (H lignin), and the other goes to further hydroxylation and methylation for S and G lignin monomers. For G lignin synthesis, only 3-site on the benzol ring is hydroxylated and methylated while S lignin requires hydroxylation and methylation of both 3-site and 5-site. After being synthesized in the cytoplasm, lignin monolignols are then transported to the cell wall, where they are polymerized by radical-coupling (Boerjan et al. 2003; Bonawitz and Chapple 2013).

2.4 Genetic engineering towards alfalfa improvement

Conventional breeding for quality improvement in alfalfa is based on phenotypic selection, which has been proved to be time-consuming and inefficient (Resende et al. 2014). Alfalfa breeding is hampered by its allogamous reproductive behavior and inbreeding (Maureira and Osborn 2004). More pronounced advances in alfalfa improvement have made use of recombinant DNA technology to modulate expressions of genes involved in forage nutritive value, biomass

yield, and stress tolerance (Kumar 2011; Kumar et al. 2013). This technology allows for the transfer of DNA sequences of interest into the plant genome to either enhance or silence the expression of target genes that determine important traits in the plant (Vogel and Jung 2001).

2.4.1 Enhance proanthocyanidins accumulation

As described above that moderate amount of PAs is capable of preventing pasture bloat, efforts have been made to enhance PAs accumulation in alfalfa. One of the targets for enhancing PAs has been the MBW complex that regulates biosynthesis of PAs and anthocyanins (Schaart et al. 2013). In order to increase the accumulation of PAs and anthocyanins in alfalfa, Ray et al. (2003) expressed three flavonoid regulatory genes from maize (*C1*, *Lc* and *B-Peru*) in alfalfa, in which C1 encodes a MYB-like protein while Lc and B-Peru encode bHLH-like structure proteins. The results showed only *Lc*-expressing alfalfa accumulated certain amounts of PAs and anthocyanins under high intensity of light or low temperature (Ray et al. 2003; Jonker and Yu 2016), which implies this accumulation of PAs and anthocyanins is both environment- and gene-dependent. Interestingly, the red color induced by light/temperature stresses faded quickly after removing stresses in greenhouse condition, while in field condition it lasted months implying natural light outdoor is sufficient in triggering this stress-induced accumulation (Ray et al. 2003). *In vitro* ruminal fermentation of *Lc*-transgenic alfalfa showed a reduced initial degradation rate of DM and nitrogen compared with its non-transgenic parental alfalfa, but with no detectable negative effects on overall degradation (Wang et al. 2006).

Progenies of this *Lc*-transgenic alfalfa were obtained by crossing to several commercial alfalfa cultivars, namely Rangelander, Rambler and Beaver that were locally grown in western Canada (Jonker et al. 2012b). Compared with their non-transgenic parents, the crossed progenies accumulated more anthocyanins with an average of 197.4 μg/mg DM, contained 3% less CP and

3% more carbohydrates (CHO), reduced the effective degradability and fermentation rate in the rumen, increased the nutrient availability to animals and reduced foaming properties (Jonker et al. 2010, 2012b, 2012a). Based on these results, new attempts were made to dual-express *C1* and *Lc* genes in alfalfa to further boost the PAs and anthocyanins content in alfalfa (Heendeniya and Yu 2017; Heendeniya et al. 2019). Ectopic expression of *R2R3-MYB* gene also has been studied in alfalfa. Hancock et al. (2014) overexpressed *Trifolium arvense* MYB14 (TaMYB14), a R2R3-MYB transcription factor, in alfalfa and white clover, and found an increase in concentration of PAs up to 1.8% of DM. Another study conducted by Verdier et al. (2012) showed that expression of *Medicago truncatula PAR (MtPAR)* gene in alfalfa resulted in enhanced PAs accumulation in alfalfa leaves.

2.4.2 Manipulation of lignin content and composition

Most of the research to decrease lignin content in alfalfa has focused on downregulation of some key genes in the lignin biosynthesis pathway. Reddy et al. (2005) downregulated *cinnamate 4-hydroxylase (C4H)* gene through antisense expression in alfalfa, which resulted in more than 7-fold of reduction in lignin content, but with no significant changes in lignin composition. In the same study, downregulation of *coumarate 3-hydroxylase (C3H)* gene resulted in a 3-fold reduction of lignin content with enriched H lignin, while downregulation of *ferulate 5-hydroxylase (F5H)* gene slightly increased G lignin and reduced S lignin. Shadle et al. (2007) down-regulated *hydroxycinnamoyl CoA: shikimate hydroxycinnamoyl transferase (HCT)* gene and found severely reduced G and S lignin monomers and enhanced H lignin. This might be because HCT is involved in 3-hydroxylation, which is a crucial step in S and G lignin synthesis as shown in Figure 2.2. Transgenic alfalfa genotypes also exhibited some pleotropic effects, including reduced biomass yield, delayed flowering and impaired vascular structure. Concomitant downregulation of *HCT*

and *C3H* produced similar results in terms of lignin content to silencing *HCT* gene alone, except for a pronounced increase (86.1%) in cellulose content (Tong et al. 2015). The authors attributed this increase to the genetic variability, growth stage of alfalfa and the measurement of cellulose. Guo et al. (2001a) down-regulated *caffeic acid 3-O-methyltransferase (COMT)* and *caffeoyl CoA 3-O-methyltransferase (CCOMT)* genes in alfalfa resulting in up to 30% and 18% of reductions in lignin content, respectively. However, the reasons for reduction of lignin were different in these two cases, as strong downregulation of *COMT* caused substantial loss in S lignin while strongly downregulation of *CCOMT* resulted in a striking reduction in G lignin. Significant increases in DM digestibility and *in vitro* gas production have been found in lignin-reduced alfalfa resulting from *COMT* and *CCOMT* down-regulation (Getachew et al. 2011). In some instances, silencing of lignin biosynthesis genes may only result in alterations in lignin composition (lignin monomer ratio) with lignin content remaining unchanged (Boerjan et al. 2003). Baucher et al. (1999) failed to reduce lignin content in alfalfa by down-regulation of *cinnamyl alcohol dehydrogenase (CAD)* gene, but such manipulation altered lignin composition by decreasing S lignin. The unchanged lignin content might be caused by the increase in other units in lignin polymerization, as larger content of aldehydes have been found in many *CAD*-silenced plants (Boerjan et al. 2003). It has been reported that a significant reduction in S/G ratio can be achieved without changing lignin content when *COMT* is reduced to lower than 20% of wild type (Guo et al. 2001a). However, the relationship between S/G ratio and forage degradability is controversial, as some transgenic lines with reduced S/G ratio had higher DM disappearance while others did not (Boerjan et al. 2003). Reduced S/G ratio resulting from *F5H*-downregulation also did not improve *in vitro* DM degradation; in contrast, this *F5H*-downregulated alfalfa had slightly lower DM degradability, which might be due to its slightly higher lignin content (Reddy et al. 2005). Silencing of COMT

and CCOMT decreased lignin content by reducing the proportion of S monomers and G monomers, respectively, and both increased DM digestibility. However, greater improvement of feed quality was achieving by silencing CCOMT than by silencing COMT, but with similar lignin content (Guo et al. 2001b). This implies that lignin composition might also affect forage digestibility.

Although reduction in lignin content and/or alteration of lignin composition in alfalfa by genetic modification increased forage digestibility (Guo et al. 2001b; Getachew et al. 2011; Tong et al. 2015), such genetic modifications were often associated with undesirable traits, such as dwarf phenotype, resulting in huge biomass loss and limiting the benefit of increased digestibility (Bonawitz and Chapple 2013). These pleotropic effects could be the results of loss of lignin itself or other related effects, such as accumulation of harmful intermediates, activation of cell wall integrity pathway, or increased susceptibility to biotic and abiotic stresses (Bonawitz and Chapple 2013). However, a promising finding was reported by McCaslin et al. (2015), in which as lignin-reduced alfalfa cultivar developed by Feed Genetics International, named HarvXtra^{TM}, had a normal (not dwarfed) phenotype. Moreover, HarvXtra^{TM} showed an increase in neutral detergent fiber (NDF) digestibility (12-15%), along with delay in the onset of flowering that allows for a more than seven-day-delay in harvest without sacrificing NDF digestibility (McCaslin et al. 2015). Such ability makes it possible to provide high yield and high-quality alfalfa, as well as low harvest cost, as proper delay in harvest can increase forage yield.

2.4.3 Improving other nutrients profiles

Genetic modification of expressions of target genes has also proven effective in enriching alfalfa with some high value nutrients. For example, Gebril et al. (2015) expressed the maize *sucrose phosphate synthase (SPS)* gene in alfalfa under the control of the constitutive CaMV35S

promoter resulting in increased growth rate and enriched crude protein content in alfalfa leaves. SPS catalyze the key reaction in the synthesis of plant sucrose, which is a main stable energy product from photosynthesis. Overexpression of SPS in alfalfa increased chlorophyll content and photosynthetic rates and increased the sucrose level in leaves, as well as root mass and nodule numbers (Gebril et al. 2015). In another study, simultaneously expressing two bacterial genes, *aspartate kinase (AK)* and *adenylylsulfate reductase (APR)*, influenced amino acid accumulation in alfalfa leading to an increase in levels of sulfur amino acids (Tong et al. 2014). AK phosphorylates aspartate, producing the substrate for the synthesis of lysine, threonine and methionine from aspartate. APR reduces sulfate into sulfite for sulfate assimilation, providing reduced sulfur for the synthesis of sulfur-containing compounds. Co-expression of these two genes increased the synthesis of sulfur amino acids, and increased other essential amino acids (EAA), such as lysine and aspartate. These results are very promising for the livestock industry as sulfur amino acids are of great importance for animal performance and production, especially for fiber growth (Galbraith 2000). Accumulation of antioxidant nutrients, such as carotenoids, could increase the tolerance of plants to abiotic stress, which allows dual improvements in both nutrient value and stress resistance (Han et al. 2008). Wang et al. (2015c) expressed *ibOr* (sweet potato orange gene, involves in carotenoid synthesis) in alfalfa resulting in an increase in carotenoid levels, and an improved tolerance to abiotic stresses; including oxidation, salinity and drought.

2.4.4 Improvement in biomass yield

Efforts have been made to improve alfalfa forage yield through conventional breeding, but with very limited success (Volenec et al. 2002; Aung 2014). More recently, molecular-based approaches to yield improvement have been attempted. For example, microRNA 156 (miR156) is a plant-specific microRNA that has been characterized in many plant species (Aung et al. 2015c).

Overexpression of miR156 in alfalfa caused transcript cleavage-based gene silencing of several *squamosa promoter binding protein-like (SPL)* genes, and enhanced biomass production and shoot branching, delayed flowering time, and improved forage quality characterized by reduced lignin and enhanced cellulose contents (Aung et al. 2015a, 2015b). The delay in flowering onset can prolong the vegetative growth, thereby increasing the biomass yield per harvest without compromising the nutritive value, same as HarvXtra^{TM} alfalfa (McCaslin et al. 2015). This is because, during floral transition, the plants switch from vegetative growth to reproductive growth and repartition their energy supply and photoassimilate to support reproductive development (Ruan et al. 2012; Tadege et al. 2015). As alfalfa is approaching maturity during this transition, The CP content and forage degradability decrease along with an increase in unavailable protein fractions (Yu et al. 2003b), which could be attributed to the decrease in leaf and stem ratio (Yari et al. 2013) and lignin accumulation in stems (Tadege et al. 2015). MiR156 is also involved in regulating biosynthesis of anthocyanidins. Overexpression of miR156 in *Arabidopsis* resulted in an increase in anthocyanins by suppressing the expression of *SPL9* gene (Gou et al. 2011). Improving nutrient absorption ability of alfalfa can also increase biomass yield under certain conditions. For example, Ma et al. (2011) expressed phytase and acid phosphatase genes in alfalfa to improve phosphorous utilization. Compared to the control, transgenic alfalfa had a 2-fold increase in biomass yield in natural soil without phosphorous supplement, and a 3-fold increase in biomass yield when phytate was the only source of phosphorous.

2.4.5 Improvement in abiotic stress resistance

Gene modification and transformation were also used to enhance the tolerance of alfalfa to abiotic stress conditions, such as cold, salt, drought, or even mitigate soil pollution. Nie et al. (2015) found that transgenic alfalfa with enhanced expression of *Ammopiptanthus mongolicus*

dehydrins (*AmDHN*) gene exhibited more resistance to cold stress (4°C). Some drought-related genes can enhance the drought and salt tolerance of alfalfa. Expression of wheat *NHX* antiporter gene, *TaNHX2*, in alfalfa resulted in an increase in salt tolerance (Zhang et al. 2012, 2014). Tang et al. (2014) increased both salt and drought tolerances of alfalfa by overexpressing *Glycine soja WRKY20* gene, which was proven to be successful in enhancing drought tolerance in *Arabidopsis*. In addition to increasing salt and drought tolerance, overexpression of alfalfa *GDP-mannose 3', 5'-epimerase (GME)* gene in *Arabidopsis* resulted in additional acid tolerance, which was attributable to the increment of ascorbate accumulation (Ma et al. 2014). This enhanced abiotic tolerance has the potential to be used in phytoremediation. Wang et al. (2015b) expressed *2,3-dihydroxylbiphenyl-1,2-dioxygenase (BphC.B)* gene, which encodes a key enzyme in catabolism of aromatic compounds, in alfalfa. This heterologous expression resulted not only in an increase in tolerance to polychlorinated biphenyls (PCBs) and 2,4-dichlorophenol (2,4-DCP), but also in a dissipation of these two contaminations in soil. Expression of *P-ATZA*, a bacterial atrazine chlorohydrolase, in tall fescue and alfalfa increased their resistance to atrazine, which was converted into hydroxyatrazine in transgenic plants (Vail et al. 2014). More recently, overexpression of miR156 in alfalfa enhanced drought resistance, as evidenced by a higher survival rate, increased root growth, reduced water loss and increased accumulation of antioxidants, ABA and compatible solutes (Arshad et al. 2017b). Expression of *SPL13* and other drought responsive genes, including *PP2C, NCED3, P5CS* and senescence-associated gene, was affected in miR156 overexpression alfalfa in response to drought. In this study it was also reported that drought tolerant phenotypes were generated by *SPL13*-silencing, which indicates that miR156 regulates drought tolerance by silencing *SPL13* (Arshad et al. 2017b). The enhanced tolerance to

abiotic stresses could make alfalfa more adaptable, enabling alfalfa to grow in more diverse conditions.

2.4.6 Molecular farming

Gene transformation in alfalfa can also be used as molecular farming to produce desirable proteins. For example, Stefanova et al. (2013) transformed human lactoferrin gene into alfalfa and successfully detected its expression in leaf tissue. Ferradini et al. (2015) used alfalfa as model plant to enhance the accumulation of heat shock protein 70 (HSP70) for therapeutic purpose. Dong et al. (2005) expressed a synthesized *sVP6* gene in alfalfa resulted in 0.28% of human group A rotavirus VP6 protein in total soluble protein. In addition, mice fed on this type of alfalfa showed higher anti-VP6 serum IgG and mucosal IgA, and such immunization also could pass to their offspring (Dong et al. 2005). The use of transgenic plants in potentially producing vaccines has been also illustrated in other studies (Aguirreburualde et al. 2013; Kim et al. 2014).

2.5 Transparent Testa8 (TT8) and Homeobox12 (HB12) genes

Observations from *Brassica napus* showed that lignin content might be positively related to expressions levels of two transcriptional factors: Transparent Testa8 (TT8) and Homeobox12 (HB12) (Li et al. 2015). Silencing of *TT8* and *HB12* genes in alfalfa affected the inner molecular structures, chemical composition, CNCPS fractions and nutrients degradations of alfalfa (Li et al. 2015, 2016a; Lei et al. 2018a, 2018c).

2.5.1 Transparent Testa8 (TT8)

TT8 functions in the phenylpropanoid pathway, which serves as sources for many secondary metabolites in plants, including flavonoids, anthocyanins and lignin (Ali and McNear 2014). TT8 encodes proteins with a bHLH (basic helix-loop-helix) structure at its C terminus,

which regulates the biosynthesis of flavonoids in plants (Nesi et al. 2000). TT8, as well as other bHLH protein, interacts with MYB and WDR proteins, forming a ternary MYB-bHLH-WDR (MBW) complex. Baudry et al. (2004) reported that TT8 acts like a bridge connecting MYB and WDR proteins in the formation of MBW complex. TT8 protein contains a bHLH domain and two binding regions: MIR- and WD-interacting regions, which combine with MYB and WD protein, respectively (Xu et al. 2015). The MBW ternary complex controls transcription levels of several late biosynthesis genes (LBGs) in phenylpropanoids pathway, including *BANYULS* (*BAN*), *Dihydroflavonol 4-Reductase (DFR)*, *Leucoanthocyanidin dioxygenase (LDOX)*, *TT19* genes, thereby regulating anthocyanins and proanthocyanins syntheses (Nesi et al. 2000; Baudry et al. 2004; Xu et al. 2015). Research showed insertion of transposable elements muted the expression of *TT8* gene, which led to a yellow seed coat of *Brassica rapa* (Li et al. 2012). Padmaja et al. (2014) reported that mutations of both homoeologous *TT8* is required for the yellow seed coat in *Brassica juncea.* Baudry et al. (2004) reported that complex of TT8 and TT2 (MYB) could also bind to *BAN* promoter; however, the activity of this complex is activated with the presence of Transparent Testa Glabra1 (TTG1) a WDR protein. Escaray et al. (2017) reported that leaf proanthocyanins levels of *Lotus corniculatus*×*tenuis* were positively correlated with expression of *MATE1*, *TT2*, *MYB14* and *TT8* genes.

Apart from regulating flavonoids syntheses, *TT8* also affects accumulations of seed fatty acids and glycosylation processes. Chen et al. (2014b) reported that *TT8* downregulated genes in fatty acids synthesis pathway, resulting in lower fatty acids accumulation and also repressed other genes for seed development and glycerolipid biosynthesis. In addition, mutation of *TT8* resulted in lower seed oil and protein contents in *Arabidopsis*, which is consistent with Qi et al. (2017). Rai et al. (2016) found *TT8* also affects glycosylation of flavonoids and nucleotides and mutation of

TT8 also led to downregulations of sugar transporters and sugar-binding proteins. Moreover, overexpression of *TT8* increased tolerances of plants to biotic and abiotic stresses (Rai et al. 2016). Qi et al. (2017) reported that ectopic expression of *Brassica napus TT8 (BnTT8)* in *Arabidopsis* fully complement the yellow seed coat, higher oil and low protein storage phenotypes, and also rescued the stress tolerance of *tt8* mutant. Studies showed that the expression of *TT8* gene is regulated by the MBW complex in a feedback regulation (Baudry et al. 2006; Xu et al. 2013). In addition, nitrogen nutrients also regulate the expression of *TT8* gene with higher concentration of ammonium decreasing expression of *TT8* and *PAP1* in *Arabidopsis* red cells (Zhou et al. 2012).

2.5.2 Homeobox12 (HB12) gene

HB12, on the other hand, belongs to homeodomain-leucine zipper class I (HD-Zip I) gene family. Homeobox genes contain a conserved DNA sequence which encodes a DNA-binding homeodomain region (Lee et al. 2001). HD-Zip is a unique homeobox gene family to plants, and the homeodomain regions in this family are tightly linked with leucine zipper motifs (Hur et al. 2014). HB12, acting as transcriptional activator, is wildly expressed in plant tissue, including leaves, flowers, stems and roots (Lee and Chun 1998; Lee et al. 2001). Previous studies showed that HB12 expression level is inducible by salt stress and abscisic acid (ABA) treatment (Shin et al. 2004; Henriksson et al. 2005). A study showed that ectopic expression of *coffee HB12 (CaH12)* gene in *Arabidopsis* increased drought tolerance of the plant (Ferreira et al. 2013). Shin et al. (2004) reported that expression of *AtHB12* increased salt tolerance of yeast by regulating sodium ion homeostasis. Lee et al. (2001) examined the structure of *Arabidopsis HB12* (*AtHB12)* gene and found putative binding sites of bHLH and MYB protein in its promoter region. Moreover, the ABA-responsive sites locate in its 5'-flanking region and the activation domain lies in its C-terminal region (Lee et al. 2001). Nobres et al.(2016) characterized the promoter of *CaHB12* gene

and found two different promoter sequences from two different ancestral species: *C. canephora* and *C. eugenioides*. The promoter that inherited from *C. canephora* is responsible for the induction from drought and ABA stress (Nobres et al. 2016).

The inducible expression of *AtHB12* by drought stress is dependent on ABA synthesis that is induced by drought, which is similar to its paralogous *AtHB7* gene (Olsson et al. 2004). Olsson et al. (2004) reported that mutation of *AtHB12* gene reduced plant sensitivity to ABA, whereas overexpression of *AtHB12 and AtHB7* resulted in a hypersensitive response to ABA. Moreover, plants with high-level expression of *AtHB12* and *AtHB7* genes showed delayed elongation and increased branching of inflorescence stems, which is similar to wild type plant during water deficit (Olsson et al. 2004). The negative regulation of *AtHB12* on inflorescence stem growth resulted from its suppressing effect on expression of *gibberellin 20-oxidase 1 (GA20ox1)* gene (Son et al. 2010). Moreover, *Arabidopsis* with overexpressed *AtHB12* gene also had higher growth rate three weeks after germination and had higher expressions of *GA3ox* genes. The up-regulation of *AtHB12* and *AtHB7* induced by ABA treatment depends of ABA-insensitive1 (ABI1), ABI2 and protein phosphatases 2C (PP2Cs) (Olsson et al. 2004; Valdés et al. 2012). In addition, *AtHB12* and *AtHB7* also activate expressions of *PP2C* genes, but repress expression of ABA receptors: *Pyrabactin resistance1-like 5 (PYL5) and PYL8* genes in feedback to ABA signaling (Valdés et al. 2012).

Expression of *AtHB12* is also inducible by virus infection. Park et al. (2011) reported that infection of *Beet severe curly top virus (BSCTV)* induced the expressions of *AtHB12* and *AtHB7* genes in *Arabidopsis*, which is dependent on the virus containing C4 gene. Transgenic plants expressed with *BSCTV C4* gene also increased *AtHB12* expression and caused stunting phenotype, curling leaves and abnormal development of inflorescence and root (Park et al. 2011). Although *AtHB12* and *AtHB7* had similar functions during drought and ABA stresses, their expressions have

a temporal pattern under normal growth conditions in *Arabidopsis* with *AtHB12* having higher expression in the early stage while *AtHB7* at late stages (Ré et al. 2014). Moreover, *AtHB12* and *AtHB7* have influences on each other's expressions and also have different functions in plant development at different stages of maturity (Ré et al. 2014). Hur et al. (2014) reported that HB12 had a positive effect on plant cell growth and the endoreduplication and blocking the function of HB12 led to decrease in leaf size and increase in leaf cell number which might due to the smaller cell size.

2.6 MicroRNA 156 (miR156) and Squamosa Promoter Binding Protein-Like (SPL) genes

MicroRNAs (miRNAs) are a class of small, non-coding regulatory RNAs with the mature sequence being about 18 to 24 nucleotides in length (Spanudakis and Jackson 2014), and they regulate gene expression particularly at post-transcriptional level through gene silencing. Since miRNAs were initially found and reported in *Caenorhabditis elegans* (Lee et al. 1993), the exploration of such small regulatory RNAs has been widely conducted among species (Aung et al. 2015c). After transcription, the inverted repeat sequences in pre-mature miRNAs fold a stem-loop structure, which is immediately detected and cleaved by Dicer complex to generate the mature and active miRNA (Spanudakis and Jackson 2014). Mature miRNAs regulate gene expression either at transcriptional or post-transcriptional level by silencing genes that contain their complementary sequences (Spanudakis and Jackson 2014). Plant miRNAs predominantly regulate the expression of transcriptional factor genes, thereby regulating a variety of processes in plant development (Aung et al. 2015c).

Of the identified plant miRNAs, miR156 is widely conserved among flowering plants (Aung et al. 2015c). The sequence information and brief description of miR156 could be found at

miRbase ("miRBase" n.d.). To date, the sequential information of 313 miR156s from different species and genome chromosomes are stored in miRbase. Most biological functions of miR156 are realized through its target *Squamosa promoter binding protein-like genes (SPLs)*. *SPLs* encode a family of putative transcriptional factors that contain a conserved SBP domain, which consists of 76 amino acids. This 76-animo-acids DNA-binding domain is crucial for SPL proteins to import in nucleus and bind to DNA sequence (Birkenbihl et al. 2005). Apart from this conserved domain, SPL proteins have massive diversity in their molecular structures and biological functions (Aung 2014; Wang and Wang 2015).

The expression of miR156 shows a temporal manner, as it is relatively high at juvenile phase and then gradually reduced with age (Wang and Wang 2015). Studies have proved that miR156 is a master switch that controls plant growth phase transitions, including both vegetative phase transition and reproductive phase transition (Bhogale et al. 2014; Wang and Wang 2015; Aung et al. 2015c; Wang 2016). The lower abundance of miR156 relieves *SPLs* from its repression effects, which activates the expression of flowering-related genes, like *Leafy (LFY)*, and *Apetala1 (AP1)*, to promote plant flowering. Substantial transgenic researches have demonstrated that overexpression of miR156 resulted in delayed flowering and enhanced branching (Bhogale et al. 2014; Aung et al. 2015b). Most of these functions are realized by its transcriptional suppression on corresponding *SPLs* in different species. miR156 targets *SPLs* by recognizing the conserved miRNA responsive elements in the coding region or 3'-UTR of *SPLs* mRNA (Wang and Wang 2015).

As we can see from Figure 2.3, *SPLs* are functionally and structurally diverse. They participate in multiple aspects in plant growth and development, including growth phase transition, branching and leaf angle and all these functions are regulatable by miR156 (Wang and Wang

2015). *SPLs* are plant-specific as no similar genes were found in animals or fungi (Birkenbihl et al. 2005; Aung et al. 2015c). They bind to the specific GTAC core motif in DNA molecule depending on the Zn^{2+} and two Zn^{2+} binding site in SBP domain. In Arabidopsis, 11 out of 17 *SPLs* are targeted by miR156 (Chen et al. 2010; Wang and Wang 2015), and can be functionally divided into three groups: *SPL3 (3,4,5)*, *SPL9 (9,15)* and *SPL10 (10, 11, 2)* (Yu et al. 2015b).

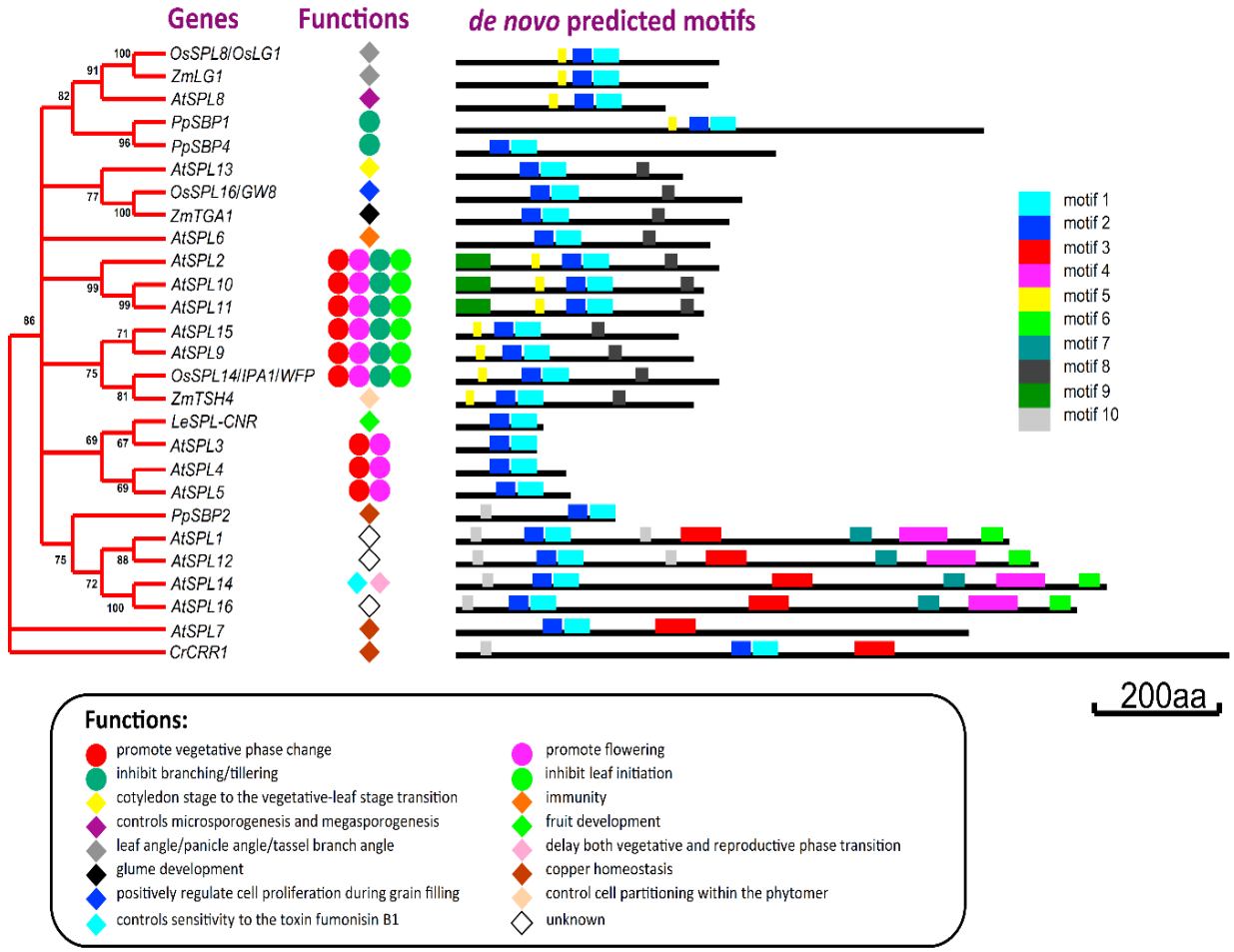

Figure 2.3 Phylogenetic tree, biological functions and structural feature of *SPLs* of several species. The phylogenetic tree was created based on the SBP domain of SPL proteins. This figure is from a review article of Wang and Wang (2015).

SPL3/4/5 are smaller and play predominant role in phase transition and flowering, while *SPL10/11/2* control morphological change of later organs (Yu et al. 2015b). The second group *(SPL9/15)* is more multi-functional and regulates growth aspects including leaf initiation, trichome

distribution and anthocyanin synthesis (Yu et al. 2015b). *SPLs* can also target miRNAs to regulate plant growth and development. For example, miR172 was found to be regulated by miR156/SPL system in potato and Arabidopsis (Wu et al. 2009; Bhogale et al. 2014). Gel retardant assays found two *SPL9*-binding sites in potato miR172 promoter region, and overexpressing miR156-resistant *SPL9* increased miR172 abundance about 5 folds under short-day condition (Bhogale et al. 2014).

2.6.1 Biological functions of miR156/SPL regulatory pathway in growth phase transition and flowering

The lifetime of plants can be broadly divided into two growth phases delimited at the time of flowering, vegetative growth phase and reproductive growth phase. The vegetative phase could be further divided into two sub-phases, juvenile phase and adult phase, based on the morphological changes and acquisition of reproductive competence (Poethig 2013; Wang and Wang 2015). MiR156 and *SPLs* play important role in both growth phase transition. As mentioned above, the expression of miR156 reduces gradually with age, and consistently, the expression levels of its target *SPLs* incline with age. The onset of flowering indicates the growth transition of plants from vegetative growth to reproductive growth, which is a crucial process in plant growth for the success in reproductive, especially for the allogamous plants as they require a synchronized flowering time with each other (Spanudakis and Jackson 2014). Researches have proved that miR156/SPL plays importance role in flowering onset. Overexpression of miR156 led to prolonged juvenile phase and delayed in flowering in many plant species, such as potato (Bhogale et al. 2014), alfalfa (Aung et al. 2015b), tomato (Zhang et al. 2011), rice (Xie et al. 2006b) and maize (Chuck et al. 2007). This repression on flowering onset relies on the involvement of many other transcriptional factors or miRNAs and flowering genes.

In Arabidopsis, *AtSPL3/4/5* directly activate three transcriptional factors, *Leafy (LFY)*, *Fruitfull (FUL)* and *Apetala1 (AP1)*, which are essential for flowering regulation as elevation of

any of these three regulators could accelerate flowering (Yamaguchi et al. 2009). *AtSPL9* promotes plant flowering by activating miR172, which suppresses *AP2*-type flowering repressors genes, such as *Target of Eat1 (Toe1), Toe2*, *Toe3 Schlafmutze (SMZ),*and *Schnarchzapfen (SNZ)* (Yamaguchi and Abe 2012; Wang and Wang 2015). These *AP2*-type genes are proposed to repress the expression of *Flowering Locus T (FT)*, which is a floral inducer capable of activating *AP1* and *FUL* genes (Mathieu et al. 2009).

The regulatory function of miR156/SPL is also regulated by other genes and biotic/abiotic factors. For example, *BdVIL4*, a *Vernalization Insensitive 3 (VIN3)* like gene in *Brachypodium distachyon*, controls flowering and branching by downregulating *miR156* (An et al. 2015). Exogenous application of sugar repressed *miR156* expression and thereby promoting plant growth transition (Yang et al. 2013). Light also affects *miR156* expression in a tissue-specific way. Potatoes grown under short-day condition had lower *miR156* level in leaves and stems but had 8-fold higher *miR156* level in stolons compared with those grown under long-day photoperiod (Bhogale et al. 2014).

2.6.2 Biological functions of miR156/SPL regulatory pathway in branching and internode growth

Branching and internode growth are important for plant growth as they are crucial for competing for light. Shoot branching includes two stages, the formation of axillary buds in the axils of leaves, and its following outgrowth (Beveridge and Kyozuka 2010). Branching is fine-regulated by cytokinin and strigolactone through the *TB1/FC1/BRC1* pathway (Kebrom et al. 2013). *Teostine Branched 1 (TB1)*, and its orthologs *Fine Clum1 (FC1)* in rice, *Brached 1 (BRC1)* in Arabidopsis, encode class II *TCP (Teosinte Branched1*, *Cycloidea*, and *PCF)* transcription factors (Wang and Wang 2015). *TB1* is a negative regulator of branching, and functions like an

integrator in branching regulation as its expression is concomitantly regulated by other signals, such as light and phytohormones (Kebrom et al. 2013).

One of the common phenotypes of miR156 OE plants is the enhanced branching, resulting in a bushy appearance (Aung et al. 2015b; Gao et al. 2016). Like flowering control, this stimulation in branching is also SPL-mediated. Overexpression of *OsSPL14*, the ortholog of *AtSPL9*, in rice promoted panicle branching (Miura et al. 2010). Although the clear mechanism behind branching control is still unknown, one possible pathway is via the *TB1/FC1/BRC1* pathway (Wang and Wang 2015). Lu et al. (2013) reported the transcriptional factor *Ideal Plant Architecture1 (IPA1)* encoded by *OsSPL14* can promote *TB1* expression in rice to suppress rice tillering. In addition, a decrease in strigolactone content was found in miR156-overexpressing potato under both long-day and short-day condition (Bhogale et al. 2014).

A decrease in internode length concomitant with an increase in node number were also found in alfalfa miR156 OE plants (Aung 2014; Gao et al. 2016). However, in most researches, the decreased internode length outweighs the increased node number, leading to a decrease in plant height (Zhang et al. 2011; Wang et al. 2011; Aung 2014). One exception is found in *MsmiR156* OE alfalfa, which showed no height difference between miR156 OE plants and wild type (Aung 2014). To date, it is still unclear how miR156 affects plant heights.

2.6.3 Biological functions of miR156/SPL regulatory pathway in leaf development

In Arabidopsis, 8 out of 16 *SPLs* control leaf development. Among them, *AtSPL3/4/5* regulate trichome distribution in first leaf; *AtSPL11/12* control laminar shape in vegetative phase; and *AtSPL9/15* affect leaf shape (Chen et al. 2010). The regulatory functions of *SPLs* in leaf development are not limited to one area. *AtSPL9* was also reported to affect trichome initiation in petal via *Trichomeless 1 (TCL1)* (Yu et al. 2010). Similar effect on trichome by *SPL10* was also

found in *Arabidopsis* (Shikata et al. 2009). Almost all these leaf-regulating *SPLs* are targeted by miR156 (Rhoades et al. 2002). Overexpression of miR156 in plants caused smaller leaves (Zhang et al. 2011; Wang et al. 2011) and increased trichome density (Aung 2014; Gao et al. 2016). Apart from leaf shape/size and trichome distribution, miR156/SPL might also involve in the regulation of leaf/branch angle. Evidence comes from the finding that *Liguleless1 (LG1)*, *AtSPL8*-homolog gene, controls leaf joint formation and branch angle in maize and rice (Wang and Wang 2015). However, more research is needed to confirm this potential function.

2.6.4 Biological functions of miR156/SPL regulatory pathway in root development and nodulation

The miR156/SPL pathway also functions in root development and nodulation. Martin et al. (2009) reported that overexpression of miR156 in potato caused an approximate 3-fold reduction in root fresh weight. Overexpression of miR156 in rice resulted in more roots but with smaller size (Xie et al. 2012), implying that miR156 might play a role in root branching. This implication was confirmed by the study of Yu et al. (2015b), who reported that overexpression of miR156 in *Arabidopsis* increased the number of lateral roots. The author proposed that at least one group of *SPLs*: *SPL3*, *SPL9* and *SPL10* was responsible for this regulation, with *SPL10* playing the most prominent role. However, the role that miR156/SPL plays in root development might be species-specific, as overexpression of *MsmiR156* in alfalfa caused longer roots (Aung et al. 2015a).

In addition, the miR156/SPL also plays a role in legume nodulation. In the study of Aung et al. (2015a), the root nodule number was increased in *MsmiR156* OE lines. However, other studies reported a reduction of nodulation reduction in miR156 OE plants. In contrast to the positive effect of *MsmiR156*, ectopic expression of *LjmiR156* (miR156 from *Lotus japonicus*) in alfalfa reduced nodulation (Aung et al. 2015b). In another study conducted in soybean,

overexpression of miR156 reduced the expression of miR172, which promotes nodule number by suppressing *AP2* transcriptional factor (Yan et al. 2013).

2.6.5 Other biological functions of miR156/SPL regulatory pathway

In addition to the functions described above, miR156/SPL also functions in other aspects in plant growth and development. For example, this regulatory pathway is involved in potato tuberization as overexpression of miR156 resulted in reduced tuber yield and produce aerial tuber (Bhogale et al. 2014). This tuberization regulation might be realized by regulating miR172 expression, which was found to be an inducer of tuberization in potato (Martin et al. 2009). In line with this suggestion, the expression level of miR172 was reduced by about 80% in the leaves and stolons of miR156 OE potatoes. In addition, the expression of *StSP6A* (paralog of *FT*) was also reduced in leaves. Researchers also reported the functions of miR156/SPL in anthocyanin synthesis (Gou et al. 2011) and environmental stress resistance (Stief et al. 2014; Arshad et al. 2017a). Although miR156/SPL shows similar functions in flowering and branching control among land plants, its function also can be species-specific, such as tuberization in potato and nodulation in legume. This specificity might come from neo-functionalization despite the phylogenetic closeness of *SPLs* (Preston et al. 2012; Wang and Wang 2015). It should be noted that *SPLs* names are not sequential nor equivalent among species. For instance, the *Arabidopsis AtSPL9* gene is more homologous-closed to rice *OsSPL14* (Wang and Wang 2015), instead of the corresponding *OsSPL9* which is found to be the ortholog of *AtSPL7* (Tang et al. 2016).

2.7 Advanced structure study for quality assessment

Gene modification for improving alfalfa quality and stress tolerance could induce molecular structural changes on a molecular basis. Transformation of alfalfa with *Lc* gene, aiming to enhance the accumulation of PAs and anthocyanins, decreased model-fitted alpha-helix and

beta-sheet and increased other protein structures (Yu et al. 2009). This result indicates that protein structure varies between transgenic and non-transgenic alfalfa, which could have an influence on their protein nutrient availability. This is because molecular structures of feedstuff are closely related to the nutritive value of forage for animals. Yu et al. (2005a) reported that high possessions of beta-sheet could reduce the degradability of protein, and an increase in beta-sheet/alpha-helix ratio by heat process was associated with an increase in PC protein fraction, which is the undegradable protein in Cornell Net Carbohydrate and Protein System (CNCPS).

The molecular structural changes induced by gene modification are detectable by advanced structural analytical techniques. Such structural analysis can provide various information on molecular chemistry of tested samples and these structural data can be linked to forage quality and nutrient availability to animals (Yu 2004). Such linkage between molecular structure and forage quality makes structural analysis a promising tool in forage breeding for quality selection. Moreover, optical structural analysis is more rapid and cost-effective than conventional wet chemical analysis, and it requires less sample amount and less preparations/pretreatment. These advantages could reduce the selection time in breeding cycle. To date, there are three common methods used to analyze molecular structures of feedstuffs: near infrared reflectance spectroscopy (NIRS), Global-sourced Fourier transformed infrared spectroscopy (FTIR), and synchrotron radiation-based IR microspectroscopy (SR-IMS).

2.7.1 Near Infrared Reflectance Spectroscopy

Near infrared reflectance spectroscopy (NIRS) was initially used to measure moisture in grains, fruits and vegetables in 1960s (Hart et al. 1962; Gold 1964; Bengera and Norris 1968). Since then, this rapid and cost-effective analytical tool has been well-established as a means for analyzing food and feed samples in terms of components content (Shenk and Westerhaus 1985;

Xiccato et al. 2003; Nie et al. 2009; Plans et al. 2012). NIRS measures the reflectance and absorption of light in the 700–2500 nm region depending on rotational and vibrational energies associated with H-bonding, like O–H, N–H and C–H (Corson et al. 1999; Halgerson et al. 2004; Dixon and Coates 2015). This dependent relationship on H-bonding implies no inorganic minerals can be directly measured by NIRS as they don't absorb energy in NIR region (Halgerson et al. 2004). However, through their associations with organic matters, some minerals can still be accurately predicted by NIRS. Halgerson et al. (2004) reported that accurate prediction of K, Ca and P could be achieved by NIRS, while Mg, S and other micro minerals like Fe, Mn and Si were poorly predicted.

2.7.2 Fourier Transformed Infrared Reflectance Spectroscopy

Unlike dispersive spectroscopy using a monochromatic beam, Fourier transformed infrared reflectance spectroscopy (FTIR) uses a polychromatic beam as a light source. This polychromatic beam is initially interfered by an interferometer, which contains a configuration of mirrors, to generate different combinations of light. After measuring the absorption of various combinations of light, the raw absorption data are analyzed in silico through mathematical procedures, Fourier transformation (Stuart 2004), which is the main characteristic of FTIR. The light used by FTIR can have a wide range of wavelengths, including near-IR, mid-IR, and far-IR. This technique has been used in several studies (Jackson and Mantsch 1995; Baker et al. 2014), including a nutritional-related structure study of alfalfa. Marković et al. (2012) evaluated the lignin profiles in alfalfa leaves and stems at different maturity stages using attenuated total reflectance (ATR)-FTIR spectroscopy, and found differences between leaves and stems, as leaf lignin mainly consisted of G lignin while stem lignin contained both G and S lignin. Another study conducted by Yari et al. (2013) investigated the protein structure of alfalfa at three different maturity stages (early bud, late

bud, and early flower) by using FTIR spectroscopy, as well as the relationship between structural profiles and nutrient availability to ruminants. FTIR spectroscopy detected a decrease in the alpha-helix to beta-sheet ratio of protein secondary structures as alfalfa approached maturity, which was negatively related to nutrient supply to ruminants. The studies of Badhan et al. (2014) and Jonker et al. (2012a) showed the capability of FTIR spectroscopy in exploring the structural changes in alfalfa induced by gene modification.

2.7.3 Synchrotron Radiation-Based Fourier Transform IR Microspectroscopy

When FTIR spectroscopy was combined with microscopy and synchrotron radiation, a new analytical tool was created, which is known as synchrotron radiation-based Fourier transform FTIR microspectroscopy (SR-IMS) (Yu 2004). Unlike traditional wet techniques, SR-IMS is capable of analyzing tissues at the cellular and molecular levels without destruction of inherent structures due to the high brightness of synchrotron light, which is much brighter than those used in NIRS and FTIR. Taking advantage of its high brightness light, SR-IMS is capable of detecting the concentrations and specific chemical structures of macromolecular molecules, like proteins, lipids, carbohydrates, and nucleic acids. To date, this advanced technique has been used to explore the intrinsic molecular structures of various feedstuffs. By using this technique, Yu et al. (2004) successfully obtained the nutritional information of barley in terms of spectral and chemical characteristics and biological components distribution. This advanced technique is also capable of exploring structural changes induced by feed processing. According to the results of Doiron et al. (2009), heating time had an influence on molecular structures of flaxseeds, and such influence affected its rumen degradation. Zhang and Yu (2014) applied this bioanalytical technique to identify molecular changes in response to heat-processing in different types of oil seeds and found

that moisture heating had a greater impact than dry heating in terms of the penetration of heat into the intrinsic tissue.

Molecular structural changes in alfalfa tissue induced by gene transformation have also been explored by using molecular structural analytical techniques (Yu et al. 2009; Yu 2010; Li et al. 2015, 2016a). Li et al. (2015) explored the effects of silencing TT8 and HB12 by RNAi on the chemical profile and carbohydrate structure in alfalfa. Results showed that silencing of TT8 and HB12 increased NDF content and NDF digestibility but had negative influences on the digestibility of rapidly degradable CHO and total CHO in rumen. It was reported that the carbohydrate structural changes induced by gene silencing were closely related to the nutritive value of transgenic alfalfa, such as the bioenergy value and fractions of carbohydrate determined using CNCPS system (Li et al. 2016a).

Genetic engineering is a promising tool for targeted improvement of forage quality. Recently, numerous studies have been conducted to improve alfalfa's nutritive value, biomass yield, and stress resistance, as well as to use alfalfa as a platform in molecular farming to produce vaccines and other desirable proteins. In terms of nutritive value of alfalfa, more research is needed to further boost the accumulation of PAs and anthocyanins as current levels are not adequate for bloat prevention. Moreover, gene modification could induce molecular structural changes in alfalfa, and such structural changes are closely correlated with the nutritive value and nutrient availability for animals. Advanced structural analytical techniques could be used as a rapid tool for the assessment of forage quality of newly modified alfalfa lines. Theses advanced analytical tools for measuring structural changes were well-developed and proven to be powerful in analyzing the nutritive value of genetically modified alfalfa. By measuring the reflectance and absorption of infrared light, it is possible to not only explore the concentration and distribution of

chemical components, but also image their secondary structural characteristics and molecular structure ratios. More studies are needed to further establish correlations between molecular structure and nutrient degradation and availability for animals.

2.8 Objectives and Hypotheses

2.8.1 Objectives

This research involves genetic modified alfalfa plants from two individual researches, silencing of *TT8* and *HB12* (Project 1), and overexpression of miR156 relative to *SPL6/13* silencing (Project 2). The objectives of this study were to investigate the effects of such genetic modifications on chemical composition, inherent molecular structures, *in vitro* ruminal and post-ruminal degradations and modeling nutritive values of alfalfa forage. Moreover, this research also aimed to explore the relationships between molecular structures and nutritive values (Project 3). This study aimed to explore the effect of silencing *TT8* and *HB12* genes, overexpressing miR156 and silencing *SPL6* and *SPL13* genes on:

- chemical composition, CNCPS fractions and degradations and energy values of alfalfa.
- molecular structures of alfalfa with ATR-FTIR by univariate and multivariate analysis.
- molecular structures of alfalfa leaves with synchrotron based FTIR and chemical mapping of alfalfa leaves.
- *in vitro* fermentation characteristics, including productions of gas, NH_3 and VFA during fermentation, degradation and degradational kinetics of DM and NDF.
- fractional microbial protein synthesis (LMN, LAMN and FAMN) and CP degradation and degradational kinetics with the Daisy II incubator.
- post-ruminal protein degradation and predicted protein availability with nutritive modelling of alfalfa.

Furthermore, this study also aimed to explore the relationship between molecular structure and nutritive profiles of alfalfa.

2.8.2 Hypotheses

It was hypothesized that silencing *TT8* and *HB12* genes, overexpressing miR156 and silencing *SPL6* and *SPL13* genes could:

- alter chemical composition and thereby influencing CNCPS fractions and degradations as well as impact energy values of alfalfa
- induce changes in molecular structures of alfalfa, which could be detected with ATR-FTIR by univariate and multivariate analysis
- change molecular structures and chemical localization in alfalfa leaves, which could be detected with synchrotron-powered spectroscopy
- influence *in vitro* fermentation characteristics of alfalfa, including productions of gas, NH_3 and VFA production, and DM and NDF degradation and degradational kinetics.
- affect microbial protein synthesis and CP degradation in the rumen, as well as predicted protein availability with nutritive modelling.

Furthermore, this study also aimed to explore the relationship between molecular structure and nutritive profiles of alfalfa.

CHAPTER 3

EFFECTS OF SILENCING *TT8* AND *HB12* GENES ON MOLECULAR STRUCTURES AND NUTRITIVE VALUES OF ALFALFA IN RUMINANT LIVESTOCK SYSTEM

3.1 Effects of silencing *TT8* and *HB12* genes on bioactive compounds, chemical composition, CNCPS fractions and energetic values of alfalfa

Abstract: The objectives of this study were to investigate the effects of silencing *TT8* and *HB12* genes on bioactive compounds, chemical composition, CNCPS fractions and degradations, and bioenergetic values of alfalfa. Five *TT8*-silenced (TT8i) and eleven *HB12*-silenced (HB12i) along with four non-transgenic control (WT) alfalfa samples were selected for this study. Alfalfa plants were grown in a greenhouse and harvested at mid-vegetative stage. Results showed that HB12i had higher lignin contents, while TT8i had higher phenolic compounds ($P<0.05$). Both transformed alfalfa genotypes had higher carbohydrate (CHO), contributed by higher fiber and sugar, therefore providing more digestible fiber ($P<0.05$). Both transformed alfalfa plants had lower crude protein (CP) and provided less rumen degradable protein (RDCP) ($P<0.05$). Moreover, the soluble true protein fraction (PA2) in protein pool was lower in transformed alfalfa ($P<0.05$). In terms of truly digestive nutrients and energetic values, transformed alfalfa had lower tdFA and higher tdNDF ($P<0.05$). In addition, HB12i had lower tdCP and energetic values ($P<0.05$), while TT8i was not different from WT.

Chemical composition and CNCPS fractions data of this chapter has been previously published. Lei, Y., Hannoufa, A., Prates, L.L., Shi, H., Wang, Y., Biligetu, B., Christensen, D., and Yu, P. 2018. Effects of TT8 and HB12 Silencing on the Relations between the Molecular Structures of Alfalfa (Medicago sativa) Plants and Their Nutritional Profiles and In Vitro Gas Production. J. Agric. Food Chem. 66: 5602–5611. doi:10.1021/acs.jafc.8b01573.

In conclusion, RNAi silencing of *TT8* and *HB12* genes in alfalfa increased fiber content and decreased CP content, which could improve the nutrient balance of alfalfa. Compared with HB12i plants, TT8i alfalfa had comparable available fiber, protein and energy while having improved nutrient balance.

3.1.1 Introduction

Significant advances have been achieved in genetic engineering-based breeding of agricultural crops in recent years (Lei et al. 2017). Compared to conventional breeding, genetic engineering is more efficient, more accurate, and less time-consuming. Taking advantage of the advanced molecular techniques and up-to-date bioinformatics tools, genetic engineering is extremely powerful in manipulating important agronomic traits of plants to meet human needs (Vogel and Jung 2001; Kumar 2011; Kim et al. 2014; Ferradini et al. 2015). Apart from developing new genetic technologies, research efforts have also focused on identification and characterization of genes that have the potential to improve forage quality. Transparent Testa8 (TT8) and Homeobox12 (HB12) are two transcription factors in plants. *TT8* encodes a bHLH (basic helix-loop-helix) protein which interacts with myeloblastosis oncogene (MYB) and WD40-repeat proteins to form a ternary complex (Nesi et al. 2000; Qi et al. 2017). This complex controls transcription of late biosynthesis genes in the phenylpropanoid pathway, thereby regulating biosynthesis of anthocyanins and proanthocyanidins (Schaart et al. 2013; Xu et al. 2015). The HB12, on the other hand, belongs to the homeodomain-leucine zipper class I (HD-Zip I) family and is more related to drought resistance in plants. The expression of *HB12* increased when plants were treated with salt or abscisic acid (Olsson et al. 2004; Ré et al. 2014). Observations from *Brassica napus* showed that expression levels of *TT8* and *HB12* genes are positively associated with lignin content (Li et al. 2015), indicating their potential use as targets towards lignin reduction in forage crops.

Although alfalfa (*Medicago sativa* L.) contains favorable nutrient content and has good palatability, the relatively high lignin content and rapid degradation of protein are two drawbacks that limit the utilization of alfalfa forage (Lei et al. 2017). The rapid degradation of protein in the rumen can lead to rumen bloat in grazing animals, causing huge economic losses to producers

(Jonker et al. 2012a). In contrast, high lignin content of alfalfa hinders the degradation of carbohydrate and other nutrients (Lei et al. 2017). Altogether, these two drawbacks make alfalfa more imbalanced in terms of ruminal nutrient synchronization. Therefore, we transformed alfalfa with TT8 and HB12 RNAi constructs to explore the effect of silencing these two genes on chemical profiles, CNCPS fractions and *in vitro* gas productions of alfalfa. Meanwhile, the Attenuated Total Reflectance Fourier Transform Infrared (ATR-FTIR) spectroscopy was used to explore relationships between nutritional and fermentation profiles with structural spectral structures. We hypothesized that genetic transformations could alter the chemical and nutritional profiles of alfalfa, and that such alterations could affect the *in vitro* fermentation of alfalfa and could be closely related to spectral structures.

3.1.2 Materials and Methods

3.1.2.1 Alfalfa transformation and samples harvest

Both transformed and non-transformed wild type (WT) alfalfa samples were obtained from Agriculture Agri-Food Canada (AAFC) Saskatoon Research Center. Details about designing and making RNAi constructs of *TT8* and *HB12*, transformation of alfalfa, growth conditions of alfalfa plants, and harvests method were described in our previous publications (Li et al. 2015, 2016a). Briefly, total RNA was extracted from alfalfa for cDNA synthesis, and making RNAi constructs for *TT8* and *HB12* by using Gateway systems and pHellsgate12 vector. Afterwards, RNAi constructs were used to transform alfalfa explants via *Agrobacterium tumefaciens* according to Aung et al. (Aung et al. 2015a). There were 11 HB12 RNAi (HB12i) and 5 TT8 RNAi (TT8i) alfalfa plants generated via gene transformation. Transformed plants were then transplanted in a greenhouse with each transformed plant in an individual pot propagated from cuttings. Alfalfa plants were grown under normal greenhouse conditions of 21–23 °C, 16/8 h light/dark rhythm,

and 70% of humidity and harvested at mid vegetative stage. Alfalfa plants were then freeze-dried and stored in individual bags with each bag containing samples from one pot in the greenhouse. There were 11 bags of HB12i, 5 bags of TT8i and 4 bags of WT plants. Bags were considered as replicates for each alfalfa genotype. Samples were ground through a 1 mm sieve (Retsch ZM-200, Retsch Inc., Germany) for chemical analysis.

3.1.2.2 Cell wall residue, lignin and total phenolic extraction

Cell wall residue (CWR) of alfalfa sample was isolated with phosphate buffer and Triton X-100 method as described in (Brinkmann et al. 2002). About 10 mg of CWR was then used to determinate lignin content of alfalfa sample using thioglycolate-alkaline (TGA) method as descried in (Brinkmann et al. 2002). Lignin content was quantified with the OD reading at 280 nm using a UV/VIS spectrophotometer (Helios^{TM} Zeta, Thermo Scientific, Madison, WI, USA). A calibration curve (R^2=0.9999) developed with commercial lignin (Sigma-Aldrich, Oakville, ON, Canada) was used for the calculation. Lignin content was calculated on the basis of both CWR and dry matter DM. Total phenolic content was quantified with Folin-Ciocalteu (F-C) method according to (Ainsworth and Gillespie 2007). About 50 mg f ground samples were incubated in 3.5 mL of 80% (v/v) methanol and vortexed for 20 min at 2500 rpm using a multi-tube vortexer. Extracts were then centrifuged at 1800 rpm for 10 min and the supernatant was used for the quantification of total phenolic content. The supernatant was combined with F-C reagent and sodium carbonate for color development and then OD reading was taken at 765 nm with a UV/VIS spectrophotometer (Helios^{TM} Zeta, Thermo Scientific, Madison, WI, USA). A calibration curve (R^2=0.9982) developed with gallic acid in 50% methanol was used for the calculation.

3.1.2.3 Chemical composition analysis

Contents of dry matter (DM), ash, crude protein (CP) and ether extract (EE) in alfalfa samples were analyzed according to the AOAC methods (Horwitz and Latimer 2005). Neutral detergent fiber (NDF), acid detergent fiber (ADF) and acid detergent lignin (ADL) were analyzed using ANKOM A200 Filter Bag Technique following the procedure provided by ANKOM Technology (ANKOM Technology 2014). Neutral detergent insoluble crude protein (NDICP), acid detergent insoluble crude protein (ADICP) and non-protein nitrogen (NPN) were determined according to the procedure described by Licitra et al. (1996). Soluble crude protein (SCP) was analyzed according to the method of Roe et al. (1990). Total starch was determined using the Megazyme method (McCleary et al. 1997), and sugar content was analyzed according to Dubois's method (DuBois et al. 1956) . Moreover, total carbohydrate content (CHO) and non-fiber carbohydrate (NFC) were calculated according to Higgs et al.(2015).

3.1.2.4 CNCPS fractions and rumen degradation

The updated version (v6.5) of Cornell Net Carbohydrate and Protein System (CNCPS) was used to evaluate CNCPS carbohydrate and protein fractions (Higgs et al. 2015; Van Amburgh et al. 2015). The CNCPS divides carbohydrate into eight fractions, CA1, CA2, CA3, CA4, CB1, CB2, CB3, and CC; divides protein into five fractions, PA1, PA2, PB1, PB2, and PC. As alfalfa hay rarely contains organic acids (Li et al. 2015) and ammonia, we calculated CA4 (sugar), CB1 (starch), CB2 (soluble fiber), CB3 (digestible fiber), CC (indigestible fiber) in carbohydrate fractions and PA2 (soluble true protein), PB1 (insoluble true protein), PB2 (fiber-bound protein), PC (indigestible protein) in protein fractions in the current study. The CNCPS carbohydrate and protein fractions were evaluated on total carbohydrate (CHO) and CP basis, respectively.

Rumen degradable and undegradable CNCPS fractions were then evaluated based on their degradations in and the passage rates from the rumen. The equation for ruminal degradation of each CNCPS fraction was: $D = K_d/(K_d + K_p)$, where *D* was the degradation of each fraction; K_d was the fractional degradation rate of each fraction; K_p was the passage rate out of rumen of each fraction. Rumen degradable CNCPS fractions were then evaluated as the products of CNCPS fractions (%DM) and their corresponding degradations, except for the C fractions in CHO and protein pools as they were regarded as undegradable in the rumen. Rumen undegradable CNCPS fractions were calculated as differences between CNCPS fractions and rumen degradable CNCPS fractions. The fractional degradation rates K_d of each fraction of alfalfa were obtained from the database of NDS professional (RUM&N, RE, Italy), which is a commercial software based on CNCPS. The passage rate K_p of alfalfa was set at 4.5% (Tamminga et al. 1994; Doiron et al. 2009). Ruminal degradable total CHO (RDCHO) and total protein (RDCP) were calculated as the sums of all degradable fractions in carbohydrate and protein pools, respectively. Ruminal undegradable carbohydrate (RUCHO) and protein (RUCP) were the sums of undegradable fractions and corresponding C fractions (CC and PC), respectively.

3.1.2.5 Truly Digestible Nutrients and Energetic Values

Truly digestible nutrients and energetic values of transformed and WT alfalfa were evaluated according to NRC Dairy (2001). Truly digestive nutrients were truly digestive NDF (tdNDF), truly digestive NFC (tdNFC), truly digestive CP (tdCP) and truly digestive FA (tdFA). Bio-energetic values were DE_{1x}, DE_{3x}, ME_{1x}, ME_{3x}, NE_L, NE_m, and NE_g. The subscript of *1x* or *3x* means the feed intake level of the animal at one time or three times of maintenance level. Three times level of maintenance was regarded as at production level of feed intake (NRC Dairy 2001).

Subscripts of *L*, *m*, and *g* with NE mean the net energy for lactation at productive level of intake (3x in this case), for maintenance and for body weight gain, respectively.

3.1.2.6 Statistical analysis

PROC MIXED procedure in SAS 9.4 (SAS Institute, Inc., Cary, NC, USA) was used for data analysis. The model was: $Y_{ij} = \mu + \mathrm{trt}_i + \varepsilon_{ij}$, where Y_{ij} was the dependent variable, μ was the population mean, trt_i was the treatment effect, and ε_{ij} was the random error. Prior to variance analysis, observations with Studentized residual greater than 2.5 were considered as outliers and removed from the dataset. Differences between WT and transformed alfalfa were determined with contract statement. The Tukey-Kramer method was used in multi-comparison after variance analysis and a SAS macro called "pdmix800" (Saxton 1998) was used to denote the letter for each treatment mean at the significance level of 0.05. Normality of residual of each variable was tested by using PROC UNIVARIATE in SAS 9.4 with Normal and Plot options.

3.1.3 Results and Discussion

3.1.3.1 Effect of silencing TT8 and HB12 on cell wall residue, lignin and total phenolic contents of alfalfa

Cell wall residue, lignin and total phenolic contents of transformed and WT alfalfa are shown in Table 3.1.1. There were no significant differences between alfalfa genotypes in terms of CWR content (P>0.05), which accounted for more than 70% of DM mass of alfalfa. The lignin content was demonstrated on both CWR basis and DM basis. Compared with WT and TT8i alfalfa, HB12i alfalfa had higher lignin content (P<0.01). In contrast, TT8i alfalfa had higher phenolic contents compared with WT and HB12i (P<0.01). Moreover, contrast results showed transformed alfalfa had higher phenolics compared with WT (P<0.01). The CWR content in this study was slightly higher compared with alfalfa samples in the second project (Chapter 4.1). This might be

attributed to differences of harvest time for alfalfa samples. Alfalfa samples were harvested at early vegetative phase in the second project, compared with mid vegetative stage in the current study. As alfalfa approaching maturity, the proportion of stem increases and leaf ratio decreases (McCaslin et al. 2015), which might be responsible for the slightly higher CWR content in this study.

Table 3.1.1 Effects of silencing *TT8* and *HB12* genes on cell wall residue, lignin and total phenolic contents of alfalfa: Comparison of gene transformed with wild type.

Items	WT	Transformed Alfalfa		SEM [1]	P value	Contrast [2]
		HB12i	TT8i			W vs G
Cell Wall Residue (CWR, % DM)						
CWR	71.45	72.76	72.26	1.694	0.858	0.653
Lignin Content						
Lignin (mg/g CWR)	9.26b	14.04a	9.57b	0.9522	0.001	0.067
Lignin (mg/g DM)	6.62b	10.24a	6.94b	0.765	0.003	0.076
Phenolic Extraction (mg/g DM)						
Phenolics	2.77b	2.99b	3.28a	0.069	0.001	0.001

[1] SEM, standard error of mean; Means with different letters in each row differ significantly at $P<0.05$.
[2] Contrast between wild type and gene transformed alfalfa.

Lignin content of WT and TT8i alfalfa were lower than those alfalfa samples in the second study (Chapter 4.1) and previous studies on miR156 overexpression in alfalfa (Aung et al. 2015a, 2015b). Research showed that lignin content increases with alfalfa maturity (Marković et al. 2012); however, the alfalfa plants were more mature in the current study compared with the second project. Therefore, the lower lignin content might more likely due to the differences in planting area, cultivation year and growth conditions. Apart from programed biosynthesis, lignin content could be increased by various biotic and abiotic stresses (Vanholme et al. 2010). HB12 belongs to the Homeodomain-Leucine Zipper (HD-Zip) family and is inducible with abscisic acid (ABA) and water stress (Olsson et al. 2004; Son et al. 2010; Park et al. 2011). To our knowledge, there were no publications elucidating the relationship between HB12 and lignin.

The total phenolic extraction was about 3 mg/g of DM weight, which agrees with alfalfa samples in the second project (Chapter 4.1). Phenolics function as plant metabolic intermediates (Dewanto et al. 2002) and antioxidants (Ainsworth and Gillespie 2007), and mainly consist of flavonoids, tannins and anthocyanins. The phenolics content of alfalfa in the current study was lower than those in a previous study (Aung et al. 2015b). This discrepancy could result from differences in growth condition, harvest time and cultivation years between studies. The TT8 protein is a transcriptional factor in phenylpropanoid pathway, which serves as the source of lignin, flavonoids, phenolics and other metabolites(Vogt 2010). The *TT8* gene encodes a beta-helix-loop-helix protein, which works with MYB protein and WD40 as a tricomplex that controls the biosynthesis of anthocyanins(Xu et al. 2015). The reason that silencing *TT8* increased phenolic contents might be the redistribution in phenylpropanoid pathway where intermediates following to syntheses of flavonoids rather than anthocyanins and proanthocyanins.

3.1.3.2 Effect of silencing TT8 and HB12 on chemical profiles

Chemical compositions of transformed and WT alfalfa are shown in Table 3.1.2. Compared with WT control, transformed alfalfa had lower DM, ash, CP, EE, and starch, but higher OM, CHO, NDF, ADF, ADL, NDICP, ADICP, and sugar ($P<0.05$). WT had the highest DM, ash and EE content and the lowest OM content, while HB12i and TT8i had the lowest DM and ash, respectively ($P<0.05$). TT8i had the highest OM followed by HB12i. The EE content of TT8i was not different from both HB12i and WT; however, WT was significantly higher than HB12i ($P<0.05$). In carbohydrate profile, both TT8i and HB12i were higher in CHO, NDF, ADF and lower in starch relative to WT ($P<0.05$). HB12i had higher sugar and ADL than WT, while TT8i was not significantly different from either of them ($P>0.05$). In protein profile, HB12i had the lowest CP, followed by TT8i with WT being the highest. HB12i had higher NDICP than WT,

while TT8i did not differ from WT and HB12i. Both TT8i and HB12i had higher ADICP content relative to WT (P<0.05).

Table 3.1.2 Effects of silencing *TT8* and *HB12* genes on chemical and nutrient profile of alfalfa: Comparison of gene transformed with wild type.

Items [1] (%DM)	WT	Transformed Alfalfa		SEM [2]	P value	Contrast [3] W vs G
		HB12i	TT8i			
DM	92.97a	91.73c	92.18b	0.109	<0.001	<0.001
Ash	9.43a	8.36b	7.53c	0.206	<0.001	<0.001
OM	90.57c	91.64b	92.47a	0.206	<0.001	<0.001
EE	2.18a	1.02b	1.66ab	0.198	<0.001	0.01
Carbohydrate profile						
CHO	62.95b	70.26a	68.05a	0.845	<0.001	<0.001
NFC	38.29	37.51	36.31	0.994	0.45	0.31
NDF	26.80b	34.18a	33.89a	0.995	<0.001	<0.001
ADF	19.78b	25.39a	25.35a	1.006	<0.001	<0.001
ADL	4.36b	5.89a	5.27ab	0.264	<0.001	<0.001
Starch	8.64a	1.23b	1.54b	0.299	<0.001	<0.001
Sugar	4.21b	5.48a	5.06ab	0.287	0.02	0.01
Protein profile						
CP	25.02a	20.73c	22.75b	0.521	<0.001	<0.001
NDICP	1.75b	2.27a	2.15ab	0.122	0.03	0.02
ADICP	0.44b	0.71a	0.65a	0.029	<0.001	<0.001
SCP	9.46	8.68	9.60	0.298	0.05	0.44
NPN	5.70	4.40	4.77	0.643	0.36	0.21

[1] DM, dry matter; OM, organic matter; EE, ester extract; CHO, total carbohydrate; NFC, non-fiber carbohydrate; NDF, neutral detergent fiber; ADF, acid detergent fiber; ADL, acid detergent lignin; NDICP, neutral detergent insoluble crude protein; ADICP, acid detergent insoluble crude protein; SCP, soluble protein; NPN, non-protein nitrogen.
[2] SEM, standard error of mean; Means with different letters in each row differ significantly at P<0.05.
[3] Contrast between wild type and transgenic alfalfa (W vs G).

A previous pilot study with a smaller population size showed similar trends in NDF and starch contents, but other nutrient profiles showed opposite trends or no significant differences (Li et al. 2015). Higher ash content of transformed alfalfa was found in the pilot study, while in the current study both TT8i and HB12i had lower ash content. There were no significant differences between alfalfa populations in DM, EE, ADF, ADL and sugar contents. Moreover, no significant differences were detected in NFC content, while WT alfalfa had higher NFC in the pilot study. Nevertheless, nutrients amount of alfalfa was comparable between our studies. Such differences in statistical results might result from our research populations. In the pilot study, only two alfalfa replicates of each genotype were selected, while in the present study 4 WT, 12 HB12i, and 5 TT8 alfalfa replicates were used. Moreover, the extent of gene silencing varies between different RNAi populations, which may lead to variations in its effect, as observed in the studies on miR156 (Aung et al. 2015a, 2015b). Thus, a lower number of plants in alfalfa populations might increase the incidence of sampling error. At the same time, more replicates can reduce random variations in statistical analysis.

Our previous publication did not report on protein profiles of transformed and WT alfalfa (Li et al. 2015). Compared with alfalfa cultivars in a study of Yu et al. (2003b), alfalfa populations in the present study had lower NDF, ADF, ADL, NDICP, and ADICP. Differences in variety and harvest time might account for these discrepancies in chemical composition. Alfalfa varieties of Pioneer and Beaver were used in the study of Yu et al. (2003b), which were different from our alfalfa clone N4.4.2. Harvest time, as suggested in Li et al. (2015), might also play a role in the chemical variation. Alfalfa harvested at different growth stages varied in nutrients profile; NDF and ADF contents increased while CP decreased when alfalfa approaching maturity from early bud to early bloom (Yu et al. 2003b).

3.1.3.3 Effect of silencing TT8 and HB12 on CNCPS Fractions

Table 3.1.3 shows CNCPS carbohydrate and protein fractions of transformed and WT alfalfa in the percentage of CHO and CP, respectively. In carbohydrate fractions, both transformed alfalfa genotypes had higher percentages of CB3 and lower CB1 percentages compared with WT ($P<0.05$). CB1 is the starch fraction and is rapidly degradable in the rumen. In terms of CC proportion, HB12i was higher than WT ($P < 0.05$), while TT8i was not significantly different from neither HB12i nor WT. The reduction of CB1 fraction was also observed in our pilot study (Li et al. 2016). However, we found higher proportions of CB3 and CC of carbohydrate in transformed alfalfa, especially in HB12i, which were not observed in the pilot study. Such differences in carbohydrate pools reflected the chemical differences between our studies, which might be attributed to the increment of population size of the present study. In protein fractions, HB12i and TT8i had higher proportion of PA2 and lower proportion of PB1 compared with WT ($P<0.01$). PB1 is the insoluble true protein in protein pools. The decreases of PB1 in transformed alfalfa were responsible for their lower CP content. There were no differences among alfalfa plants in PB2 proportion. HB12i was the highest in PC proportion, followed by TT8i, with WT being the lowest ($P < 0.01$). Our previous publication did not report protein fractions of TT8i and HB12i, so other publications were used for comparison.

Tremblay et al. (2003) used an older version of CNCPS, in which protein was partitioned into five (A, B1, B2, B3 and C) fractions (Sniffen et al. 1992), to evaluate protein fractions of early-bloom alfalfa of different genotypes and cultivars. After adapting their results into the updated CNCPS, the average proportions of PB2 and PC in their alfalfa populations were 2.8 and 3.9, respectively. Compared with their results, PB2 was higher and PC was lower in the present study. Cutting stage might be responsible for these differences. According to Yu et al. (2003b), who assessed the effect of cutting stage on CNCPS fractions of alfalfa, PC increased while PB2

decreased with the maturity of alfalfa from early bud to early bloom. In this study, higher unavailable PC fraction was found in transformed alfalfa, indicating a maturity-like down-regulatory effect of *TT8* and *HB12* on protein fractions. In contrast, maturity had the opposite effects on carbohydrate fractions, as transformed alfalfa contained higher CC fraction that was found to decrease with maturity (Yu et al. 2003b).

Table 3.1.3 Effects of silencing *TT8* and *HB12* genes on CNCPS fractions of alfalfa: Comparison of gene transformed with wild type.

Items [1]	WT	Transformed Alfalfa		SEM [2]	P value	Contrast [3] W vs G
		HB12i	TT8i			
Carbohydrate fractions (%CHO)						
CA4	6.68	7.83	7.45	0.451	0.21	0.13
CB1	11.77a	1.75b	2.26b	0.699	<0.001	<0.001
CB2	38.85	40.68	40.49	1.173	0.53	0.29
CB3	38.18b	42.39a	43.51a	1.051	0.01	<0.001
CC	4.53b	7.35a	6.30ab	0.619	0.01	0.01
Protein fractions (%CP)						
PA2	37.78b	42.69a	42.17a	0.687	<0.001	<0.001
PB1	53.78a	46.09b	48.37b	1.060	<0.001	<0.001
PB2	6.68	7.69	6.62	0.669	0.36	0.60
PC	1.76c	3.37a	2.85b	0.126	<0.001	<0.001

[1] CA4, water-soluble carbohydrate, sugar; CB1, starch; CB2, soluble fiber; CB3, digestible fiber; CC, indigestible fiber; PA2, soluble true protein; PB1, insoluble true protein; PB2, fiber-bound protein; PC, indigestible protein

[2] SEM, standard error of mean; Means with different letters in each row differ significantly at $P<0.05$.

[3] Contrast between wild type and transgenic alfalfa (W vs G).

The impact of genetic modifications on nutrient profiles and CNCPS fractions of alfalfa was previously reported by Jonker et al. (2010). The transformation of *Lc* gene in alfalfa, which increased anthocyanidins accumulation (Jonker et al. 2012a), increased total carbohydrate content and tended to increase slowly degradable fiber and unavailable protein fractions. Different results

were found in rapidly degradable protein fractions in *Lc* and *C1* co-transformed plants (Heendeniya et al. 2019).To our knowledge, there are no other publications that explore the influence of genetic modifications on CNCPS fractions other than our pilot study (Li et al. 2015, 2016a).

3.1.3.4 Effect of silencing TT8 and HB12 on rumen degradations of CNCPS fractions

The rumen degradable and undegradable CNCPS fractions of transgenic and WT alfalfa are shown in Table 3.1.4. In general, HB12i and TT8i alfalfa had higher degradable carbohydrate fractions and lower protein fractions. The HB12i had higher RDCA4 compared to WT ($P<0.05$), but TT8 was not significantly different from neither HB12i nor WT. Both HB12i and TT8i had lower RDCB1, but higher RDCB2 and RDCB3 in comparison with WT ($P<0.05$). Similar patterns of results were also found in rumen undegradable carbohydrate fractions, which resulted from discrepancies in CNCPS fractions(Lei et al. 2018b). Both HB12i and TT8i were equally higher for RUCB2, RUCB3, RUCHO and lower for RUCB1 compared to WT ($P<0.05$). The HB12i had higher RUCA4 and RUCC compared to WT ($P<0.05$), while TT8i showed no significant difference relative to HB12i and WT ($P>0.05$). In terms of ruminal degradation of protein fractions, both HB12i and TT8i had lower RDPB1, RDCP and RUPB1 with HB12i even lower than TT8i, but higher RUPC. Moreover, HB12i had lower RUCP compared with WT, while TT8i was not different from either of them.

Table 3.1.4 Effects of silencing *TT8* and *HB12* genes on rumen degradable and undegradable CNCPS fractions in alfalfa: Comparison of gene transformed with wild type.

Items [1] (%DM)	WT	Transformed Alfalfa		SEM [2]	P value	Contrast [3]
		HB12i	TT8i			W vs G
Rumen degradable CHO						
RDCA4	3.66b	4.77a	4.4ab	0.250	0.02	0.01
RDCB1	7.20a	1.02b	1.28b	0.249	<0.001	<0.001
RDCB2	22.7b	26.62a	25.36a	0.473	<0.001	<0.001
RDCB3	7.64b	9.76a	10.28a	0.389	<0.001	<0.001
RDCHO	41.86	41.84	41.33	0.539	0.71	0.72
Rumen degradable protein						
RDPA2	7.52	6.91	7.64	0.237	0.05	0.44
RDPB1	9.33a	6.71c	7.65b	0.23	<0.001	<0.001
RDPB2	0.73	0.84	0.81	0.06	0.44	0.26
RDCP	17.77a	14.58c	16.1b	0.371	<0.001	<0.001
Rumen undegradable CHO						
RUCA4	0.55b	0.71a	0.66ab	0.037	0.02	0.01
RUCB1	1.44a	0.21b	0.26b	0.050	<0.001	<0.001
RUCB2	3.89b	4.57a	4.35a	0.081	<0.001	<0.001
RUCB3	6.55b	8.37a	8.82a	0.335	<0.001	<0.001
RUCHO	22.7b	27.84a	26.72a	0.635	<0.001	<0.001
Rumen undegradable protein						
RUPA2	1.93	1.77	1.96	0.061	0.05	0.44
RUPB1	4.09a	2.94c	3.35b	0.101	<0.001	<0.001
RUPB2	0.63	0.72	0.69	0.051	0.49	0.30
RUCP	7.25a	6.07b	6.65a	0.178	<0.001	<0.001

[1] RD**, rumen degradable CNCPS fractions; RU**, rumen undegradable CNCPS fractions; CA4, water-soluble carbohydrate, sugar; CB1, starch; CB2, soluble fiber; CB3, digestible fiber; CC, indigestible fiber; PA2, soluble true protein; PB1, insoluble true protein; PB2, fiber-bound protein; PC, indigestible protein; CHO, carbohydrate; CP, crude protein.
[2] SEM, standard error of mean; Means with different letters in each row differ significantly at P<0.05.
[3] Contrast between wild type and transgenic alfalfa (W vs G).

Our results suggested that both transgenic alfalfa genotypes provided more slowly degradable carbohydrates and less rumen degradable protein, which is consistent with our previous publication in chemical composition and CNCPS fractions (Lei et al. 2018b). Chemically, both transgenic alfalfa genotypes had higher fiber but lower CP content (Lei et al. 2018b). A previous pilot study conducted on a smaller alfalfa population (n=2) reported rumen degradable CNCPS carbohydrate fractions(Li et al. 2015) and found similar results in RDCB1 and RUCB1. However, the pilot study failed to detected the differences in RUCB2, RDCB2, RDCB3, RUCB3 and RUCHO(Li et al. 2015). Furthermore, lower RDCHO was observed in transgenic alfalfa in the pilot study, which showed no differences in the current study. The discrepancies between our studies might be attributed to the differences in population size. The current study used a larger alfalfa population (5 TT8i, 11 HB12i and 4 WT) compared with the pilot study (n=2 for all alfalfa genotypes). Lei et al. (2018a) reported that the population size of samples had an impact on statistical results of spectral parameters in alfalfa. This effect of population size might be attributed to the variations in the extent of genetic modification, as shown in the miR156 studies (Aung et al. 2015a, 2015b).

3.1.3.5 Effect of silencing of TT8 and HB12 on truly digestible nutrients and energetic values

Truly digestible nutrients, total digestible nutrients and energetic values of transgenic and WT alfalfa are shown in Table 3.1.5. Transformed alfalfa had equally higher tdNDF and lower tdCP in comparison with WT ($P<0.01$). Moreover, HB12i was lower than WT in tdFA, while TT8i was not different from neither HB12i nor WT. In terms of TDN and bioenergetic values, HB12i was lower compared with TT8i and WT ($P<0.05$). The TT8i had comparable TDN and energy values to WT, although it was numerically lower. The increased tdNDF of TT8i offset the decreases in tdCP and tdFA, thereby maintaining its energy level.

Table 3.1.5 Effects of silencing *TT8* and *HB12* genes on truly digestive nutrients and bio-energetic values in alfalfa: Comparison of gene transformed with wild type.

Items [1]	WT	Transformed Alfalfa		SEM [2]	P value	Contrast [3] W vs G
		HB12i	TT8i			
Truly digestive nutrients (%DM)						
tdNFC	37.52	36.76	35.58	0.974	0.45	0.31
tdCP	24.49a	19.53b	21.99a	0.645	<0.001	<0.001
tdFA	1.18a	0.18b	0.66ab	0.155	<0.001	<0.001
tdNDF	10.46b	13.48a	13.87a	0.515	<0.001	<0.001
Total digestible nutrients (%DM)						
TDN1x	68.12a	63.19b	65.93a	0.757	<0.001	<0.001
Bio-energetic values (Mcal/Kg)						
DE1x	3.20a	2.92b	3.07a	0.038	<0.001	<0.001
DE3x	3.01a	2.82b	2.92a	0.025	<0.001	<0.001
ME3x	2.59a	2.40b	2.50a	0.025	<0.001	<0.001
NEl3x	1.63a	1.50b	1.57a	0.017	<0.001	<0.001
NEm	1.71a	1.51b	1.62a	0.028	<0.001	<0.001
NEg	1.10a	0.92b	1.02a	0.025	<0.001	<0.001

[1] tdNFC, truly digestive non-fiber carbohydrate; td, truly digestive crude protein; tdFA, truly digestive fatty acid; tdNDF, truly digestive neutral detergent fiber; TDN1x, total digestible nutrients at one time of maintenance level; DE1x, digestible energy at one time maintenance level; DE3x, digestible energy at three times maintenance level; ME3x, metabolizable energy at three times maintenance level; NEl3x, net energy for lactation at three times maintenance level; NEm, net energy for maintenance; NEg, net energy for growth. 3x represents the production level of feed intake.
[2] SEM, standard error of mean; Means with different letters in each row differ significantly at P<0.05.
[3] Contrast between wild type and transgenic alfalfa (W vs G).

Yu et al.(2003b) reported the effect of alfalfa variety and maturity on energetic values of alfalfa, which were lower than our results. This difference might result from the differences in harvest time. The earliest harvest date in Yu's study was early bud stage, while our samples were harvested at early-to-mid vegetative phase. Overall, the estimated energetic values of alfalfa in the present study was equivalent to published values (Belyea et al. 1999; Vahdani et al. 2014). In the pilot study (Li et al. 2016a), both tdNFC and tdCP were lower in transgenic alfalfa, and no differences were found in tdFA and tdNDF. Moreover, there were no differences between alfalfa genotypes in truly digestible nutrients and energetic values in the pilot study, although energy values were numerically lower in transgenic alfalfa, especially in HB12i (Li et al. 2016a). The differences in energy values between our results again could be attributed to population size.

3.1.4 Conclusion

Silencing of *HB12* and *TT8* genes in alfalfa increased fiber content and decreased CP content, which could improve the nutrient balance of alfalfa. Moreover, silencing of *HB12* gene resulted in higher lignin content, while silencing of *TT8* gene leaded to higher phenolics content. In addition, silencing of *TT8* gene had equivalent energy values and truly digestible CP compared with silencing *HB12* gene.

3.2 Effects of silencing *TT8* and *HB12* genes on molecular structures of alfalfa by ATR-FTIR spectroscopy

Abstract: This study investigated the spectral changes in alfalfa molecular structures induced by silencing of *Transparent Testa 8* (*TT8)* and *Homeobox 12* (*HB12)* genes with univariate and multivariate analyses. *TT8*-silenced (TT8i), *HB12*-silenced (HB12i) and wild type (WT) alfalfa were grown in a greenhouse under normal conditions and were harvested at early-to-mid vegetative stage. Samples were free-dried and grounded through 0.02 mm sieve for spectra collections with attenuated total reflectance Fourier transform infrared (ATR-FTIR) spectroscopy. Afterwards, both univariate and multivariate analyses were conducted on amide, carbohydrate and lipid regions. Univariate results showed that silencing of *TT8* and *HB12* genes affected peak heights of most total carbohydrates (TC) and structural carbohydrates (STC), and structural carbohydrates area (STCA) in carbohydrate regions; and β-sheet height, amide areas, and ratios of amide I/II and α-helix/β-sheet in amide region; and symmetric CH_2 (SyCH2), asymmetric CH_2 ($AsCH_2$) and (a)symmetric CH_2 and CH_3 area (ASCCA) in the lipid region. Multivariate analysis showed that both hierarchy cluster analysis (HCA) and principal component analysis (PCA) clearly separated WT from transgenic plants in all carbohydrate regions and (a)symmetric CH_2 and CH_3 (ASCC) lipid region. In the amide region, PCA separated WT, TT8i and HB12i into different groups, while HCA clustered WT into a separate group. In conclusion, silencing of *TT8* and *HB12* affected intrinsic molecular structures of both amide and carbohydrate profiles in alfalfa, and multivariate analyses successfully distinguished gene-silenced alfalfa from WT control.

A version of this chapter has been previously published. Lei, Y., Hannoufa, A., Christensen, D., Shi, H., Prates, L.L., and Yu, P. 2018. Molecular Structural Changes in Alfalfa Detected by ATR-FTIR Spectroscopy in Response to Silencing of TT8 and HB12 Genes. International Journal of Molecular Sciences 19: 1046. doi:10.3390/ijms19041046.

3.2.1 Introduction

Fourier-transform infrared (FTIR) spectroscopy is an analytical technique that uses a polychromatic light source allowing for simultaneous collection of spectral absorption data from a wide range of electromagnetic spectra (Lei et al. 2017). The absorption data is closely correlated to the vibrational intensities of the molecular bonds of chemical functional groups of samples (Pumure et al. 2015). Compared with conventional wet analysis, FTIR is rapid, direct and has been widely used in many fields, such as biodiesel (Mueller et al. 2013), food science (Chen et al. 2018), medical research (Rai et al. 2018), and plant science (Fahey et al. 2017). Moreover, FTIR spectroscopy requires only small little amounts of samples (Stuart 2004), which is very useful for the preliminary evaluation of forage quality at the early stages of genetic breeding. FTIR spectroscopy can be divided into three categories according to its spectroscopic sampling mode; transmission, transflection and attenuated total reflection (ATR) (Baker et al. 2014). In ATR-FTIR spectroscopy, the IR beam goes through a crystal and reflects at the interface of the crystal and the sample on it. The reflection of IR beam creates an evanescent wave (4~6 μm) which can penetrate the sample on the crystal surface (Baker et al. 2014; Fahey et al. 2017). Recently, this technique has been used to detect the molecular changes induced by genetic modifications. Heendeniya and Yu (2017) applied this technique to dual-transgenic (*Lc* and *C1*) alfalfa and found that transgenic alfalfa had higher amide area and amide I/II height ratios, and lower heights in some carbohydrate peaks. Secondary protein structures were also analyzed in this project, and α-helix/β-sheet height ratio was found higher in dual-transgenic alfalfa.

Recently, our group generated two genotypes of transgenic alfalfa TT8i and HB12i, with silenced TT8 and HB12 genes, respectively). TT8 (Transparent Testa8) and HB12 (Homeodomain Leucine Zipper Class I) are two transcriptional factors in the phenylpropanoid pathway, which serves as the source of many secondary metabolites. A pilot study previously reported on the

carbohydrate structural features and the structural-nutrition relationships in TT8i and HB12i (Li et al. 2015, 2016a). In the current study, we explored univariate structural features in amide, carbohydrate and lipid-related regions. And we also used two multivariate analyses on all spectral structural regions to distinguish different genotypes.

3.2.2 Materials and Methods

3.2.2.1 RNAi transformation, growth condition and sampling

Information on the making of RNAi constructs and transformation of alfalfa, growth conditions and sampling methods was previously described Chapter 3.1. There were 5 TT8 RNAi (TT8i, n=5), 11 HB12 RNAi (HB12i, n=11) and 4 wild type (WT, n=4). Samples were ground through a 0.12 mm sieve (Retsch ZM-200, Retsch Inc., Germany).

3.2.2.2 ATR-FTIR spectroscopy

Molecular FTIR spectra of each sample were obtained by using JASCO FT/IR-4200 with ATR (JASCO Corp., Tokyo, Japan) at the University of Saskatchewan, Canada. The FTIR spectra were obtained at mid-IR region (ca. 4000-700 cm^{-1}) at a resolution of 4 cm^{-1} with 128 scans (SpectraManager II software). Five subsamples of each sample were measured, generating five spectra for each sample. Figure 3.2.1 shows the example spectra of transgenic and WT alfalfa.

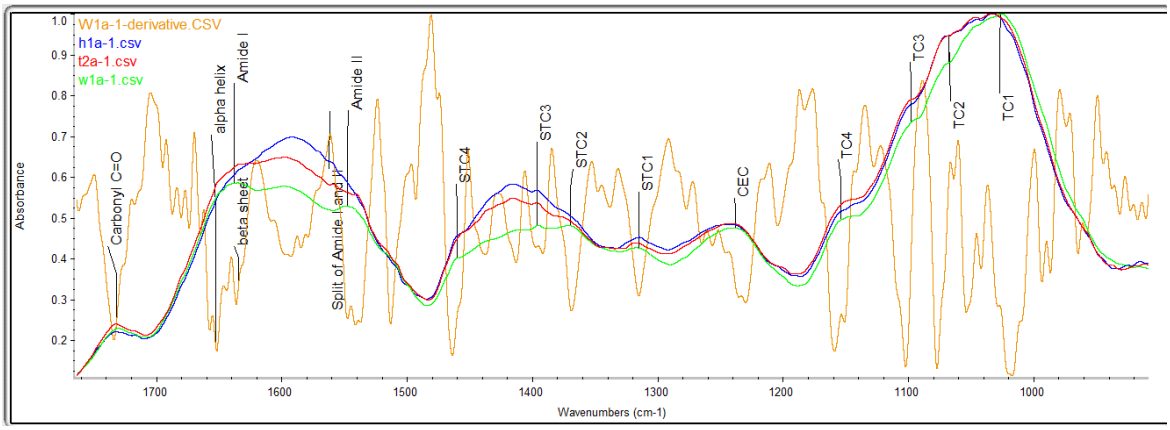

(a)

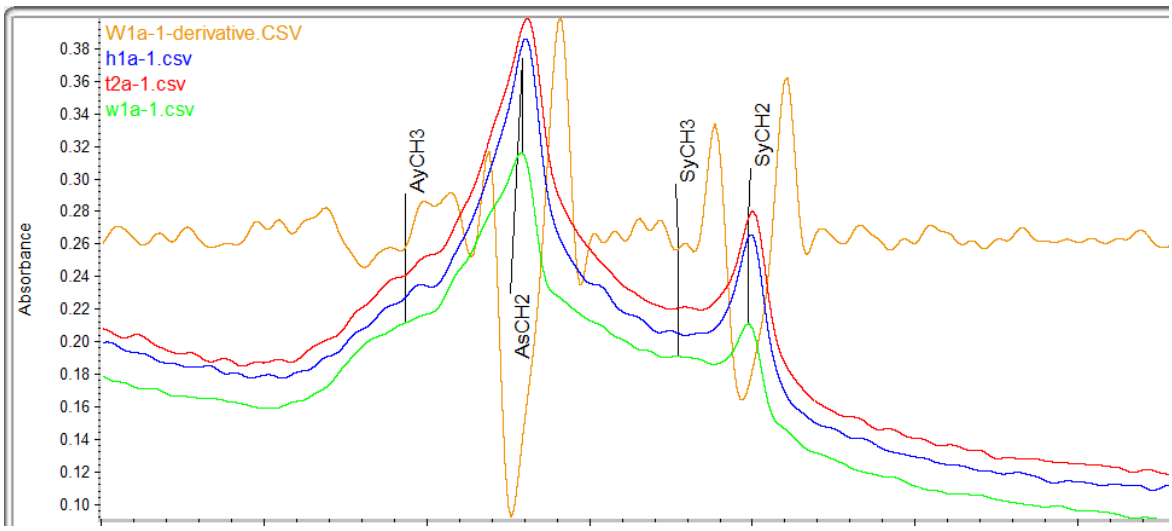

Figure 3.2.1 Example of normalized and derivative spectra of transgenic and WT alfalfa with annotations.

(**a**) Carbonyl C=O (CCO), Amide and carbohydrate (CHO) region; (**b**) Symmetric and asymmetric CH2 and CH3 (ASCC) region. TC1-4 and STC1-4 are four peaks in total carbohydrate (TC) and structural carbohydrate (STC) regions, respectively; CEC, cellulosic compounds region; SyCH2, symmetric CH2; SyCH3, symmetric CH3; AsCH2, asymmetric CH2; AsCH3, asymmetric CH3. W1a-1.csv, t2a-1.csv, h1a-1.csv are spectral examples of WT, TT8i and HB12i alfalfa. W1a-1-derivative.csv is the second derivative of w1a spectrum, showing as an example.

3.2.2.3 Univariate analysis

IR spectra were preprocessed by using OMNIC 7.3 software (Spectra Tech, Madison, WI, USA) before measurements of peak height and area. First, each IR spectrum was normalized and then its second derivative was generated and autosmoothed. The normalized spectra and smoothed second derivatives were then saved as "csv" files. Afterwards, all five spectra of each sample along with its second derivatives were read in excel and processed by using Excel® Macro for peak and area measurements. The Excel® Macro consisting of two Modules: 1. Input all five csv-form spectra and five csv-form second derivatives into sheet1; 2. Automatically calculate peak heights and areas for each spectrum of five subsamples, then output the results into sheet2 (see Sup-1, Macro template). Peak heights and areas were calculated with baseline correction (Figure 3.2.2). Peak heights equaled to total peak heights subtract the baseline heights at the peak wavenumber.

Peak areas were calculated as total peak areas subtract the areas below the baseline. Total peak areas were determined as the cumulative area between every two adjacent wavenumbers under the spectrum, which were calculated as a trapezoidal shape. Wavenumbers of peaks and baseline points were determined according to the experiential wavenumbers (Xin and Yu 2014; Yan et al. 2014; Li et al. 2015).

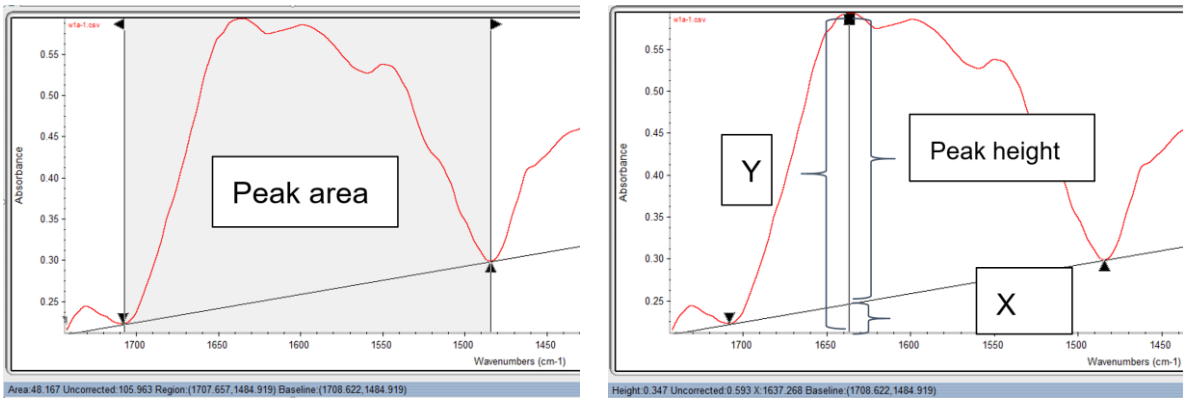

(**a**) (**b**)

Figure 3.2.2 Illustrations of peak area and peak height measurements.

(**a**) Peak area measurement. Corrected peak area equals the total area below the red spectrum minus the area below the baseline (straight black line); (**b**) Peak height measurement. Corrected peak height equals the total height (Y) minus the height below the baseline (X).

Peaks and areas were measured in three regions: carbohydrate (CHO, ca. 1484-941 cm^{-1}), Amide (ca. 1710-1484 cm^{-1}) and lipid-related region (ca. 1781-1710 cm^{-1} and 3000-2761 cm^{-1}). Within CHO region, wavenumbers were further divided into total CHO (TC, ca. 1178-941 cm^{-1}), structural CHO (STC, ca. 1484-1178 cm^{-1}), and cellulosic compounds (CEC, ca. 1283-1178 cm^{-1}). TC contains four major peaks at ca. 1149 (TC4), 1104 (TC3), 1074 (TC2), and 1026 (TC1) cm^{-1}; STC also contains four major peaks at ca. 1453 (STC4), 1397 (STC3), 1370 (STC2), and 1317 (STC1) cm^{-1}; CEC centers at ca. 1237 cm^{-1}. Areas of each sub-CHO regions (TCA, STCA, and CECA) were measured according to their baselines. In amide region, unlike cereal spectra (Damiran and Yu 2010), sub-regions of amide I and amide II of alfalfa were overlapped in the current study (Figure 5a and Figure 6a). Therefore, a common baseline of ca. 1710-1484 cm^{-1} was

used to determine peak heights in amide region. For the heights of protein secondary structures, the second derivatives were used in assisting the determination. Amide I, amide II, α-helix and β-sheet peak at ca. 1649, 1540, 1653 and 1629 cm^{-1}, respectively. Although no subdivision of amide region was performed, total amide area (AA) was divided into two subareas, amide I area (AIA) and amide II area (AIIA), by ca.1575 cm^{-1}. This was confirmed by a common peak in second derivatives of all IR spectra, and it also is the normal split point of amide I and II in cereal samples (Damiran and Yu 2010). Moreover, ratios of some variables were calculated in amide region, including α-helix/β-sheet, amide I/amide II, AIA/AIIA, AIA/AA. The lipid-related region contains two parts, carbonyl C=O region (CCO, ca. 1781-1710 cm^{-1}) and (a)symmetric CH_2 and CH_3 region (ASCC, ca. 3000-2761 cm^{-1}). CCO centers at ca. 1733 cm^{-1}. ASCC features four major peaks at ca. 2955 cm^{-1} (asymmetric CH_3, AsCH3), 2920 cm^{-1} (asymmetric CH_2, AsCH2), 2872 cm^{-1} (symmetric CH_3, SyCH3), and 2850 cm^{-1} (symmetric CH_2, SyCH2). Areas of carbonyl C=O region (CCOA) and (a)symmetric CH_2 and CH_3 region (ASCCA) were also measured with their corresponding baselines.

3.2.2.4 Multivariate analysis

Hierarchical cluster analysis (HCA) and principle component analysis (PCA) were performed on each region of IR spectra. In addition to all regions (CHO, TC, STC, CEC, amide, lipid) described above in univariate analysis, the whole spectrum region (ca. 4000-700 cm^{-1}) and fingerprint region (ca. 1800-800 cm^{-1}) were also analyzed. Both HCA and PCA were performed in R 3.4.2 software (R Core Team 2017) with STATS package in Rsutdio® environment. Initially, all five spectra (csv files) of each sample were input into R software, and then spectra from all samples were integrated into one R object (one dataset). Afterwards, eight sub-datasets (four carbohydrate regions, one amide region, two lipid-related regions and one fingerprint region) were

created from the whole dataset according to wavenumber range described previously. HCA and PCA were performed on all eight sub-regions and the whole region. For HCA, the mean spectra of each sample were calculated with aggregate() function in order to clarify the HCA cluster dendrogram. After that, dist() function was used for calculating the sample distance with Euclidean method. Function hclust() was then used for HCA clustering with Ward.D method by using squared Euclidean distance. The dendrograms of HCA were plotted with plot() function. All R functions mentioned above are from STATS package. For PCA, prcomp() function in STATS package was used with both *center* and *scale* options setting as true. Then, PCA plots were generated with ggbiplot() function with *ellipse* and *circle* options setting as true, and *var.axes* option setting as false, and options of o*bs.scale* and *var.scale* were set to 1. Function ggbiplot() was from GGBIPLOT package (Vu 2018).

3.2.2.5 Statistical analysis

Procedure MIXED of SAS 9.4 software (SAS Institute, Inc., Cary, NC, USA) was used to analyze univariate variables in IR spectra. The model used was: $Y_{ijk} = u + geno_i + sub(geno)_j + \varepsilon_{ijk}$, where Y_{ijk} was the independent variable; μ_i was the mean of all samples; $geno_i$ was the fixed genotype effect; $sub(geno)_j$ as a random effect; ε_{ijk} was the random error. Prior to variance analysis, a SAS Macro with the same model was used to remove all outliers with a criterion of Studentized Residual greater than 2.5. Contrast statement was used to compare WT with transgenic alfalfa. The Tukey-Kramer method was used for multi-comparison among genotypes. A SAS macro called "pdmix800" (Saxton 1998) was used to denote the letter for each treatment mean at the significance level of 0.05. Proc UNIVARIATE with Normal and Plot options was used to test the normality of the residue of each variable. Significance level was set as $P<0.05$.

3.2.3 Results and Discussion

3.2.2.1. Effects of silencing TT8 and HB12 genes on carbohydrate structure-related spectral profiles of alfalfa

The CHO structural parameters of transgenic and WT alfalfa are shown in Table 3.2.1. Three of the four major TC peak heights were affected by alfalfa transformation with TT8 and HB12 RNAi constructs. There were no significant differences between alfalfa genotypes for TC1 peak height, although transformed alfalfa tended to have lower TC1 heights ($P<0.1$). In contrast, both TC2 and TC3 heights were increased in transformed alfalfa compared with WT control ($P<0.001$). Height and area of CEC were significantly decreased in transformed alfalfa compared with WT. All structural carbohydrate (STC) spectral parameters were affected by genetic transformation. STC1 peak height was higher in HB12i alfalfa, while TT8i was not significantly different from WT control. HB12i had the highest STC2, STC3, and STC4 peak heights; whereas TT8i was not different from WT in STC2 and STCA. WT alfalfa had the lowest STC3 and STC4 followed by TT8i. Chemically, transgenic alfalfa had higher NDF and ADF contents, with HB12i having the highest values (Chapter 3.1). Our data suggested a positive correlation exists between structural parameters and chemical components.

The current results are not in accordance with the results of a previous pilot study, which was conducted on a smaller population size (Li et al. 2015). In that pilot study, either no differences were found in peak heights or differences were opposite to the current study. The discrepancies in the results of the two studies could be attributed to multiple factors. First, the IR spectra were not normalized in the pilot study, which led to low values in peak heights and areas. Variations in sample thickness under ATR-FTIR determination could affect the results, and such variations could be eliminated through the normalization process. Second, only two replicates of each

genotype were used in the pilot study. The smaller size of the alfalfa population might lead to sampling error.

Table 3.2.1 Effects of silencing *TT8* and *HB12* genes on carbohydrate structural parameters of alfalfa: Comparison of gene transformed with wild type.

Items [1]	WT	Transgenic Alfalfa		SEM [2]	P value	Contrast [3]
		HB12i	TT8i			W vs G
Total carbohydrate related spectral profiles						
TC1	0.630	0.610	0.608	0.0086	0.223	0.088
TC2	0.500b	0.551a	0.539a	0.0078	0.001	<0.001
TC3	0.344b	0.381a	0.376a	0.0050	<0.001	<0.001
TC4	0.154	0.152	0.152	0.0032	0.919	0.688
TCA	75.507	78.553	78.034	0.8721	0.064	0.029
Cellulosic compounds related structural profiles						
CEC	0.084a	0.071b	0.073b	0.0024	0.006	0.002
CECA	3.121a	2.503b	2.408b	0.1506	0.015	0.004
Structural carbohydrate related structural profiles						
STC1	0.096b	0.107a	0.099ab	0.0027	0.014	0.083
STC2	0.157ab	0.164a	0.150b	0.0028	0.004	0.994
STC3	0.170c	0.234a	0.193b	0.0053	<0.001	<0.001
STC4	0.127c	0.170a	0.151b	0.0037	<0.001	<0.001
STCA	29.111b	35.445a	30.964b	0.5923	<0.001	<0.001

[1] TC1-TC4, four major peaks at ca. 1026 (TC1) 1074 (TC2), 1104 (TC3) and 1149 (TC4) cm^{-1} in TC region, respectively; TCA, peak area of TC region; CEC, cellulosic compounds (ca. 1237 cm^{-1}); CECA, peak area of CEC region. STC1-STC4, four major peaks at ca. 1317 (STC1), 1370 (STC2), 1397 (STC3) and 1453 (STC4) cm^{-1}, respectively.
[2] SEM, standard error of mean; Values with same letter in each row are not significantly different at P>0.05.
[3] Contrast between WT and transgenic alfalfa;

Notably, an additional peak was found in both TC and STC regions in the current study, which was absent in the pilot study of Li et al. (2015, 2016a). This is because different methods were used to obtaining structural parameters. In the pilot study, only peaks shown in the IR spectrum were included in the analysis. However, there was an inconsistency in the wavenumber of the second total CHO peak, either ca. 1100 cm^{-1} or 1075 cm^{-1}, in published studies (Yang et al. 2014; Li et al. 2015; Heendeniya and Yu 2017; Ban et al. 2017; Refat et al. 2017b). This inconsistency indicates that there were individual peaks at these two wavenumbers; however, one of them might have overlapped with other peaks because of the feature of FTIR spectra (Ami et al. 2013). Thus, in the present study, second derivatives were used as references to measure the overlapped peaks.

Plots of HCA and PCA multivariate analyses of three carbohydrate sub-regions (TC, CEC, and TC) and the whole CHO region are shown in Figure 3.2.3. Both HCA and PCA clearly separated WT from TT8i and HB12i transgenic plants in all carbohydrate regions. In HCA dendrograms of TC, STC and CHO, WT was clustered in a different group at heights arounds 4, 7 and 10, respectively. This indicated there were significant differences between WT and transgenic alfalfa in these carbohydrate regions. The HCA dendrogram of CEC region clustered alfalfa populations into three groups at the height of 0.7 with most of WT replicates clustering in a separate group. Nevertheless, HCA clustering failed to separate TT8i and HB12i transgenic alfalfa in carbohydrate regions. Similarly, PCA plots of TC and CHO regions also plotted transgenic alfalfa populations together. However, HB12i and TT8i were distinguished from each other in PCA plots of CEC and STC regions with little overlaps, especially in STC region. Transgenic alfalfa genotypes were separated at the scale of second principle component (PC2). The first

principle components of TC, CEC, STC and CHO regions explained 71.8%, 98.3%, 90.5%, and 79.0% of population variances, respectively.

In the pilot study, Li et al. (Li et al. 2016a) did multivariate analyses on TC, STC, NTC (non-structural carbohydrate) and CEC regions and found that all genotypes overlapped with each other and were indistinguishable from each other in all carbohydrate regions. This failure in distinguishing alfalfa genotypes could be attributed to the population size and normalization processing. Multivariate analyses of carbohydrate regions implied that WT differed from transgenic alfalfa populations in every carbohydrate profile. From the PCA plots of TC and CHO region, WT was clearly separated from transgenic alfalfa on PC1 axil with WT at the positive side while transgenic alfalfa at negative side. Thus, we plotted PC1 loading against wavenumber for PCA results of TC and CHO (Figure 3.2.1). Except for the region close to ca. 1020 cm^{-1} (around ca. 990-1026 cm^{-1}), all other wavenumber variables contributed negatively to PC1.

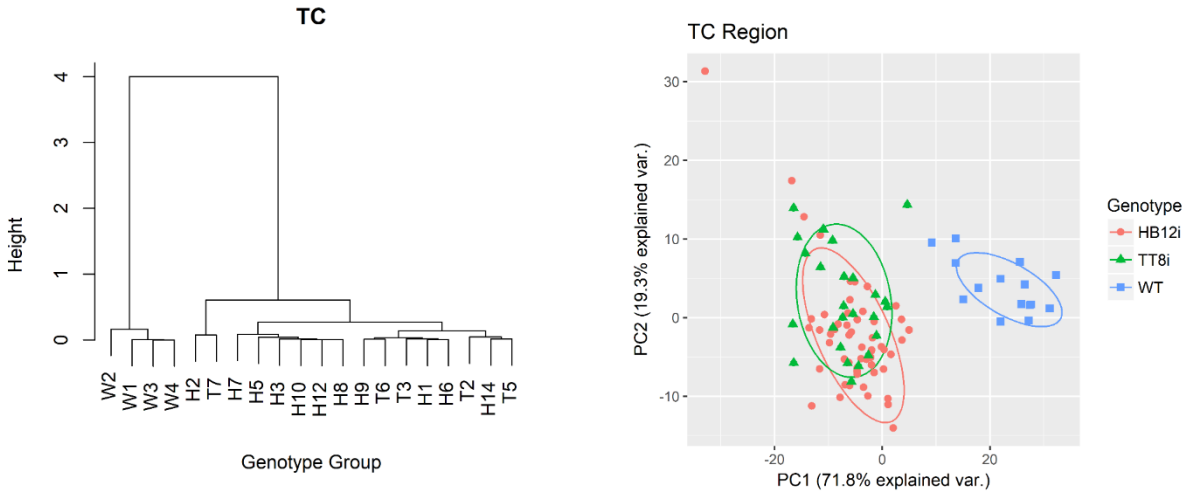

(a) (b)

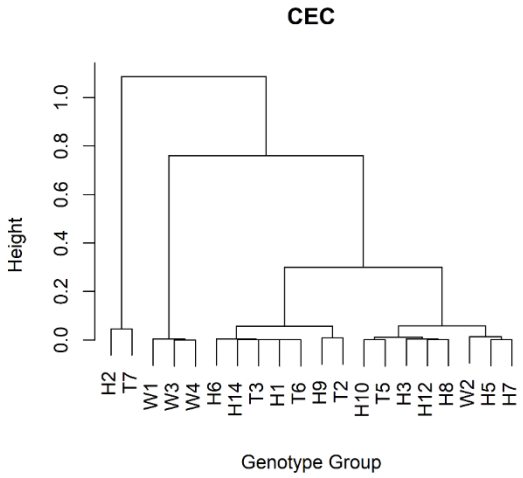
CEC
Height
0.0
0.2
0.4
0.6
0.8
1.0
H2
T7
W1
W3
W4
H6
H14
T3
H1
T6
H9
T2
H10
T5
H3
H12
H8
W2
H5
H7
Genotype Group

(c)

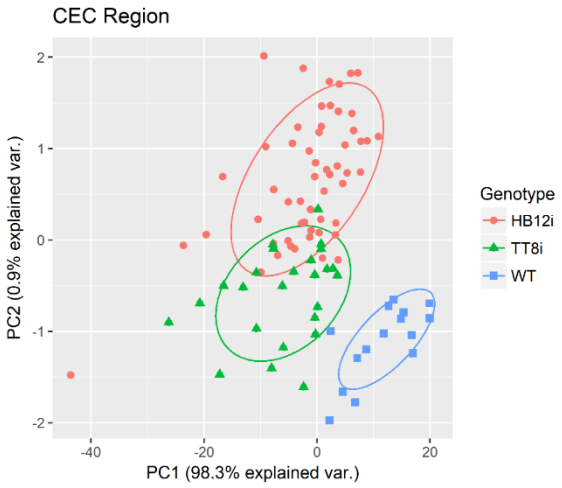
CEC Region
PC2 (0.9% explained var.)
2
1
0
-1
-2
-40
-20
0
20
PC1 (98.3% explained var.)
Genotype
HB12i
TT8i
WT

(d)

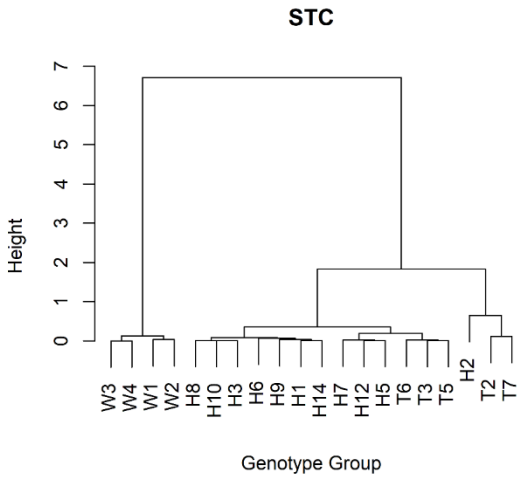
STC
Height
0
1
2
3
4
5
6
7
W3
W4
W1
W2
H8
H10
H3
H6
H9
H1
H14
H7
H12
H5
T6
T3
T5
H2
T2
T7
Genotype Group

(e)

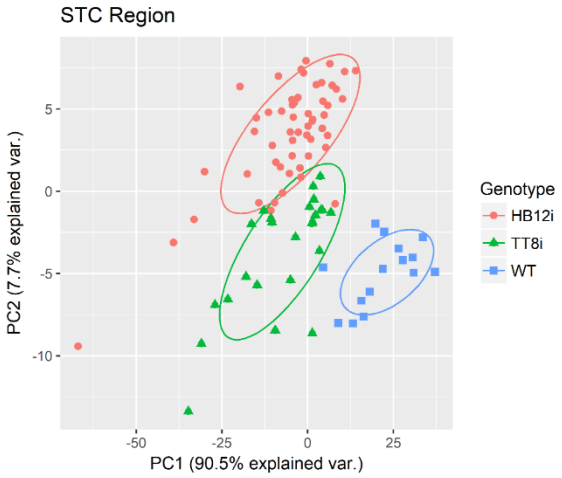
STC Region
PC2 (7.7% explained var.)
5
0
-5
-10
-50
-25
0
25
PC1 (90.5% explained var.)
Genotype
HB12i
TT8i
WT

(f)

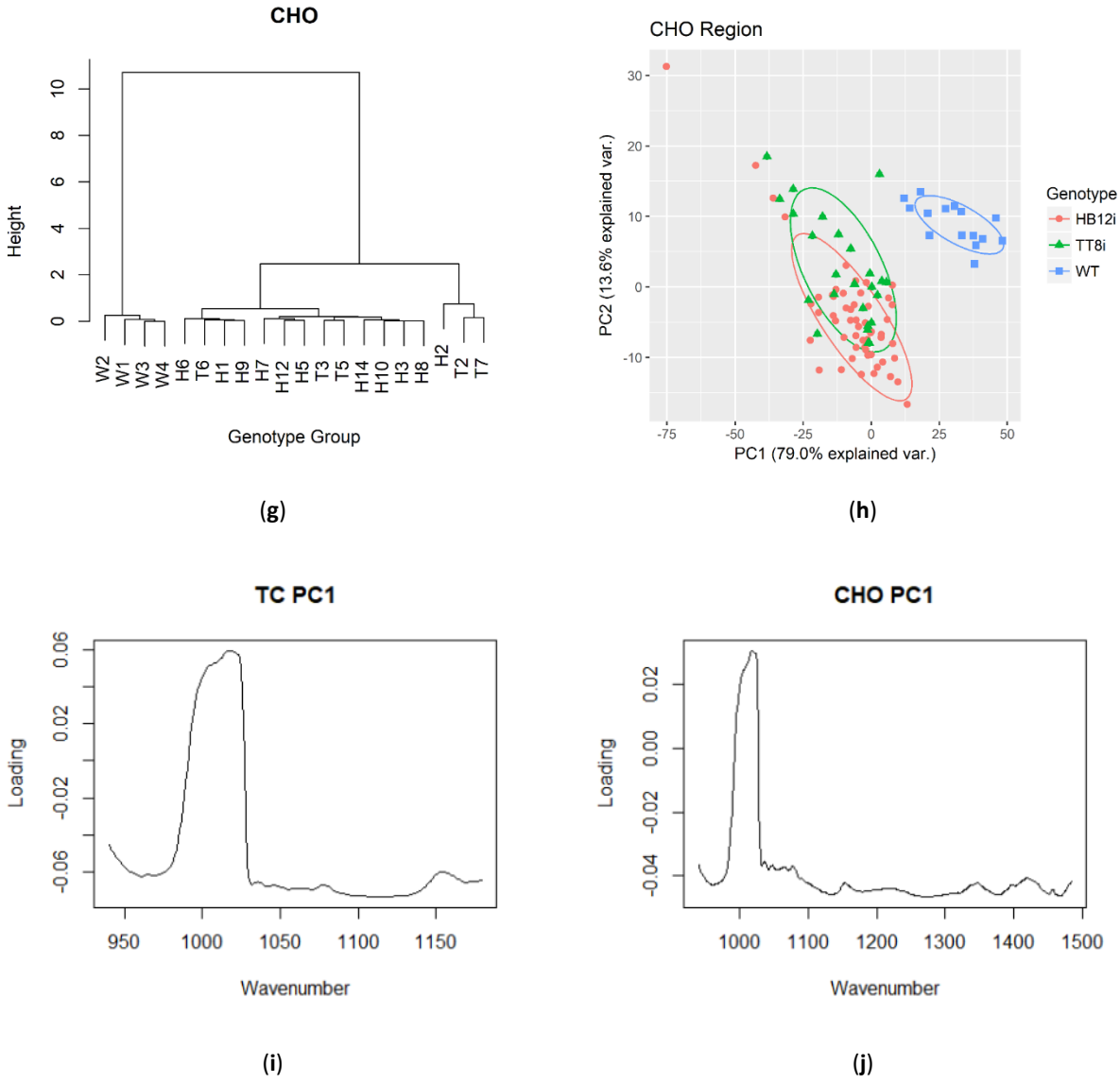

Figure 3.2.3 HCA dendrograms and PCA plots of carbohydrate regions of transgenic and WT control.

TC, total carbohydrate (ca. 1178-941 cm^{-1}); CEC, cellulosic compounds (ca. 1283-1178 cm^{-1}); STC, structural carbohydrate (baseline ca. 1484-1178 cm^{-1}); CHO, whole carbohydrate region (ca. 1484-941 cm^{-1}). (**a**) HCA dendrogram of TC; (**b**) PCA plot of TC; (**c**) HCA dendrogram of CEC; (**d**) PCA plot of CEC; (**e**) HCA dendrogram of STC; (**f**) PCA plot of STC; (**g**) HCA dendrogram of CHO; (**h**) PCA plot of CHO; (**i**) PC1 loading of TC against wavenumber; (**j**) PC1 loading of CHO against wavenumber.

3.2.2.2. Effects of silencing TT8 and HB12 gens on amide and protein secondary structure related spectral profiles of alfalfa

Amide region of FTIR spectrum, baseline of ca. 1484-1710 cm^{-1}, normally contains two main peaks in high protein samples, amide I and amide II (Yu et al. 2009). However, in the current study, amide I and II overlapped and were visibly indistinguishable from each other in most transgenic alfalfa FTIR spectra, which was consistent with the study of Yari et al (2017). As shown in Table 3.2.2, there were no significant differences in amide I peak height among alfalfa populations (P=0.508). In amide II peak height, variance analysis and multiple comparison showed some inconsistency. A significant P value of 0.043 was obtained from the F test of variance analysis; however, multiple comparison results among populations were not significant due to the strictness of Tukey-Kramer method. This situation occurs when the P value is close to 0.05, and different comparison methods come to different decisions on whether to reject the H0 hypothesis.

The amide I to amide II ratio was higher in TT8i ($P<0.01$), compared to HB12i and WT control. The amide I to amide II ratio in TT8i unveiled the ambiguous results of amide II height, confirming a lower amide II height in TT8i populations. There were no significant differences in α-helix secondary structures among alfalfa populations. TT8i and HB12i had numerically equal height value of β-sheet, which was higher than that of WT control ($P<0.001$). The differences of β-sheet carried out to α-helix/β-sheet ratio, as both transgenic alfalfa genotypes had lower α-helix/β-sheet ratio with HB12i having the lowest ratio. The higher ratio of β-sheet in transgenic alfalfa could hinder the utilization and availability of protein and reduce protein value. This is because proteins with higher proportion of β-sheet secondary structure are more resistant to enzymatic digestion (Yu 2005a).

Another study by Yu et al. (2009) evaluated the effects of *Lc* gene transformation, which was aimed at increasing the accumulation of anthocyanidins, on protein secondary structural ratios

in alfalfa. Both ratios of α-helix and β-sheet were decreased in *Lc*-transgenic alfalfa. Transformation with HB12 and TT8 RNAi also affected amide areas in alfalfa. HB12i had higher AA compared with TT8i and WT control. Higher AIA and AIIA were also found in HB12i, which were significantly higher than WT and TT8i, respectively. TT8i and WT were not significantly different from each other in terms of AIA and AIIA. The results of our chemical analysis showed lower crude protein content in both transgenic alfalfa plants with HB12i having the lowest CP (Chapter 3.1), indicating a negative relationship between amide areas and CP content.

Table 3.2.2 Effects of silencing *TT8* and *HB12* genes on amide structural parameters of alfalfa: Comparison of gene transformed with wild type.

Items	WT	Transgenic Alfalfa		SEM [1]	P value	Contrast [2]
		HB12i	TT8i			W vs G
Amide heights and spectral ratio profiles						
Amide I	0.358	0.339	0.348	0.0096	0.349	0.255
Amide II	0.274	0.271	0.242	0.0088	0.043	0.163
Amide I/Amide II	1.313b	1.256b	1.428a	0.0246	<0.001	0.385
Secondary structures heights and ratio profiles						
α-helix	0.346	0.331	0.335	0.0082	0.451	0.257
β-sheet	0.342b	0.386a	0.374a	0.0076	0.002	0.002
α-helix/β-sheet	1.017a	0.858c	0.895b	0.0090	<0.001	<0.001
Amide area and ratio profiles						
Amide area (AA)	49.882b	55.216a	50.727b	1.2236	0.006	0.076
Amide I area (AIA)	33.788b	38.027a	35.891ab	0.7861	0.003	0.008
Amide II area (AIIA)	16.094ab	17.147a	14.836b	0.4884	0.006	0.877
AIA/AIIA	2.097c	2.221b	2.444a	0.0307	<0.001	<0.001
AIA/AA	0.677c	0.689b	0.709a	0.0029	<0.001	<0.001

[1] SEM, standard error of mean; Values with same letter in each row are not significantly different at P>0.05.
[2] Contrast between WT and transgenic alfalfa;

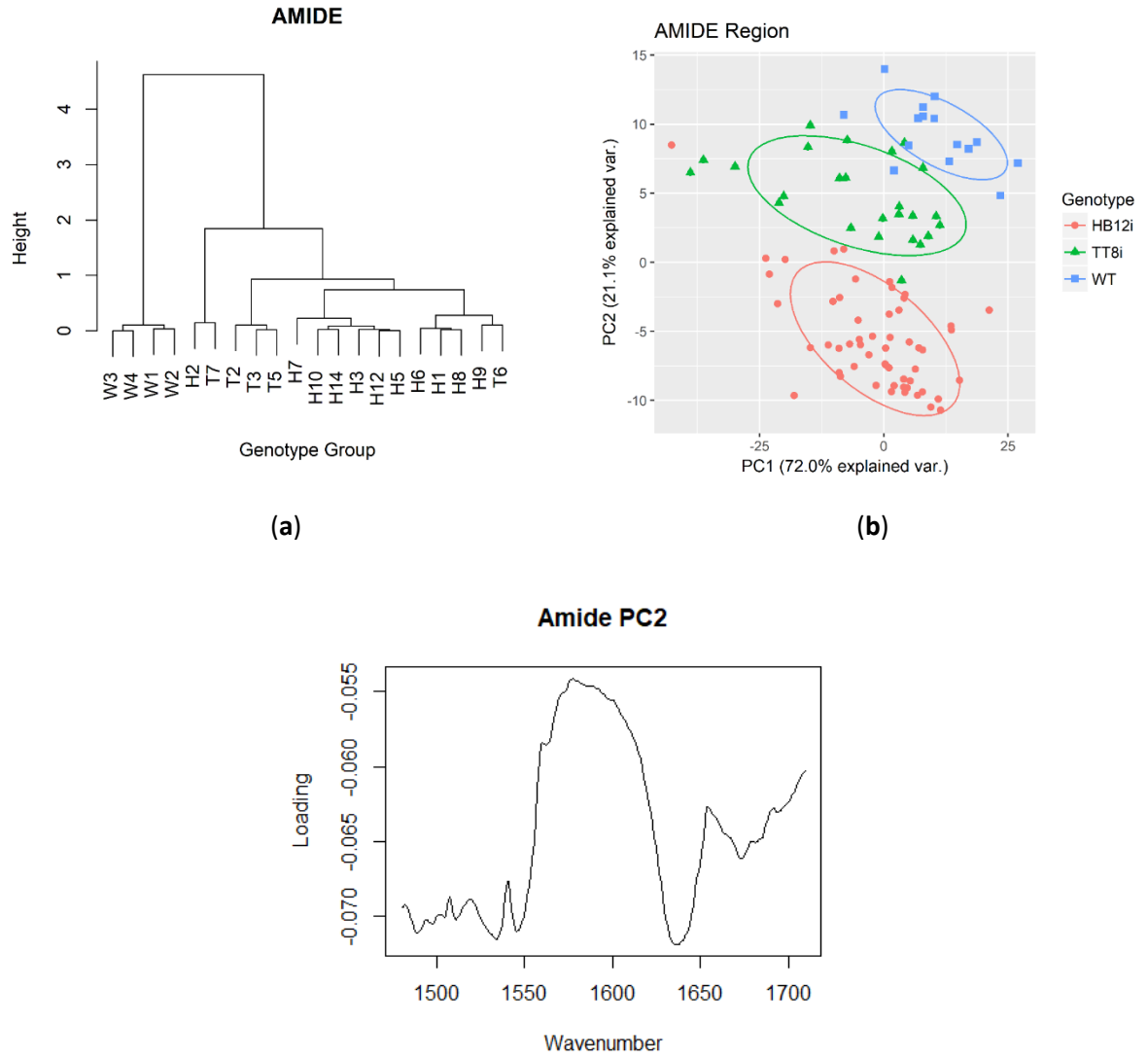

Figure 3.2.4 HCA dendrograms and PCA plots of amide region of transgenic and WT control. Baseline of amide region is ca. 1710-1484 cm^{-1}. (**a**) HCA dendrogram of amide region; (**b**) PCA plot of amide region; (**c**) PC2 loading of amide region against wavenumber.

Previous reports in the literature showed both amide heights and areas were positively correlated to CP content in cereals (Yan et al. 2014; Peng et al. 2014). However, Chen et al. (2014a) reported no significant relationships existed between amide spectral profiles and CP content. There might be more factors affecting the spectral profiles in chemical compositions of feedstuffs, such

as sources, types and processing methods of samples. It should be noted that IR spectra in these previous studies were not normalized, which might also contribute to this discrepancy. HCA dendrograms and PCA plots of the amide region are shown in Figure 3.2.4. In HCA dendrograms, WT was clustered in a group at the height above 4. Moreover, most of HB12i alfalfa sub-genotypes (except for H2) were clustered in a group at the height around 0.8. Similar results were also obtained in PCA plots of the first two PCs, with PC1 and PC2 explained 72.0% and 21.1 % of total population variances. WT, HB12i, and TT8i were separated into different ellipses at PC2 axil. Plot of PC2 loadings against wavenumber variables are also shown in Figure 3.2.4. All variables negatively contributed to PC2, with variables of ca. 1480-1550 cm^{-1} and regions close to ca.1640 cm^{-1} outweighed others.

3.2.2.3 Effects of silencing TT8 and HB12 on lipid-related structure spectral profiles of alfalfa

There are two regions relating to lipid profiles of samples in MIR spectrum, carbonyl C=O ester stretching region (ca. 1710-1781 cm^{-1}) and (a)symmetric CH_2 and CH_3 stretching region (ASCC, ca. 3000-2761 cm^{-1}) (Abeysekara et al. 2013; Xin and Yu 2014; Xin et al. 2014). As shown in Table 3.2.3, there were no spectral differences in carbonyl C=O ester region, as neither CCO nor CCOA showed significant differences between alfalfa populations. As to ASCC region, transformed alfalfa had higher SyCH2 and AsCH2 heights and ASCCA compared with WT ($P<0.001$). There were no significant differences were detected in SyCH3 between alfalfa genotypes; however, HB12i had higher AsyCH3 peak compared with WT alfalfa. Interestingly, similar increases of SyCH2, AsCH2 and ASCCA were found in early-flowering alfalfa compared with early- and late-bud stage (Yari et al. 2017). As nutrient values of alfalfa decrease after flowering, these spectral results might indicate lower nutrient availability of HB12i population.

Figure 3.2.5 shows HCA dendrograms and PCA plots of lipid-related IR regions. All alfalfa populations were indistinguishable from each other in CCO region by neither HCA nor PCA. However, in ASCC region, WT was separated from its transgenic counterparts in both HCA and PCA. In PCA plots, WT ellipse was only little overlapped with TT8i ellipse and totally separated from HB12i ellipse. PC1 of CCO and AASC regions explained 97.3% and 85.5% of total population variances.

Table 3.2.3 Effects of silencing *TT8* and *HB12* genes on lipid-related structural parameters of alfalfa: Comparison of gene transformed with wild type.

Items [1]	WT	Transgenic Alfalfa		SEM [2]	P value	Contrast [3]
		HB12i	TT8i			W vs. G
Carbonyl C=O ester height and area profiles						
CCO	0.059	0.058	0.061	0.0026	0.661	0.772
CCOA	1.637	1.671	1.820	0.0898	0.360	0.382
Symmetric and asymmetric of CH2 and CH3 profiles						
SyCH2	0.098b	0.132a	0.122a	0.0044	<0.001	<0.001
SyCH3	0.058	0.062	0.062	0.0013	0.085	0.033
AsCH2	0.178b	0.237a	0.217a	0.0071	<0.001	<0.001
AsCH3	0.060b	0.066a	0.064ab	0.0015	0.020	0.023
ASCCA	11.442b	13.334a	12.852a	0.3195	0.002	0.001

[1] CCO, carbonyl C=O (centers at ca. 1733 cm^{-1}); CCOA, peak area of CCO region (baseline ca. 1781-1710 cm^{-1}). SyCH2, symmetric CH_2 (ca. 2850 cm^{-1}); SyCH3, symmetric CH_3 (ca. 2872 cm^{-1}); AsCH2, asymmetric CH_2 (ca. 2920 cm^{-1}); AsCH3, asymmetric CH_3 (ca. 2955 cm^{-1}); ASCCA, peak area of asymmetric and symmetric CH_2 and CH_3 (baseline ca. 3000-2761 cm^{-1}).
[2] SEM, standard error of mean; Values with same letter in each row are not significantly different at P>0.05.
[3] Contrast between WT and transgenic alfalfa.

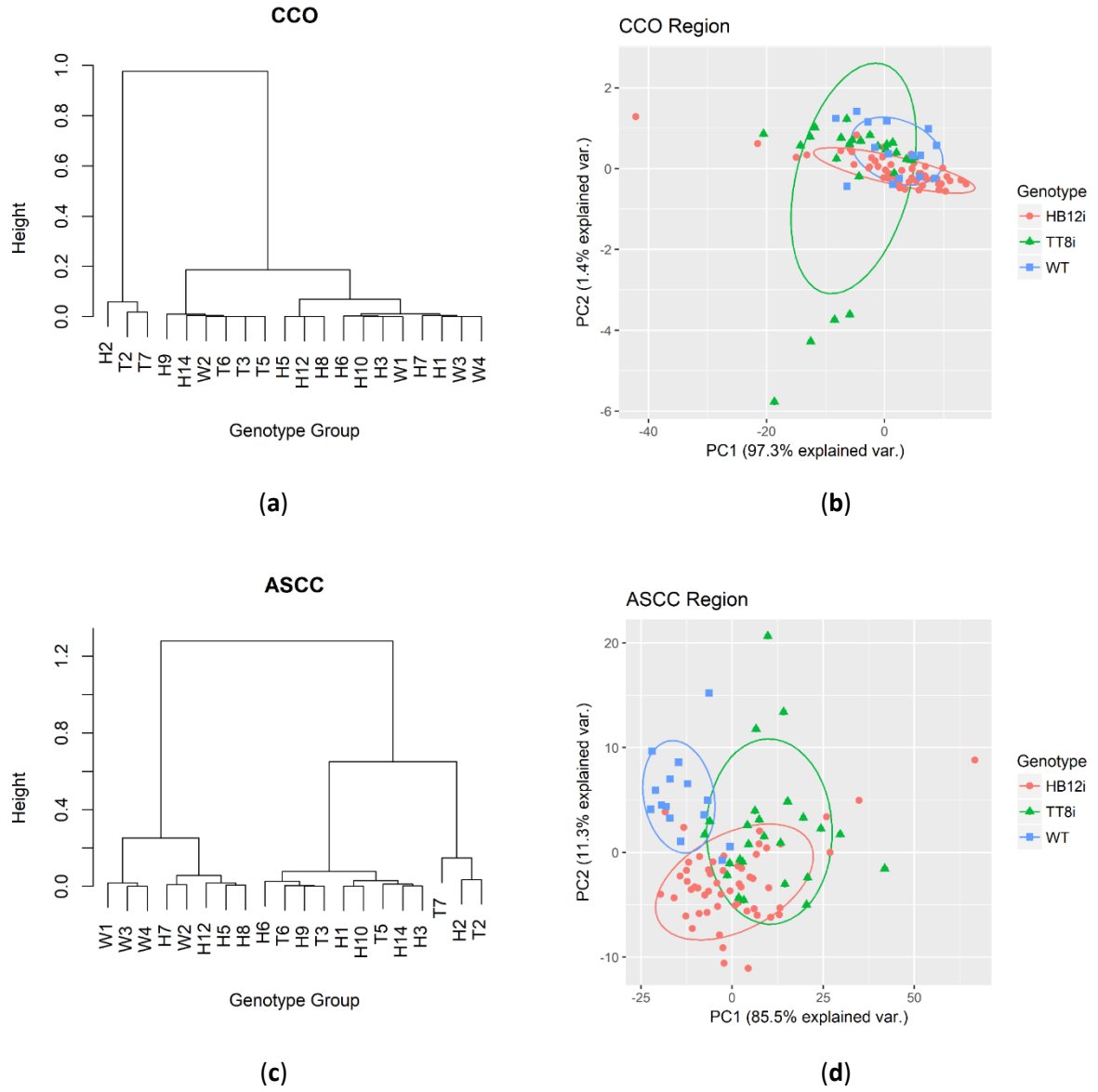

Figure 3.2.5 HCA dendrograms and PCA plots of lipid-related regions of transgenic and WT control.

CCO, carbonyl C=O region (ca. 1710-1781 cm^{-1}); ASCC, asymmetric and symmetric CH2 and CH3 region (ca 3000-2761 cm^{-1}). (**a**) HCA dendrogram of CCO region; (**b**) PCA plot of CCO region; (**c**) HCA dendrogram of ASCC region; (**b**) PCA plot of ASCC region.

3.2.3.4 Multivariate analysis in fingerprint and whole region

HCA dendrograms and PCA plots of fingerprint region and whole mid-IR region transgenic and WT control are shown in Figure 3.2.6. As shown in the figure, both HCA and PCA clustered WT into a separated group in fingerprint and whole mid-IR regions. In HCA

dendrograms, WT was separated from transgenic populations at the heights over 15 and 25 in fingerprint region and whole mid-IR region, respectively. In PCA plots of fingerprint region, PC1 and PC2 explained 72.7% and 16.2% of population variations, respectively. In whole mid-IR region, PCA results showed that PC1 and PC2 explained 61.7% and 18.5% variations, respectively.

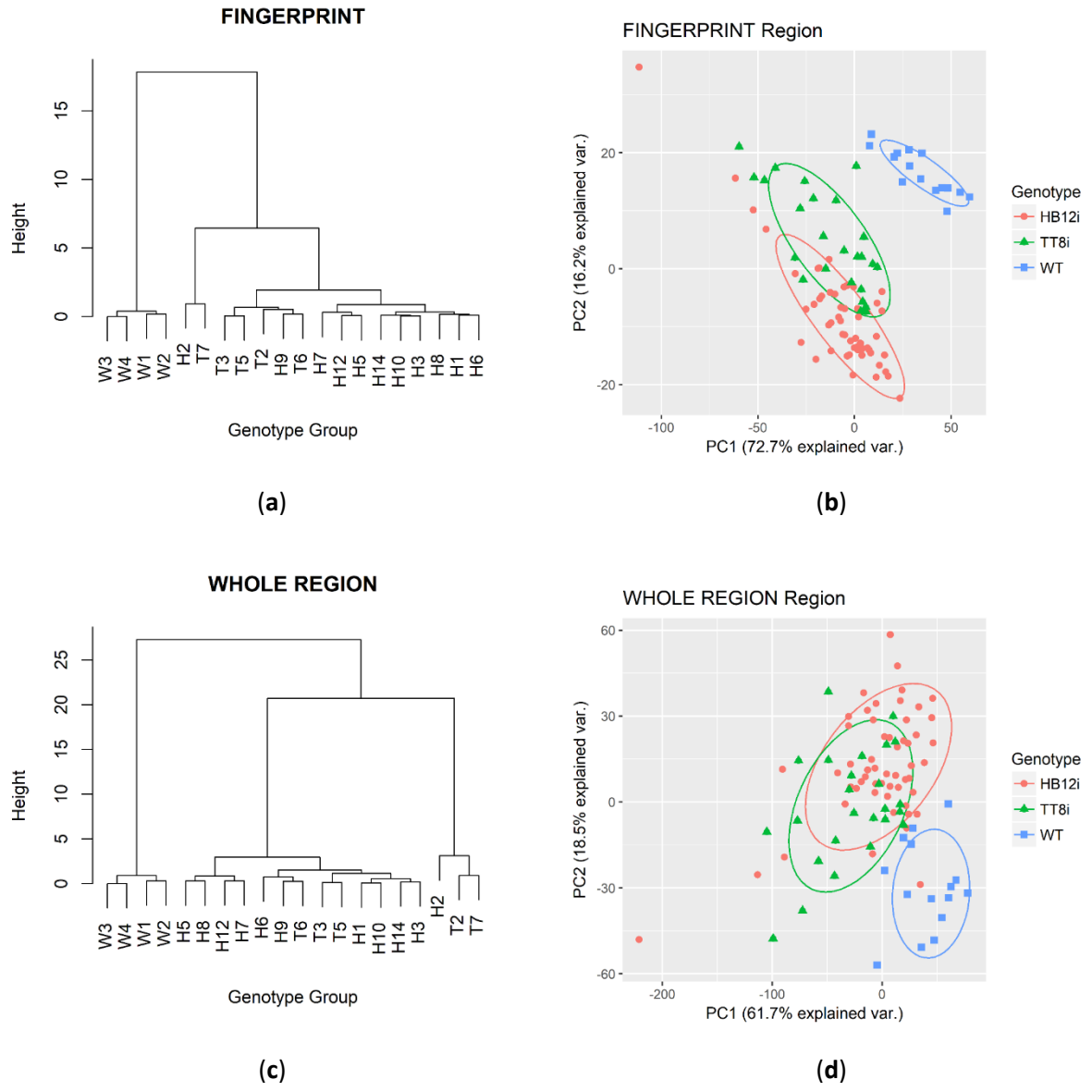

Figure 3.2.6 HCA dendrograms and PCA plots of whole region and fingerprint region of transgenic and WT control.

Baseline of fingerprint region and whole region are ca. 1800-800 cm^{-1} and ca. 4000-700 cm^{-1}, respectively. (**a**) HCA dendrogram of fingerprint region; (**b**) PCA plot of fingerprint region; (**c**) HCA dendrogram of whole IR region; (**b**) PCA plot of whole IR region.

3.2.4 Conclusions

In conclusion, genetic transformation of alfalfa with TT8 RNAi and HB12 RNAi affected molecular spectral structures. Silencing of *TT8* and *HB12* genes affected both amide and carbohydrate intrinsic molecular structures in alfalfa, and such structural changes could be detected by ATR-FTIR spectroscopy. Both HCA and PCA multivariate analyses separated from transformed alfalfa in all CHO regions and ASCC region, while all genotypes were successively separated in amide region.

3.3 Effects of silencing *TT8* and *HB12* genes on molecular structure and chemical mapping of alfalfa leaves by synchrotron based FTIR spectroscopy

Abstract: The objectives of this study were to determine the molecular structural changes and chemical mapping of alfalfa leaves induced by silencing of *TT8* and *HB12* genes in alfalfa. Five alfalfa leaves from each alfalfa genotype were selected for FTIR spectra collection and chemical mapping with synchrotron-based FTIR spectroscopy (SR-IMS). Peak heights and areas of regions same as Chapter 3.2 were analyzed. For chemical mapping, peak areas of previous regions were mapped for each sample. Results showed there were no differences between alfalfa genotypes in carbohydrate, amide and ASCC regions ($P>0.05$). However, transformed alfalfa had higher peak height and area of CCO, compared with WT ($P<0.05$). Chemical maps for carbohydrate, amide and lipid-related regions were successfully obtained. HB12i had higher TC and STC intensity in the mesophyll and epidermises, whereas TT8i and WT only had higher intensity in their epidermises. All alfalfa genotypes had higher intensity of amide and ASCC area in their mesophylls. Interestingly, localization of amide was opposite to TC and STC. In addition, higher intensity of CCO area was observed in HB12i cell contents, which not found in TT8i and WT. However, HB12i had lower lignin intensity in leaf cells, while higher intensity of lignin could be found in mesophylls of TT8i and WT. In conclusion, silencing of *HB12* gene in alfalfa increased carbonyl compound in leaf tissues, which implies higher lipid deposition in the leaf. Moreover, amide compounds were located mainly in leaf mesophyll area, while carbohydrates largely lied in the epidermis tissue. Furthermore, Chemical mapping with SR-IMS is a good tool to localize chemical compounds in plant leaf tissue.

3.3.1 Introduction

Alfalfa (*Medicago* sativa) is one of the most widely cultivated legume forage crops owing to its high forage quality and good palatability and adaptability (Lei et al. 2017). However, like any other legumes, alfalfa contains relatively high lignin content, which hinders the degradation of other nutrients and thereby limits its usage (Lei et al. 2017). Genetic modifications towards lignin reduction in alfalfa have been reported with downregulations of lignin synthesis genes (Baucher et al. 1999; Guo et al. 2001a; Pu et al. 2009; Getachew et al. 2011). And there was one commercial low-lignin alfalfa line released by Monsanto® been approved in many countries (Canada 2015). Apart from biosynthesis genes, regulation of transcriptional factors might also affect lignin deposition in plants. Recent observations showed that two transcriptional factors: Transparent Testa 8 (TT8) and Homeobox 12 (HB12), might be positively correlated to lignin contents (Li et al. 2015). Therefore, expression levels of these two transcriptional factors were downregulated in alfalfa via RNAi technique in attempts to decrease lignin contents. To our surprise, chemical analysis shows that silencing of *HB12* resulted in higher lignin content (Chapter 3.1) (Lei et al. 2018b). However, other nutritional profiles were also influenced by such genetic modifications. Transgenic alfalfa genotypes showed enhanced fiber content and lower protein content, which could be useful for grazing purpose.

Nutritive values of forages are not only related to their chemical composition, but also depend on their inherent molecular structures. Barley samples with similar protein composition degraded differently in the rumen due to structural differences (Yu 2007). Therefore, to fully evaluate the nutritive value of transgenic alfalfa, molecular studies were also conducted to explore the genetic effects on intrinsic molecular structures of alfalfa. Our previous study evaluated the structural features of homogenously ground alfalfa samples with ATR-FTIR spectroscopy (Lei et al. 2018a). Silencing of *TT8* and *HB12* genes increased total carbohydrate (TC) and structural

carbohydrate (STC) and asymmetric and symmetric CH_2 and CH_3 (ASCC) parameters of alfalfa (Lei et al. 2018a). However, the spectral analysis was conducted with ground samples with no details in alfalfa leaves and stems in terms of their molecular structures. Plant leaves are the main site for photosynthesis, which involves a chain of biochemical reactions to capture solar energy and convert it to carbohydrate (Tanaka and Makino 2009). Alfalfa leaves accounted for about half of plant biomass at vegetative stage (McCaslin et al. 2015) and thereby have critical contributions to alfalfa nutritive values. Therefore, this study aimed to explore the effects of silencing *TT8* and *HB12* genes on the molecular structures of alfalfa leaves with synchrotron-based FTIR microspectroscopy (SR-IMS).

The SR-IMS is a rapid, non-invasive and non-destructive bioanalytical technique and is capable of exploring functional groups within plant samples at the cellular and subcellular levels (Yang and Yu 2017). This technique utilizes synchrotron light, which is 1000 times brighter than conventional light, to detect structural information of biological samples with higher accuracy and small effective source size (Liu and Yu 2016). Moreover, SR-IMS technique is able to provide information on chemical localizations through chemical mapping analysis (Yu et al. 2003c, 2019; Miller and Dumas 2006). Therefore, this study also attempted to explore the effects of silencing *TT8* and *HB12* genes on chemical localizations in alfalfa leaves.

3.3.2 Materials and Methods

3.3.2.1 Alfalfa leaf sample and FTIR microspectroscopic window preparation

Freeze-dried leaves of HB12i, TT8i and WT alfalfa were collected for cross section. Cross section and window preparation were conducted at Western College of Veterinary Medicine, University of Saskatchewan. Alfalfa leaves were embedded with paraffin at -20 ºC in a microtome and then cut into 6 μm thickness cross sections. Paraffin was then removed with xylene and cross

section of alfalfa leaves were immediately transferred to BaF_2 windows (13 × 1 mm disk; Part 015-3015, Spectral systems) for synchrotron FTIR spectra collection and chemical mapping. There were five leave windows prepared for each genotype of alfalfa.

3.3.2.2 Synchrotron light source and FTIR microspectroscopy

The spectra collection and chemical mapping were carried out at the Advanced Light Source in Lawrence Berkeley National Laboratory (LBNL), U.S. Department of Energy (DOE, Berkeley, CA). The spectroscopic images were recorded with a Nicolet Magna IR-760 spectroscopy (Thermo Nicolet) equipped with a Continuum IR microscope (Spectra Tech), a KBr Beamsplitter and a mercury cadmium telluride (MCT/A) detector. The spectrometer was related to a synchrotron light beam with an energy level of 500 mA.

3.3.2.3 Spectra collection and chemical mapping

The spectra were collected in the mid-IR range (4000-750 cm^{-1}) with 64 scans at a resolution of 8 cm^{-1}. Aperture size was set at ca. 10 × 10 μm and collection was set as absorbance mode. Visible images of alfalfa sample were obtained with a charge-coupled device camera. Before sample spectra collection, a background spectrum was collected from a blank area free of sample. For each sample window, 15 to 20 spectra were collected at spots avoiding the follicle facilitated by visible image (Figure 3.3.1). Spectral parameters of peak heights and peak areas were analyzed with the same methods as Chapter 3.2 (Lei et al. 2018a). Spectral regions of interest were total carbohydrate (TC), cellulosic compounds (CEC), structural carbohydrate (STC), amide, carbonyl C=O (CCO) and asymmetric and symmetric CH_2 and CH_3 (ASCC) region.

As for chemical mapping, a spatial area of 130 × 170 μm from one randomly selected sample window were mapped for each sample. Chemical mapping was performed with OMNIC 7.3 software (Spectra Tech). Frequency between 2200-1950 cm^{-1} was straightened because of one

noise peak appeared in this region. Then, spectra were automatic baseline corrected and scale normalized to eliminate the effect of sample sickness. Chemical mapping of functional groups was focused on TC, STC, CEC, amide, CCO, ASCC and lignin regions.

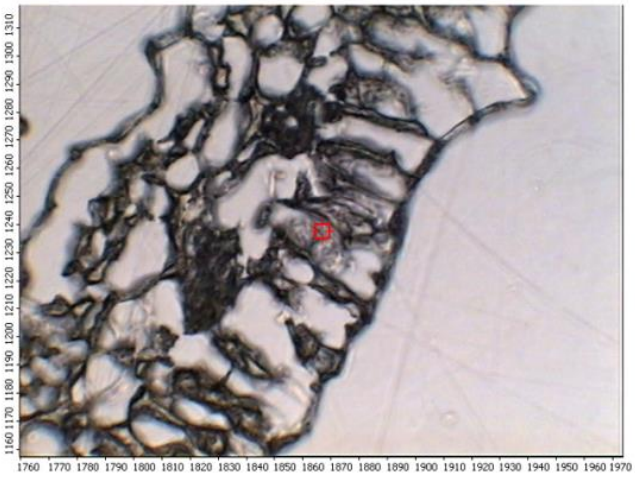

Figure 3.3.1 Example of visible image of alfalfa leave samples. Red square cursor shows the spot of spectra collection.

3.3.2.4 Statistical analysis

Procedure MIXED of SAS 9.4 software (SAS Institute, Inc., Cary, NC, USA) was used to analyze univariate variables of spectral parameters. The model used was same as Chapter 3.2, which was: $Y_{ijk} = u + geno_i + sub(geno)_j + \varepsilon_{ijk}$, where Y_{ijk} was the independent variable; μ_i was the mean of all samples; $geno_i$ was the fixed genotype effect; $sub(geno)_j$ as a random effect; ε_{ijk} was the random error. Prior to variance analysis, a SAS macro with the same model was used to remove all outliers with a criterion of Studentized Residual greater than 2.5. Contrast statement was used to compare WT with transgenic alfalfa. The Tukey-Kramer method was used for multi-comparison among genotypes. A SAS Macro called "pdmix800" (Saxton 1998) was used to denote the letter for each treatment mean at the significance level of 0.05. Proc UNIVARIATE with Normal and Plot options was used to test the normality of the residue of each variable. Significance level was set as $P<0.05$ and trend was set at $0.05<P<0.10$.

3.3.3 Results and Discussion

3.3.3.1 Effects of silencing TT8 and HB12 genes on carbohydrate spectral parameters of alfalfa leaves with synchrotron based FTIR spectroscopy

Carbohydrate structural parameters of leaves cross sections of transformed and WT alfalfa are shown in Table 3.3.1. There were no significant differences between alfalfa genotypes in terms of carbohydrate spectral parameters ($P>0.05$). The contrasting results showed that transformed alfalfa genotypes tended to have lower TC4 compared with WT alfalfa ($P<0.1$). Compared with carbohydrate parameters of homogenous samples in Chapter 3.2, peak heights and areas for TC and STC regions were dramatically lower for alfalfa leaves.

In addition, carbohydrate parameters of alfalfa leaves in this project were comparable to those in the second project (Chapter 4.3). This might be caused by the differences in structures and chemical compositions of homogenous alfalfa samples and alfalfa leaves. A previous study showed that alfalfa leaves contain more protein and less fiber compared with alfalfa stems (Marković et al. 2012). Moreover, alfalfa stems account for about half of alfalfa biomass at vegetative stage of alfalfa (McCaslin et al. 2015). In addition, our correlation study showed that TC and STC parameters were negatively correlated with CP and starch, but positively correlated with fiber and total carbohydrate (Chapter 5.1). Therefore, these spectral differences suggested alfalfa leaves might have higher CP and starch, but lower fiber compared with homogenous samples, which was in line the previous study (Marković et al. 2012).

Table 3.3.1 Effects of silencing *TT8* and *HB12* genes on carbohydrate structural parameters of leaves: Comparison of gene transformed with wild type.

Items[1]	WT	Transformed Alfalfa		SEM [2]	P value	Contrast [3]
		HB12i	TT8i			W vs G
Total Carbohydrate Peaks and Area						
TC1	0.275	0.204	0.204	0.0313	0.251	0.104
TC2	0.195	0.174	0.174	0.0224	0.767	0.477
TC3	0.128	0.124	0.120	0.0143	0.933	0.759
TC4	0.098	0.067	0.070	0.0107	0.146	0.056
TCA	30.977	25.775	25.499	3.5135	0.511	0.258
Cellulosic Compounds Peak and Area						
CEC	0.070	0.064	0.062	0.0037	0.297	0.139
CECA	3.474	3.259	3.049	0.1425	0.159	0.104
Structure Carbohydrate Peaks and Area						
STC1	0.068	0.064	0.060	0.0072	0.752	0.539
STC2	0.038	0.041	0.040	0.0062	0.942	0.768
STC3	0.057	0.058	0.058	0.0054	0.974	0.834
STC4	0.056	0.061	0.060	0.0059	0.785	0.502
STCA	12.734	12.642	11.619	1.3917	0.817	0.740
Lignin Peak						
Lignin	0.037	0.031	0.032	0.0035	0.502	0.274

[1] TC1-TC4, four major peaks at ca. 1026 (TC1) 1074 (TC2), 1104 (TC3) and 1149 (TC4) cm^{-1} in TC region, respectively; TCA, peak area of TC region; CEC, cellulosic compounds (ca. 1237 cm^{-1}); CECA, peak area of CEC region; STC1-STC4, four major peaks at ca. 1317 (STC1), 1370 (STC2), 1397 (STC3) and 1453 (STC4) cm^{-1}, respectively.

[2] SEM, standard error of mean. Values with same letter in each row are not significantly different at $P>0.05$.

[3] W vs G, contrast between WT and genetic modified alfalfa.

3.3.3.2 Effects of silencing TT8 and HB12 genes on amide and lipid-related spectral parameters of alfalfa leaves with synchrotron based FTIR spectroscopy

Table 3.3.2 shows amide and lipid-related structural parameters of leaf cross sections of transformed and WT alfalfa. There were no significant differences between alfalfa genotypes in amide and ASCC peak heights and areas ($P>0.05$). In contrast, HB12i alfalfa had significantly higher CCO peak height compared with WT ($P<0.05$). Moreover, both TT8i and HB12i alfalfa had higher CCOA compared with WT ($P<0.01$). Study on homogenous samples showed no significant differences between alfalfa genotypes in terms of CCO parameters (Chapter 3.2) (Lei et al. 2018a). The CCO is the carbonyl C=O ester band that centers at 1740 cm^{-1}, which is reported to be more likely aldehyde, ester and carboxylic acids (Coates 2006; Fahey et al. 2017). This result suggested that transformed alfalfa might have higher contents of these chemical compounds in leaves compared with WT alfalfa.

Compared with homogenous alfalfa samples in Chapter 3.2, alfalfa leaves had higher heights of Amide I, α-helix, β-sheet, CCO and ASCC peaks, but lower CCOA. The ASCC parameters were about double the values, while amide areas of alfalfa leaves were equivalent to those homogenous samples in Chapter 3.2. The higher values of ASCC parameters were consistent with the second project (Chapter 4.3). Our correlation study showed that ASCC peak heights and ASCCA were negatively correlated with fiber and positively correlated with sugar of alfalfa, although the correlations were weak. This might explain, to some extent, the differences between homogenous samples and alfalfa leaves in amide and ASCC regions.

Table 3.3.2 Effects of silencing *TT8* and *HB12* genes on amide and lipid-related structural parameters of alfalfa leaves: Comparison of gene transformed with wild type.

Items [1]	WT	Transformed Alfalfa		SEM [2]	P value	Contrast [3]
		HB12i	TT8i			W vs G
Amide Peak Heights and Areas						
Amide I	0.532	0.467	0.435	0.0397	0.277	0.139
Amide II	0.301	0.276	0.268	0.0236	0.630	0.364
α-sheet	0.490	0.445	0.412	0.0366	0.373	0.215
β-helix	0.505	0.450	0.415	0.0401	0.333	0.183
Amide Area	59.256	55.975	52.268	4.0255	0.501	0.337
Amide I Area	39.861	37.731	34.677	2.6603	0.417	0.302
Amide II Area	19.395	18.083	17.592	1.4558	0.690	0.418
Carbonyl C=O (CCO) Peak Height and Area						
CCO	0.021b	0.038a	0.036ab	0.0042	0.043	0.014
CCOA	0.458b	1.011a	1.024a	0.1023	0.007	0.001
Asymmetric and symmetric CH2 and CH3 (ASCC) Peak Heights and Area						
SyCH2	0.214	0.216	0.230	0.0267	0.901	0.809
SyCH3	0.113	0.120	0.114	0.0087	0.828	0.712
AsCH2	0.356	0.357	0.357	0.0407	1.000	0.982
AsCH3	0.125	0.124	0.111	0.0102	0.570	0.585
ASCCA	23.427	23.754	23.313	2.1320	0.988	0.969

[1] CCO, carbonyl C=O; CCOA, carbonyl C=O area; SyCH2, symmetric CH2 (ca. 2850 cm^{-1}); SyCH3, symmetric CH3 (ca. 2872 cm^{-1}); AsCH2, asymmetric CH2 (ca. 2920 cm^{-1}); AsCH3, asymmetric CH3 (ca. 2955 cm^{-1}); ASCCA, peak area of asymmetric and symmetric CH2 and CH3 (baseline ca. 3000–2761 cm^{-1}).
[2] SEM, standard error of mean. Values with same letter in each row are not significantly different at P>0.05.
[3] Contrast between wild type (WT) and transgenic alfalfa;

3.3.3.3 Effects of silencing TT8 and HB12 genes on chemical mapping of alfalfa leaves with synchrotron based FTIR spectroscopy

Visible images and chemical mappings of HB12i, TT8i and WT alfalfa leaves are shown in Figure 3.3.2, Figure 3.3.3 and Figure 3.3.4, respectively. In general, amide had the highest intensity in alfalfa leaves and were mainly deposited in the mesophyll areas of alfalfa leaves. The ASCC region had the second higher intensity and were also located in mesophyll area mainly. In contrast, carbohydrate regions, like TC and STC regions, had comparably lower intensity. For carbohydrate functional groups, HB12i had higher TC and STC intensity compared with TT8i and WT. Moreover, TC and STC functional groups in HB12i were distributed both in the mesophyll and epidermises, whereas in TT8i and WT they were only observed in epidermises of alfalfa leaves. As for CEC region, it could be found both in mesophyll areas and epidermises and was significantly lower in WT alfalfa leaves compared with transformed alfalfa.

All alfalfa genotypes had higher intensity of amide and ASCC area in their mesophylls. The amide region was reported to be closely related to proteins and the first peak of which was used to characterize protein secondary structures (Yu 2005a). Around 75% of leaf proteins are concentrated in cell mesophylls and about 80% of which are stored in chloroplasts where photosynthesis take place (Fiorentini and Galoppini 1983). The HB12i had the highest amide intensity, followed by TT8i with WT being the lowest. In addition, high intensity of CCO area was observed in HB12i cell contents, which were nearly neglectable in TT8i alfalfa. In addition, HB12i had higher ASCC intensity compared with TT8i and WT alfalfa leaves. As for lignin intensity, HB12i had the lowest lignin intensity, which was almost neglectable in leaf cells. In contrast, TT8i had several high-intensity spots of lignin in the mesophyll area, but the intensity was still lower than WT alfalfa.

Lignin polymers start to deposit in secondary cell wall during cell wall maturation and keep the stem strength of plants (Boerjan et al. 2003). Moreover, it makes cell wall waterproof and protects cell wall from microbial degradation (Boerjan et al. 2003; Vanholme et al. 2010). Our chemical analysis shows HB12i had higher lignin contents compared with other genotypes, which were opposite to lignin deposition in alfalfa leaves. This discrepancy suggested that HB12i might either have higher stem ratio or higher lignin deposition in stems, compared with other genotypes. Yu et al. (2009) analyzed protein structural features with synchrotron based FTIR technique between *Lc*-transgenic alfalfa and non-transgenic (WT) control and found transgenic alfalfa had lower alpha helix and beta sheet structures compared with WT alfalfa. However, there were no chemical mappings reported regarding to distinguish chemical deposition in *Lc*-transgenic alfalfa. Previous studies have reported chemical images of corn grains (Yu et al. 2004b), feather (Yu et al. 2004a) and plant tissues (Yu et al. 2003c, 2019) and revealed the intrinsic structural features of these ingredients. To our knowledge, this study was the first to illustrate the effects of genetic modification on chemical mappings of alfalfa leaves.

3.3.4 Conclusion

In conclusion, silencing of *HB12* gene in alfalfa increased carbonyl compounds in leaf tissues, which implies higher lipid deposition in leaves of HB12i alfalfa. Moreover, amide compounds were located mainly in mesophyll of leaves, whereas carbohydrates were largely concentrated in epidermis tissue. Furthermore, chemical mapping with synchrotron based FTIR spectroscopy is a good tool to localize chemical compounds in plant leaf tissue.

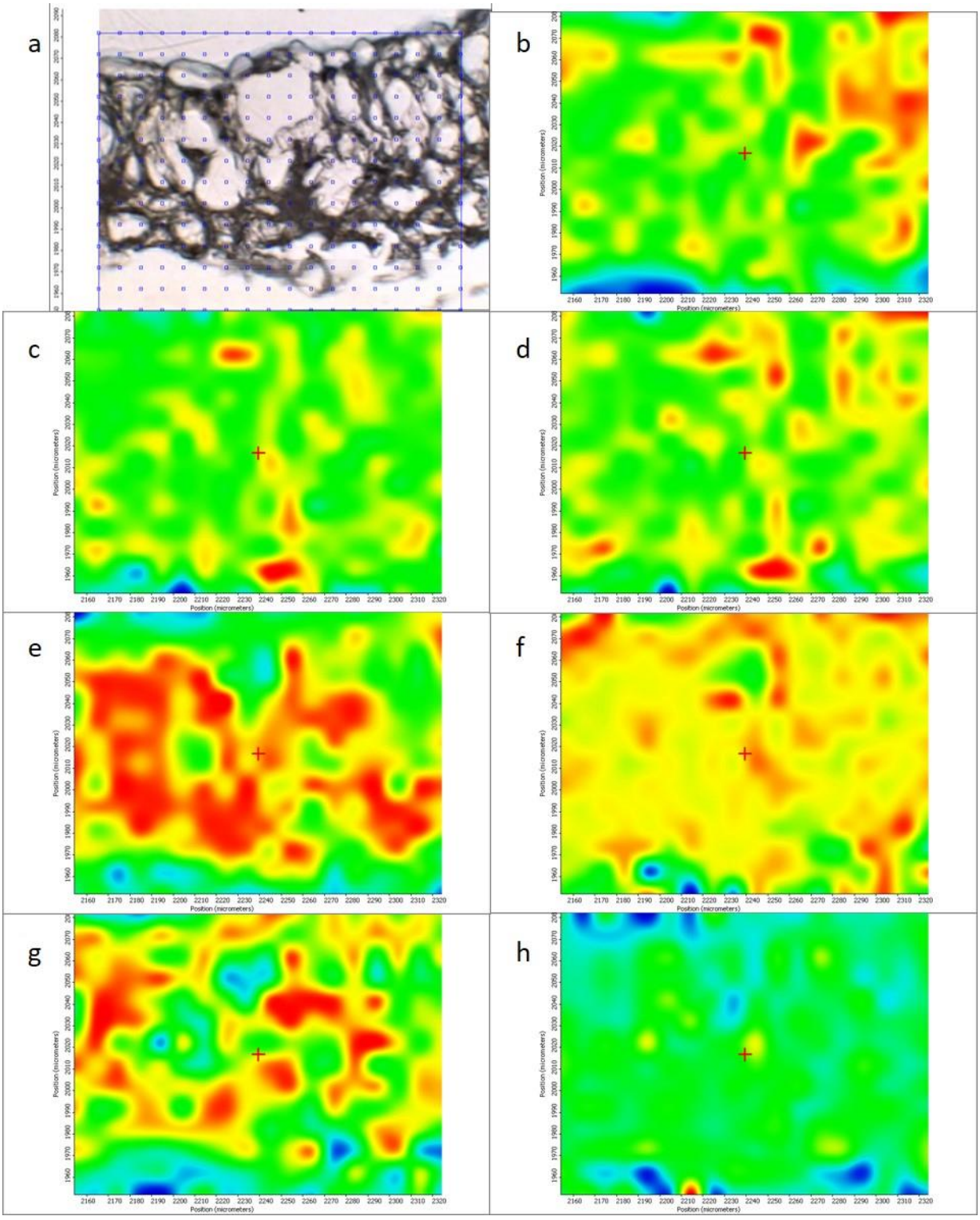

Figure 3.3.2 Chemical Mapping of HB12i alfalfa leaves in nutritional related spectral regions.

Figures are original visible image (a), and chemical group maps of total carbohydrate (TC, b), cellulosic compounds (CEC, c), structural carbohydrate (STC, d), amide (e), carbonyl C=O (CCO, f), asymmetric and symmetric CH2 and CH3 (ASCC, g) and lignin (h) regions.

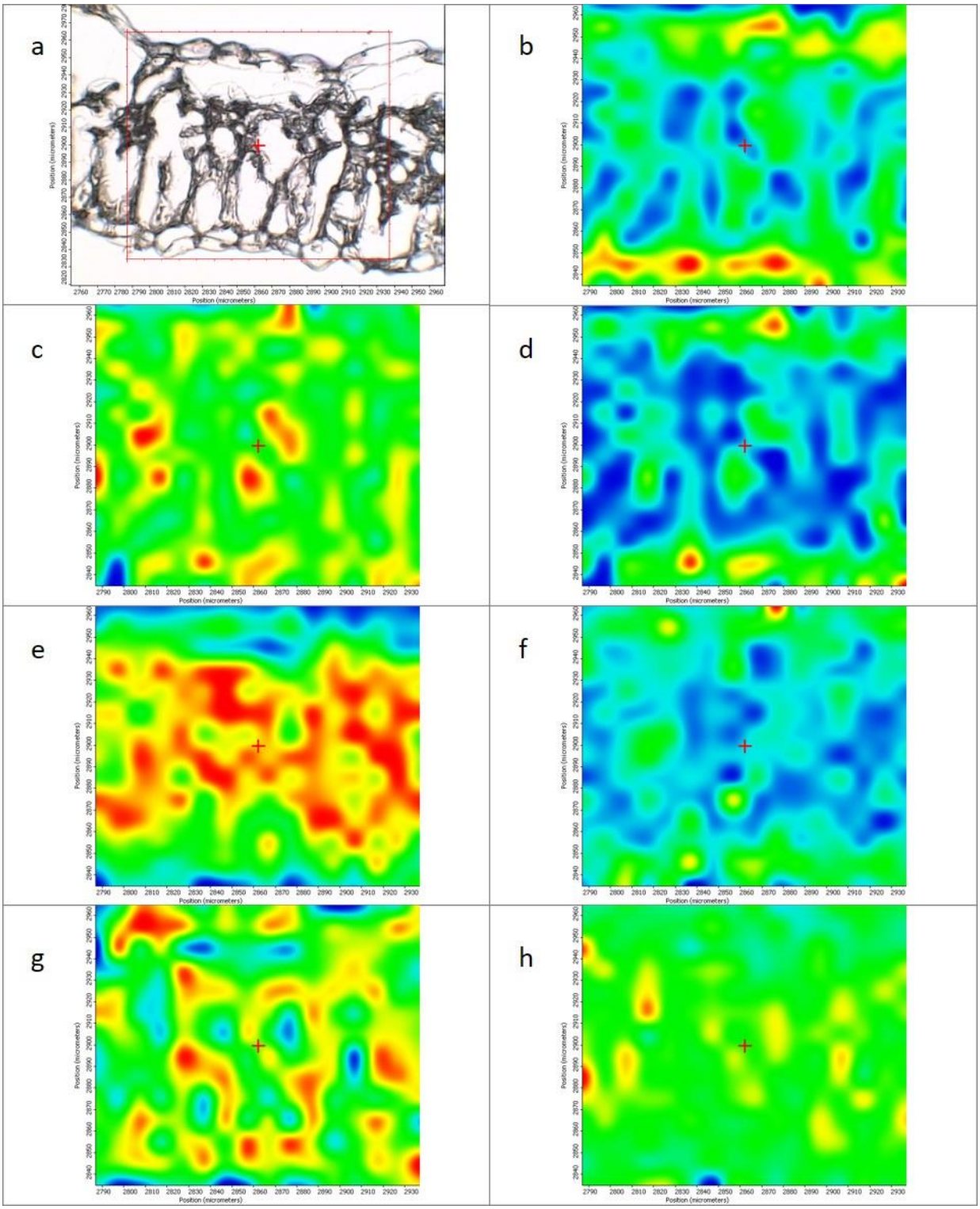

Figure 3.3.3 Chemical Mapping of TT8i alfalfa leaves in nutritional related spectral regions.

Figures are original visible image (a), and chemical group maps of total carbohydrate (TC, b), cellulosic compounds (CEC, c), structural carbohydrate (STC, d), amide (e), carbonyl C=O (CCO, f), asymmetric and symmetric CH2 and CH3 (ASCC, g) and lignin (h) regions.

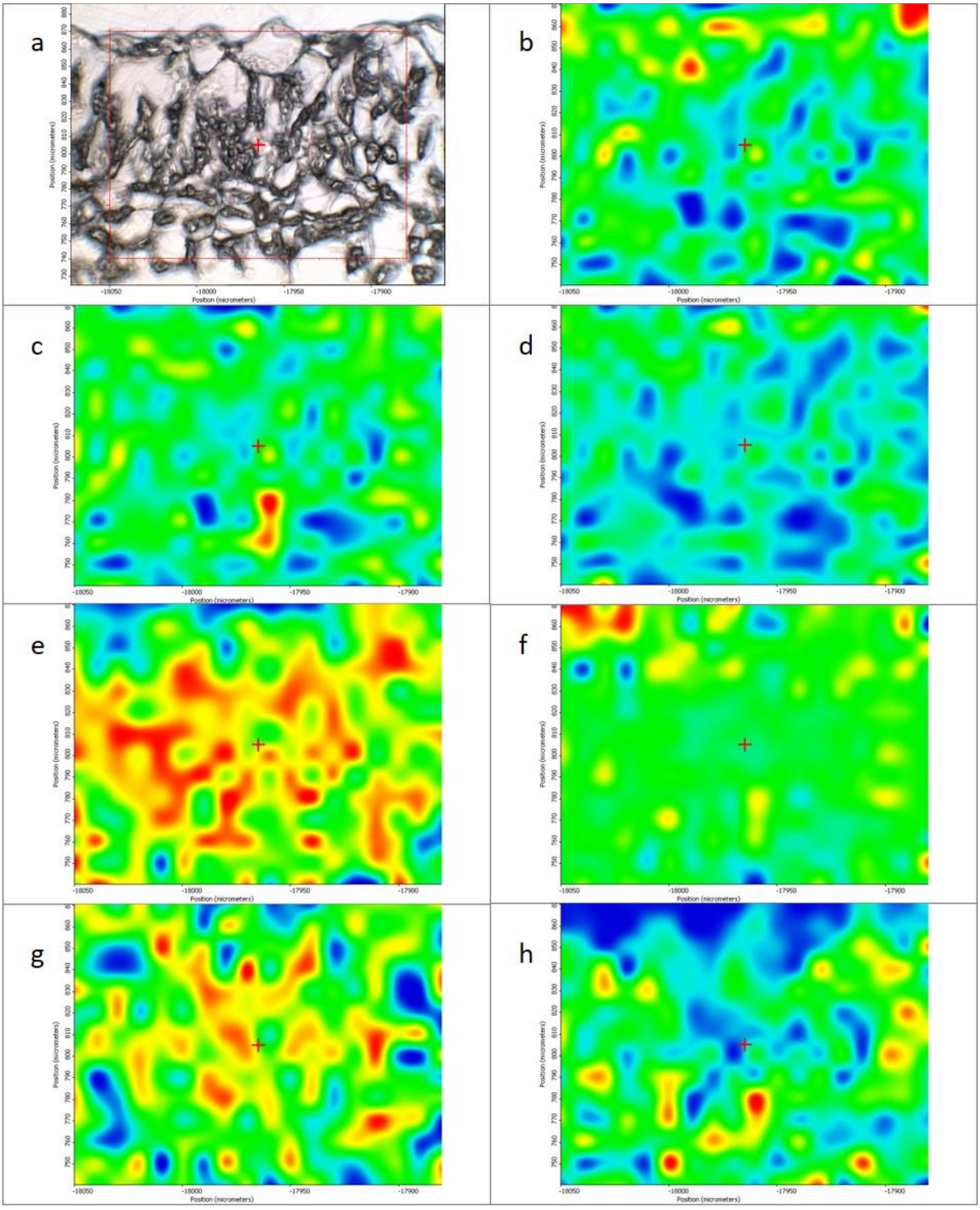

Figure 3.3.4 Chemical Mapping of WT alfalfa leaves in nutritional related spectral regions.

Figures are original visible image (a), and chemical group maps of total carbohydrate (TC, b), cellulosic compounds (CEC, c), structural carbohydrate (STC, d), amide (e), carbonyl C=O (CCO, f), asymmetric and symmetric CH_2 and CH_3 (ASCC, g) and lignin (h) regions.

3.4 Effects of silencing *TT8* and *HB12* genes on *in vitro* fermentation characteristics of alfalfa

Abstract: This study was conducted to evaluate the effects of silencing of *TT8* and *HB12* genes on *in vitro* fermentation characteristics of alfalfa. Alfalfa samples were incubated in vials with rumen fluid and buffer for 0, 2, 4, 8, 12, 24, 48 h. Gas production were measured at each time point, while NH3 and VFA production were measured at 4, 12, 24 and 48 h. Production kinetics were determined for gas, acetate, propionate and total VFA. Moreover, DM and NDF degradation and kinetics were determined. Results showed that HB12i had lower gas, VFA and ammonia productions compared with TT8i and WT, and both transformed alfalfa plants had lower DM degradation than WT ($P<0.05$). In addition, TT8i had higher ammonia production at 48 h of fermentation compared with HB12i and WT ($P<0.05$). Moreover, transformed alfalfa had lower propionate, butyrate and long-chain VFA in comparison with WT ($P<0.05$). There were no differences in NDF degradation and degradational kinetics ($P>0.05$). In conclusion, silencing *HB12* gene significantly decreased ruminal DM degradation, gas, ammonia and VFA productions of alfalfa, whereas silencing *TT8* gene decreased DM degradation and long-chain VFA production.

Gas production data of this chapter has been published. Lei, Y., Hannoufa, A., Prates, L.L., Shi, H., Wang, Y., Biligetu, B., Christensen, D., and Yu, P. 2018. Effects of TT8 and HB12 Silencing on the Relations between the Molecular Structures of Alfalfa (Medicago sativa) Plants and Their Nutritional Profiles and In Vitro Gas Production. J. Agric. Food Chem. 66: 5602–5611. doi:10.1021/acs.jafc.8b01573.

DM and NDF degradation and ammonia production data of this chapter has been accepted in Journal of the Science of Food and Agriculture.

3.4.1 Introduction

Gene transformation has been a powerful tool in plant breeding by regulating gene expressions or introducing new genes to plants. Target genes could be either synthetic genes or regulating genes that function in the pathway for desired traits. For forage crops, efforts have been making towards nutritional and adaptive improvements for decades (Budak and Spangenberg 2015). As the "queen of forages" and a model plant of legume, alfalfa (*Medicago sativa*) has been a popular forage species in plant genetic research (Maureira and Osborn 2004; Li and Brummer 2012). Like any other legume plants, alfalfa contains relatively high lignin content that limits its utilization (Soest 1994; Lei et al. 2018b). Researches have been focusing on the reduction of lignin with regulating genes in lignin biosynthesis pathway (Boerjan et al. 2003). Reports of lignin reduction have been made with single- or dual- downregulations of several synthetic genes, such as HCT and C3H(Tong et al. 2015), COMT and CCOMT (Guo et al. 2001a), CAD (Fu et al. 2011) et al., which control crucial steps in lignin biosynthesis.

Observations from canola (*Brassica napus*) suggested that other regulating genes in phenylpropanoid pathway which are not directly related to lignin synthesis might also have an influence on lignin content (Li et al. 2015). *Brassica napus* with low lignin content was found to have low expressions for two transcriptional factors, *Homeobox 12 (HB12)* and *Transparent Testa 8 (TT8)* that serves in phenylpropanoid pathway (Li et al. 2015). Therefore, downregulation of *HB12* and *TT8* genes were conducted in alfalfa to explore the effects of silencing *HB12* and *TT8* on lignin synthesis and nutritive values of alfalfa. Although lignin content was found higher in *HB12*-silenced genotypes, more changes in chemical compositions and nutrient profiles were observed in transformed alfalfa (Lei et al. 2018b). Such as both transformed alfalfa genotypes had higher degradable fiber and lower soluble true protein, which could lead to better-balanced nutrient synchronization and are less likely to induce rumen bloat. To better understand the nutrient profiles

of transformed alfalfa genotypes, productions of gas, ammonia and volatile fatty acids (VFA) and degradations of dry matter (DM) and neutral detergent fiber (NDF) were determined with *in vitro* fermentation in the current study.

3.4.2 Materials and Methods

3.4.2.1 Alfalfa samples

Alfalfa samples were same as Chapter 3.1. Details in regarding to alfalfa transformation, growth condition and harvest could be found in Chapter 3.1. There were 11 HB12 RNAi (HB12i), 5 TT8 RNAi (TT8i) and 4 wild type (WT) control alfalfa samples used in this study.

3.4.2.2 In vitro gas production fermentation

In vitro gas production fermentation was conducted at Lethbridge Research and Development Center of AAFC (Alberta, Canada), according to the description of Wang et al. (2006) with minor modifications. About 0.3 g of ground samples was placed in ANKOM F57 bags and then incubated with rumen fluid and buffer solution in a 125 mL serum vial. Rumen fluid was collected from three Angus heifers at the Research Center farm after morning feeding. Samples were incubated for 48 h in the incubator at 39 Celsius degrees with two experimental runs. Two replicates of each alfalfa sample and two blanks were withdrawn from the incubator after 2, 4, 8, 12, 24 and 48 h of incubation.

3.4.2.3 Gas, ammonia and VFA productions and kinetics

Gas production was measured at 2, 4, 8, 12, 24, 48 h for all samples available by using a water replacement equipment, according to Wang et al. (2006). For ammonia-N and VFA analyses, 1.6 mL fermentation fluid was sampled at 4, 12, 24 and 48 h and mixed with 0.3 mL of 1% H_2SO_4

and 20% metaphosphoric acid, respectively. VFA and ammonia-N were analyzed with gas chromatograph (model 5890, Hewlett-Packard Lab, Palo Alto, CA, USA).

Production kinetics of gas and VFA were calculated with the non-linear model of $P = a(1 - e^{-c(t-lag)})$ according to the description of Jonker et al. (2012b). In this model, P was gas production at the time of t, a was asymptotic gas production, c was the fractional rate (%/h), t was the incubation hours, and lag was the initial delay of gas production onset. Average production (AP) was calculated as $AP = a \times c \div (2 \times (ln2 + c \times lag))$, according to Jonker et al. (2012b).

3.4.2.4 DM and NDF degradation and kinetics

Degradation kinetics of DM and NDF were determined according to Refat et al. (2017b). The nonlinear model for DM kinetics determination was $R_t = U + (100 - S - U)e^{-K_d(t-T_0)}$, where R_t was the residue after *t* hours of fermentation (%); U was undegradable fractions (%); S was soluble fractions (washable fractions at 0 h, %); K_d was the fractional degradation rate (%/h); t was each time point; T_0 was the lag time of degradation (h). The degradable fraction (D) of DM was calculated as: $D = 100 - S - U$. The nonlinear model for NDF kinetics was: $R_t = U + (100 - U) \times e^{-K_d(t-T_0)}$, and the symbols in this model have the same meanings as the previous one. The degradable fraction (D) was calculated as: $D = 100 - U$. The effective degradation of DM was calculated as: $ED_{DM} = S + D \times K_d/(K_d + K_p)$, while effective degradation of NDF was calculated as $ED_{NDF} = D \times K_d/(K_d + K_p)$. The passage rate ($K_p$) was assumed as 4.5% per hour according to Jonker et al. (2012b).

3.4.2.5 Statistical analysis

The Mixed procedure of SAS 9.4 (SAS Institute, Inc., Cary, NC, USA) was used to analyze data. The model for nutrients degradation was $Y_{ij} = \mu + Trt_{ij} + \varepsilon_{ij}$, where Y_i was the nutritive

variable; μ was the population mean; Trt_i was the genotype effect; ε_i was the random error. The model for gas, ammonia and VFA production data was: $Y_{ij} = \mu + Trt_i + Run_j + \varepsilon_{ij}$, where Run_j was the effect of experiment run. The degree of freedom was estimated with Kenward Roger method. Prior to variance analysis, outliers were detected and removed when Studentized residuals were greater than 2.5. Contrast statement was used to determine the difference between WT and transformed alfalfa, and the Tukey-Kramer method was used for multi-treatment comparison. The "pdmix800" Macro (Saxton 1998) was used to letter-group treatment means. Normality test of residual data was performed using Shapiro Wilk method by using Univariate Procedure with Normal and Plot options. Significance level was set at $\alpha<0.05$.

3.4.3 Results and Discussion

3.4.3.1 Effects of silencing TT8 and HB12 genes on in vitro gas production of alfalfa

Gas production kinetics and accumulative production after hours of fermentation are shown in Table 3.4.1. In the nonlinear model of estimating gas kinetics, *a* is the asymptotic gas production that refers to total gas production. As shown in Table 3.4.1, HB12i had lower asymptotic gas production compared to WT ($P < 0.001$) but was not different from TT8i. There were no significant differences in gas fractional production rate (*c*) and lag time ($P > 0.05$). The average gas production (AP) of HB12i was lower compared to WT and TT8i. Jonker et al. (2012b) determined the gas production kinetics of *Lc*-transgenic and non-transgenic alfalfa, and found that green-*Lc* alfalfa had lower asymptotic and average gas production but equally high production rate, compared to non-transgenic control alfalfa. The asymptotic and average gas production and production rate of the current study were lower than that in Jonker's study (Jonker et al. 2012b), which might be attributed to differences in alfalfa cultivar, harvest time, rumen fluid fluctuation and sample amount used in the fermentation.

Cumulative gas production after hours of fermentation showed that HB12i had lower gas production during the fermentation (P<0.05), compared to TT8i and WT alfalfa. Although the gas production of TT8i was numerically lower than that of WT, there were no statistically significant differences relative to WT during the fermentation (P > 0.05). Gas produced in rumen fermentation consists mainly of carbon dioxide and methane, which comes from the hydrolysis of carbohydrates to pyruvate and acetate (Russell and Rychlik 2001; Getachew et al. 2004).

Table 3.4.1 Effects of silencing *TT8* and *HB12* genes on accumulative gas production of alfalfa during *in vitro* fermentation: Comparison of gene transformed with wild type.

Items [1]	WT	Transformed Alfalfa		SEM [2]	P value	Contrast P [3]
		HB12i	TT8i			W vs G
Gas production kinetics						
a (mL/g DM)	170.33a	144.64b	159.20ab	5.089	<0.001	0.01
c (%/h)	9.04	8.10	8.47	1.411	0.28	0.20
Lag time (h)	0.21	0.34	0.08	0.116	0.07	0.98
AP (mL)	10.70a	8.04b	9.64a	1.640	<0.001	<0.001
Accumulative gas production after hours of fermentation (mL/g DM)						
2 h	28.76a	20.56b	25.94a	4.889	<0.001	<0.001
4 h	45.53a	34.47b	42.14a	6.928	<0.001	<0.001
8 h	82.85a	64.64b	78.53a	9.836	<0.001	<0.001
12 h	111.43a	87.13b	100.96a	9.760	<0.001	<0.001
24 h	149.39a	122.68b	136.56a	11.379	<0.001	<0.001
48 h	164.53a	137.81b	154.78a	4.878	<0.001	0.01

[1.] a, asymptotic production (mL/g DM); c, production fractional rate (%/h); lag time, initial delay of production onset (h); AP, average production at half of asymptotic production (mL), which was calculated as $AP = a \times c \div (2 \times (ln2 + c \times lag))$.
[2.] SEM, standard error of mean; Means with different letters in each row differ significantly at P<0.05.
[3.] Contrast between wild type and transgenic alfalfa (W vs G).

Meanwhile, nitrogen is also essential for bacterial biomass synthesis. The HB12i had lower CP but higher fiber-bound protein and indigestible protein, which might limit the nitrogen availability in the fermentation. The positive relationship between CP and gas production was

consistent with previous studies (Ndlovu and Nherera 1997; Larbi et al. 1998; Jonker et al. 2012b). However, Getachew et al. (2004) reported that gas production was negatively related to CP and NDF based on the study on 12 feedstuffs. This indicates that the low gas production from HB12i might be the integrated result from its low CP and high NDF.

3.4.3.2 Effect of silencing of TT8 and HB12 on in vitro ammonia production of alfalfa

Ammonia production during *in vitro* fermentation is shown in Table 3.4.2. Ammonia productions were calculated both as milligram per gram DM sample fermented (mg/g DM) and milligram per gram nitrogen fermented (mg/g N). At 4 h point, HB12i had lower ammonia production both based on DM and N compared with WT and TT8i. At 24 h, HB12i had lower production than WT when calculated based on DM. At 48 h, HB12i had the lowest ammonia production based on DM, while HB12i was the highest. When calculated based on N, there were no differences between WT and TT8i, both of which were higher than HB12i.

Our ammonia production results were comparable to a previous study (Wang et al. 2006). The lower ammonia production of HB12i could be explained with its low content of rumen degradable protein. When feed particles reach the rumen, dietary proteins are degraded by microbes eventually to ammonia nitrogen, which serves as the nitrogen source to most ruminal bacteria (Yang et al. 2010). Therefore, lower ammonia production was observed for HB12i as less rumen degradable protein was provided. When ammonia production exceed the requirement of bacteria, the excessive ammonia is absorbed by the rumen and will be converted to urea in the liver (Tas et al. 2006). Unlike *in vivo* environment, the *in vitro* incubator would not absorb ammonia during the fermentation, which could lead to an increase in ammonia concentration overtime.

Table 3.4.2 Effects of silencing *TT8* and *HB12* genes on ammonia production of alfalfa during *in vitro* fermentation: Comparison of gene transformed with wild type.

Time (h)	WT	Transgenic Alfalfa		SEM [1]	P value	Contrast [2]
		HB12i	TT8i			W vs G
NH3 production (mg/g DM)						
4	9.54a	4.90b	9.55a	2.078	<0.001	0.076
12	7.75	6.27	6.58	2.685	0.592	0.373
24	13.46a	8.68b	11.04ab	1.737	0.010	0.028
48	22.37b	11.39c	32.12a	2.358	<0.001	0.847
NH3 production (mg/g N)						
4	244.40a	150.48b	267.10a	63.405	0.006	0.334
12	193.00	193.26	176.00	79.847	0.928	0.848
24	335.45	264.32	305.15	49.956	0.271	0.259
48	624.11a	350.85b	879.63a	70.483	<0.001	0.925

[1] SEM, standard error of mean; values with different letters in each row are significant different at P<0.05.
[2] Contrast between wild type and transgenic alfalfa (W vs G).

3.4.3.3 Effects of silencing TT8 and HB12 on in vitro VFA productions of alfalfa

Total VFA, acetate and propionate productional kinetics of transformed and WT alfalfa are shown in Table 3.4.3. The HB12i had lower asymptotic and average production of total VFA compared with WT and TT8i (P<0.05). As for acetate production, HB12i had lower asymptotic production compared with TT8i (P<0.05), but not different from WT. Additionally, both WT and TT8i had higher average production of acetate than HB12i (P<0.05). In terms of propionate production, WT had the highest asymptotic production, followed by TT8i with HB12i had the lowest (P<0.05). Also, HB12i had lower production rate and average production of propionate compared with WT and TT8i (P<0.05). In addition, both transgenic alfalfa genotypes had lower lag time than WT (P<0.05). The VFA productions of transformed and WT alfalfa at each time points are shown in Figure 3.4.1. In general, WT had higher VFA productions than transformed alfalfa, except for acetate and total VFA which were not different from TT8i. Also, TT8i had

higher propionate, isobutyrate and isovalerate compared with HB12i. Moreover, both transgenic alfalfa genotypes had higher C2 to C3 ratio compared with WT during *in vitro* fermentation.

Table 3.4.3 Effects of silencing *TT8* and *HB12* genes on VFA production kinetics of alfalfa during *in vitro* fermentation: Comparison of gene transformed with wild type.

Items [1]	WT	Transformed Alfalfa		SEM [2]	P value	Contrast [3]
		HB12i	TT8i			W vs G
Total VFA production kinetics						
a	6.47a	5.67b	6.27a	0.395	<0.001	0.016
c	8.09	5.98	7.58	1.747	0.094	0.241
lag	0.64	0.51	0.25	0.221	0.507	0.394
AP	0.35a	0.22b	0.31a	0.053	<0.001	0.005
Acetate production kinetics						
a	3.89ab	3.65b	4.06a	0.168	0.003	0.786
c	8.70	6.62	7.75	1.558	0.126	0.156
lag	0.62	0.50	0.19	0.217	0.398	0.353
AP	0.23a	0.16b	0.22a	0.035	0.001	0.033
Propionate production kinetics						
a	1.55a	1.30c	1.42b	0.069	<0.001	<0.001
c	9.50a	6.45b	8.72a	1.530	0.001	0.036
lag	0.70a	0.21b	0.18b	0.121	0.019	0.005
AP	0.10a	0.06b	0.08a	0.012	<0.001	<0.001

[1.] a, asymptotic production (mmol/g DM); c, production fractional rate (%/h); lag time, initial delay of production onset (h); AP, average production at half of asymptotic production (mmol), which was calculated as $AP = a \times c \div (2 \times (ln2 + c \times lag))$.

[2.] SEM, standard error of mean; Means with different letters in each row differ significantly at P<0.05.

[3.] Contrast between wild type and transgenic alfalfa (W vs G).

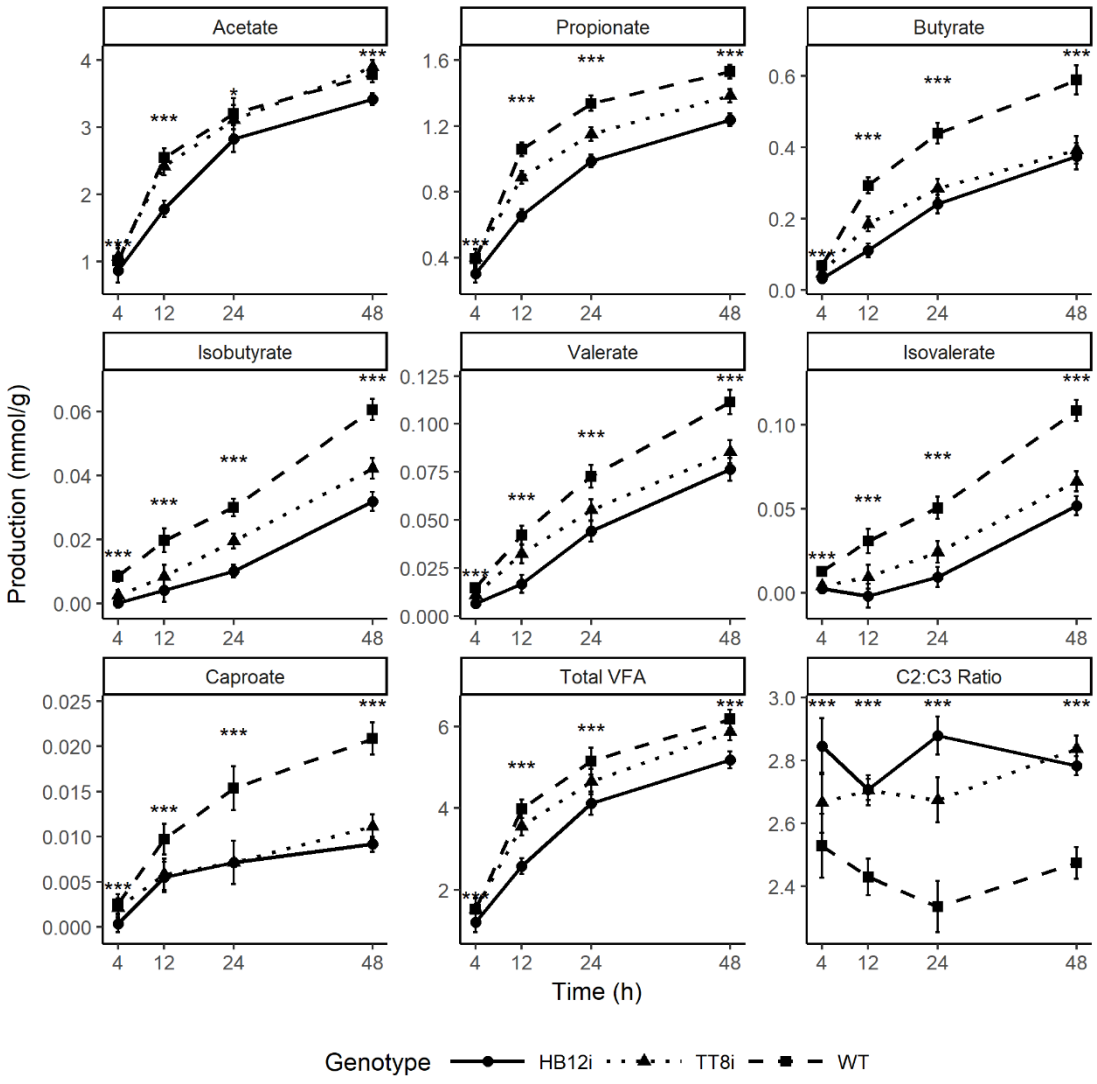

Figure 3.4.1 Volatile fatty acids production of transformed and WT alfalfa during *in vitro* incubation. *, P<0.05; **, P<0.01; ***, P<0.001.

VFA are end products of nutrients fermented in the rumen and serve as the major energy source for ruminants (Zeineldin et al. 2018). Lower DM degradation of transformed alfalfa were to be blamed for lower VFA production as less substrates were provided to microbes. Study reported that VFA productions were positively correlated with gas production during *in vitro* fermentation (Getachew et al. 2004). The VFA production patterns of our alfalfa samples were consistent with their gas production as HB12i also had lower gas production compared with TT8i and WT (Lei et al. 2018b). Individual VFA production are mainly derived from specific substrates,

such as cellulose for acetate, starch and protein for propionate, and soluble fiber for butyrate (Bannink et al. 2006; Jonker et al. 2012b). Similar acetate production between WT and TT8i suggests similar cellulose content between them. Moreover, lower butyrate production from transformed alfalfa implies lower soluble fiber contents. However, CNCPS method estimated that both transgenic alfalfas had higher soluble fiber contents on DM basis than WT (Lei et al. 2018b). This conflict could be resulted from experimental errors of misclassifying nutrients in chemical analysis (Soest 1994) and modeling errors in predicting VFA from substrate sources(Bannink et al. 2006). Berthiaume et al. (2010) reported alfalfa with high non-structural carbohydrates had low C2 to C3 ratio, which is in line with our study as WT had higher starch and comparable sugar (Lei et al. 2018b).

3.4.3.4 Effects of silencing TT8 and HB12 on in vitro DM and NDF degradations of alfalfa

The *in vitro* DM and NDF degradational kinetics of transformed and WT alfalfa are shown in Table 3.4.4. For DM kinetics, both HB12i and TT8i were higher for undegradable fraction (U, %), but lower for degradable fraction (D, %) and effective degradations ($P<0.05$). The fractional degradation rate K_d of HB12i was higher than that of WT ($P<0.05$), but not different from TT8i ($P>0.05$). In contrast, there were no significant differences in NDF degradation kinetics between alfalfa genotypes ($P>0.05$). Degradations of DM and NDF at each time point are illustrated in Figure 3.4.2. The DM degradation of WT was higher than transgenic alfalfa after 8 h of incubation and remained higher afterwards ($P<0.05$), with no differences between HB12i and TT8i ($P>0.05$). In contrast, there were no significant difference found in NDF degradation between alfalfa genotypes ($P>0.05$). Given the fact that transgenic alfalfa genotypes had higher NDF contents (Lei et al. 2018b), the similarity in NDF degradation indicates a higher amount of degradable NDF for transgenic alfalfa, which could supply more energy.

Table 3.4.4 Effects of silencing *TT8* and *HB12* genes on DM and NDF degradational kinetics of alfalfa during *in vitro* fermentation: Comparison of gene transformed with wild type.

Items [1]	WT	Transformed Alfalfa		SEM [2]	P value	Contrast [3]
		HB12i	TT8i			W vs G
DM degradational kinetics (%)						
U	34.86b	44.28a	43.09a	1.183	<0.001	<0.001
S	39.25	41.33	39.68	0.782	0.117	0.254
D	25.89a	14.39b	17.23b	1.261	<0.001	<0.001
K_d (%/h)	19.71b	32.68a	28.20ab	0.025	0.006	0.006
ED	60.25a	53.87b	54.42b	0.913	<0.001	<0.001
NDF degradational kinetics (%)						
U	30.60	39.84	35.99	7.037	0.654	0.463
D	69.40	60.16	64.01	7.037	0.654	0.463
K_d (%/h)	2.91	3.96	3.58	1.152	0.813	0.596
ED	23.75	24.47	24.43	2.541	0.979	0.844

[1] U, undegradable fraction; S, soluble fraction; D, degradable fraction; K_d, degradation rate; ED, effective degradation.
[2] SEM, standard error of mean. Means with different letters in each row differ significantly at P<0.05.
[3] Contrast between wildtype and genetic transformed alfalfa.

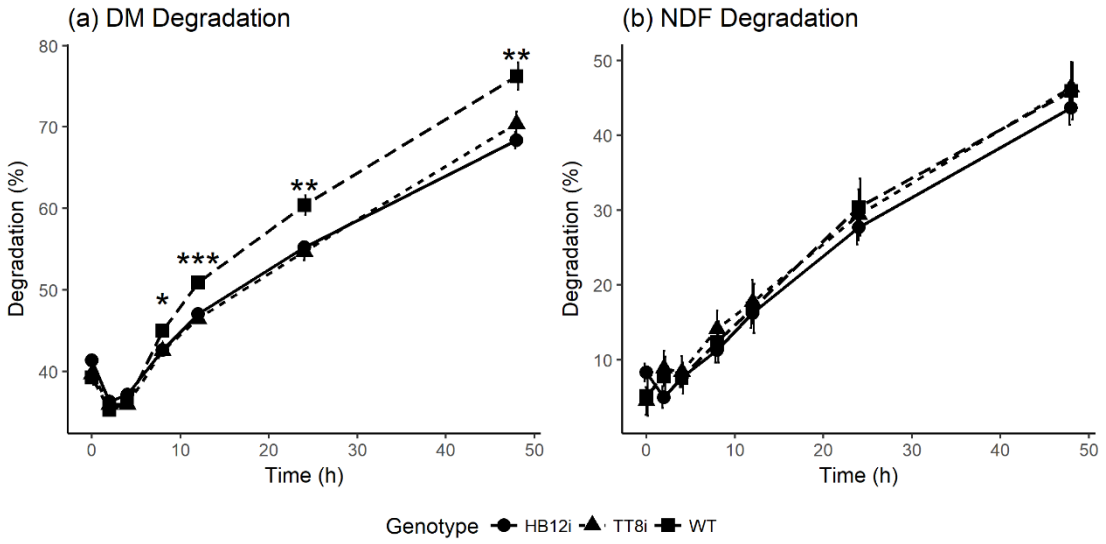

Figure 3.4.2 Dry matter and natural detergent fiber degradations of transformed and WT alfalfa during *in vitro* incubation. *, P<0.05; **, P<0.01; ***, P<0.001.

Jonker et al.(2012b) analyzed *in vitro* DM and CP degradation of *Lc*-transgenic alfalfa populations with similar incubation methods. Among the *Lc*-alfalfa populations, green and light-purple-green alfalfa plants had higher undegradable DM fraction and lower ED_{DM} than WT, which were comparable to transformed alfalfa in the current study. The similarity in DM degradation could be attributed to similar changes in chemical composition induced by genetic modification. Like TT8i and HB12i transgenic alfalfa, green and light-purple-green *Lc*-alfalfa plants also had higher fiber and lower CP compared to WT. A previous pilot study measured *in vitro* DM and NDF degradations after 30 and 240 h of fermentation by using Daisy II incubator (Ankom Technology, Fairport, NY) (Li et al. 2015). It was reported that TT8i had higher DM degradations at 30 h fermentation compared to WT, while HB12i was not different from WT. Both TT8i and HB12i had higher NDF degradation at 30 h fermentation. Compared with the present study, both DM and NDF degradations were higher in the pilot study. This discrepancy might result from differences in fermentation runs, incubation methods, and population size.

3.4.4 Conclusion

In conclusion, silencing *HB12* gene significantly decreased ruminal DM degradation and productions of fermentation end products of alfalfa, whereas silencing *TT8* gene decreased DM degradation and long-chain VFA production. In general, silencing of *TT8* gene had fewer negative influences on rumen fermentation of alfalfa.

3.5 Effects of silencing *TT8* and *HB12* genes on microbial synthesis, protein degradation and digestion, and nutritive modeling of alfalfa

Abstract: This study aimed to determine the effect of silencing *TT8* and *HB12* genes on CP degradation and digestion, fractional microbial nitrogen (MN) and protein metabolic parameters of alfalfa. Alfalfa samples of 11 HB12-silenced (HB12i), 5 TT8-silenced (TT8i) and 4 WT were incubated with rumen fluid and N^{15} labelled ammonium sulfate for 0, 4, 8, 12, and 24 h using Daisy II incubator. Residue from 12 h were used to determine intestinal digestion of rumen undegraded CP (IDRUP). CP degradation and degradational kinetics and fractional MN were determined. Protein availability was estimated with DVE/OEB and NRC (2001) models and feed milk value (FMV) were calculated based on both models. Results showed that both transgenic alfalfa genotypes had lower CP degradation at the end of fermentation while HB12i had lower effective CP degradation. Moreover, HB12i had lower LAMN and higher FAMN at 24 h of fermentation compared with others. Both nutritional systems showed that HB12i had the lowest microbial protein (MCP) and highest ENDP (lowest ECP), followed by TT8 with WT. DVE/OEB system showed that HB12i had lower total available protein and FMV, whereas there were no significant differences found in NRC-2001 system. In conclusion, silencing of *HB12* increased protein solubility and initially degradation of alfalfa, while decreased protein effective degradation and availability. In contrast, silencing of *TT8* gene increased protein solubility but did not affect protein effective degradation and overall availability to animals.

A version of this chapter has been published. Lei, Y.; Hannoufa, A.; Prates, L. L.; Christensen, D.; Wang, Y.; Yu, P. Silencing TT8 and HB12 Decreased Protein Degradation and Digestion, Microbial Synthesis, and Metabolic Protein in Relation to Molecular Structures of Alfalfa (Medicago Sativa). J. Agric. Food Chem. 2019, 67 (28), 7898–7907. https://doi.org/10.1021/acs.jafc.9b02317.

3.5.1 Introduction

Alfalfa (Medicago sativa.) is one of the most cultivated forages worldwide and is regarded as the "Queen of forage" due to its high nutritive value and good palatability (Lei et al. 2018c). However, alfalfa contains relatively high lignin content, which hinders degradations of other nutrients (Li et al. 2015; Lei et al. 2017). Moreover, fresh alfalfa possesses high rapidly degradable protein, which could lead to rumen bloat of ruminants grazing on pure alfalfa pasture (Jonker et al. 2012a). Researches have been focusing on solving these drawbacks with both genetic and traditional techniques. In terms of bloating issue, traditional phenotype selection resulted in a cultivar named AC Grazeland that has lower initial digestion due to thick cell walls (Goplen et al. 1993; Jonker et al. 2012a). Besides, researchers have also attempted to engineer accumulation of anthocyanins and proanthocyanins in alfalfa leaves and stems to slow down protein degradation in the rumen (Ray et al. 2003; McCaslin et al. 2015). As for lignin issue, downregulation of lignin biosynthesis genes has been reported to reduce lignin content and alter lignin composition in alfalfa. For instance, the commercial low-lignin alfalfa cultivar that Monsanto® released was generated by downregulation of *caffeoyl CoA 3-O-methyltransferase (CCOMT)* gene and has been approved in many countries (FAO 2014). Also, downregulations of other genes in lignin synthesis pathway have also been reported (Guo et al. 2001a; Marita et al. 2003; Nakashima et al. 2008; Dien et al. 2011).

Apart from lignin biosynthesis genes, transcriptional factors of Homeobox12 (HB12) and Transparent Testa8 (TT8) have also been proposed to affect lignin content (Li et al. 2015). Therefore, alfalfa genotypes with silenced *HB12* and *TT8* genes were generated to explore such effects on lignin content and nutritive values of alfalfa. Although silencing of *HB12* resulted in higher lignin content in alfalfa, such genetic modification decreased protein content and increased fiber content, which might be suitable for grazing condition (Lei et al. 2018c). Moreover,

transgenic alfalfa also showed alterations in molecular structure (Lei et al. 2018a) and *in vitro* fermentation profiles (Chapter 3.4). The current study aimed to evaluate the effects of silencing *HB12* and *TT8* genes in alfalfa on protein degradation and intestinal digestion, microbial protein synthesis and protein metabolic profiles. In addition, correlations and regressions between these nutritional profiles and Fourier transform infrared (FTIR) spectral parameters were also determined.

3.5.2 Materials and Methods

3.5.2.1 Gene transformation and sample information

Alfalfa samples used in this study were same as chemical study (Chapter 3.1). Details in alfalfa transformation, growth condition and harvest have been described in Chapter 3.1. There were 11 HB12 RNAi (HB12i), 5 TT8 RNAi (TT8i) and 4 wild type (WT) alfalfa samples used in this study.

3.5.2.2 Daisy II fermentation procedure

Daisy II fermentation was conduced at the University of Saskatchewan according to manufacture's instruction manual (Ankom Technology, USA). Alfalfa samples were weighed into F57 Ankom bags and incubated in Daisy II incubation jars at 39 °C with 1 L rumen fluid: buffer (1:2, v/v) solution. Rumen fluids were collected from two cannulated Holstein cows fed with total mixed ration (TMR) at the Rayner Diary Research and Teaching Facility (Saskatoon, Canada). Bags of same alfalfa genotype were incubated in one jar for 0, 4, 8, 12, 24 h with sample amounts gradually increased from 0.3 g to 0.6 g. There were 4 bags for 12 h and 2 bags for other time points. Ammonium sulfate labeled with N^{15} were added at 0.5 g/L for determinations of microbial synthesis during incubation. Corresponding bags were withdrawn at each time point for total N

and N^{15} isotope analyses. Bags withdrawn at 8 h were washed with running tap water, while bags for other time points were processed according to procedures below.

3.5.2.3 Microbial nitrogen partition

Microbial nitrogen (MN) partition and isolation were performed according to references (Wang et al. 2006; Jonker et al. 2012b). Corresponding bags were removed from fermentation jars at 4, 12 and 24 h and washed with 10 mL of dH_2O for three times with Stomacher® 400 Circulator (Seward Ltd., UK). Washed liquids were combined and centrifuged initially at 1000 rtf for 10 min to removed residue, and then recentrifuged at 20,000 rtf for 30 min to precipitated loosely attached microbial nitrogen (LAMN). Then microbes were washed twice with 20 mL dH_2O with vigorous vortex and recentrifuged.

Liquid samples of 10 mL were also collected at 4, 12 and 24 h to isolated liquid associated microbial nitrogen (LMN) with same centrifugation procedure. LAMN and LMN samples were resuspend in 5 mL dH_2O and freeze-dried. Prewashed bags were rewashed with running tap water until water is colorless and then oven-dried at 55 C for 24 h, same as duplicate bags withdrawn at 8h and another two bags at 12 h. Dried residue from same time point for each sample were combined and ball ground with Retsch MM 200 (Retsch GmbH, Haan, Germany). Afterwards, ground residue, LMN and LAMN were analyzed for N content and N^{15} enrichment (APE) with Costech ECS4010 elemental analyzer (Costech Analytical Technologies Inc., USA) coupled to a Delta V mass spectrometer with Conflo IV interface (Thermo Scientific, Germany). MN in residue nitrogen (RN) was regarded as firmly attached microbial nitrogen (FAMN) and was assumed to have same APE as LAMN and was estimated as: $FAMN = (APE\ in\ RN \times RN)/APE\ in\ LAMN$.

3.5.2.4 Three-step intestinal digestion

Residue from 12 h of Daisy II incubation were used in three-step intestinal digestion according to Theodoridou and Yu (2013b). About 200 mg residue were soaked in 10 mL of 0.1 N HCl containing 1 g of pepsin/L at 38 ºC for 1 h. Then, solution was neutralized with 0.5 mL 1 N NaOH and mixed with 13.5 mL of pancreatin. Mixed solution was then vortexed and incubated at 38 ºC for 24 h, followed by addition of 3 mL of trichloroacetic acid (TCA) to precipitate undigested proteins. Solution was then centrifuged at 10, 000 rtf for 15 min and supernatants were then used for N analysis with Kjeldahl method. Intestinal digestion of rumen undegradable protein (IDRUP) was calculated as TCA-soluble N divided by total N in residue.

3.5.2.5 CP degradation and degradational kinetics

The CP degradations at each time point were calculated based on RN values. The CP degradational kinetics was estimated with nonlinear procedure with SAS 9.4 (SAS Institute Inc., USA). Model for CP degradational kinetics was same as DM (Refat et al. 2017b), which was $R_t = U + (100 - S - U)e^{-K_d(t-T_0)}$, where R_t is fermentation residue at t time point (%); U is undegradable fractions (%); S is soluble fractions (%); K_d is degradation rate (%/h); t is time point; T_0 is lag time of degradation (h). Degradable fraction (D) of CP was calculated as $D = 100 - S - U$. Effective degradation of CP was calculated as $ED_{CP} = S + D \times K_d/(K_d + K_p)$, where K_p is the passage rate and was assumed at 4.5%/h (Jonker et al. 2012b).

3.5.2.6 Protein metabolic characteristics and feed milk value with the Dutch DVE/OEB system and NRC-2001 system

Protein metabolic characteristics of alfalfa samples were estimated with the Dutch protein evaluation system (DVE/OEB) (Tamminga et al. 1994; Duinkerken et al. 2011) and NRC-2001 system (NRC Dairy 2001). Detailed calculations of these two systems were previously described

(Yu et al. 2003a; Theodoridou and Yu 2013b). Availabilities of microbial protein (MCP), endogenous protein (ENDP for DVE/OEB system and ECP for NRC system) and rumen undegradable protein (RUP) were estimated. MCP was estimated with both available energy and nitrogen, and degraded protein balance (DPB for NRC system and OEB for DVE/OEB system) was calculated as the differences between these two estimated MCP values. For available energy, fermentation organic matter (FOM) was used in the DVE/OEB system, whereas total digestible nutrients (TDN) was used in NRC-2001 system. The total truly absorbed protein (DVE for DVE/OEB system and MP for NRC system) was then used to calculate the feed milk value (FMV) according to Theodoridou and Yu (2013b).

3.5.2.6 Statistical Analyses

The Mixed procedure of SAS 9.4 (SAS Institute Inc., USA) was used with CRD model $Y_{ij} = \mu + Trt_i + \varepsilon_{ij}$, where Y_{ij} was the nutritive variable; μ was the population mean; Trt_i was the genotype effect; ε_{ij} was the random error. Observations with Studentized residual greater than 2.5 were considered as outliers and removed. Degrees of freedom were estimated with Kenward Roger method and multi-comparison were performed with Tukey-Kramer method. Treatment means were lettered with "pdmix800" macro(Saxton 1998). Differences between WT and transformed alfalfa were determined with contrast statements. Normality test of residual data were conducted with Proc Univariate using Shapiro-Wilk method. Significance level was set at $\alpha<0.05$ and trend was set at $0.05<\alpha<0.1$.

3.5.3 Results and Discussion

3.5.3.1 Effects of silencing TT8 and HB12 on in vitro CP degradation and digestion of alfalfa

The *in vitro* protein degradation kinetics and IDRUP are shown in Table 3.5.1. Both transgenic alfalfa genotypes had higher undegradable and soluble fractions and lower degradable

fractions compared with WT (P<0.05). HB12i had higher degradational rate and lower effective CP degradation compared with other genotypes (P<0.01). In terms of IDRUP, there were no differences between alfalfa genotypes (P=0.117). The CP degradations at each time point are shown in Figure 3.5.1. Both transgenic genotypes had higher degradation at 0 h (soluble fraction) than WT, while TT8i was not different from WT at 4 h and both were lower than HB12i (P<0.01). At the end of fermentation (24 h), WT had the highest degradation, followed by TT8i with HB12i had the lowest degradation (P<0.001).

The maturity-like chemical composition of transformed alfalfa might to be blamed for their lower CP degradation, especially for HB12i (Lei et al. 2018c). Chemical analysis showed that HB12i had higher neutral detergent insoluble protein (NDICP) and both transformed alfalfa had higher acid detergent insoluble protein (ADICP) (Lei et al. 2018c). Both NDICP and ADICP are negatively correlated with CP degradation because of their resistance to rumen degradation.

Table 3.5.1 Effects of silencing *TT8* and *HB12* genes on *in vitro* CP degradation kinetics and intestinal digestion of alfalfa: Comparison of gene transformed and wild type.

Items [1]	WT	Transformed Alfalfa		SEM [2]	P value	Contrast [3]
		HB12i	TT8i			W vs G
CP ruminal degradational kinetics						
U (%)	7.41b	23.81a	17.76a	1.958	<0.001	<0.001
S (%)	43.96b	52.04a	53.38a	1.994	0.026	0.008
D (%)	48.63a	28.86b	24.15b	3.033	<0.001	<0.001
K_d (%/h)	12.86b	24.67a	15.60b	2.581	0.008	0.067
ED_{CP} (%)	79.66a	71.90b	75.70a	1.073	<0.001	0.002
Intestinal digestion of rumen undegradable protein (IDRUP)						
IDRUP (%)	72.26	65.70	68.29	1.994	0.117	0.082

[1] U, undegradable fraction; S, soluble fraction; D, degradable fraction; K_d, degradation rate; ED, effective degradation.
[2] SEM, standard error of mean. Means with different letters in each row differ significantly at P<0.05.
[3] Contrast between wildtype and genetic transformed alfalfa.

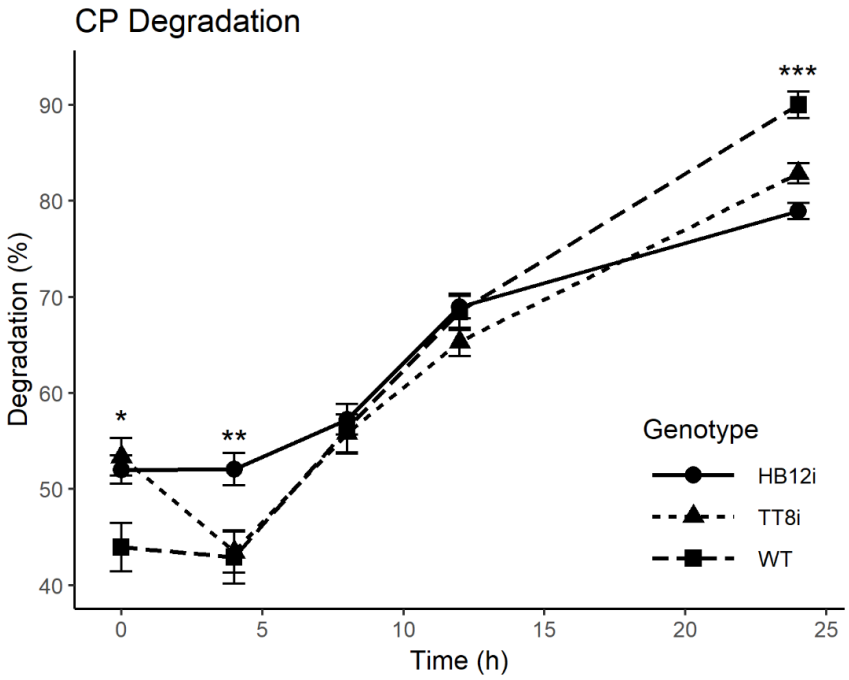

Figure 3.5.1 *In vitro* CP degradations of transformed and WT alfalfa. *, P<0.05; **, P<0.01; ***, P<0.001.

Maturity had a similar effect on chemical composition and CP degradation of alfalfa with more matured plant containing less CP and had lower effective CP degradation (Yari et al. 2012b). The effective CP degradation of alfalfa in the present study was about 75%, which is higher than those in ref (Yari et al. 2012b). This discrepancy could be attributed to the maturity of plants at harvest. Alfalfa samples of this study were harvested at vegetative stage, while those in ref (Yari et al. 2012b) were harvested at bud or early flower stage. The IDRUP result implied similar quality of rumen undegradable protein (RUP) for each genotype and about 68% RUP were available for the animal in the small intestine.

3.5.3.2 Effects of silencing TT8 and HB12 on microbial nitrogen profiles of alfalfa

The APE data of fractional microbial nitrogen are shown in Table 3.5.2. For LMN profiles, HB12i had higher APE than other genotypes during the fermentation except for at 12 h, when it was not different from WT but still higher than TT8i (P<0.05). Although there were no differences

in APE of LAMN at 4 h, HB12i was higher than WT and TT8i at 12 h and higher than WT at 24 h (P<0.01). In terms of APE of RN, HB12i was higher than WT at 4 h of fermentation (P<0.01). And at 12 h, HB12i was the highest, followed by TT8i with WT being the lowest (P<0.001). The fractional microbial nitrogen based on residue are reported in Table 3.5.3. HB12i had higher LAMN per gram of residue at 4 h than others (P=0.001); however, it was the lowest at 24 h with WT been the highest (P<0.001). As for FAMN production, HB12i was lower than TT8i at 4 h and 12 h and higher than WT at 24 h (P<0.05). Results of FAMN to RN ratio showed that both transgenic genotypes were higher than WT at 4 h and 12 h (P<0.01).

Table 3.5.2 Effects of silencing *TT8* and *HB12* genes on N^{15} enrichment (atom excess %) of fractional N during Daisy II fermentation: Comparison of gene transformed and wild type

Time (h)	WT	Transformed Alfalfa		SEM [1]	P value	Contrast [2] W vs G
		HB12i	TT8i			
Liquid associated microbial N (LMN)						
4	2.287b	3.906a	2.299b	0.019	<0.001	<0.001
12	3.495ab	3.842a	3.166b	0.173	0.018	0.971
24	2.848b	3.904a	2.956b	0.047	<0.001	<0.001
Loosely attached microbial N (LAMN)						
4	4.728	5.251	4.778	0.162	0.036	0.221
12	5.812b	6.857a	5.804b	0.206	0.001	0.090
24	5.515b	6.395a	5.936ab	0.161	0.005	0.011
Residue microbial N (RN)						
4	0.716b	1.014a	0.905ab	0.055	0.008	0.007
12	1.148c	1.750a	1.457b	0.074	<0.001	0.001
24	1.678	1.998	1.811	0.105	0.116	0.142

[1] SEM, standard error of mean. Means with different letters in each row differ significantly at P<0.05.
[2] Contrast between wildtype and genetic transformed alfalfa.

Table 3.5.3 Effects of silencing *TT8* and *HB12* genes on fractional microbial nitrogen during Daisy II fermentation of alfalfa: Comparison of gene transformed and wild type.

Time (h)	WT	Transformed Alfalfa		SEM [1]	P value	Contrast [2]
		HB12i	TT8i			W vs G
Loosely attached microbial N (LAMN, mg/g residue)						
4	1.403b	2.475a	1.770b	0.175	0.001	0.010
12	6.695	5.798	5.654	0.403	0.254	0.104
24	15.006a	6.140c	8.453b	0.609	<0.001	<0.001
Firmly attached microbial N (FAMN, mg/g residue)						
4	6.011ab	5.607b	6.786a	0.319	0.031	0.679
12	7.145ab	6.629b	7.903a	0.372	0.045	0.816
24	5.506b	6.573a	6.433ab	0.260	0.04	0.015
FMAN to residual N (RN) ratio (FAMN/RN)						
4	15.252b	19.310a	18.942a	0.711	0.005	0.002
12	19.740b	25.495a	25.084a	0.706	<0.001	<0.001
24	30.395	30.833	30.470	1.368	0.964	0.894

[1] SEM, standard error of mean. Means with different letters in each row differ significantly at P<0.05.
[2] Contrast between wildtype and genetic transformed alfalfa.

Microbial growth in the rumen relies on both energy and nitrogen supply (Clark et al. 1992). For most bacteria in the rumen, ammonia is their primary nitrogen source (Yang et al. 2010). Therefore, introduction of N^{15} labeled ammonia sulphate would be helpful in tracing microbial synthesis during the fermentation. The higher APE of LAMN than LMN was consistent with previous study (Wang et al. 2006), implying higher N assimilation in particle-attached microbes. This might result from the higher nutrient availability in attached condition. In general, HB12i had higher APE than other genotypes, which might be attributed to its lower CP content. As microbes growing, lower N supply from feed particle might lead to a higher incorporation of N^{15} from ammonia sulphate. As for fractional MN, HB12i had higher initial LAMN than others because of its higher initial CP degradation, which provided more available nitrogen. Once again, the lower LAMN for both transgenic genotypes at the end of fermentation, especially for HB12i,

might be explained with their lower CP content. Most feed protein was degraded in the end of fermentation and total N supply was highest for WT and lowest for HB12i given their CP content (Lei et al. 2018c) and degradation. For FMAN, both transformed genotypes were higher at the end of fermentation, which might be resulted from their higher amount of feed residue (Chapter 3.4) that provided more surface area for microbial attachment. The higher FAMN of transformed alfalfa also contributed to their higher FAMN to RN ratio in the beginning of fermentation. Notably, FAMN to RN ratio were about 30% for alfalfa, which was in agreement with previous study (Wang et al. 2006). The high percentage of MN in RN could lead to an underestimation of CP degradation.

3.5.3.4 Effects of Silencing TT8 and HB12 on protein metabolic parameters and feed milk value of alfalfa with DVE/OEB and NRC-2001 Systems

Protein metabolic parameters and feed milk values with DVE/OEB and NRC-2001 systems are shown in Table 3.5.4 and Table 3.5.5, respectively. In DVE/OEB system, HB12i had lowest fermentable organic matter (FOM), microbial protein (MCP) and absorbable MCP (AMCP) after TT8i and WT had highest MCP profiles ($P<0.001$). The NRC-2001 system showed similar results except that there were no differences in MCP based on total digestible nutrient (TDN). The DVE/OEB system showed HB12i had highest endogenous protein (ENDP), followed by TT8i with WT had the lowest, which were opposite to NRC system ($P<0.001$). This is because DVE/OEB system considered ENDP as losses for total absorbable protein (DVE), whereas NRC regarded endogenous protein (ECP) as parts of metabolizable protein (MP) (Theodoridou and Yu 2013b). Therefore, calculations for endogenous protein were opposite for these two systems.

Table 3.5.4 Predicted protein supply and feed milk value to dairy cattle of transformed and WT alfalfa with DVE/OEB system

Items [1]	WT	Transformed Alfalfa		SEM [2]	P value	Contrast [3]
		HB12i	TT8i			W vs G
Absorbable microbial protein (AMCP, g/Kg DM)						
FOM	642.29a	544.11c	604.52b	8.506	<0.001	<0.001
MCP_{FOM}	96.35a	81.62c	90.68b	1.276	<0.001	<0.001
MCP_{RDP}	188.20a	143.48c	166.04b	4.414	<0.001	<0.001
$AMCP_{DVE}$	61.42a	52.03c	57.81b	0.814	<0.001	<0.001
Endogenous protein (ENDP, g/Kg DM)						
ENDP	16.27c	24.60a	19.32b	0.514	<0.001	<0.001
Absorbable rumen undegraded protein (ARUP, g/Kg DM)						
RUP_{DVE}	54.95	64.89	61.49	3.025	0.106	0.069
$ARUP_{DVE}$	39.76	42.73	42.10	2.941	0.786	0.523
Total truly absorbed protein (DVE, g/Kg DM)						
DVE	84.50a	70.30b	84.02a	2.407	0.001	0.043
Degraded protein balance (OEB, g/Kg DM)						
OEB	91.86a	61.87b	75.36ab	4.735	0.002	0.003
Feed milk value (FMV, Kg milk/Kg feed)						
FMV_{DVE}	1.72a	1.43b	1.71a	0.049	<0.001	0.041

[1] FOM, fermentable organic matter; MCP_{FOM}, predicted microbial protein synthesized based on energy (FOM); MCP_{RDP}, predicted microbial protein synthesized based on rumen degradable protein (RDP); RUP, rumen undegraded protein.
[2] SEM, standard error of mean. Means with different letters in each row differ significantly at $P<0.05$.
[3] Contrast between wildtype and genetic transformed alfalfa.

Table 3.5.5 Predicted protein supply and feed milk value to dairy cattle of transformed and WT alfalfa with NRC-2001 system

Items [1]	WT	Transformed Alfalfa		SEM [2]	P value	Contrast [3]
		HB12i	TT8i			W vs G
Absorbable microbial protein (AMCP, g/Kg DM)						
MCP_{TDN}	83.45a	79.76b	81.63a	0.466	<0.001	<0.001
MCP_{RDP}	164.60a	127.43c	146.31b	3.733	<0.001	<0.001
$AMCP_{NRC}$	53.69a	51.21c	52.24b	0.261	<0.001	<0.001
Absorbable rumen undegraded protein (ARUP, g/Kg DM)						
RUP_{NRC}	49.50	58.46	55.39	2.726	0.106	0.069
$ARUP_{NRC}$	35.82	38.49	37.93	2.651	0.786	0.524
Absorbable endogenous protein (AECP, g/Kg DM)						
ECP	11.04a	10.89c	10.95b	0.013	<0.001	<0.001
AECP	4.42a	4.36c	4.38b	0.006	<0.001	<0.001
Total metabolizable protein (MP, g/Kg DM)						
MP	93.93	93.98	94.55	2.757	0.983	0.931
Degraded protein balance (DPB, g/Kg DM)						
DPB	94.65a	55.50c	75.80b	4.170	<0.001	<0.001
Feed milk value (FMC, Kg milk/Kg feed)						
FMV_{NRC}	1.91	1.91	1.92	0.056	0.981	0.928

[1] MCP_{TDN}, predicted microbial protein synthesized based on energy (TDN); MCP_{RDP}, predicted microbial protein synthesized based on rumen degradable protein (RDP); RUP, rumen undegraded protein; ECP, endogenous protein.
[2] SEM, standard error of mean. Means with different letters in each row differ significantly at $P<0.05$.
[3] Contrast between wildtype and genetic transformed alfalfa.

Both systems found no differences in rumen undegradable protein (RUP) profiles, which is line with intestinal digestion trial. The DVE/OEB system showed HB12i had lower DVE compared with WT and TT8i (P=0.001), whereas there were no differences in MP between genotypes calculated with NRC-2001 system. As for degraded protein balance (OEB in DVE/OEB system, DPB in NRC system), WT was higher than HB12i in DVE/OEB system (P<0.01), and higher than both transformed alfalfa in NRC-2001 system (P<0.001). Moreover, DVE/OEB system found HB12i had lower feed milk value compared with WT and TT8i (P<0.001), which was not found with NRC-2001 system.

Metabolizable protein for ruminant includes microbial protein, rumen undegraded protein and endogenous protein. Microbial protein accounts for a large amount of total absorbable protein, especially when dietary protein is insufficient (Clark et al. 1992). Synthesis of MCP depends on both energy and protein supply and are estimated with the limiting one in DVE/OEB and NRC-2001 systems (Tamminga et al. 1994; NRC Dairy 2001). Transformed alfalfa, especially HB12i, had lower MCP compared with WT either based on energy or nitrogen in both nutritional systems. This implies that transformed alfalfa had lower supply of energy as it is the limiting factor for alfalfa, which is consistent with their energy values (Chapter 3.1). Moreover, transformed alfalfa also had lower protein content compared with WT (Lei et al. 2018c). Endogenous protein consists of mucins, digestive enzymes, dead epithelium cells and so on (Dave et al. 2014), and is estimated with different concepts in DVE/OEB and NRC-2001 system. The DVE/OEB system considers it as losses for DVE and is more related to undigested DM (Tamminga et al. 1994; Theodoridou and Yu 2013b). In contrast, NRC-2001 system regards it as a part of MP and is morel related with DM content (NRC Dairy 2001; Theodoridou and Yu 2013b). Therefore, the contrast pattern of endogenous protein between genotypes were opposite for these two systems. Also, HB12i was

considered to have more loss or less contribution from endogenous protein according to DVE/OEB and NRC-2001 systems, respectively.

The DVE values were lower than MP values in the current study, which is consistent with previous studies on alfalfa forage (Yu et al. 2003a; Yari et al. 2012b). Notably, estimation differences were greater for samples with low CP, such as HB12i in this study and late-harvest samples in studies of Yu (Yu et al. 2003a) and Yari (Yari et al. 2012b). This suggests that CP content is more crucial on estimations for available protein in DVE/OEB system, compared with NRC-2001 system. Protein metabolic characteristics of this study were comparable to Yu's study (Yu et al. 2003a) and higher than those in Yari's study (Yari et al. 2012b). Given the fact that alfalfa samples were harvested at similar stages in Yu's and Yari's studies, discrepancies in protein metabolic characteristics might be attributed to not only differences in harvest time, but also to varieties, cultivation year and cultivation locations.

3.5.4 Conclusion

In conclusion, silencing of *HB12* and *TT8* genes in alfalfa decreased CP degradation especially for the silencing of *HB12* gene. Moreover, transformed alfalfa had lower microbial protein and total available protein compared with WT. Nevertheless, such alteration in protein profiles could lead to a better nutrient balance for transgenic alfalfa plants.

CHAPTER 4
COMPARATIVE EFFECTS OF OVEREXPRESSION OF MIR156 AND SILENCING OF SPL6 AND SPL13 GENES ON MOLECULAR STRUCTURES AND NUTRITIVE VALUES OF ALFALFA IN RUMINANT SYSTEM

4.1 Effects of overexpression of miR156 on bioactive compounds, chemical composition, CNCPS fractions and energetic values of alfalfa: in comparison with silencing *SPL6* and *SPL13* genes

Abstract: This study aimed to explore the comparative effects of overexpressing miR156 with individually silencing *SPL6* and *SPL13* genes on bioactive compounds, chemical profiles, CNCPS fractions and degradation, and bioenergy values of alfalfa. Three sub-genotypes of miR156 OE, SPL6 RNAi and SPL13 RNAi grown in a greenhouse with WT and harvested at early vegetative stage were used for this study. There were two replicates and three harvests of each sub-genotype for the bioactive study and chemical analysis, respectively. Results showed that miR156 OE had lower fiber and higher energy compared with all other genotypes. Moreover, miR156 OE also had higher insoluble true protein than WT and SPL13 RNAi and higher starch compared with SPL13 RNAi. In conclusion, overexpression of miR156 decreased fiber content of alfalfa and provided more insoluble true protein and energy to animals. SPL6 RNAi was more similar to miR156 OE alfalfa in chemical composition, indicating that *SPL6* gene plays an important role in the miR156 overexpression event.

4.1.1 Introduction

MicroRNAs (miRNAs) are a class of small, non-coding regulatory RNAs containing about 18 to 24 nucleotides (Spanudakis and Jackson 2014). They regulate gene expression particularly at post-transcriptional level through gene silencing. Plant miRNAs predominantly regulate the expression of transcriptional factor genes, thereby regulating a variety of processes in plant development (Aung et al. 2015c). Among those identified plant miRNAs, miR156 is highly conserved among flowering plants (Aung et al. 2015c). The expression of miR156 shows a temporal manner, as it is relatively high at juvenile phase and then gradually reduced with age (Wang and Wang 2015). Studies showed that miR156 is a master switch that controls plant growth phase transitions, from vegetative phase to reproductive phase (Bhogale et al. 2014; Wang and Wang 2015; Aung et al. 2015c; Wang 2016). Most functions of miR156 are fulfilled via its transcriptional suppression of target *Squamosa promoter binding protein-like genes (SPL)*. *SPL* genes encode a family of transcriptional factors containing a conserved SBP domain, which consists of 76 amino acids (Wang and Wang 2015).

Since miR156 is highly expressed in early vegetative phase, overexpression of miR156 might prolong the vegetative growth by delaying flowering, which would lead to higher biomass yield and better nutritive value. A previous study showed that overexpression of miR156 delayed the onset of flowering, enhanced branching, and increased root length and biomass yield in alfalfa (Aung et al. 2015a). In addition, among alfalfa *SPL* genes, *SPL6* and *SPL13* were confirmed to be downregulated by overexpressing miR156 (Aung et al. 2015a, 2015b). However, comprehensive influences of overexpressing miR156 on nutritive values of alfalfa remains unclear. To explore the roles of *SPL6* and *SPL13* genes play in miR156 OE event, *SPL6* and *SPL13* silenced (SPL6 RNAi and SPL13 RNAi) alfalfa were generated with RNAi technique. This study was conducted to explore the effects of overexpressing miR156 on chemical composition, CNCPS fractions and

degradations, and energetic values of alfalfa. Meanwhile, we also aimed to discover the effects of silencing *SPL6* and *SPL13* genes on these nutritional profiles in comparison with miR156 overexpression.

4.1.2 Materials and Methods

4.1.2.1 Alfalfa samples and growth conditions

Alfalfa samples of microRNA156 overexpression (miR156 OE), *SPL6*-silenced (SPL6 RNAi) and *SPL13*-silenced (SPL13 RNAi) were obtain from London Research and Development Centre, AAFC (London, ON). There were three sub-genotypes for each transformed alfalfa (A11, A11a and A17 for miR156 OE; 6-405, 6-425, 6-428 for SPL6 RNAi; 13-2, 13-5, 13-6 for SPL13 RNAi). A sub-genotype of transformed alfalfa means plants from an individual transformation event. Details of alfalfa transformation for miR156 OE was described by (Aung et al. 2015a). The alfalfa miR156 precursor was amplified from cDNA template and then cloned into pENTR/D-TOPO entry vector. Then, miR156 fragment was then cloned into pBINPLUS vector and transferred into Agrobacterium tumefaciens, which was used for the transformation of alfalfa explants. For SPL6 and SPL13 RNAi alfalfa, RNAi technique was used.

Three sub-genotypes for each transformed genotype were grown with wild type (WT, non-transformed N4.4.2) control in a greenhouse. Transformed and WT alfalfa were propagated from existing plants. New cuttings were inserted in growing media for root development and then transferred into plastic pots with four root-cutting in each pot. There were three pots for each sub-genotypes of transformed alfalfa and six pots for WT control. All plants were grown under normal conditions and harvested three times from June to September with a 25 days interval. Upon each harvest, samples of each genotype from all available pots were combined and then stored at -20

ºC freezer. Three harvests were considered block effects in statistical analysis. Then, samples were freeze-dried and ground through 1 mm sieve for chemical analysis.

4.1.2.2 Cell wall residue, lignin and total phenolic content determination

Two replicates of fresh alfalfa samples for each genotype were harvested at early vegetative stage and ground with liquid nitrogen for the analyses of cell wall residue (CWR), lignin and phenolic compounds. Procedures for determination of these compounds were previously described in Chapter 3.1.

4.1.2.3 Chemical analysis, CNCPS fractions and degradations and energetic values

Procedures of analysis for Chemical composition and evaluations for CNCPS fractions and energetic values were same as project one. See details in Chapter 3.1.

4.1.2.4 Statistical analysis

The Mixed procedure of SAS 9.4 (SAS Institute, Inc., Cary, NC, USA) was used to analyze data. The model for kinetics and degradation was: $Y_{ijk} = \mu + G_i + S_j(G_i) + H_k + \varepsilon_{ijk}$, where Y_{ijk} was the dependent variable; μ was the population mean; G_i was the genotype effect; $S_j(G_i)$ was the random sub-genotype effect nested in genotype effect; H_k was the random harvest effect, ε_{iik} was the random error. The degree of freedom was estimated with Kenward Roger method. Prior to variance analysis, outliers were detected with "residual" option in Model statement with a Studentized residual greater than 2.5. Contrast statement was used to determine the difference between WT and transformed alfalfa, SPL RNAi and WT, and SPL RNAi and miR156 OE alfalfa. The Tukey-Kramer method was used in multi-treatment comparison. The "pdmix800" macro (Saxton 1998) was used to letter grouping the treatment mean. Normality test of the residual data

was performed using Shapiro Wilk method by using Univariate Procedure with Normal and Plot options. Significance level was set at $P<0.05$ and trend was set at $0.05<P<0.10$.

4.1.3 Results and Discussion

4.1.3.1 Comparative effects of overexpressing miR156 and silencing SPL6 and SPL13 genes on bioactive compounds of alfalfa

There were no differences in cell wall residue, lignin content and phenolic compounds between alfalfa genotypes (Table 4.1.1). Cell wall residue accounted for about 60% of dry weight (DW) of alfalfa, in agreement with the first project on TT8/HB12 silenced alfalfa (Chapter 3.1).

Table 4.1.1 Cell wall residue, lignin and phenolic contents of miR156 OE in comparison with SPL6 RNAi, SPL13 RNAi and WT alfalfa

Items	Cell Wall Residue (CWR, %DW)	Lignin (mg/g CWR)	Lignin (mg/g DW)	Phenolic Extraction (mg/g DW)
WT	60.21	21.56	12.98	3.80
miR156 OE	58.78	20.00	11.75	3.46
SPL13 RNAi	56.97	20.53	11.72	3.56
SPL6 RNAi	63.09	19.48	12.20	3.18
SEM [1]	2.945	1.626	1.563	0.216
P value	0.430	0.875	0.975	0.368
Contrast [2]				
WT vs GM	0.690	0.770	0.612	0.830
SPL vs WT	0.448	0.799	0.498	0.917
SPL vs miR156	0.232	0.997	0.482	0.800

[1] SEM, standard error of mean;
[2] WT vs GM, contrast between wild type and gene transformed alfalfa; SPL vs WT, contrast between SPL RNAi and wild type; SPL vs miR156, contrast between SPL RNAi and miR156 OE.

Lignin contents of alfalfa samples in the current study were higher than those discovered in the first project for HB12i TT8i, but was consistent with previous report on miR156 OE alfalfa (Aung et al. 2015a). However, lignin contents were slightly lower in two miR156 OE subgenotypes (A17 and A11a) that had higher expression of miR156 (Aung et al. 2015a). In contrast, were no

differences between miR156 OE and WT in the current study although miR156 OE was numerically lower than WT. The discrepancy in lignin content is mostly likely caused by genotype selection in the current study. Except for these two subgenotypes of miR156 OE, another subgenotype of miR156 (A11) was also included in miR156 OE in order to compared with SPL RNAi and WT. And this subgenotype (A11) was not different from WT in lignin content (Aung et al. 2015a). In terms of total phenolic content, it was about 3.5 mg/g DW in the present study, which was comparable to the first project (HB12/TT8), and both were lower than alfalfa expressing heterologous miR156 from *Lotus japonicus* (Aung et al. 2015b). The differences in phenolic compounds might be attributed to origin of miR156 gene, gene expression level, growth condition, and harvest time.

4.1.3.2 Comparative effects of overexpressing miR156 and silencing SPL6 and SPL13 genes on chemical composition of alfalfa

Chemical composition data of miR156 OE, SPL6 and SPL13 RNAi and WT are shown in Table 4.1.2. Although there were no significant differences in DM between alfalfa genotypes ($P=0.063$), contrast results showed miR156 OE had higher DM than SPL RNAi genotypes ($P=0.01$). As for carbohydrate profiles, overexpression of miR156 had significant effects on NFC, NDF, ADF and starch contents of alfalfa. The miR156 OE had higher NFC and starch compared with SPL13 RNAi ($P<0.05$), but lower NDF and ADF compared with all other genotypes ($P<0.01$). Moreover, miR156 OE alfalfa had lower sugar content than SPL RNAi according to contrast results ($P=0.02$). In terms of protein profiles, contrast results showed that transformed alfalfa tended to have higher CP ($P=0.069$) and had higher ADICP ($P<0.05$) compared with WT. There were no significant differences between WT and SPL RNAi alfalfa in terms of chemical composition ($P>0.05$).

Table 4.1.2 Chemical composition of miR156 OE in comparison with SPL6 RNAi, SPL13 RNAi and WT alfalfa

Items (%DM)[1]	Alfalfa Genotypes				SEM [2]	P value	Contrast [3]		
	WT	miR156 OE	SPL13 RNAi	SPL6 RNAi			G vs W	S vs W	S vs M
DM	92.59	92.70	92.44	92.38	0.207	0.063	0.614	0.279	0.010
Ash	9.27	8.89	9.02	8.72	0.366	0.483	0.283	0.284	0.910
EE	3.44	3.93	3.91	3.95	0.393	0.794	0.350	0.361	0.999
OM	90.73	91.11	90.98	91.28	0.366	0.483	0.283	0.284	0.910
Carbohydrate profiles									
CHO	61.09	58.61	59.58	60.08	1.639	0.140	0.113	0.221	0.088
NFC	34.07ab	35.88a	33.62b	34.55ab	0.858	0.014	0.464	0.983	0.004
NDF	27.90a	23.72b	26.92a	26.46a	1.201	0.007	0.044	0.222	0.002
ADF	23.34a	19.73b	22.35a	21.96a	1.051	0.001	0.006	0.053	0.000
ADL	5.21	4.80	5.23	5.20	0.378	0.256	0.650	0.990	0.054
Starch	4.77ab	6.26a	4.11b	5.37ab	0.931	0.004	0.492	0.959	0.003
Sugar	7.08	6.48	7.21	7.09	0.455	0.093	0.657	0.826	0.020
Protein profiles									
CP	26.21	28.22	27.48	27.26	1.335	0.120	0.069	0.134	0.100
NDICP	0.88	0.99	0.96	0.94	0.124	0.761	0.421	0.503	0.572
ADICP	0.49	0.59	0.62	0.61	0.131	0.164	0.038	0.029	0.398
SCP	12.27	12.78	12.93	12.50	0.955	0.553	0.372	0.403	0.851

[1] DM, dry matter; OM, organic matter; EE, ester extract; CHO, total carbohydrate; NFC, non-fiber carbohydrate; NDF, neutral detergent fiber; ADF, acid detergent fiber; ADL, acid detergent lignin; NDICP, neutral detergent insoluble crude protein; ADICP, acid detergent insoluble crude protein; SCP, soluble protein;

[2] SEM, standard error of mean. Means with different letters in each row differ significantly at $P<0.05$.

[3] G vs W, contrast between WT and transgenic alfalfa; S vs W, contrast between SPL RNAi and WT; S vs M, contrast between SPL RNAi and miR156 OE

Yari et al. (2012a) reported no differences in starch and sugar content between alfalfa samples harvested at early bud, late bud and early flowering stages. Moreover, starch content in Yari's study was much lower than the current study, implying a maturity effect on starch content of alfalfa as samples were younger in the current study. Interestingly, there was an opposite pattern between starch and sugar content of alfalfa, which is in line with the first project. However, previous study on injured alfalfa reported a positive correlation between sugar and starch concentration in alfalfa leaves (Pirone et al. 2005). Reasons behind this phenomenon are unclear but might be related to starch synthesis from sugar and starch turnover. Overall, fiber content was lower, and CP was higher in the current study compared with the first project, which might be resulted from differences in harvest time. Alfalfa samples were harvested at early vegetative stage compared with those in the first project (Chapter 3.1). Moreover, miR156 OE had lower fiber and higher protein content than other genotypes in the current study. This might be because miR156 OE was at an even earlier vegetative growth stage compared with other genotypes, suggesting that the prolonging effect of miR156 OE might start at a very early stage and likely throughout the vegetative growth. Studies reported that miR156 also controls plant transition from juvenile vegetative stage to adult stage (Wu et al. 2009).

4.1.3.2 Comparative effects of overexpressing miR156 and silencing SPL6 and SPL13 genes on CNCPS fractions and degradations of alfalfa

The CNCPS fractions and rumen degradations of CNCPS fractions miR156 OE, SPL6 RNAi, SPL13 RNAi and WT alfalfa are shown in Table 4.1.3 and Table 4.1.4, respectively. In terms of carbohydrate fractions, miR156 OE had higher CB1, RDCB1 and RUCB1 than SPL13 RNAi ($P<0.01$), and lower CB3, RDCB3 and RUCB3 than other genotypes ($P<0.01$). Moreover, contrast results showed miR156 OE had lower CA4, RDCA4, RUCA4 and RUCHO compared

with SPL6 and SPL13 RNAi ($P<0.05$). As for protein fractions, miR156 OE had higher PB1 (%DM), RDPB1 and RUPB1 compared with WT and SPL13 RNAi. Also, contrast results showed transformed alfalfa tended to have higher RDCP ($P=0.083$) and had higher RUCP compared with WT ($P<0.05$), largely due to higher values of miR156 OE. Ruminal degradable and undegradable CNCPS fractions had same patterns as CNCPS fractions. This is because rumen degradation of CNCPS fractions were estimated for each sample with same calculations based on degradation rate and passage rate.

In CNCPS carbohydrate fractions, CA4 and CB1 are sugar and starch, respectively (Higgs et al. 2015). Differences in CA4 and CB1 between alfalfa genotypes derived directly from their differences in chemical composition. The CB3, on the other hand, is calculated with adjusted NDF and ADF and represents digestible fiber of feed ingredient (Higgs et al. 2015). The lower CB3 of miR156 OE mainly resulted from its lower NDF content, therefore lower total digestible fiber is expected from miR156 OE. In CNCPS protein fractions, PB1 is the insoluble true protein and is calculated by CP subtracting other fractions (Higgs et al. 2015) and is degraded in a moderate rate in the rumen (Van Amburgh et al. 2015). The higher PB1 of miR156 OE implies an overall slower degradation of protein for this genotype, which is good for ruminal nutrient synchronization. Compared with the first project, alfalfa samples in the current study had higher PA2 and PB1 fractions, which is largely because of higher CP in the current study.

Table 4.1.3 CNCPS fractions of miR156 OE in comparison with SPL6 RNAi, SPL13 RNAi and WT alfalfa

Items [1]	Alfalfa Genotypes				SEM [2]	P value	Contrast [3]		
	WT	miR156 OE	SPL13 RNAi	SPL6 RNAi			G vs W	S vs W	S vs M
Carbohydrate Fractions (%DM)									
CA4	7.08	6.48	7.21	7.09	0.455	0.093	0.657	0.826	0.020
CB1	4.77ab	6.26a	4.11b	5.37ab	0.931	0.004	0.492	0.959	0.003
CB2	22.22	23.14	22.31	22.09	1.791	0.505	0.757	0.982	0.171
CB3	14.51a	10.60b	13.41a	13.04a	0.803	0.004	0.059	0.260	0.002
CC	12.51	11.52	12.55	12.49	0.907	0.256	0.648	0.992	0.054
Carbohydrate Fractions (%CHO)									
CA4	11.60	11.06	12.09	11.82	0.686	0.090	0.907	0.500	0.015
CB1	7.88ab	10.69a	6.97b	9.00ab	1.688	0.002	0.368	0.928	0.001
CB2	36.32	39.46	37.43	36.71	2.624	0.215	0.378	0.667	0.071
CB3	23.74	19.27	23.31	21.68	1.187	0.102	0.242	0.520	0.039
CC	20.46	19.62	21.04	20.78	1.280	0.563	0.986	0.735	0.168
Protein Fractions (%DM)									
PA2	12.27	12.78	12.93	12.50	0.955	0.553	0.372	0.403	0.851
PB1	13.06b	14.46a	13.60b	13.82ab	0.575	0.016	0.023	0.078	0.009
PB2	0.38	0.40	0.39	0.32	0.076	0.804	0.919	0.818	0.554
PC	0.49	0.59	0.62	0.61	0.131	0.164	0.038	0.029	0.398
Protein Fractions (%CP)									
PA2	46.74	45.04	47.02	45.79	1.622	0.103	0.396	0.718	0.057
PB1	49.87	51.41	49.46	50.75	1.261	0.219	0.562	0.841	0.124
PB2	1.49	1.42	1.41	1.16	0.265	0.789	0.697	0.629	0.633
PC	1.91	2.14	2.31	2.30	0.553	0.197	0.078	0.049	0.202

[1] CA4, water-soluble carbohydrate, sugar; CB1, starch; CB2, soluble fiber; CB3, digestible fiber; CC, indigestible fiber; PA2, soluble true protein; PB1, insoluble true protein; PB2, fiber-bound protein; PC, indigestible protein;

[2] SEM, standard error of mean. Means with different letters in each row differ significantly at $P<0.05$.

[3] G vs W, contrast between WT and transgenic alfalfa; S vs W, contrast between SPL RNAi and WT; S vs M, contrast between SPL RNAi and miR156 OE

Table 4.1.4 Rumen degradable and undegradable CNCPS fractions of miR156 OE in comparison with SPL6 RNAi, SPL13 RNAi and WT alfalfa

Items (%DM) [1]	Alfalfa Genotypes					Contrast [3]		
	WT	miR156 OE	SPL13 RNAi	SPL6 RNAi	SEM [2]	P value	G vs W	S vs W	S vs M
Rumen degradable carbohydrate fractions									
RDCA4	6.36	5.82	6.48	6.38	0.410	0.093	0.653	0.830	0.020
RDCB1	4.15ab	5.44a	3.57b	4.67ab	0.810	0.004	0.487	0.967	0.003
RDCB2	19.69	20.50	19.77	19.57	1.588	0.509	0.758	0.983	0.173
RDCB3	8.83a	6.45b	8.16a	7.94a	0.489	0.004	0.059	0.261	0.002
RDCHO	39.03	38.21	37.98	38.55	1.092	0.764	0.444	0.465	0.938
Rumen degradable protein fractions									
RDPA2	10.30	10.71	10.84	10.48	0.801	0.555	0.375	0.406	0.858
RDPB1	9.83b	10.88a	10.23b	10.40ab	0.432	0.016	0.023	0.078	0.009
RDPB2	0.23	0.24	0.24	0.20	0.046	0.816	0.914	0.820	0.577
RDCP	20.36	21.84	21.31	21.08	1.146	0.135	0.083	0.157	0.108
Rumen undegradable carbohydrate fractions									
RUCA4	0.71ab	0.66b	0.73a	0.72ab	0.045	0.036	0.689	0.783	0.005
RUCB1	0.63ab	0.82a	0.53b	0.70ab	0.121	0.003	0.525	0.907	0.002
RUCB2	2.53	2.64	2.54	2.52	0.203	0.473	0.747	0.980	0.154
RUCB3	5.68a	4.15b	5.25a	5.10a	0.314	0.004	0.058	0.259	0.002
RUCC	12.51	11.52	12.55	12.49	0.907	0.256	0.648	0.992	0.054
RUCHO	22.06	20.39	21.60	21.52	1.075	0.126	0.232	0.495	0.040
Rumen undegradable protein fractions									
RUPA2	1.98	2.06	2.08	2.02	0.153	0.542	0.354	0.390	0.812
RUPB1	3.23b	3.58a	3.36b	3.42ab	0.143	0.016	0.023	0.077	0.010
RUPB2	0.15	0.16	0.15	0.13	0.030	0.784	0.927	0.816	0.520
RUPC	0.49	0.59	0.62	0.61	0.131	0.164	0.038	0.029	0.398
RUCP	5.85	6.38	6.17	6.17	0.210	0.092	0.046	0.092	0.090

[1] RD**, rumen degradable CNCPS fractions; RU**, rumen undegradable fractions. CA4, water-soluble carbohydrate, sugar; CB1, starch; CB2, soluble fiber; CB3, digestible fiber; CC, indigestible fiber; PA2, soluble true protein; PB1, insoluble true protein; PB2, fiber-bound protein; PC, indigestible protein;
[2] SEM, standard error of mean. Means with different letters in each row differ significantly at $P<0.05$.
[3] G vs W, contrast between WT and transgenic alfalfa; S vs W, contrast between SPL RNAi and WT; S vs M, contrast between SPL RNAi and miR156 OE

4.1.3.2 Comparative effects of overexpressing miR156 and silencing SPL6 and SPL13 genes on truly digestive nutrients and energy values of alfalfa

Overexpression of miR156 in alfalfa significantly affected truly digestive nutrient and energy values (Table 4.1.5). The miR156 OE had higher tdNFC than SPL13 RNAi ($P<0.05$), and lower tdNDF than other genotypes ($P<0.01$). The miR156 OE contained higher starch compared with SPL13 RNAi, which explains its higher tdNFC. In addition, contrast results showed miR156 OE tended to have higher tdCP than other genotypes ($P<0.01$). Moreover, miR156 OE had higher TDN than other alfalfa genotypes ($P<0.01$).

In terms of energy values, miR156 OE was higher than WT and SPL13 RNAi in DE, ME, NE_L and NE_g and was highest in NE_m compared with other alfalfa genotypes. There were no significant differences between miR156 OE and SPL6 RNAi in terms of energy values (except for NE_m), suggesting that *SPL6* gene might play a more important role than *SPL13* gene during miR156 overexpression event. There were no significant differences between SPL6 RNAi and SPL13 RNAi and between WT and SPL RNAi alfalfa. Truly digestive nutrients content and energy values of alfalfa samples were equivalent to the first project and previous publications (Belyea et al. 1999; Yari et al. 2012a; Li et al. 2016a). Energy values of feed ingredient were estimated from TDN, which were calculated with truly digestive NFC, CP, FA and NDF according to NRC-2001 system (NRC Dairy 2001). The higher values of tdNFC and tdCP of miR156 OE alfalfa overweighed its lower tdNDF content, resulting in higher TDN and energy values. Like the first project, tdNFC had the highest contribution to energy values for alfalfa forage, followed by tdCP and tdNDF.

Table 4.1.5 Truly digestive nutrients and energetic values of miR156 OE in comparison with SPL6 RNAi, SPL13 RNAi and WT alfalfa

Items [1]	Alfalfa Genotypes				SEM [2]	P value	Contrast [3]		
	WT	miR156 OE	SPL13 RNAi	SPL6 RNAi			G vs W	S vs W	S vs M
Truly digestive nutrients (%DM)									
tdNFC	33.39ab	35.16a	32.95b	33.86ab	0.840	0.014	0.462	0.981	0.004
tdCP	25.62	27.53	26.81	26.53	1.442	0.117	0.077	0.154	0.088
tdFA	2.44	2.93	2.91	2.95	0.393	0.794	0.350	0.361	0.999
tdNDF	10.90a	8.44b	10.23a	9.98a	0.463	0.001	0.026	0.184	<0.001
Total digestible nutrients (%DM)									
TDN1x	68.39b	71.49a	69.55b	70.01b	0.892	0.001	0.009	0.060	0.001
TDN3x	64.37b	66.35a	65.11b	65.40b	0.571	0.001	0.009	0.061	0.001
Bioenergetic values (Mcal/ Kg)									
DE_{1x}	3.22b	3.38a	3.29b	3.30ab	0.055	0.011	0.015	0.054	0.006
DE_{3x}	3.03b	3.14a	3.08b	3.09ab	0.040	0.013	0.017	0.058	0.008
ME_{1x}	2.64b	2.77a	2.70b	2.71ab	0.045	0.008	0.010	0.039	0.005
ME_{3x}	2.62b	2.72a	2.66b	2.67ab	0.041	0.015	0.019	0.064	0.009
NE_L	1.65b	1.73a	1.68b	1.69ab	0.029	0.012	0.017	0.060	0.007
NE_m	1.73b	1.84a	1.78b	1.79b	0.039	<0.001	0.003	0.029	<0.001
NE_g	1.12b	1.21a	1.15b	1.16ab	0.034	0.010	0.017	0.065	0.005

[1] tdNFC, truly digestive non-fiber carbohydrate; tdCP, truly digestive crude protein; tdFA, truly digestive fatty acid; tdNDF, truly digestive neutral detergent fiber; TDN, total digestible nutrients; DE, digestible energy; ME, metabolizable energy at three times maintenance level; NE_L, net energy for lactation at three times maintenance level; NE_m, net energy for maintenance; NE_g, net energy for growth. Subscripts of 1x and 3x represent one time and three times of feed intake.

[2] SEM, standard error of mean. Means with different letters in each row differ significantly at $P<0.05$.

[3] G vs W, contrast between WT and transgenic alfalfa; S vs W, contrast between SPL RNAi and WT; S vs M, contrast between SPL RNAi and miR156 OE

4.1.4 Conclusion

In conclusion, overexpression of miR156 decreased fiber content of alfalfa and provided more insoluble true protein and energy to animals. There were no significant differences between SPL6 RNAi and SPL13 RNAi and between SPL RNAi and WT alfalfa in chemical composition, CNCPS fractions and energy values. However, SPL6 RNAi was more similar to miR156 OE compared with SPL13 RNAi, indicating *SPL6* gene might play a more important role in the event of miR156 overexpression.

4.2 Effects of overexpression of miR156 on molecular structures of alfalfa with ATR-FTIR spectroscopy: in comparison with silencing *SPL6* and *SPL13* genes

Abstract: This study was conducted to investigate the comparative effects of overexpressing miR156 with silencing *SPL6* and *SPL13* genes on the inherent molecular structure of alfalfa with ATR-FTIR spectroscopy. Alfalfa samples used were same as Chapter 4.1. Peak heights and peak areas from spectral regions were measured and analyzed. Both multivariate analyses methods of PCA and HCA were used to analyze spectral data. Results showed that all transformed alfalfa had lower peak heights and areas for TC, CEC and amide regions, but higher for lipid-related region compared with WT ($P<0.05$). Both SPL RNAi genotypes had lower peak heights and areas in STC region than WT ($P<0.05$); however, miR156 OE was not different from them. In addition, both SPL RNAi had higher area ratio of amide I to II and total amide area ($P<0.05$). The multivariate results showed that WT could be separated from transformed alfalfa in the lipid region with both methods. Furthermore, WT could also be isolated in WTC and CEC regions with PCA analysis. However, all transformed genotypes overlapped with each other and both PCA and HCA could not separate them. In conclusion, overexpression of miR156 had similar effects on molecular structure of alfalfa as silencing of SPL6 and SPL13 genes. All genetic transformations resulted in lower carbohydrate and amide parameters and higher lipid parameters. Moreover, multivariate analyses showed there were huge differences in lipid region between transformed and WT alfalfa.

4.2.1 Introduction

MicroRNA 156 (miR156) is an plant specific microRNA that controls plant transition from vegetative stage to reproductive stage (Aung et al. 2015c). Most functions of miR156 are exerted via its regulation of *Squamosa Promoter Binding Protein-Like (SPL)* genes, which encode proteins with a conservative DNA binding SPB domain (Wang and Wang 2015). Studies reported that miR156 regulates plant growth and development, especially controls the growth transition from vegetative growth to reproductive growth (Wang et al. 2009; Wang 2016). Plants express high level of miR156 at early stage and then expression of miR156 gradually decreases with maturity; in contrast, the expression levels of miR156-target SPL genes gradually increase (Chen et al. 2010). Then, SPL genes promote the expression of miR172, which accelerate plant flowering via its regulations on other genes (Wu et al. 2009; Chen et al. 2010; Wang and Wang 2015). Therefore, overexpressing miR156 in forages might prolong the vegetative growth and thereby increasing the biomass yield of forages.

Alfalfa is one of the most widely planted legume forages around the world due to its good nutritive value and adaptability (Cash and Hu 2009). The yield of alfalfa forage depends on both varieties and management (Undersander et al. 2011). Research showed that overexpression of miR156 delayed the onset of flowering and thereby prolonged the vegetative growth of alfalfa, leading to an increase in biomass yield (Aung et al. 2015a, 2015b). In addition, miR156 overexpression (miR156 OE) alfalfa also showed enhanced shoot branching, trichome densities and root length, and decreased expression of *SPL6* and *SPL13* genes (Aung et al. 2015a). However, influences of miR156 overexpression on the inherent molecular structures of alfalfa remains unclear. Molecular structures have important impacts on nutrients degradation and availability of feed ingredient. Samples with similar protein composition have different degradation patterns due to differences in inherent molecular structures (Yu 2007). For instance, β-sheet structure of protein

could resistance enzymatic degradation and a higher ratio of β-sheet structure in protein could result in lower protein availability (Yu 2005a).

Fourier transform infrared (FTIR) spectroscopy is a non-destructive analytical technique that gives structural information of samples (Stuart 2004; Ami et al. 2013). This rapid spectral tool can be used not only on pure molecules but also complex compounds (Ami et al. 2013). The attenuated total reflection (ATR)-FTIR spectroscopy have been used to explore the molecular structures of several feed ingredients, such as canola (Theodoridou and Yu 2013a), barley (Prates et al. 2018b), sorghum (He et al. 2019), silage (Refat et al. 2017a), and alfalfa (Lei et al. 2018a). In the current study, this technique was used to evaluate the effects of overexpression miR156 OE on inherent molecular structures of alfalfa in comparison with silencing *SPL6* and *SPL13* genes.

4.2.2 Materials and Methods

4.2.2.1 Alfalfa samples

Alfalfa samples used in this study were same as previous study (Chapter 4.1). Samples were ground through a 0.12 mm sieve (Retsch ZM-200, Retsch Inc., Germany) for spectral collection.

4.2.2.2 Spectral collection, univariate and multivariate analyses

Procedures of spectral collection, univariate and multivariate analyses were same as first project. See details in Chapter 3.2.

4.2.2.3 Statistical analysis

The Mixed procedure of SAS 9.4 (SAS Institute, Inc., Cary, NC, USA) was used to analyze univariate spectral data. The model for univariate data was: $Y_{ijk} = \mu + G_i + S_j(G_i) + H_k + \varepsilon_{ijk}$, where Y_{ijk} was the dependent variable; μ was the population mean; G_i was the genotype effect;

$S_j(G_i)$ was the sub-genotype effect nested in genotype effect; H_k was the random harvest effect, ε_{iik} was the random error. The degree of freedom was estimated with Kenward Roger method. Prior to variance analysis, outliers were detected with "residual" option in Model statement with a Studentized residual greater than 2.5. Contrast statement was used to determine the difference between WT and transformed alfalfa, SPL RNAi and WT, and SPL RNAi and miR156 OE alfalfa. The Tukey-Kramer method was used in multi-treatment comparison. The "pdmix800" macro (Saxton 1998) was used to letter grouping the treatment mean. Normality test of the residual data was performed using Shapiro-Wilk method by using Univariate Procedure with Normal and Plot options. Significance level was set at $\alpha<0.05$.

4.2.3 Results and Discussion

4.2.3.1 Comparative effects of overexpressing miR156 and silencing SPL6 and SPL13 genes on carbohydrate structure of alfalfa

Carbohydrate structural profiles of miR156 OE, SPL6 RNAi, SPL13 RNAi, and WT alfalfa are shown in Table 4.2.1. In total carbohydrate (TC) and cellulosic compounds (CEC) region, transformed alfalfa had lower peaks and areas, except for TC4, compared with WT ($P<0.01$). Besides, contrast results showed both SPL6 RNAi and SPL13 RNAi alfalfa genotypes had lower TC4 height compared with WT ($P<0.05$). In terms of structural carbohydrate (STC) region, SPL6 RNAi and SPL13 RNAi had lower STC2, STC3, STC4 and STCA compared with WT ($P<0.05$). As for STC1, both SPL RNAi tended to be lower than WT according to contrast results ($P=0.085$). There were no significant differences in carbohydrate structures between miR156 OE and SPL RNAi alfalfa ($P>0.05$). TC and STC parameters of alfalfa samples in the current study were lower, while CEC parameters were higher than those alfalfa samples in the first project (Lei et al. 2018a), especially for those in TT8 and HB12 silenced alfalfa.

Table 4.2.1 Carbohydrate structural profiles of miR156 OE alfalfa in comparison with SPL6 RNAi, SPL13 RNAi and WT alfalfa

Items [1]	Alfalfa Genotypes				SEM [2]	P value	Contrast [3]		
	WT	miR156 OE	SPL13 RNAi	SPL6 RNAi			G vs W	S vs W	S vs M
Total carbohydrate parameters									
TC1	0.532a	0.489b	0.493b	0.499b	0.0071	0.007	0.001	0.002	0.182
TC2	0.454a	0.421b	0.422b	0.415b	0.0063	0.001	<0.001	<0.001	0.419
TC3	0.310a	0.295b	0.295b	0.291b	0.0043	<0.001	<0.001	<0.001	0.555
TC4	0.140	0.137	0.131	0.133	0.0041	0.110	0.087	0.049	0.078
TCA	64.313a	61.677b	61.970b	62.225b	0.5062	0.014	0.001	0.002	0.213
Cellulosic compounds parameters									
CEC	0.090a	0.076b	0.080b	0.077b	0.0027	0.001	<0.001	<0.001	0.144
CECA	4.555a	3.705b	3.862b	3.735b	0.1511	0.001	<0.001	<0.001	0.173
Structural carbohydrate parameters									
STC1	0.081	0.071	0.074	0.073	0.0032	0.174	0.055	0.085	0.287
STC2	0.146a	0.131ab	0.122b	0.119b	0.0059	0.009	0.004	0.002	0.017
STC3	0.170a	0.151ab	0.143b	0.139b	0.0106	0.010	0.004	0.002	0.036
STC4	0.133a	0.131a	0.123b	0.121b	0.0045	0.004	0.021	0.005	0.002
STCA	28.660a	25.887ab	25.366b	24.691b	1.2530	0.019	0.005	0.004	0.152

[1] TC1-TC4, four major peaks at ca. 1026 (TC1) 1074 (TC2), 1104 (TC3) and 1149 (TC4) cm^{-1} in TC region, respectively; TCA, peak area of TC region; CEC, cellulosic compounds (ca. 1237 cm^{-1}); CECA, peak area of CEC region; STC1-STC4, four major peaks at ca. 1317 (STC1), 1370 (STC2), 1397 (STC3) and 1453 (STC4) cm^{-1}, respectively.

[2] SEM, standard error of mean; Values with different letter in each row differ significantly at $P > 0.05$.

[3] G vs W, contrast between WT and transgenic alfalfa; S vs W, contrast between SPL RNAi and WT; S vs M, contrast between SPL RNAi and miR156 OE

Our previous study showed that TC and STC structural parameters were positively correlated with fiber and total carbohydrate content and negatively correlated with DM and protein(Lei et al. 2018c). The transformed alfalfa in the first projects had higher NDF and lower CP compared with alfalfa samples in the current study. However, controversy results were found in STC parameters in the current study, as miR156 OE was not different from WT in STC parameters. The previous section (Chapter 4.1) showed miR156 OE had higher insoluble true protein but lower fiber compared with WT and SPL RNAi alfalfa. Moreover, CEC parameters showed opposite correlations with chemical composition of alfalfa compared with STC and TC parameters (Lei et al. 2018c). These discrepancies suggest correlations between structural parameters and chemical composition vary for samples with vast differences. Heendeniya and Yu (2017) co-expressed *Lc* and *C1* gene in alfalfa and observed lower peak heights of STC2, CEC, TC1 and TC4 compared with non-transformed alfalfa.

4.2.3.2 Comparative effects of overexpressing miR156 and silencing SPL6 and SPL13 genes on amide and lipid structures of alfalfa

Amide and lipid-related structural parameters of miR156 OE, SPL6/13 RNAi and WT alfalfa are shown in Table 4.2.2 and Table 4.2.3, respectively. Similar to carbohydrate parameters, transformed alfalfa had lower peaks and areas in amide region ($P<0.05$). Moreover, both SPL6 and SPL13 RNAi had higher Amide I/II ratio than miR156 OE ($P<0.01$), and higher ratios of Amide I area (AIA) to Amide II area (AIIA) and AIA to all amide area (AA) compared with WT ($P<0.01$). To the contrary, transformed alfalfa had higher carbonyl C=O area (CCOA) and Asymmetric CH_3 (AsCH3). Furthermore, miR156 OE had higher symmetric CH_2 and (a)symmetric CH_2 and CH_3 area (ASCCA) compared with WT ($P<0.05$). Overall, there were no significant differences in amide and lipid parameters between miR156 OE and SPL6/13 RNAi alfalfa ($P>0.05$).

Table 4.2.2 Amide structural profiles of miR156 OE alfalfa in comparison with SPL6 RNAi, SPL13 RNAi and WT alfalfa

Items [1]	Alfalfa Genotypes				SEM [2]	P value	Contrast [3]		
	WT	miR156 OE	SPL13 RNAi	SPL6 RNAi			G vs W	S vs W	S vs M
Amide heights and ratio									
Amide I	0.396a	0.342b	0.334b	0.327b	0.0204	0.012	0.002	0.002	0.203
Amide II	0.296a	0.256b	0.241b	0.234b	0.0150	0.007	0.002	0.002	0.035
Amide I/II	1.339ab	1.335b	1.387a	1.396a	0.0198	0.016	0.117	0.032	0.004
Protein secondary structure and ratio									
α-helix	0.382a	0.328b	0.322b	0.316b	0.0207	0.021	0.004	0.004	0.358
β-sheet	0.367a	0.326b	0.319b	0.314b	0.0185	0.022	0.005	0.004	0.258
α/β	1.040	1.006	1.009	1.004	0.0250	0.622	0.224	0.236	0.975
Amide area and ratio									
AA	53.624a	46.347b	44.452b	42.839b	2.8714	0.008	0.002	0.002	0.068
AIA	34.988a	31.013b	30.301b	29.293b	1.7221	0.014	0.004	0.003	0.134
AIIA	18.636a	15.334b	14.151b	13.546b	1.1680	0.006	0.002	0.001	0.037
AIA/AIIA	1.881b	2.039ab	2.161a	2.178a	0.0596	0.012	0.007	0.004	0.018
AIA/AA	0.653b	0.670ab	0.683a	0.684a	0.0062	0.014	0.007	0.004	0.021

[1] Amide I/II, ratio of Amide I to Amide II; α/β, ratio of α-helix to β-sheet; AA, total amide area; AIA, amide I area; AIIA, amide II area.
[2] SEM, standard error of mean; Values with different letter in each row differ significantly at P > 0.05.
[3] G vs W, contrast between WT and transgenic alfalfa; S vs W, contrast between SPL RNAi and WT; S vs M, contrast between SPL RNAi and miR156 OE

Like the first project, amide region in this study also had only one obvious peak (Lei et al. 2018a). Thus, second derivative spectra were used to locate amide peaks along with secondary structural parameters. Amide and lipid-related parameters in the current study are equivalent to those in the first project. Previous study reported that protein secondary structure β-sheet is negatively correlated with protein availability to animals, as this structure is resistance to enzyme

digestion (Yu 2005a). Lower β-sheet in transformed alfalfa implies better protein utilization for these genotypes. In Heendeniya and Yu's study, alfalfa with co-expression of *Lc* and *C1* genes showed higher ratio of Amide I to Amide II and α-helix to β-sheet (Heendeniya and Yu 2017).

Table 4.2.3 Lipid-related structural profiles of miR156 OE alfalfa in comparison with SPL6 RNAi, SPL13 RNAi and WT alfalfa

Items [1]	Alfalfa Genotypes				SEM [2]	*P*	Contrast [3]		
	WT	miR156 OE	SPL13 RNAi	SPL6 RNAi			G vs W	S vs W	S vs M
Carbonyl C=O height									
CCO	0.037	0.040	0.034	0.037	0.0019	0.220	0.963	0.694	0.080
CCOA	-0.208b	0.512a	0.369a	0.445a	0.0647	<0.001	<0.001	<0.001	0.062
Symmetric and asymmetric CH2 and CH3 parameters									
SyCH2	0.110b	0.137a	0.131ab	0.126ab	0.0067	0.052	0.022	0.041	0.104
SyCH3	0.060	0.063	0.062	0.061	0.0016	0.227	0.172	0.259	0.266
AsCH2	0.231	0.267	0.256	0.252	0.0106	0.113	0.049	0.088	0.138
AsCH3	0.064b	0.074a	0.075a	0.073a	0.0023	0.009	0.002	0.002	0.831
ASCCA	12.233b	14.044a	13.815a	13.543ab	0.4552	0.035	0.009	0.014	0.235

[1] CCO, carbonyl C=O (centers at ca. 1733 cm^{-1}); CCOA, CCO peak area; SyCH2, symmetric CH2 (ca. 2850 cm^{-1}); SyCH3, symmetric CH3 (ca. 2872 cm^{-1}); AsCH2, asymmetric CH2 (ca. 2920 cm^{-1}); AsCH3, asymmetric CH3 (ca. 2955 cm^{-1}); ASCCA, peak area of asymmetric and symmetric CH2 and CH3 (baseline ca. 3000–2761 cm^{-1}).
[2] SEM, standard error of mean; Values with different letter in each row differ significantly at P > 0.05.
[3] G vs W, contrast between WT and transgenic alfalfa; S vs W, contrast between SPL RNAi and WT; S vs M, contrast between SPL RNAi and miR156 OE

Another study on *Lc* alfalfa by Yu et al. found lower α-helix and β-sheet in *Lc* alfalfa leaves compared with non-transgenic alfalfa (Yu et al. 2009). Also, there were no differences in α-helix to β-sheet ratio between *Lc* and non-transformed alfalfa. In terms of lipid profiles, CCOA for WT were found negative which is because baseline of CCO area in WT alfalfa were smaller than other

genotypes and thereby CCOA of WT was compromised by the area above the baseline. Yari et al. reported increases in symmetric CH2 ($SyCH_2$), asymmetric CH2 ($AsCH_2$) and ASCCA when alfalfa approaching to maturity from bud stage (Yari et al. 2017), which is opposite to our results as miR156 OE alfalfa was expected to at an early growth stage compared with WT. This might because maturity has different effect on alfalfa structure before and after bug stage, as seen in starch content (Yari et al. 2012a).

4.2.3.3 Multivariate analyses of miR156 OE, SPL6 and SPL13 RNAi, and WT alfalfa

Plots of principle component analysis (PCA) and hierarchical cluster analysis (HCA) of alfalfa spectral regions are shown in Figure 4.2.1 and Figure 4.2.2, respectively. With PCA analysis, the first components accounted for more than 90% of population variations for STC, CEC and lipid regions, and more than 75% for CHO and Amide region. The first two components could explain more than 80% of population variations, which suggested principle components were successfully obtained to represents the original spectral dataset. In PCA plots, WT could be separated from transformed alfalfa in STC, CEC and lipid regions. Similar results also were observed in HCA dendrograms. WT was clearly clustered in a group in lipid region and was distinguishable from SPL6 and SPL13 RNAi in TC region. And, replicates of SPL6 RNAi had more similarity to each other in carbohydrate region than in amide and lipid regions. Both multivariate analyses failed to distinguish transformed alfalfa from each other, which implies that transformed alfalfa genotypes had similar molecular structures. Multivariate analyses are used to reduce data dimension when the original dataset contains many variables and are especially useful for high-dimensional spectral data (Ami et al. 2013). Studies have been using multivariate analyses to detect molecular differences in many feed ingredients (Yu 2005b; Abeysekara et al. 2013; Heendeniya and Yu 2017).

4.2.3 Conclusion

In conclusion, overexpression of miR156 and silencing of *SPL6* and *SPL13* genes decreased carbohydrate and amide spectral parameters, and increased lipid parameters. However, there were no significant differences among transformed alfalfa genotypes in molecular strucutres. The similarity in univariate spectral parameters suggested that overexpression of miR156 had similar effects in molecular structure of alfalfa as silencing *SPL6* and *SPL13* genes individually. Moreover, multivariate analyses showed there were huge differences in lipid region between transformed and WT alfalfa.

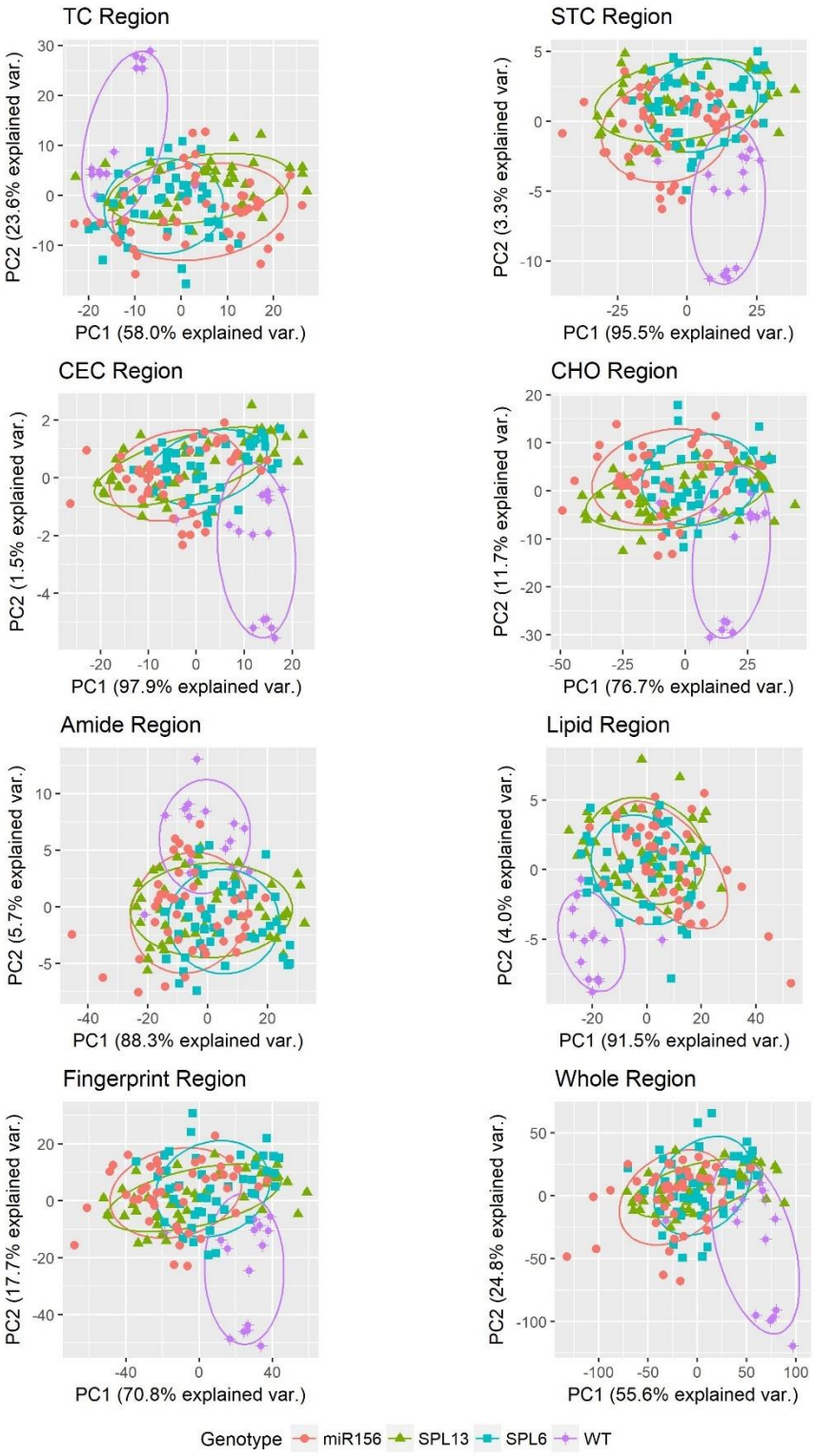

Figure 4.2.1 Principle component analysis (PCA) plots of functional regions in ATR-FTIR spectra of miR156 OE alfalfa in comparison with SPL6 RNAi, SPL13 RNAi and WT.

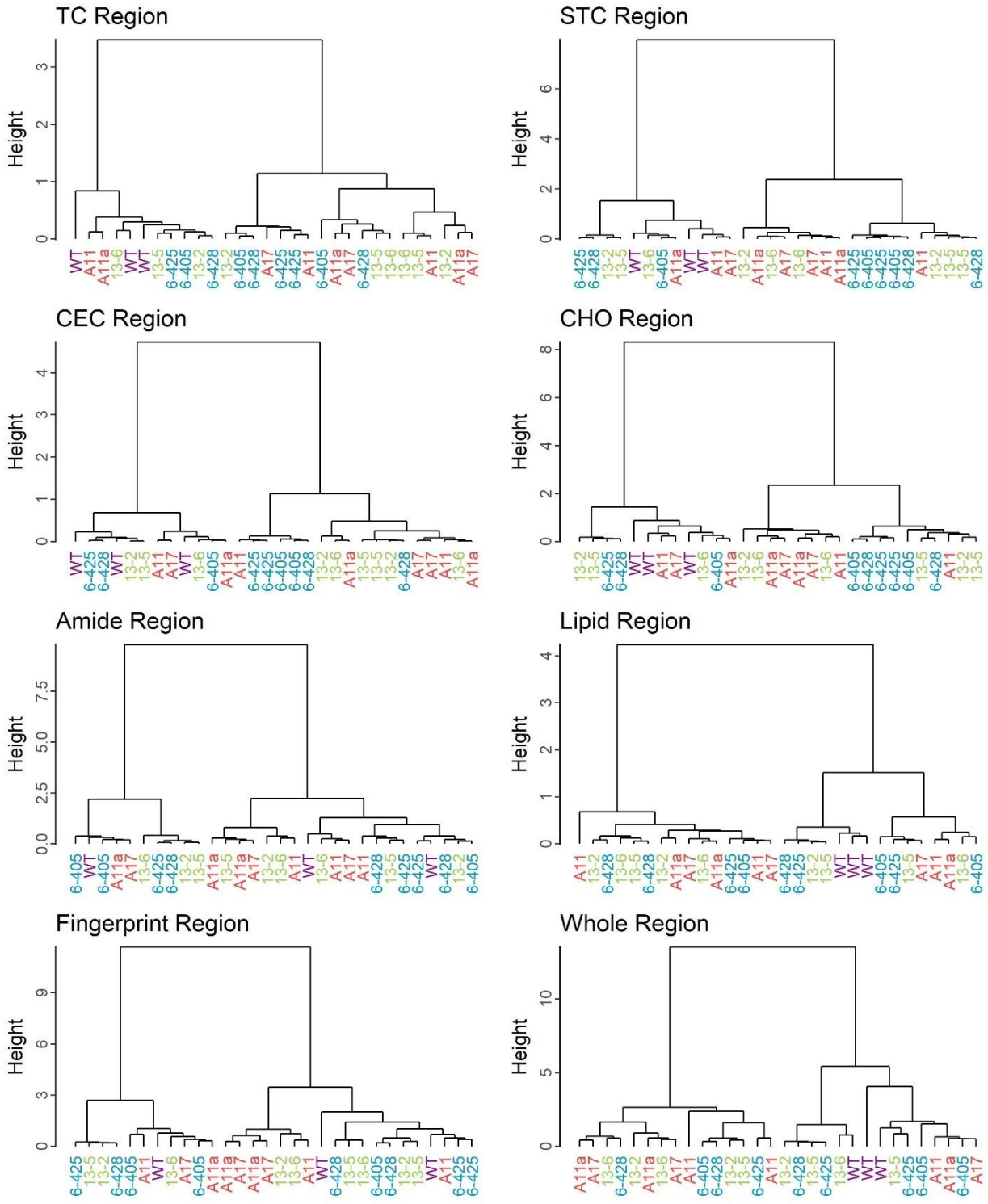

Figure 4.2.2 Hierarchical cluster analysis (HCA) plots of functional regions in ATR-FTIR spectra of miR156 OE alfalfa in comparison with SPL6 RNAi, SPL13 RNAi and WT.

4.3 Effects of overexpression of miR156 on molecular structure and chemical mapping of alfalfa leaves with synchrotron based FTIR spectroscopy: in comparison with silencing *SPL6* and *SPL13* genes

Abstract: This study was conducted to explore the effects of overexpression of miR156 on the molecular structure and chemical compounds localization of alfalfa leaves in comparison with silencing *SPL6* and *SPL13* genes. Five alfalfa leaves from miR156 OE, SPL6 RNAi and SPL13 RNAi and WT were used for univariate analysis of peaks. One window for each alfalfa genotype was selected for chemical mapping. Univariate analysis showed that miR156 OE had higher peak heights and area in TC region, while lower in CEC and amide regions compared with SPL6 RNAi ($P<0.05$). All transformed alfalfa had lower lignin peak height than WT ($P<0.05$). In CCO region, SPL13 RNAi had lower peak heights and area than WT, and lower heights than SPL6 RNAi ($P<0.05$). Chemical mappings were successfully obtained for each alfalfa genotype. TC and STC functional groups were mainly located in epidemical areas in miR156 OE, SPL6 RNAi and WT, while they were located more evenly in SPL13 RNAi alfalfa leaves. Moreover, SPL6 RNAi had lower intensities of STC and CCO, while SPL13 RNAi had lower intensities of CEC and amide compared with other genotypes. In terms of lignin area, SPL13 RNAi had the highest intensity followed by WT with no significant differences between miR156 OE and SPL6 RNAi. In general, amide area had the highest intensity, followed by ASCC and CCO area with carbohydrate areas being the lowest. Moreover, carbohydrate compounds were largely located in epidemical areas, while amide and lipid were mainly located in mesophyll areas of alfalfa leaves. In conclusion, overexpression of miR156 and silencing of *SPL6* and *SPL13* genes affected molecular structure and chemical localizations in alfalfa leaves. Also, alfalfa leaves had higher amide intensity over other compounds, followed by lipids and carbohydrates.

4.3.1 Introduction

Alfalfa (*Medicago sativa*) is a perennial legume forage with high nutritive value and good palatability, which makes alfalfa a good source of feed roughage and is largely used in ruminant diets (Radović et al. 2009; Lei et al. 2017). One great feature of alfalfa forage is its high biomass yield that is not only important in animal husbandry but also enables its potential in biofuel industry (Radović et al. 2009; Badhan et al. 2014). Biomass yield of alfalfa is affected by many factors, such variety, climate, soil type, harvest management and cultivation plan (Undersander et al. 2011). Varieties with low fall dormancy (FD) and low winter hardiness provide higher yield (Undersander et al. 2011). Low dormancy varieties (high FD score) could grow more in fall and have better forage quality, but they are less likely to survive winter if planted in cold areas (Putnam et al. 2005). Cutting schedule also affects biomass yield. As alfalfa grows, total biomass yield increases but forage quality decreases because of great increase from stems (McCaslin et al. 2015). Therefore, it is recommended to harvest alfalfa at early-bud stage to maximum profitability (Undersander et al. 2011). To obtain higher biomass yield without sacrifice forage quality, one potential approach is to prolong its vegetative growth that delays flowering time.

MicroRNA 156 (miR156) is a plant specific microRNA and is conserved in many flowering species (Aung et al. 2015c). miR156 controls plant transitions both from juvenile vegetative stage to adult vegetative stage and from adult stage to reproductive stage (Wu et al. 2009; Wang and Wang 2015). The expression level of miR156 is higher in early vegetative stage and then decline gradually with age (Wang et al. 2009). Studies showed that overexpression of miR156 suppress the expression of its target genes, *Squamosa Promoter Binding Protein-Like (SPL)* genes, and delayed the onset of flowering in *Arabidopsis* (Wu and Poethig 2006; Gandikota et al. 2007). Apart from increasing biomass yield in alfalfa, overexpression of miR156 also resulted in enhanced shoot branching and trichome density and increased root length (Aung et al. 2015a).

Moreover, *SPL6* and *SPL13* genes were downregulated in miR156 overexpression (miR156 OE) alfalfa (Aung et al. 2015a, 2015b). To explore the effects of *SPL6* and *SPL13* genes in the event of miR156 OE, *SPL6- and SPL13*-silenced (SPL6 RNAi and SPL13 RNAi, respectively) alfalfa were generated with RNAi technique. However, little is known on structural changes of inherent molecular structure of alfalfa induced by miR156 OE and *SPL6/13* silencing.

Synchrotron based FTIR microspectroscopy (SR-IMS) is a rapid and non-destructive bioanalytic technique, which can explore molecular chemistry under cellular level (Yu 2006). Compared with conventional light source, synchrotron beam light is 1000 times brighter, which enables a higher signal-to-noise ratio and small effective source size (Miller and Dumas 2006). This study aimed to explore the effects of overexpressing miR156 on inherent molecular structures of alfalfa leaves in comparison with silencing *SPL6* and *SPL13* genes. Moreover, chemical image method was used to determine the effects of such genetic modification on localizations of chemical components in alfalfa leaves.

4.3.2 Materials and Methods

4.3.2.1 Alfalfa leaf sample

Alfalfa genotypes were same as previous study (Project 4.2). There were three sub-genotypes of miR156 OE, SPL6 RNAi and SPL13 RNAi been selected with WT alfalfa in this study. Five alfalfa leaves from each genotype were freeze-dried for cross section and BaF2 window preparation. Procedures for cross section and window preparation were previous described in Chapter 3.3.

4.3.2.2 Synchrotron light source, FTIR spectra collection and chemical mapping

Information about synchrotron light source, FTIR spectral collection and chemical image mapping procedures were same as the first project. Details can be found in Chapter 3.3.

4.3.2.3 Statistical analysis

Procedure MIXED of SAS 9.4 software (SAS Institute, Inc., Cary, NC, USA) was used to analyze univariate variables data. The model for univariate data was: $Y_{ijk} = \mu + G_i + S_j(G_i) + H_k + \varepsilon_{ijk}$, where Y_{ijk} was the dependent variable; μ was the population mean; G_i was the genotype effect; $S_j(G_i)$ was the sub-genotype effect nested in genotype effect; H_k was the random harvest effect, ε_{iik} was the random error. Prior to variance analysis, a SAS macro with same model was used to remove all outliers with a criterion of Studentized Residual greater than 2.5. Contrast statement was used to compare WT with transgenic alfalfa and between transformed alfalfa. The Kenward-Roger method was used for estimation of degree of freedom and Tukey-Kramer method was used for multi-comparison among genotypes. Proc Univariate with Normal and Plot options was used to test the normality of the residue of each variable. Significance level was set at $P<0.05$ and trend was set at $0.05<P<0.10$.

4.3.3 Results and Discussion

4.3.3.1 Comparative effects of overexpressing miR156 and silencing SPL6 and SPL13 genes on carbohydrate and lignin structures of alfalfa leaves

Carbohydrate and lignin structural parameters of miR156 OE, SPL6 and SPL13 RNAi and WT alfalfa leaves are shown in Table 4.3.1. The miR156 OE had higher TC1 and TC4 than SPL6 RNAi, and higher TCA compared with WT and SPL6 RNAi ($P<0.05$). As for TC2 and TC3 peaks, miR156 OE tended to be higher than WT and SPL RNAi ($P<0.1$). In terms of CEC parameters, both miR156 OE and SPL13 RNAi had lower CEC than SPL6 RNAi ($P<0.01$) and miR156 OE had lower CECA than SPL6 RNAi ($P<0.05$). Although there were no significant differences in STC parameters, miR156 tended to have higher STC1 and STC2 heights compared with other

genotypes (P<0.10). As for lignin peak height, all transformed alfalfa had lower values compared with WT (P<0.01).

Table 4.3.1 Carbohydrate and lignin structural parameters of leaf cross sections of miR156 OE in comparison with SPL6 RNAi, SPL13 RNAi and WT alfalfa.

Items [1]	Alfalfa Genotypes						Contrast [3]		
	WT	miR156 OE	SPL6 RNAi	SPL13 RNAi	SEM 2	P value	G vs W	S vs W	S vs M
Total Carbohydrate (TC) Peaks and Area									
TC1	0.201ab	0.405a	0.245b	0.360ab	0.0396	0.030	0.061	0.144	0.041
TC2	0.158	0.257	0.182	0.235	0.0236	0.076	0.105	0.206	0.087
TC3	0.100	0.161	0.116	0.144	0.0136	0.064	0.091	0.194	0.062
TC4	0.076ab	0.162a	0.090b	0.139ab	0.0159	0.020	0.060	0.161	0.023
TCA	24.504b	44.057a	28.573b	39.576ab	4.1624	0.043	0.083	0.183	0.053
Cellulosic Compounds (CEC) Peak and Area									
CEC	0.061ab	0.054b	0.069a	0.061b	0.0024	0.000	0.971	0.326	<0.001
CECA	3.213ab	2.643b	3.468a	2.986ab	0.1447	0.013	0.433	0.953	0.006
Structural Carbohydrate (STC) Peaks and Area									
STC1	0.031	0.063	0.037	0.050	0.0074	0.063	0.139	0.329	0.033
STC2	0.051	0.084	0.057	0.070	0.0076	0.064	0.146	0.338	0.036
STC3	0.062	0.085	0.072	0.080	0.0074	0.294	0.173	0.256	0.288
STC4	0.053	0.068	0.064	0.069	0.0045	0.242	0.083	0.098	0.771
STCA	11.794	18.328	14.049	16.283	1.5174	0.101	0.098	0.196	0.082
Lignin Peak									
Lignin	0.030a	0.015b	0.020b	0.020b	0.0016	0.008	0.003	0.007	0.020

[1] TC1-TC4, four major peaks at ca. 1026 (TC1) 1074 (TC2), 1104 (TC3) and 1149 (TC4) cm^{-1} in TC region, respectively; TCA, peak area of TC region; CEC, cellulosic compounds (ca. 1237 cm^{-1}); CECA, peak area of CEC region; STC1-STC4, four major peaks at ca. 1317 (STC1), 1370 (STC2), 1397 (STC3) and 1453 (STC4) cm^{-1}, respectively.
[2] SEM, standard error of mean. Values with different letters in each row differ significantly at P>0.05.
[3] G vs W, contrast between genetic modified alfalfa and WT; S vs W, contrast between SPL RNAi and WT; S vs M, contrast between SPL RNAi and miR156 OE

Statistical patterns for carbohydrate structure in alfalfa leaves were different from whole alfalfa samples as shown in Chapter 4.2, indicating there are significant structural differences in alfalfa leaves and stems. Structural differences between leaves and whole alfalfa samples were also found in the first project. In the current study, all transformed alfalfa had lower carbohydrate parameters than WT for homogenous samples, but miR156 OE tented to have higher TC and STC parameters in leaves compared with other genotypes. Given the correlations between carbohydrate and chemical composition (Chapter 5.1), miR156 OE alfalfa might contain more carbohydrate in its leaves compared with other genotypes. Compared with STC parameters, larger differences were found in TC parameters especially for TC1 and TCA. TC1 is the peak centers at 1025 cm^{-1} and are reported to be more related to starch (Damiran and Yu 2010). Contrast results showed that miR156 OE had higher TC1 peak than other genotypes, indicating higher starch content in miR156 OE leaves. This might be the reason for higher starch of miR156 OE (Chapter 4.1), as miR156 OE was reported to have more bushy phenotype (Aung et al. 2015a). Lignin peak centers at ca. 1515 cm^{-1} (Prates et al. 2018b) and was more obvious in alfalfa leaves spectra compared with whole alfalfa samples, therefore it was determined in the current study. All transformed alfalfa showed lower lignin peak compared with WT ($P<0.01$) and miR156 OE was even lower than SPL6/13 RNAi according to contrast results ($P<0.05$). This suggested that miR156 OE alfalfa had lower lignin content in its leaves compared with WT, which might explain the lower lignin of some miR156 OE sub-genotypes (Aung et al. 2015c).

4.3.3.2 Comparative effects of overexpressing miR156 and silencing SPL6 and SPL13 genes on amide and lipid structures of alfalfa leaves

Amide and lipid-related structural parameters of miR156 OE, SPL6 and SPL13 RNAi and WT alfalfa leaves are shown in Table 4.3.2. For amide parameters, miR156 OE had lower Amide

II and Amide II area (AIIA) than SPL6 RNAi ($P<0.05$) and lower alpha-helix, beta-sheet, Amide Area (AA) and Amide I area (AIA) compared with both SPL RNAi alfalfa ($P<0.01$). Although there were no differences between WT and SPL RNAi, contrast results indicated that SPL RNAi had higher amide parameters compared with WT ($P<0.01$), largely due to high values of SPL6 RNAi. In terms of CCO parameters, SPL13 RNAi had lower CCO and CCOA compared with WT ($P<0.05$) and lower CCO compared with both WT and SPL13 RNAi. Furthermore, there were no differences in ASCC parameters between alfalfa genotypes ($P>0.05$), although contrast results showed SPL RNAi tended to be higher than miR156 OE in SyCH3 and AsCH3 peaks.

Like carbohydrate structures, amide and lipid structural parameters of alfalfa leaves were also different from whole alfalfa samples in previous study (Chapter 4.2). Both SPL6 RNAi and SPL13 RNAi were greater than miR156 OE and WT in β-sheet and amide areas, which were reported to be negatively related to protein content in alfalfa (Lei et al. 2018c). This suggested that SPL RNAi alfalfa had lower protein content in their leaves, especially compared with miR156 OE. Since β-sheet structure is more resistant to enzyme digestion (Yu 2005a), proteins in SPL RNAi alfalfa leaves might be also less available compared with miR156 OE. CCO peak at 1740 cm^{-1} is the C=O ester stretching band that are related to lipid compounds (Xin and Yu 2014; Doiron and Yu 2017). Yari et al.(2017) evaluated lipid parameters of alfalfa differed in maturity and found higher AsCH2, SyCH2 and ASCCA when alfalfa reach to early flowering stage.

Table 4.3.2 Amide and lipid-related structural parameters of leaf cross sections of miR156 OE in comparison with SPL6 RNAi 13 RNAi and wild type (WT) alfalfa.

Items [1]	Alfalfa Genotypes				SEM [2]	P value	Contrast [3]		
	WT	miR156 OE	SPL6 RNAi	SPL13 RNAi			G vs W	S vs W	S vs M
Amide Peaks and Areas									
Amide I	0.449ab	0.352b	0.515a	0.476a	0.0220	0.004	0.973	0.215	0.001
Amide II	0.298ab	0.229b	0.336a	0.298ab	0.0173	0.010	0.697	0.508	0.002
α-sheet	0.399ab	0.357b	0.505a	0.479a	0.0227	0.005	0.201	0.036	0.001
β-helix	0.439ab	0.322b	0.475a	0.434a	0.0213	0.004	0.403	0.648	0.001
AA	57.639ab	44.409b	64.719a	58.687a	3.1582	0.008	0.731	0.432	0.002
AIA	38.659ab	30.337b	43.910a	40.216a	2.0287	0.006	0.873	0.315	0.001
AIIA	18.982ab	13.902b	20.620a	18.198ab	1.0981	0.010	0.423	0.808	0.002
Carbonyl C=O (CCO) Peak and Area									
CCO	0.035a	0.026ab	0.032a	0.024b	0.0030	0.048	0.120	0.167	0.517
CCOA	0.836a	0.609ab	0.606ab	0.407b	0.0954	0.045	0.044	0.029	0.286
Asymmetric and Symmetric CH2 and CH3 (ASCC) Peaks and Area									
SyCH2	0.182	0.150	0.185	0.198	0.0253	0.481	0.915	0.815	0.157
SyCH3	0.103	0.093	0.106	0.108	0.0056	0.202	0.940	0.658	0.047
AsCH2	0.296	0.260	0.310	0.332	0.0437	0.581	0.946	0.723	0.215
AsCH3	0.102	0.094	0.120	0.120	0.0112	0.234	0.614	0.346	0.060
ASCCA	20.112	18.774	22.031	22.794	1.9989	0.392	0.728	0.480	0.118

[1] AA, amide area; AIA, amide I area; AIIA, amide II area. [4] CCO, carbonyl C=O; CCOA, carbonyl C=O area. [5] SyCH2, symmetric CH_2 (ca. 2850 cm^{-1}); SyCH3, symmetric CH_3 (ca. 2872 cm^{-1}); AsCH2, asymmetric CH_2 (ca. 2920 cm^{-1}); AsCH3, asymmetric CH_3 (ca. 2955 cm^{-1}); ASCCA, peak area of asymmetric and symmetric CH_2 and CH_3 (baseline ca. 3000–2761 cm^{-1}).

[2] SEM, standard error of mean. Values with different letters in each row differ significantly at P>0.05.

[3] G vs W, contrast between genetic modified alfalfa and WT; S vs W, contrast between SPL RNAi and WT; S vs M, contrast between SPL RNAi and miR156 OE;

4.3.3.3 Chemical image mapping of alfalfa leaves of miR156 OE, SPL6 and SPL13 RNAi compared with WT with Synchrotron based FTIR spectroscopy

Visible images and chemical mappings of miR156 OE, SPL6 and SPL13 RNAi and WT alfalfa leaves are shown in Figure 4.3.1, Figure 4.3.2, Figure 4.3.3 and Figure 4.3.4, respectively. For carbohydrate components mappings, TC and STC functional groups were mainly located in epidemical areas in miR156 OE, SPL6 RNAi and WT, and were located more evenly in SPL13 RNAi alfalfa leaves. Compared with miR156 OE and WT, both SPL RNAi alfalfa had lower TC intensity. Moreover, SPL6 RNAi had lower STC intensity and SPL13 RNAi had lower CEC intensity compared with other genotypes. There were not many differences between miR156 OE and WT alfalfa in carbohydrate distributions and intensities. To the contrary of carbohydrate region, amide region had highest intensity in mesophyll condensed areas of alfalfa leaves, followed by ASCC and CCO regions. Compared with other genotypes, SPL13 RNAi alfalfa had lower intensity of amide area. As for CCO area, miR156 OE was highest while SPL6 RNAi was lowest intensity with no significant differences between SPL13 RNAi and WT. Moreover, all transformed alfalfa had higher ASCC intensity especially for miR156 OE which had the highest intensity. In terms of lignin area, SPL13 RNAi had the highest intensity followed by WT with no significant differences between miR156 OE and SPL6 RNAi. Compared with conventional light source, synchrotron light is 100-1000 times brighter, making it a better light source for FTIR spectroscopy (Miller and Dumas 2006). Thanks to its high brightness, synchrotron light had smaller effective source size with higher signal to noise ratio (Miller and Dumas 2006). This feature enables synchrotron-based FTIR spectroscopy to evaluate molecular chemistry at ultra-spatial resolution of 3-10 μm (Yu 2004; Yang and Yu 2017). Therefore, synchrotron images could localize chemical functional groups of plant samples at cellular and subcellular dimensions (Yu et al. 2004a).

Chemical images revealing structural features of corn grains (Yu et al. 2004b), feather (Yu et al. 2004a) and plant tissues (Yu et al. 2003c, 2019) have been reported.

4.3.4 Conclusion

In conclusion, overexpression of miR156 had higher TC and STC spectral parameters and lower CEC and amide parameters compared with silencing of *SPL6* gene in alfalfa leaves. Moreover, all transformed alfalfa had lower lignin peaks in alfalfa leaves compared with WT. Chemical mapping showed that alfalfa leaves had higher amide intensity over other compounds, followed by lipids and carbohydrates. In conclusion, overexpression of miR156 and silencing of *SPL6* and *SPL13* genes significantly affected molecular structures and chemical localizations in alfalfa leaves.

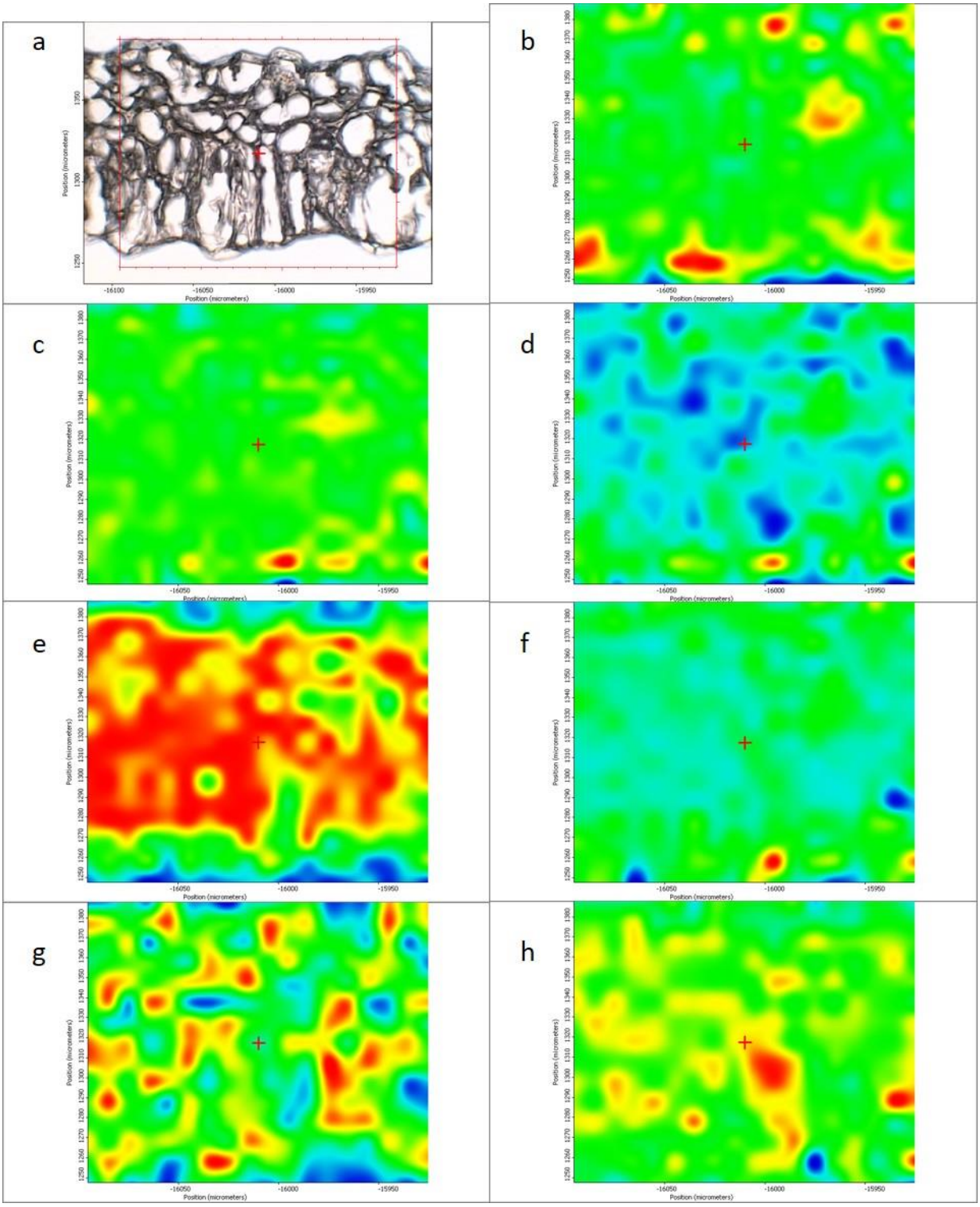

Figure 4.3.1 Chemical mapping of SPL6 RNAi (6-425) alfalfa leave in nutritional related spectral regions.

Figures are original visible image (a), and chemical group maps of total carbohydrate (TC, b), cellulosic compounds (CEC, c), structural carbohydrate (STC, d), amide (e), carbonyl C=O (CCO, f), asymmetric and symmetric CH_2 and CH_3 (ASCC, g) and lignin (h) regions.

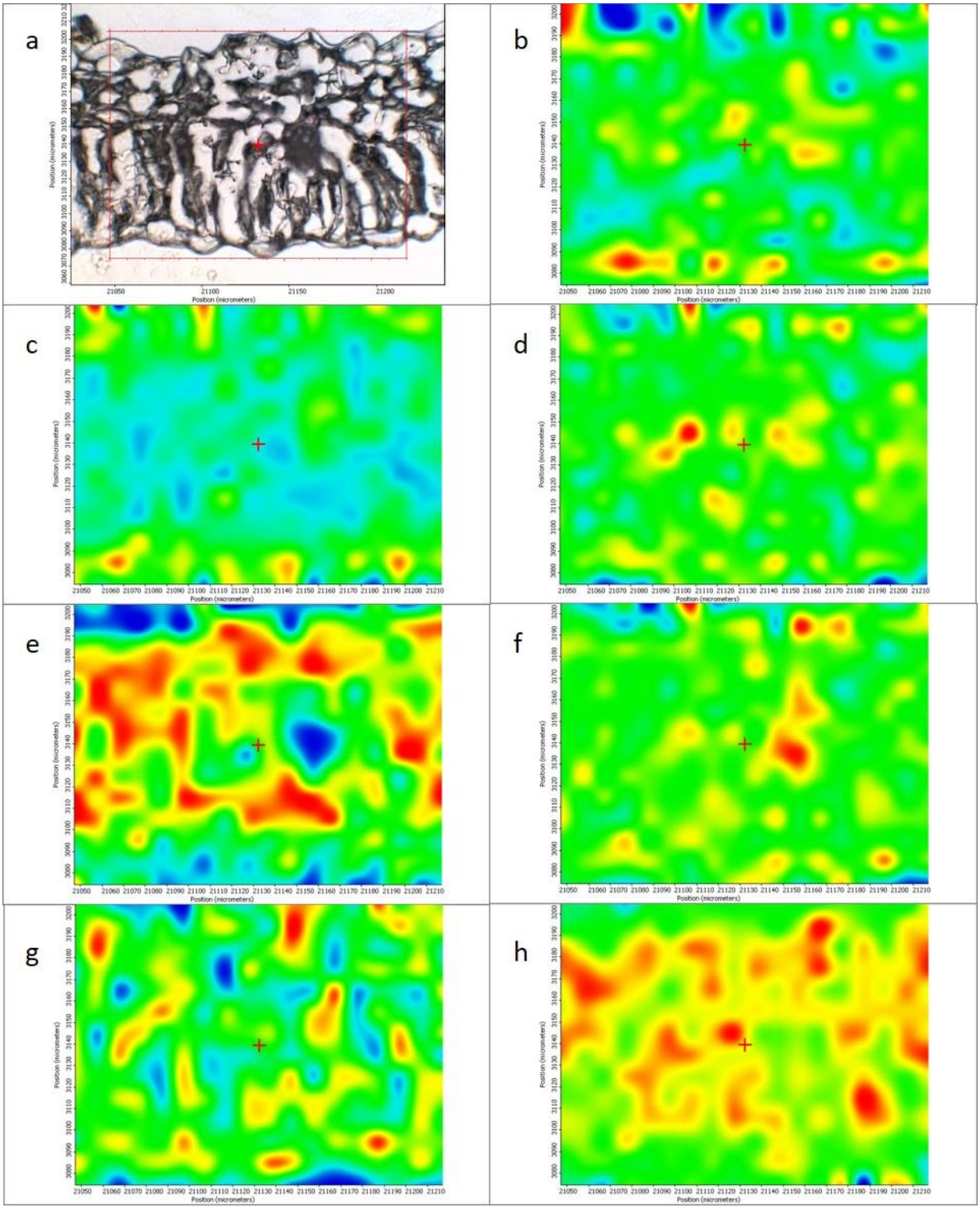

Figure 4.3.2 Chemical mapping of SPL13 RNAi (13-5) alfalfa leave in nutritional related spectral regions.

Figures are original visible image (a), and chemical group maps of total carbohydrate (TC, b), cellulosic compounds (CEC, c), structural carbohydrate (STC, d), amide (e), carbonyl C=O (CCO, f), asymmetric and symmetric CH_2 and CH_3 (ASCC, g) and lignin (h) regions.

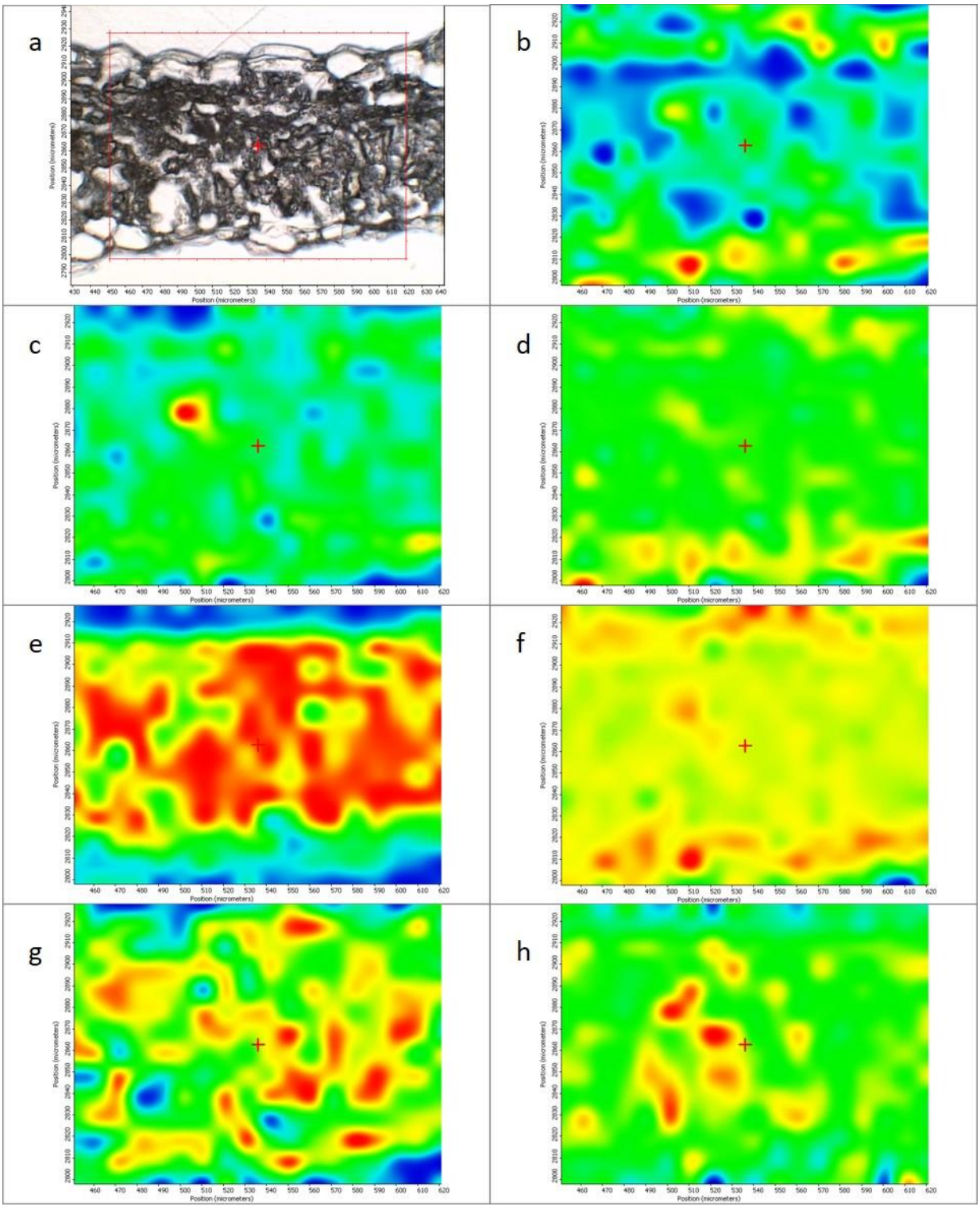

Figure 4.3.3 Chemical mapping of miR156 OE (A17) alfalfa leave in nutritional related spectral regions.

Figures are original visible image (a), and chemical group maps of total carbohydrate (TC, b), cellulosic compounds (CEC, c), structural carbohydrate (STC, d), amide (e), carbonyl C=O (CCO, f), asymmetric and symmetric CH_2 and CH_3 (ASCC, g) and lignin (h) regions.

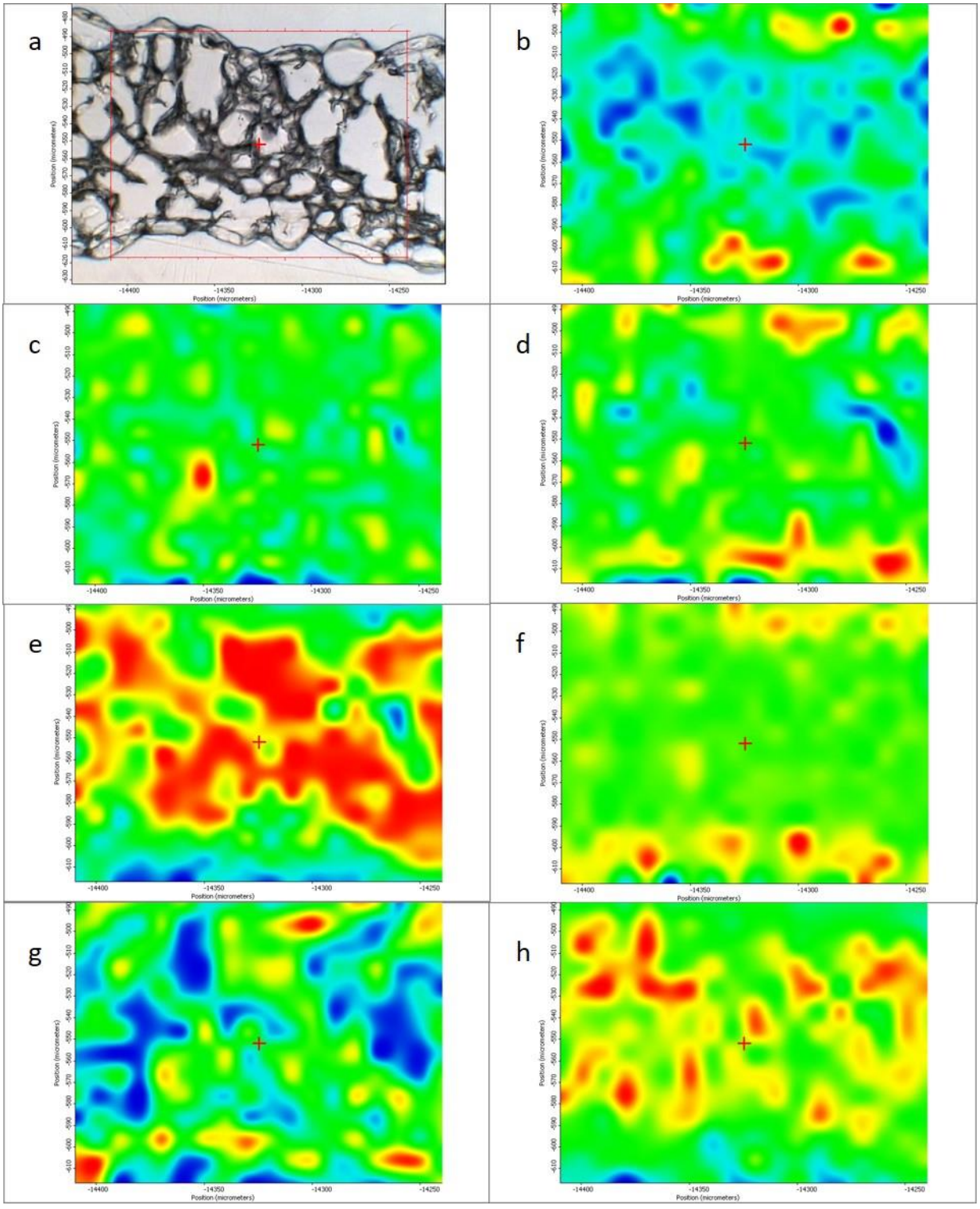

Figure 4.3.4 Chemical mapping of WT alfalfa leave in nutritional related spectral regions.

Figures are original visible image (a), and chemical group maps of total carbohydrate (TC, b), cellulosic compounds (CEC, c), structural carbohydrate (STC, d), amide (e), carbonyl C=O (CCO, f), asymmetric and symmetric CH_2 and CH_3 (ASCC, g) and lignin (h) regions.

4.4 Effects of overexpression of miR156 on *in vitro* fermentation characteristics of alfalfa: in comparison with silencing *SPL6* and *SPL13* genes

Abstract: The objectives of this study were to investigate the effects of overexpression of miR156 on *in vitro* fermentation characteristics of alfalfa in comparison with silencing *SPL6* and *SPL13* genes. Three subgenotypes for miR156 OE, SPL6 RNAi and SPL13 RNAi grown with WT in a greenhouse and harvested three times were used in this study. Production of gas, VFA and ammonia and degradations of DM and NDF were determined. Results showed there were no differences in gas production kinetics between alfalfa genotypes ($P>0.05$), although SPL RNAi had higher asymptotic gas production in contrast to WT. As for nutrient degradation, miR156 OE had higher soluble DM compared with SPL RNAi genotypes, and higher effective DM degradation than WT and SPL13 RNAi ($P<0.05$). In terms of ammonia production, SPL13 RNAi was higher at 12 h than WT and miR156 OE ($P<0.05$). There were no differences in acetate, propionate, butyrate and total VFA production between alfalfa genotypes ($P>0.05$). However, SPL13 RNAi had higher asymptotic production for total VFA than WT, and higher for acetate than miR156 OE ($P<0.05$). In addition, SPL RNAi had higher long-chain VFA compared with WT and miR156 OE ($P<0.05$). In conclusion, overexpression of miR156 increased DM degradation of alfalfa, but had no other influences on rumen fermentation. In contrast, silencing of *SPL6* and *SPL13* had more impacts on fermentation features, especially for silencing of *SPL13* gene. Moreover, miR156 OE was more different from SPL13 RNAi than from SPL6 RNAi, implying a more important role of *SPL6* gene.

4.4.1 Introduction

Alfalfa (*Medicago sativa*) is an important perennial legume forage and is widely cultivated and utilized around the world (Lei et al. 2017). Alfalfa production in North America accounts about 40~50% of world total production by cultivation area (Volenec et al. 2002; Cash and Hu 2009). Compared with other forages, alfalfa contains high protein and lower NDF, which is especially beneficial for high-production dairy cows (Berthiaume et al. 2010). The forage quality of alfalfa is affected by many factors, with the most important one being the age at harvest (Belyea et al. 1999). Forage quality of alfalfa decreases with age, while biomass yield increases (McCaslin et al. 2015). Therefore, to maximize profitability, commercial harvest of alfalfa usually takes place at early-bud stage when both yield and quality are relatively high. One solution to this dilemma between yield and quality is to prolong the vegetative growth of alfalfa, which could increase biomass yield without compromise or even increase forage quality (Tadege et al. 2015).

Genetic engineering has been an effective approach in alfalfa improvement for decades (Volenec et al. 2002; Kumar 2011; Li and Brummer 2012). It alters agronomic traits of plants by manipulating genes of interest, which is more efficient and accurate compare with conventional breeding (Lei et al. 2017). MicroRNA 156 (miR156), one of plant specific microRNA, has been reported as a main control for plant growth transition (Wang 2016). This microRNA controls transition of both from juvenile stage to adult stage and from adult phase to reproduction phase (Wu et al. 2009; Wang and Wang 2015). MiR156 regulates its target genes, *Squamosa Promoter Binding Protein-Like (SPL)* genes, which in turn affect expression of miR172 to control the onset of flowering (Wu et al. 2009). A previous study showed that overexpression of miR156 in alfalfa delayed flowering, enhanced shoot branching, increased trichome density and biomass yield (Aung et al. 2015a, 2015b). Moreover, two target *SPL* genes of miR156, *SPL6* and *SPL13*, were repressed in miR156 overexpression alfalfa (miR156 OE). However, little is known about the ruminal

degradation profiles of miR156 OE alfalfa. Moreover, it was also unclear about the effects of silencing *SPL6* and *SPL13* genes individually on degradational profiles of alfalfa and how different they are from miR156 OE in terms of ruminal degradation. Therefore, this study aimed to determine the effects of overexpression miR156 on *in vitro* fermentation features of alfalfa in comparison with silencing of *SPL6* and *SPL13* genes.

4.4.2 Materials and Methods

4.4.2.1 Alfalfa samples

Alfalfa samples were same as Chapter 4.1. There were three subgenotypes for miR156 OE, SPL6 RNAi and SPL13 RNAi. Alfalfa plants were grown in a greenhouse and harvested three times for both transformed alfalfa and WT control.

4.4.2.2 In vitro fermentation

The *in vitro* fermentation was conducted at the Department of Animal and Poultry Science, University of Saskatchewan. Rumen fluid were collected from two rumen-cannulated lactating Holstein cows. Fermentation procedure was same as previous project (Chapter 3.4), except for the measurement of gas production. Gas production was measured with an electronic pressure transducer (Model PX4200-015GI; Omega Engineering, Inc., Laval, QC, Canada). Calculation of gas production from pressure values was performed according to Refat et al. (2017a).

4.4.2.3 Statistical analysis

Production kinetics of gas, total VFA, acetate and propionate and degradational kinetics of DM and NDF were estimated with non-liner model same as the first project. Detailed description in kinetics estimation can be found in Chapter 3.4.

The Mixed procedure of SAS 9.4 (SAS Institute, Inc., Cary, NC, USA) was used to analyze fermentation data. The model used was: $Y_{ijk} = \mu + G_i + S_j(G_i) + H_k + \varepsilon_{ijk}$, where Y_{ijk} was the dependent variable; μ was the population mean; G_i was the genotype effect; $S_j(G_i)$ was the sub-genotype effect nested in genotype effect; H_k was the random harvest effect, ε_{iik} was the random error. The degree of freedom was estimated with Kenward-Roger method. Prior to variance analysis, outliers were detected with "residual" option for Studentized Residual greater than 2.5. Contrast statement was used to determine the difference between WT and transformed alfalfa, and the Tukey-Kramer method was used in multi-treatment comparison. The "pdmix800" macro (Saxton 1998) was used to letter grouping the treatment mean. Normality test of the residual data was performed using Shapiro-Wilk method by using Univariate Procedure with Normal and Plot options. Significance level was set at $P<0.05$ and trend as set at $0.05<P<0.10$.

4.4.3 Results and Discussion

4.4.3.1 Comparative effects of overexpressing miR156 and silencing SPL6 and SPL13 genes on in vitro gas production of alfalfa

Cumulative gas production and production kinetics of miR156 OE, SPL6 RNAi, SPL13 RNAi, and WT alfalfa are shown in Table 4.4.1. There were no significant differences between alfalfa genotypes in the beginning until 12 h of fermentation, when SPL13 RNAi tended to have higher gas production than WT ($P<0.10$). At 24 h, SPL13 RNAi tended to have higher gas production compared with miR156 OE ($P<0.10$). Moreover, contrast results showed significant differences among SPL RNAi and miR156 OE alfalfa ($P<0.05$). In terms of gas production kinetics, the asymptotic gas production tended to be significant among genotypes and SPL RNAi were higher than WT according to contrast results ($P<0.05$). There were no significant differences for other production kinetics among alfalfa genotypes ($P>0.05$).

Table 4.4.1 Gas production during *in vitro* fermentation of miR156 OE alfalfa in comparison with SPL6 RNAi, SPL13 RNAi alfalfa and WT control

Items [1]	Alfalfa Genotypes				SEM [2]	P value	Contrast [3]		
	WT	miR156 OE	SPL13 RNAi	SPL6 RNAi			G vs W	S vs W	S vs M
Gas production after hours of incubation (mL/g DM)									
2 h	27.27	24.24	26.08	24.28	1.046	0.171	0.135	0.202	0.375
4 h	52.39	47.30	51.79	49.34	1.917	0.167	0.302	0.525	0.092
8 h	89.14	85.09	86.81	85.01	3.383	0.824	0.454	0.500	0.792
12 h	108.97	114.13	124.65	117.15	9.829	0.058	0.109	0.057	0.095
24 h	143.68ab	140.77b	153.65a	149.74ab	8.550	0.056	0.384	0.144	0.013
48 h	161.21	169.20	175.02	177.37	10.096	0.104	0.058	0.035	0.103
Gas production kinetics									
a (mL/g DM)	161.75	169.97	175.27	178.59	10.507	0.091	0.052	0.032	0.101
c (%/h)	9.74	9.14	9.37	8.64	0.473	0.433	0.338	0.321	0.788
Lag time (h)	0.07	0.23	0.36	0.25	0.171	0.128	0.071	0.050	0.335
AP (mL)	11.25	10.71	11.51	10.69	0.602	0.343	0.675	0.825	0.391

[1] a, asymptotic gas production; c, production fractional rate; lag time, initial delay of production onset; AP, average production at half of asymptotic production, $AP = a \times c \div (2 \times (ln2 + c \times lag))$.
2 SEM, standard error of mean; Means with different letters in each row differ significantly at P<0.05.
3 G vs W, contrast between wild type and transgenic alfalfa; S vs W, contrast between SPL RNAi and WT; S vs M, contrast between SPL RNAi and miR156 OE.

Gas production is an indirect index for nutrient degradation in the rumen. Gas is produced from substrate fermentation and consists mainly of carbon dioxide and methane (Russell and Rychlik 2001; Kamalak et al. 2009). Studies reported that gas production was negatively correlated with NDF, ADF and ADL content (Ndlovu and Nherera 1997; Getachew et al. 2004). However, the relationship between gas production and CP content was controversial, as both negative and positive correlations were reported (Larbi et al. 1998; Getachew et al. 2004). In the current study, SPL13 RNAi had higher gas production at 24 h of fermentation compared with miR156 OE.

Moreover, contrast results showed SPL RNAi had higher asymptotic gas production compared with WT but was not different from miR156 OE. Chemically, there were no significant differences between SPL RNAi and WT, except that SPL RNAi tended to have lower ADF than WT alfalfa (Chapter 4.1). This might explain the slightly higher gas production of SPL RNAi compared with WT alfalfa. Compared with HB12i and TT8i alfalfa in the first project (Chapter 3.4), alfalfa in this study had higher gas production. HB12i and TT8i alfalfa had higher NDF and lower CP compared with alfalfa samples in the current study (Lei et al. 2018c), which was in consistent with those correlations studies (Ndlovu and Nherera 1997; Larbi et al. 1998). According to those correlation studies, we could expect higher gas production from miR156 OE as it had lower NDF (Chapter 4.1); however, this was not observed in this study. This indicates that NDF has less effects on gas production when its level is low, which is in agreement with Getachew et al. (2004).

4.4.3.2 Comparative effects of overexpressing miR156 and silencing SPL6 and SPL13 genes on in vitro VFA production of alfalfa

Table 4.4.2 illustrates VFA production kinetics of miR156 OE, SPL6 RNAi, SPL13 RNAi and WT alfalfa. Genetic modification of overexpressing miR156 and silencing SPL6 and SPL13 genes had significant on asymptotic production of total VFA and acetate. The SPL13 RNAi had higher total VFA compared with WT and higher acetate compared with miR156 OE ($P<0.05$). The production rate of acetate tended to be higher for miR156 OE compared with other genotypes according to contrast results ($P<0.05$). Besides, there were no significant differences between alfalfa genotypes in terms of propionate production. Productions of each individual VFA during fermentation are shown in Figure 4.4.1. There were no significant differences between alfalfa genotypes for short-chain VFA; however, significant differences were observed in long-chain VFA during *in vitro* fermentation. At 4 h, both SPL RNAi genotypes had higher valerate and

isovalerate compared with miR156 OE (P<0.01). At 12 h, SPL13 RNAi had higher isobutyrate and isovalerate compared with WT and miR156 OE (P<0.001), and higher caproate than miR156 OE (P<0.05). In contrast, WT had higher valerate production compared with SPL6 RNAi and miR156 OE alfalfa (P<0.05). At 24 h, both SPL RNAi alfalfa had higher valerate production compared with WT control (P<0.05). In addition, there were no significant differences between alfalfa genotypes in total VFA production and C2:C3 ratio (P>0.05).

Table 4.4.2 Volatile fatty acids (VFA) production kinetics during *in vitro* fermentation of miR156 OE alfalfa in comparison with SPL6 RNAi, SPL13 RNAi alfalfa and WT alfalfa

Items [1]	Alfalfa Genotypes				SEM [2]	P value	Contrast [3]		
	WT	miR156 OE	SPL13 RNAi	SPL6 RNAi			G vs W	S vs W	S vs M
Total VFA production kinetics									
a	5.39b	6.33ab	7.79a	6.08ab	0.939	0.042	0.075	0.052	0.19
c	9.30	13.23	9.13	12.49	3.736	0.672	0.616	0.753	0.396
Lag	0.69	0.89	3.48	1.85	2.108	0.726	0.671	0.558	0.427
AP	0.36	0.46	0.37	0.40	0.107	0.480	0.582	0.803	0.169
Acetate production kinetics									
a	2.99ab	3.38b	4.70a	3.71ab	0.576	0.030	0.114	0.053	0.047
c	8.98	19.29	7.84	9.34	3.683	0.052	0.569	0.946	0.008
Lag	0.72	0.82	3.33	1.45	2.292	0.782	0.747	0.648	0.516
AP	0.20	0.36	0.20	0.21	0.071	0.190	0.572	0.945	0.054
Propionate production kinetics									
a	1.50	1.59	1.89	1.59	0.162	0.136	0.267	0.187	0.215
c	14.28	13.16	6.96	15.21	3.227	0.244	0.59	0.509	0.528
Lag	1.41	1.43	0.09	1.49	0.526	0.150	0.568	0.404	0.209
AP	0.11	0.11	0.09	0.12	0.016	0.477	0.829	0.765	0.685

1. *a*, asymptotic production (mmol/g DM); *c*, production fractional rate (%/h); lag time (h), initial delay of production onset; AP, average production at half of asymptotic production (mmol), which was calculated as $AP = a \times c \div (2 \times (ln2 + c \times lag))$.
2. SEM, standard error of mean; Means with different letters in each row differ significantly at P<0.05.
3. G vs W, contrast between wild type and transgenic alfalfa; S vs W, contrast between SPL RNAi and WT; S vs M, contrast between SPL RNAi and miR156 OE.

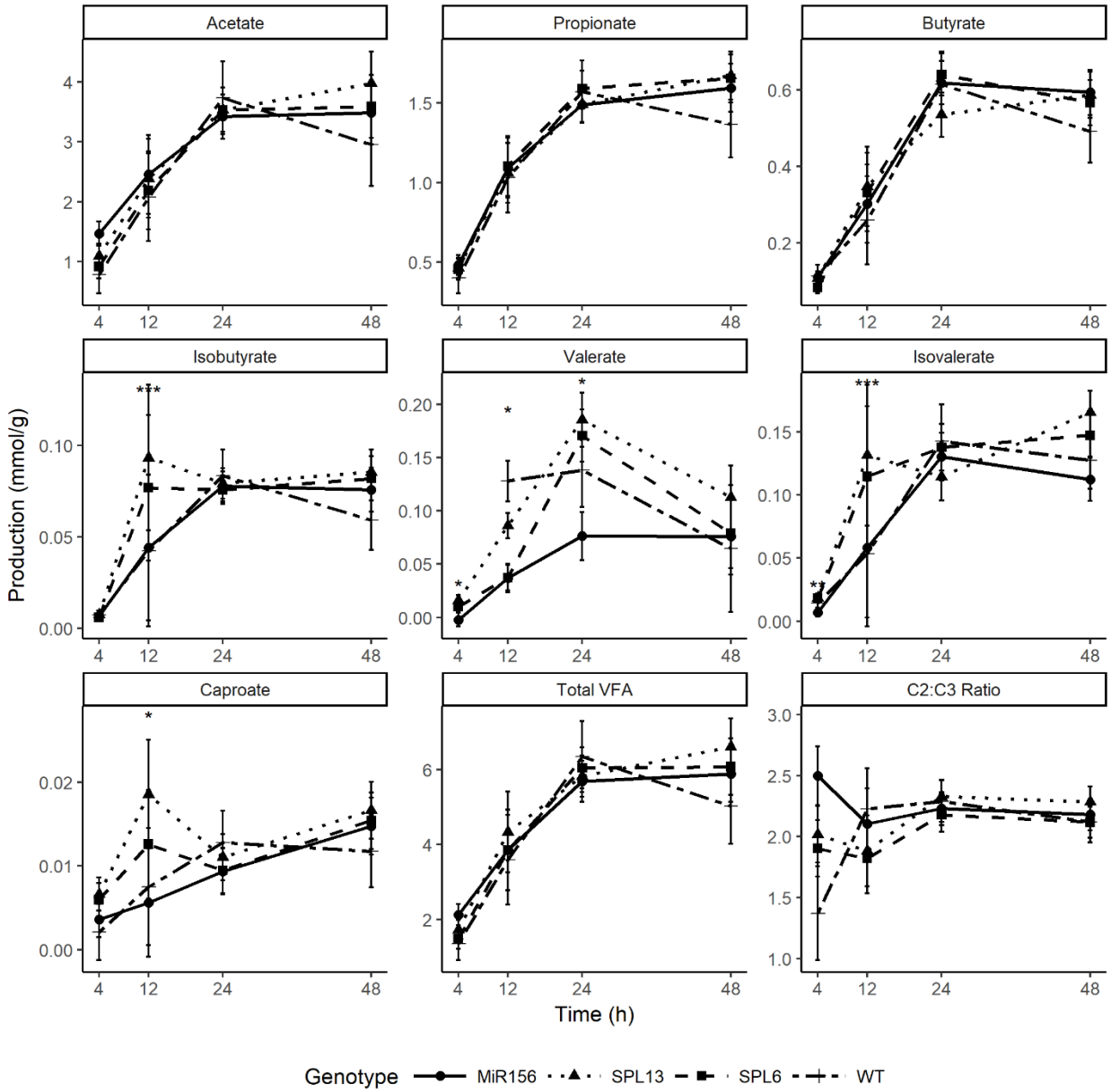

Figure 4.4.1 Volatile fatty acids (VFA) production during *in vitro* fermentation of miR156 OE alfalfa in comparison with SPL6 RNAi, SPL13 RNAi alfalfa and WT control. * means P<0.05; ** means P<0.01; *** means P<0.001.

In general, acetate and propionate accounted for more than 80% of total VFA production, while butyrate and long-chain VFAs only contributed less than 20% to total VFA production. This VFA production pattern of alfalfa is consistent with a previous study (Jonker et al. 2012b) and the first project (Chapter 3.4). The C2:C3 ratio was about 2.2, which is slightly lower than alfalfa hay in previous studies (Getachew et al. 2004; Jonker et al. 2012b). This might be attributed to the

differences in chemical compositions and experiment variations. A previous study showed that alfalfa with higher NFC was found to have low C2:C3 ratio (Berthiaume et al. 2010). Moreover, starch and protein promote propionate production while cellulose promotes acetate production (Bannink et al. 2006). Alfalfa samples in this study had lower NDF but higher CP and NFC compared with samples in previous studies, which explains the lower C2:C3 ratio. Furthermore, SPL13 RNAi had higher asymptotic production of acetate than miR156 OE alfalfa, which was consistent with their gas productions as gas and VFA productions were positively correlated with each other (Getachew et al. 2004).

4.4.3.3 Comparative effects of overexpressing miR156 and silencing SPL6 and SPL13 genes on in vitro ammonia production of alfalfa

Genetic modification of overexpressing miR156 and silencing *SPL6* and *SPL13* genes had little impacts on *in vitro* ammonia production (Figure 4.4.2). Significant differences were only observed at 12 h of fermentation, when SPL13 RNAi had higher ammonia production than miR156 OE on DM basis and higher than all other genotypes on N basis ($P<0.05$). In addition, ammonia production tended to be significant at 48 h of fermentation. The SPL6 RNAi tended to be lower than miR156 OE on DM basis and lower than SPL13 RNAi on N basis ($P<0.10$). The ammonia productions in the current study were comparable to those in the first project (except for TT8i alfalfa) and higher than those in a previous study (Wang et al. 2006). The SPL6 RNAi had similar ammonia production as WT alfalfa in the first project, while other alfalfa genotypes had similar ammonia production as TT8i RNAi in the first project (Chapter 3.4).

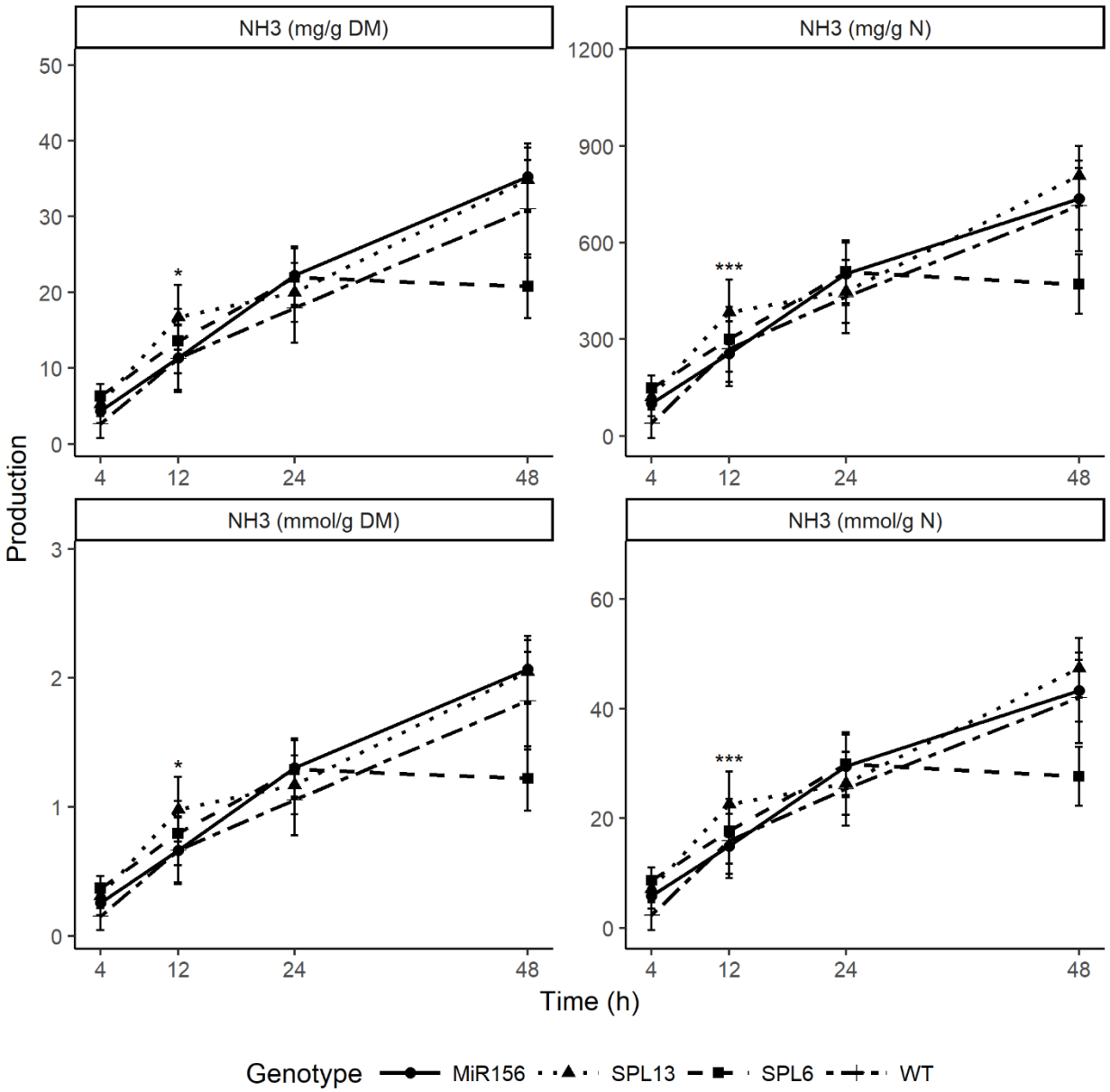

Figure 4.4.2 Ammonia production during *in vitro* fermentation of miR156 OE alfalfa in comparison with SPL6 RNAi, SPL13 RNAi alfalfa and WT control. * means P<0.05; ** means P<0.01; *** means P<0.001.

Ammonia is produced from the deamination of dietary protein during rumen fermentation, and is an important nitrogen source for most rumen bacteria (Yang et al. 2010). Bacteria utilize carbon skeleton from carbohydrate and ammonia from protein and NPN to synthesize microbial protein. When carbohydrate or energy is limited, the excessive ammonia will be absorbed via the rumen epithelia and converted into urea in the liver (Tas et al. 2006). Therefore, the ammonia

concentration is maintained in a healthy level. However, the ammonia production accumulates during *in vitro* fermentation due to the lack of absorption system, although a small amount is released with gas during gas measurement (Spanghero et al. 2018). In this study, SPL6 RNAi tended to have lower ammonia production at the end of fermentation compared with other genotypes, which might be due to a higher utilization of ammonia in microbial synthesis. Our microbial nitrogen fractional study showed that SPL6 RNAi had higher N^{15} enrichment for liquid microbial nitrogen than SPL13 RNAi (Chapter 4.5), which implies a higher microbial production in the liquid phase for SPL6 RNAi alfalfa.

4.4.3.4 Comparative effects of overexpressing miR156 and silencing SPL6 and SPL13 genes on in vitro DM and NDF degradation of alfalfa

Degradation kinetics of DM and NDF of miR156 OE, SPL6 RNAi, SPL13 RNAi and WT alfalfa are presented in Table 4.4.3. For DM degradation kinetics, miR156 OE had lower undegradable fraction (U) compared with other genotypes ($P<0.05$), but higher soluble fraction (S) compared with both SPL RNAi alfalfa ($P<0.05$). In addition, miR156 OE had higher effective DM degradation compared with WT and SPL13 ($P<0.05$), and higher than SPL RNAi group according to contrast results ($P<0.05$). In terms of NDF degradation kinetics, there were no significant differences between alfalfa genotypes ($P>0.05$). Nevertheless, miR156 OE tended to have lower undegradable fraction (U) but higher degradable fraction (D) compared with SPL RNAi group according to contrast results ($P<0.1$). Degradation of DM and NDF at each time point of each alfalfa genotypes are demonstrated in Figure 4.4.3. There were significant differences between alfalfa genotypes in DM degradation at the beginning and the end of fermentation. The miR156 OE had significant higher DM degradation than SPL RNAi alfalfa at 0 h ($P<0.01$) and

higher than SPL6 RNAi alfalfa at 2 h ($P<0.05$). At 48 h of fermentation, miR156 OE had higher DM degradation compared with SPL13 RNAi and WT alfalfa ($P<0.05$).

Table 4.4.3 Degradation kinetics of DM and NDF of *in vitro* fermentation of miR156 OE alfalfa in comparison with SPL6 RNAi, SPL13 RNAi alfalfa and WT control

Items [1]	Alfalfa Genotypes				SEM [2]	P value	Contrast [3]		
	WT	miR156 OE	SPL13 RNAi	SPL6 RNAi			G vs W	S vs W	S vs M
Dry matter (DM) kinetics (%)									
K_d (%/h)	7.72	8.41	8.85	9.10	0.706	0.651	0.348	0.288	0.456
T0 (h)	0.75	1.44	1.24	1.32	0.405	0.481	0.158	0.209	0.556
U	20.80a	17.03b	20.11a	20.20a	1.925	0.026	0.269	0.677	0.004
S	33.73ab	36.00a	32.53b	32.11b	0.825	0.002	0.882	0.269	<0.001
D	45.47	46.97	47.35	47.69	1.981	0.708	0.325	0.294	0.653
ED	62.32b	66.36a	63.72b	64.27ab	1.449	0.035	0.084	0.244	0.017
Neutral detergent fiber (NDF) kinetics (%)									
K_d (%/h)	4.72	5.58	5.82	6.01	0.820	0.808	0.410	0.378	0.699
T0 (h)	0.15	0.80	0.72	0.92	0.441	0.656	0.269	0.276	0.965
U	37.56	34.56	40.59	40.54	2.896	0.318	0.824	0.522	0.083
D	62.44	65.44	59.41	59.46	2.896	0.318	0.824	0.522	0.083
ED	30.04	34.96	32.93	34.13	1.499	0.172	0.064	0.108	0.309

1 U, undegradable fraction (%); S, soluble fraction (%); D, degradable fraction (%); K_d, degradation rate (%/h); ED, effective degradation (%).
[2] SEM, standard error of mean. Means with different letters in each row differ significantly at $P<0.05$.
[3] G vs W, contrast between wild type and transgenic alfalfa; S vs W, contrast between SPL RNAi and WT; S vs M, contrast between SPL RNAi and miR156 OE.

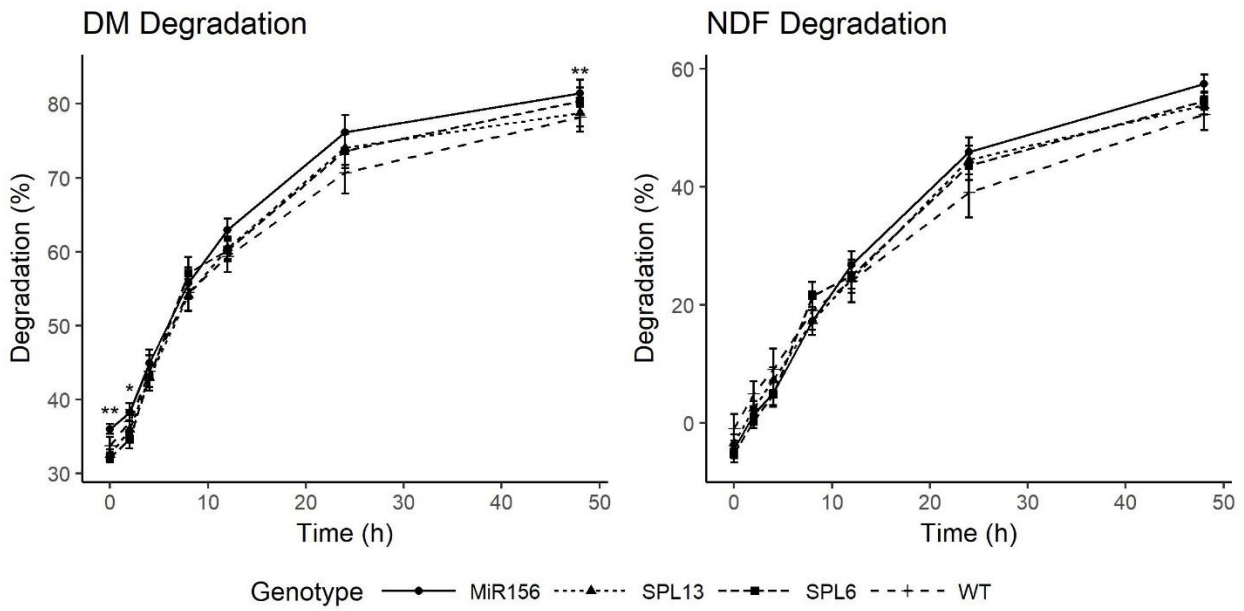

Figure 4.4.3 Degradations of dry matter and neutral detergent fiber of miR156 OE alfalfa in comparison with SPL6 RNAi, SPL13 RNAi alfalfa and WT control. * means P<0.05; ** means P<0.01; *** means P<0.001.

DM degradations of alfalfa in this study were higher compared with alfalfa samples in the first project (Chapter 3.4) and previous studies (Yu et al. 2003b; Yari et al. 2012a; Jonker et al. 2012b). This is because alfalfa samples in this study were harvest at early vegetative stage and had higher CP and lower NDF compared with those in the first project and previous studies. In contrast, Wang et al. (2006) reported similar *in vitro* DM degradation of *Lc*-transformed alfalfa, which accumulates anthocyanins in leaves and stems and had similar NDF and protein contents as samples in this study. It was the same reason for miR156 OE having higher DM degradation compared with other genotypes. Chemically, miR156 OE had higher insoluble protein and lower fiber (Chapter 3.4), which makes it more degradable in the rumen. As for NDF degradations, alfalfa samples in this study were also higher than those in the first project and previous studies, which were about 40% at 48 h of incubation (Yu et al. 2003b; Yari et al. 2012a). This could also be attributed to the differences in harvest time as alfalfa samples were younger in this study. Yu et

al. (2003b) reported that NDF degradation increased very little after 24 h of incubation for alfalfa samples harvested after early-bud stage, especially for late-harvested samples (Yu et al. 2003b). In contrast, NDF degradation in this study further increased from about 45% at 24 h to about 55% at 48 h of incubation. Nevertheless, the majority of degradable NDF was degraded within 24 h of fermentation. Furthermore, genetic modifications also had no effects on NDF degradation, which is similar to the findings of the first project (Chapter 3.4). This suggests that genetic modification might only affects NDF content but had no influences on degradability of NDF.

4.4.4 Conclusion

In conclusion, overexpression of miR156 increased DM degradation of alfalfa, but had no other influences on rumen fermentation. In contrast, silencing of *SPL6* and *SPL13* genes had more impacts on fermentation features, especially for silencing of *SPL13* gene. Moreover, miR156 OE was more different from SPL13 RNAi than from WT or SPL6 RNAi. Taken all together, we suggest that *SPL* genes might work antagonistically in miR156 overexpression event and *SPL6* gene might play a more important role than *SPL13* gene.

4.5 Effects of overexpressing miR156 on microbial synthesis, protein degradation and digestion, and nutritive modeling of alfalfa: in comparison with silencing *SPL6* and *SPL13* genes

Abstract: The objectives of this study were to explore the effects of overexpressing miR156 on microbial synthesis, protein degradation and digestion, and nutritive modeling of alfalfa in comparison with silencing *SPL6* and *SPL13* genes. Alfalfa samples used were same as Chapter 4.1. Daisy II fermentation, three-step *in vitro* digestion, and modeling methods were same as previous project (project one). Results showed that miR156 OE had lower degradational rate and degradation of CP at 4, 8 and 12 h of incubation ($P<0.05$). As for the N^{15} enrichment (APE) in MN fractions, SPL6 RNAi had higher APE in LMN at 4 h, followed by miR156 OE and WT, and SPL13 RNAi had the lowest ($P<0.05$). In terms of MN fractions, both SPL RNAi had higher LAMN than miR156 OE at 12 h of incubation ($P<0.05$). In contrast, miR156 OE had higher FAMN at 4 h than WT and SPL6 RNAi, but lower FAMN/RN ratio than WT at 24 h of incubation ($P<0.05$). For protein metabolic profiles, both DVE/OEB and NRC-2001 system showed transformed alfalfa had higher MCP_{RDP} than WT according to contrast results. In addition, miR156 OE had lower ENDP compared with WT and SPL13 RNAi ($P<0.05$) in DVE/OEB system and higher AMCP than other genotypes in NRC-2001 system ($P<0.05$). In conclusion, overexpression of miR156 reduced initial degradation and degradation rate of CP but did not affect overall CP degradation, which could improve nutrient synchronization of alfalfa in the rumen. Also, although miR156 OE provided more AMCP, there were no significant differences in total truly available protein between alfalfa genotypes.

4.5.1 Introduction

Alfalfa is one of the most widely cultivated perennial legume forages thanks to its high nutritive values and good adaptability (Cash and Hu 2009; Lei et al. 2017). Studies reported that North America contributes approximately 40~50 % of world alfalfa production by cultivation area (Volenec et al. 2002; Cash and Hu 2009). Yield of alfalfa forage is affected by many factors, such as variety, soil type and fertility, environment and cutting schedules (Undersander et al. 2011). Varieties with high fall dormancy score (less dormant) and low winterhardiness provide higher biomass yield but forage quality is relatively low (Putnam et al. 2005). This negative correlation between biomass yield and forage quality of alfalfa also exists with cutting schedule. Forage quality and NDF degradability of alfalfa declines with plant maturity (McCaslin et al. 2015). Therefore, commercial cutting for alfalfa forage is recommended at early-bud stage to maximize the profitability. One potential approach to solve this dilemma is to prolong the vegetative growth of alfalfa, which makes it possible for producing alfalfa forage with high biomass yield and high forage quality (Tadege et al. 2015).

MicroRNA 156 (miR156) is a plant specific microRNA that controls plant transitions both from juvenile stage to adult stage and from adult vegetative stage to reproductive stage (Wu et al. 2009; Wang and Wang 2015; Wang 2016). Function of miR156 for controlling flowering largely depends on its target *Squamosa promoter binding protein like (SPL)* genes, which regulate the expression of miR172 (Wu et al. 2009). Aung et al. (2015a, 2015b) reported that overexpression of miR156 delayed the onset of flowering, enhanced shoot branching and increased biomass yield of alfalfa. In addition, decreases in expression levels of *SPL6* and *SPL13* genes were also observed in miR156 overexpression (miR156 OE) alfalfa (Aung et al. 2015a, 2015b). However, the effects of such genetic modification on protein degradational and metabolic features of alfalfa remains unknown. Alfalfa contains high protein and less NDF and is very good for high-production dairy

cows (Berthiaume et al. 2010). Studies showed that protein degradational and metabolic features of alfalfa are affected by stage of maturity (Yari et al. 2012a, 2012b) and genetic modifications (Jonker et al. 2012b; Heendeniya et al. 2019). The objective of this study was to evaluate the effects of overexpressing miR156 on microbial synthesis, protein degradation and digestion, and protein metabolic characteristics of alfalfa in comparison with silencing *SPL6* and *SPL13* genes.

4.5.2 Material and Methods

4.5.2.1 Alfalfa samples

Alfalfa samples used in this study were same to Chapter 4.1. Details in sample growth, harvest and preparation could be found in Chapter 4.1.

4.5.2.2 Daisy II fermentation, Intestinal digestion, microbial nitrogen fractions and protein metabolic parameters modelling

Procedures for Daisy II fermentation, three-step intentional digestion, microbial nitrogen partition and modelling for protein metabolic parameters were same as the first project. Detailed description could be found in Chapter 3.5.

4.5.2.3 Statistic Analysis

The nonlinear model for CP degradation was same as the first project and was previously described in Chapter 3.5. The Proc Mixed of SAS 9.4 (SAS Institute, Inc., Cary, NC, USA) was used to analyze data. The model was: $Y_{ijk} = \mu + G_i + S_j(G_i) + H_k + \varepsilon_{ijk}$, where Y_{ijk} was the dependent variable; μ was the population mean; G_i was the genotype effect; $S_j(G_i)$ was the sub-genotype effect nested in genotype effect; H_k was the random harvest effect, ε_{iik} was the random error. The degree of freedom was estimated with Kenward-Roger method. Prior to variance analysis, outliers were detected with "residual" option in Model statement with a Studentized Residual greater than 2.5. Contrast statement was used to determine the difference between WT

and transformed alfalfa, SPL RNAi and WT, and SPL RNAi and miR156 OE alfalfa. The Tukey-Kramer method was used in multi-treatment comparison. The "pdmix800" macro (Saxton 1998) was used to letter grouping treatment means. Normality test of the residual data was performed using Shapiro-Wilk method by using Proc Univariate with Normal and Plot options. Significance level was set at $P<0.05$ and trend was set at $0.05<P<0.10$.

4.5.3 Results and Discussion

4.5.3.1 Comparative effects of overexpressing miR156 and silencing SPL6 and SPL13 genes on ruminal degradation and intestinal digestion of protein of alfalfa

Degradation kinetics of protein and intestinal digestion of rumen undegradable protein (IDRUP) of miR156 OE, SPL6 RNAi, SPL13 RNAi, and WT alfalfa are shown in Table 4.5.1. The miR156 OE had lower degradation rate (K_d) of protein compared with SPL13 RNAi ($P<0.05$). In addition, contrast results showed miR156 OE had lower K_d of protein compared with SPL RNAi group ($P<0.01$). Apart from K_d, there were no significant differences between alfalfa genotypes in protein degradation kinetics and intestinal digestion ($P>0.05$). However, miR156 OE alfalfa had significant lower initial CP degradation during the *in vitro* fermentation (Figure 4.5.1). At 4, 8 and 12 h of incubation, miR156 OE alfalfa had lower CP degradation compared with both SPL RNAi alfalfa ($P<0.05$), which explains the lower degradation rate of miR156 OE. This feature implies that miR156 OE alfalfa may have lower incidences for rumen bloat, which is caused by the high initial degradation of forage protein in the rumen (Jonker et al. 2012a). There were no significant differences between alfalfa genotypes in intestinal digestion of rumen undegradable protein (IDRUP) ($P>0.05$), which is same as the first project and both were about 70% (Chapter 3.5).

The CP degradation of alfalfa reached 80% at 12 h of fermentation (except for miR156 OE), which was higher than those in the first project. This could be attributed to the differences in age at cutting as alfalfa samples in the current study were harvested at an earlier age compared to

those in the first project. However, alfalfa samples in this study had equal CP degradation of 90% at 24 h of fermentation compared with WT alfalfa in the first project (Chapter 3.5). This indicates that, within a certain range, younger alfalfa is more degradable in the beginning of fermentation. Jonker et al. (2012b) examined the CP degradation of anthocyanin-accumulating *Lc*-transgenic alfalfa, which were found lower than WT control. Yari et al. (2012a) reported that alfalfa harvested at early flower stage had lower CP degradation than those harvested at early bud and late bud stages. Once again, CP degradation in the current study was higher than those in Jonker's and Yari's studies, which can be attributed to differences in stage of maturity. Alfalfa samples were harvested at a younger stage in the current study compared with those in the previous studies (Yari et al. 2012a; Jonker et al. 2012b).

Table 4.5.1 Degradation kinetics of CP and intestinal digestion of rumen undegradable CP of miR156 OE alfalfa in comparison with SPL6 RNAi, SPL13 RNAi alfalfa and WT control.

Items [1]	Alfalfa Genotypes				SEM [2]	P value	Contrast [3]		
	WT	miR156 OE	SPL13 RNAi	SPL6 RNAi			G vs W	S vs W	S vs M
Rumen degradational kinetics of CP (%)									
K_d (%/h)	25.72ab	17.30b	29.93a	26.04ab	2.093	0.015	0.694	0.505	0.003
U	11.82	9.40	12.75	12.10	1.605	0.389	0.871	0.813	0.113
S	49.82	53.60	52.57	52.52	1.679	0.419	0.160	0.215	0.444
D	38.35	36.75	34.84	35.38	1.993	0.535	0.293	0.226	0.353
ED	82.45	82.56	82.86	82.62	1.051	0.993	0.885	0.860	0.872
Intestinal digestion of rumen undegraded CP (IDRUP, %)									
IDRUP	70.48	70.51	66.96	68.9	2.286	0.235	0.27	0.628	0.135

[1] U, undegradable fraction (%); S, soluble fraction (%); D, degradable fraction (%); K_d, degradation rate (%/h); ED, effective degradation (%).
[2] SEM, standard error of mean. Means with different letters in each row differ significantly at $P<0.05$.
[3] G vs W, contrast between wild type and transgenic alfalfa; S vs W, contrast between SPL RNAi and WT; S vs M, contrast between SPL RNAi and miR156 OE.

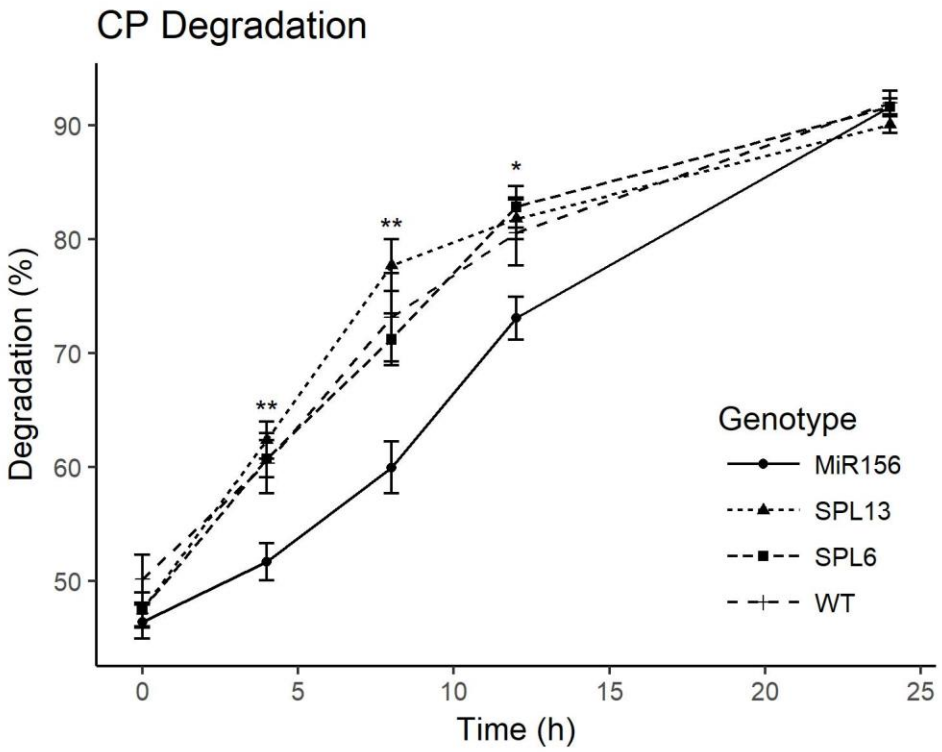

Figure 4.5.1 *In vitro* CP degradations of miR156 OE alfalfa in comparison with SPL6 RNAi, SPL13 RNAi alfalfa and WT control. *, P<0.05; **, P<0.01, ***, P<0.001.

4.5.3.2 Comparative effects of overexpressing miR156 and silencing SPL6 and SPL13 genes on fractional microbial nitrogen of alfalfa

The N^{15} enrichment (atom excess %, APE) of fractional microbial nitrogen of miR156 OE, SPL6 RNAi, and SPL13 RNAi are shown in Table 4.5.2. For liquid associated microbial N (LMN), SPL6 RNAi had significantly higher APE than miR156 OE at 4 h, followed by WT and SPL13 RNAi (P<0.001). At 12 and 24 h, SPL6 RNAi had higher APE in LMN than SPL13 RNAi (P<0.05), and both SPL RNAi were not different from WT and miR156 OE (P>0.05). For loosely attached microbial N (LAMN) and feed residue N (RN), there were no significant differences between alfalfa genotypes, although SPL RNAi tended to have higher APE in RN at 12 h of fermentation according to contrast results. The microbial N fractions and ratio of FAMN to RN of transformed and WT alfalfa are presented in Table 4.5.3. For LAMN, both SPL RNAi alfalfa were higher than miR156 and SPL6 RNAi also was higher than WT at 12 h of fermentation (P<0.05). In terms of

FAMN, miR156 OE was higher than WT and SPL6 RNAi at 4 h of incubation (P<0.05). In addition, miR156 OE also tended to be higher than SPL RNAi group at 12 h according to contrast results (P<0.1). As for FAMN/RN ratio, there were no significant differences between alfalfa genotypes although miR156 OE tended to be lower than SPL RNAi group at 12 h of incubation according to contrast results (P<0.10).

Table 4.5.2 N^{15} enrichment (atom excess %) of fractional microbial nitrogen (MN) of miR156 OE alfalfa in comparison with SPL6 RNAi, SPL13 RNAi alfalfa and WT control.

Time (h)	Alfalfa Genotypes				SEM [1]	P value	Contrast [2]		
	WT	miR156 OE	SPL13 RNAi	SPL6 RNAi			G vs W	S vs W	S vs M
Liquid associated microbial N (LMN)									
4	2.31c	2.84b	1.58d	2.95a	0.020	<0.001	0.003	0.123	<0.001
12	3.43ab	3.32ab	2.67b	4.13a	0.262	0.016	0.880	0.939	0.749
24	3.42ab	2.98ab	2.56b	3.34a	0.164	0.024	0.110	0.110	0.847
Loosely attached microbial N (LAMN)									
4	4.50	4.74	4.88	4.83	0.176	0.616	0.270	0.234	0.539
12	4.70	5.03	5.36	5.19	0.375	0.565	0.300	0.245	0.434
24	4.42	4.60	4.68	4.72	0.290	0.809	0.433	0.389	0.636
Feed residual N (RN)									
4	0.77	0.80	0.92	0.83	0.049	0.230	0.323	0.218	0.187
12	1.09	1.02	1.27	1.25	0.139	0.332	0.646	0.400	0.094
24	1.76	1.42	1.64	1.58	0.137	0.303	0.244	0.404	0.149

1 SEM, standard error of mean. Means with different letters in each row differ significantly at P<0.05.
2. G vs W, contrast between wild type and transgenic alfalfa; S vs W, contrast between SPL RNAi and WT; S vs M, contrast between SPL RNAi and miR156 OE.

SPL6 RNAi had higher APE for LMN compared with SPL13 RNAi, implying that SPL6 RNAi might have higher microbial protein production in the liquid phase. This was confirmed with the lower ammonia production of SPL6 RNAi in *in vitro* fermentation, which might be caused by a higher synthesis of microbial protein. Moreover, SPL RNAi also had higher LAMN at 12 h

of incubation compared with miR156 OE and WT. This suggested that SPL RNAi alfalfa might provide more nutrients for attached microbes at 12 h compared with WT and miR156 OE. It also might be the same reason for the higher FAMN for miR156 OE at 4 h of fermentation as it contains higher soluble fractions of protein (Table 4.5.1) and DM (Chapter 3.5).

Table 4.5.3 Fractional microbial nitrogen (MN) of miR156 OE alfalfa in comparison with SPL6 RNAi, SPL13 RNAi alfalfa and WT control.

Time (h)	Alfalfa Genotypes				SEM [1]	P value	Contrast [2]		
	WT	miR156 OE	SPL13 RNAi	SPL6 RNAi			G vs W	S vs W	S vs M
Loosely attached microbial N (LAMN, mg/g residue)									
4	3.20	2.76	3.19	2.99	0.433	0.836	0.740	0.874	0.466
12	7.62bc	7.79c	9.67ab	10.26a	0.867	0.003	0.072	0.014	0.001
24	17.07	16.91	14.20	16.87	1.374	0.147	0.493	0.350	0.218
Firmly attached microbial N (FAMN, mg/g residue)									
4	5.75b	7.03a	6.35ab	6.07b	0.446	0.001	0.022	0.147	0.001
12	5.71	7.16	6.04	6.07	0.466	0.086	0.234	0.555	0.022
24	5.90	5.72	6.60	5.95	0.570	0.456	0.788	0.612	0.284
FAMN to residual N (RN) ratio (FAMN/RN)									
4	17.16	16.91	18.06	17.25	0.630	0.530	0.805	0.631	0.293
12	23.18	20.40	23.63	24.01	1.408	0.219	0.820	0.775	0.052
24	39.84a	30.96b	34.88ab	32.28ab	1.354	0.033	0.016	0.028	0.110

[1] SEM, standard error of mean. Means with different letters in each row differ significantly at $P<0.05$.
[2] G vs W, contrast between wild type and transgenic alfalfa; S vs W, contrast between SPL RNAi and WT; S vs M, contrast between SPL RNAi and miR156 OE.

Same as the first project (Chapter 3.5), APE was higher for LAMN compared with LMN, which indicates that the attached microbes had higher N assimilation compared with suspending microbes. The higher APE for LAMN compared with LMN was also found in a previous study on *Lc*-transgenic alfalfa (Wang et al. 2006). In addition, FAMN was also higher than LAMN in this

study and the first project, which was in consistent with a previous report (Jonker et al. 2012b). The APE of microbial fraction and MN production in this study were equivalent to those in the first project (Chapter 3.5) and those in Wang's study (Wang et al. 2006). The FAMN/RN was slightly higher at 24 h of fermentation in this study compared with the first project (Chapter 3.5), and both exceeded 30%. This means more than 30% nitrogen in the feed residue was of microbial origin, which implies an underestimation of protein degradation with *in vitro* methods. Wang et al. (2006) reported that LAMN and FAMN together accounted for more than 40% of feed residue N, which is in line with our results.

4.5.3.3 Comparative effects of overexpressing miR156 and silencing SPL6 and SPL13 genes on protein metabolic parameters of alfalfa with DVE/OEB system and NRC-2001 system

Protein metabolic parameters of transformed and WT alfalfa with DVE/OEB system are shown in Table 4.5.4. There were no significant differences between alfalfa populations in fermentable organic matter (FOM), microbial protein (MCP) based on FOM and absorbable microbial protein (AMCP) ($P>0.05$). Moreover, contrast results showed transformed had higher MCP based on rumen degradable protein (RDP) compared with WT ($P=0.05$). For endogenous protein (ENDP), miR156 OE was lower than WT and SPL13 RNAi alfalfa ($P<0.05$). Contrast results showed transformed alfalfa had lower ENDP than WT ($P<0.05$) and miR156 OE was even lower than SPL RNAi ($P<0.01$). For rumen undegradable protein (RUP), there were no significant differences between alfalfa populations ($P>0.05$). In addition, there were no significant differences between alfalfa populations in total truly absorbed protein (DVE), feed milk value (FMV) and degraded protein balance (OEB). Nevertheless, contrast results showed that transformed alfalfa tended to have higher OEB values compared with WT alfalfa ($P<0. 1$).

Table 4.5.4 Predicted protein supply and feed milk value with DVE/OEB system of miR156 OE alfalfa in comparison with SPL6 RNAi, SPL13 RNAi alfalfa and WT control.

Items [1]	Alfalfa Genotypes				SEM [2]	P value	Contrast [3]		
	WT	miR156 OE	SPL13 RNAi	SPL6 RNAi			G vs W	S vs W	S vs M
Absorbable microbial protein (AMCP, g/Kg DM)									
FOM	624.46	642.75	624.88	641.35	14.762	0.149	0.294	0.454	0.231
MCP_{FOM}	93.67	96.41	93.73	96.20	2.214	0.149	0.294	0.453	0.231
MCP_{RDP}	211.27	226.45	222.47	219.95	10.277	0.127	0.050	0.099	0.200
$AMCP_{DVE}$	59.71	61.46	59.75	61.33	1.412	0.149	0.294	0.453	0.231
Endogenous protein (ENDP, g/Kg DM)									
ENDP	17.26a	15.00b	16.86a	15.73ab	1.282	0.003	0.041	0.158	0.007
Absorbable rumen undegraded protein (ARUP, g/Kg DM)									
RUP_{DVE}	50.81	54.62	52.38	52.60	4.587	0.917	0.684	0.779	0.598
$ARUP_{DVE}$	35.85	38.63	35.45	36.42	4.073	0.819	0.830	0.986	0.403
Total truly absorbed protein (DVE, g/Kg DM)									
DVE	78.31	85.45	78.14	82.86	5.649	0.229	0.401	0.633	0.136
Degraded protein balance (OEB, g/Kg DM)									
OEB	117.60	130.05	128.74	124.05	9.636	0.150	0.068	0.116	0.333
Feed milk value (FMV, Kg milk/Kg feed)									
FMV_{DVE}	1.59	1.74	1.59	1.68	0.115	0.229	0.417	0.656	0.134

[1] FOM, fermentable organic matter; MCP_{FOM}, predicted microbial protein synthesized based on energy (FOM); MCP_{RDP}, predicted microbial protein synthesized based on rumen degradable protein (RDP); RUP, rumen undegraded protein.
[2] SEM, standard error of mean. Means with different letters in each row differ significantly at $P<0.05$.
[3] G vs W, contrast between wild type and transgenic alfalfa; S vs W, contrast between SPL RNAi and WT; S vs M, contrast between SPL RNAi and miR156 OE.

Table 4.5.5 Predicted protein supply and feed milk value with NRC-2001 system of miR156 OE alfalfa in comparison with SPL6 RNAi, SPL13 RNAi alfalfa and WT control.

Items [1]	Alfalfa Genotypes				SEM [2]	P value	Contrast [3]		
	WT	miR156 OE	SPL13 RNAi	SPL6 RNAi			G vs W	S vs W	S vs M
Absorbable microbial protein (AMCP, g/Kg DM)									
MCP_{TDN}	83.68b	86.26a	84.64b	85.03b	0.743	0.001	0.009	0.061	0.001
MCP_{RDP}	183.86	197.12	193.51	191.39	8.939	0.102	0.041	0.087	0.171
$AMCP_{NRC}$	53.56b	55.27a	54.26b	54.42b	0.480	0.001	0.007	0.048	0.001
Absorbable rumen undegraded protein (ARUP, g/Kg DM)									
RUP_{NRC}	45.78	49.21	47.19	47.39	4.133	0.917	0.684	0.779	0.598
$ARUP_{NRC}$	32.30	34.80	31.93	32.81	3.670	0.820	0.830	0.986	0.403
Absorbable endogenous protein (AECP, g/Kg DM)									
ECP	11.00	11.01	10.98	10.97	0.025	0.082	0.559	0.259	0.014
AECP	4.40	4.40	4.39	4.39	0.009	0.154	0.641	0.343	0.029
Total metabolizable protein (MP, g/Kg DM)									
MP	90.25	94.53	90.56	91.62	4.018	0.623	0.639	0.846	0.257
Degraded protein balance (DPB, g/Kg DM)									
DPB	117.56	129.98	127.64	124.83	9.814	0.260	0.094	0.150	0.360
Feed milk value (FMC, Kg milk/Kg feed)									
FMV_{NRC}	1.83	1.92	1.84	1.86	0.081	0.609	0.638	0.849	0.249

1. MCP_{TDN}, predicted microbial protein synthesized based on energy (TDN); MCP_{RDP}, predicted microbial protein synthesized based on rumen degradable protein (RDP); RUP, rumen undegraded protein; ECP, endogenous protein.
2. SEM, standard error of mean. Means with different letters in each row differ significantly at $P<0.05$.
3. G vs W, contrast between wild type and transgenic alfalfa; S vs W, contrast between SPL RNAi and WT; S vs M, contrast between SPL RNAi and miR156 OE.

Table 4.5.5 shows protein metabolic parameters of transformed and WT alfalfa with NRC-2001 system. The miR156 OE alfalfa had higher MCP based on total digestive nutrients (TDN) compared with other genotypes ($P=0.001$) and contrast results showed transformed alfalfa had higher MCP based on RDP than WT ($P<0.05$). Same as with DVE/OEB system, energy was also the limit factor for MCP synthesis in NRC-2001 system. Therefore, AMCP was also calculated based on available energy and were found higher for miR156 OE compared with other genotypes ($P=0.001$). For RUP parameters, there were no significant differences between alfalfa genotypes ($P>0.05$). As for endogenous protein (ECP), contrast results showed SPL RNAi were lower than miR156 OE for ECP and absorbable ECP (AECP) ($P<0.05$), which was opposite to DVE/OEB system. This is because DVE/OEB system considers ENDP as a loss of protein, while NRC-2001 regards ECP as a part of total metabolizable protein (MP) (Theodoridou and Yu 2013b). Therefore, calculations for endogenous protein were opposite for these two nutritional systems. In addition, there were no significant differences between alfalfa genotypes in MP and FMV($P<0.05$) and transformed alfalfa tended to have higher degradable protein balance (DPB) than WT according to contrasts ($P<0.1$), which is in line with DVE/OEB system.

For total truly absorbed protein (DVE or MP) of alfalfa samples, AMCP had the most contribution followed by RUP, which was consistent with each other for these two systems. Microbial protein synthesis relies on both energy and nitrogen supply and accounts for a large amount of total absorbable protein (Clark et al. 1992). A synchronized supply of 32 g N/Kg CHO or 25 g N/Kg OM is considered to be optimum for microbial growth (Yari et al. 2012a). Both nutritional systems found unbalanced protein and energy supply for alfalfa with transformed alfalfa tending to be more unbalanced, which made energy the limiting factor for microbial protein synthesis. Previous studies also reported the unbalanced nitrogen to energy ratio of alfalfa but

degraded protein balance were lower in their studies (Yu et al. 2003a; Yari et al. 2012a, 2012b). Yari et al. (2012b) reported that degraded protein balance of alfalfa decreased with stage of maturity, which explains the lower degraded protein balance in previous studies. Alfalfa samples in studies of Yu et al. (2003a) and Yari et al. (2012b) were harvested after early bud stage, while samples were harvested at early vegetative stage in the current study.

For endogenous protein, different patterns were observed with DVE/OEB and NRC-2001 systems and the values were higher for ENDP in DVE/OEB system. This is because DVE/OEB system considers endogenous protein as a lost portion of absorbable protein and is calculated as 75 g/Kg of undigested DM (Tamminga et al. 1994; Duinkerken et al. 2011). MiR156 OE had higher DM degradation than WT and SPL13 RNAi (Chapter 4.4), which explains its lower ENDP content. However, NRC system regards endogenous protein as a contributor to total metabolizable protein and is related with DM intake (NRC Dairy 2001; Theodoridou and Yu 2013b). Truly absorbable RUP is calculated with the product of RUP with its intestinal digestion. As DVE/OEB has a coefficient of 1.11 for the *in vitro* correction (Theodoridou and Yu 2013b), ARUP values of alfalfa were higher with DVE/OEB system than NRC-2001 system.

4.5.4 Conclusion

In conclusion, overexpression of miR156 reduced the initial degradation and degradation rate of CP in the rumen; however, the overall CP degradation was not affected. This impact on CP degradation could improve the nutrient synchronization of alfalfa in the rumen. Moreover, transformed alfalfa tended to have more unbalanced protein and energy supply in the rumen for MCP synthesis. Although miR156 OE alfalfa had higher MCP synthesis according to RDP and TDN, there were no significant differences in total truly available protein between alfalfa genotypes.

CHAPTER 5
RELATIONSHIP BETWEEN MOLECULAR STRUCTURE PARAMETERS AND NUTRITIONAL PROFILES OF ALFALFA

5.1 Relationship between molecular structures and chemical composition, CNCPS fractions and energetic values of alfalfa

Abstract: This study aimed to explore the correlation between molecular structure and nutritional profiles of chemical composition, CNCPS fractions and energetic values of alfalfa. Moreover, regression models of predicting these nutritive profiles, at least some, from molecular structure parameters were also expected. Molecular structural and chemical data were obtained from previous two projects. Results showed that TC, STC and CCO profiles were negatively correlated with DM, CP, EE, SCP and sugar, but positively correlated with NDF, ADF, NDICP, CHO and NFC ($P<0.05$). However, CEC profiles, alpha/beta ratio and asymmetric CH_2/CH_3 had opposite correlations with those chemical compositions. As for CNCPS fractions and degradations, TC, STC and CCO profiles had negative correlations with rapidly degraded fractions but had positive correlations with slowly or un-degraded fractions ($P<0.05$). Like chemical results, CEC profiles, alpha/beta ratio and asymmetric CH_2/CH_3 also had opposite correlations with those CNCPS fractions. In terms of energy values, TC, STC and CCO profiles were negatively correlated with energy values, which were positively correlated with CEC profiles, alpha/beta ratio and asymmetric CH_2/CH_3. Regression equations of predicting chemical composition, CNCPS fraction and degradation, truly digestive nutrients and energy values were successfully obtained with good

estimation power. In conclusion, molecular structures of alfalfa were closely correlated with its chemical composition and nutritional profiles. Moreover, with the help of ATR-FTIR spectroscopy, we could predict these nutritional profiles with great explanation powers.

5.1.1 Introduction

Alfalfa (*Medicago sativa*) is one of the most widely cultivated perennial legume forage crop in the world due to its high nutritive values and good palatability and adaptability (Lei et al. 2017). Alfalfa hay contains high protein content and low fiber content, which makes it a very good roughage for ruminant, especially for high production dairy cows (Sánchez-Duarte and García 2017). Moreover, the deep root system of alfalfa enables it grows and flourish in arid and semi-arid conditions, and the symbiotic relationship with *Rhizobium* endorses it the capability of utilizing atmospheric nitrogen (Lei et al. 2017). However, utilization of alfalfa is limited by some drawback, such as high lignin content and rapid degradable protein (Lei et al. 2017). To solve these drawbacks and further improve alfalfa, genetic transformation has been used in alfalfa breeding for decades (Li and Brummer 2012; Lei et al. 2017). Such genetic modifications induced changes in molecular structures of alfalfa and affected its nutritional profiles. Transformation of maze *Lc* gene in alfalfa resulted in accumulations of anthocyanin, which could improve protein degradation in the rumen, and changes in carbohydrate and amide spectral parameters (Yu et al. 2009; Jonker 2011; Heendeniya and Yu 2017).

Fourier transform infrared (FTIR) spectroscopy is a rapid and non-destructive tool for analyzing inherent molecular structures of samples in many research disciplines (Stuart 2004; Bassbasi et al. 2014; Bekiaris et al. 2015; Chen et al. 2018). Researchers have implemented this technique in feed nutrition in recent years in attempt to explore the internal molecular structures of feed ingredients in mid infrared (IR) range (Shi and Yu 2017; Prates and Yu 2017). Studies showed that the molecular structures of feedstuffs are closely correlated with their nutritional profiles and nutrient availability to the animal (Theodoridou and Yu 2013a; Peng et al. 2014; Xin et al. 2014; Prates et al. 2018a). However, correlations between spectral parameters and nutritional profiles are not consistent for different feed ingredients, implying unique correlation patterns for

different feeds (Theodoridou and Yu 2013a; Xin and Yu 2013a). This suggests that to better utilize this technique in predicting of nutritional profiles of a feed ingredient, the unique relationship between its spectral parameters with FTIR spectroscopy and nutritional profiles need to be studied in a large scale. Therefore, this study used spectral parameters and chemical composition, CNCPS fractions and energy values of alfalfa samples from Chapter 3 and Chapter 4 to study the structural-nutritional relationships for alfalfa forage

5.1.2 Materials and Methods

Spectral parameters, chemical composition, CNCPS fractions and degradations, truly digestive nutrients and energetic values of alfalfa were obtained from previous two projects.

5.1.2.1 Spectral data

Spectral parameters include peak heights and areas of spectral regions. Peak heights were total carbohydrate (TC), structural carbohydrate (STC), cellulosic compounds (CEC), Amide I, Amide II, α-helix, β-sheet, carbonyl C=O (CCO), symmetric CH_2 (SyCH2), asymmetric CH_2 (AsCH2), symmetric CH_3 (SyCH3) and asymmetric CH_3 (AsCH3). Peak areas were TC area (TCA), STC area (STCA), CEC area (CECA), Amide area (AA), Amide I area (AIA), Amide II area (AIIA), CCO area (CCOA), and asymmetric and symmetric CH_2 and CH_3 area (ASCCA).

5.1.2.2 Chemical data

Chemical composition included dry matter (DM), ash, crude protein (CP), ether extract (EE), neutral detergent fiber (NDF), acid detergent fiber (ADF), acid detergent lignin (ADL), neutral detergent insoluble crude protein (NDICP), acid detergent insoluble crude protein (ADICP), soluble crude protein (SCP), starch, sugar, total carbohydrate (CHO) and non-fiber carbohydrate (NFC).

5.1.2.3 CNCPS fractions and rumen degradation data

CNCPS fractions included carbohydrate fractions of sugar (CA4), starch (CB1), soluble fiber (CB2), digestible fiber (CB3), and indigestible fiber (CC) and protein fractions of soluble true protein (PA2), insoluble true protein (PB1), fiber-bound protein (PB2) and indigestible protein (PC). As rumen degradable CNCPS fractions had similar pattern as rumen undegradable fractions in regards of their correlations with spectral parameters. Therefore, only rumen degradable carbohydrate (RDCHO) and rumen degradable crude protein (RDCP) and rumen undegradable (RU) fractions were selected for correlation and regression study.

5.1.2.4 Truly digestive nutrients and energy data

Truly digestive nutrients included truly digestive NFC (tdNFC), truly digestive CP (tdCP), truly digestive fatty acids (tdFA), truly digestive NDF (tdNDF) and total digestible nutrients (TDN). Energetic values included digestive energy (DE), metabolizable energy (ME), net energy for lactation at productive level (NE_L), net energy for maintenance (NE_m) and net energy for growth (NE_g).

5.1.2.5 Correlation study

Correlations and regressions between nutritional profiles and spectral parameters were performed with R software (R Core Team 2017). Correlation coefficients and their significances were obtained with the *rcorr()* function in HMISC package. Prior to correlations analysis, normality of each variable was tested with the *shapiro-test()* function in STATS package. Correlations involved non-normally distributed variables were performed with "Spearman method", while others were performed with "Pearson" method. Correlation coefficient matrix between spectral and nutritional profiles were then visualized with Corrplot function from CORRPLOT package. Positive correlation coefficients were showed in red color while negative

coefficients were presented in blue color. The darker the color, the higher the absolute coefficient values. Significant level was set at $P<0.05$ and insignificant correlation coefficients were left in white color.

5.1.2.6 Multilinear regression

Multiple linear regressions of predicting nutritional profiles from spectral parameters were conducted with the *lm()* function in STATS package. Then, the *alias()* function in STATS package was used to identify predictors that were completely linearly dependent on other predictors. The complete aliased predictors were then deleted, and the *vif()* function from CAR package was used to check the variance inflation factor (VIF) of each predictor. The predictor that had the highest VIF, which was greater than 10, was removed from the model. The linear modeling was re-conducted until the VIF values of all predictors were lower than 10. Afterwards, the *step()* function with "direction = both" was used to select the linear model that had the lowest AIC value. Then, predictors with significance level of $P>0.05$ were removed from the model. Models with an R^2 greater than 0.7 were selected to report in this study.

5.1.3 Results and Discussion

5.1.3.1 Correlations between spectral parameters and chemical composition of alfalfa

Among spectral parameters, carbohydrate parameters were more closely correlated with chemical composition of alfalfa compared with amide and lipid-related parameters (Figure 5.1.1). Parameters of TC, STC, AIA/AIIA, AIA/AA, CCO and CCOA were negatively correlated with DM, CP, EE, SCP, starch and sugar, but positively correlated with NDF, ADF, NDICP, CHO an NFC. Moreover, STC parameters also had weak positive correlations with ADICP, while AIA/AIIA, AIA/AA, CCO and CCOA had weak positive correlations with ADL. Like TC and STC parameters, beta sheet, AA and AIA were negatively correlated with CP, EE, SCP, starch and

sugar but positively correlated with NDF, NDICP, CHO and NFC. In contrast, CEC, CECA, α-helix to β-sheet ratio (alpha/beta), AsCH2 and AsCH3 had opposite correlations with chemical composition, compared with TC and STC parameters. As for Amide I, Amide II, Amide I/II, alpha helix, AIIA, SyCH2, SyCH3 and ASCCA, only weak correlations or no significant correlations were observed with chemical composition.

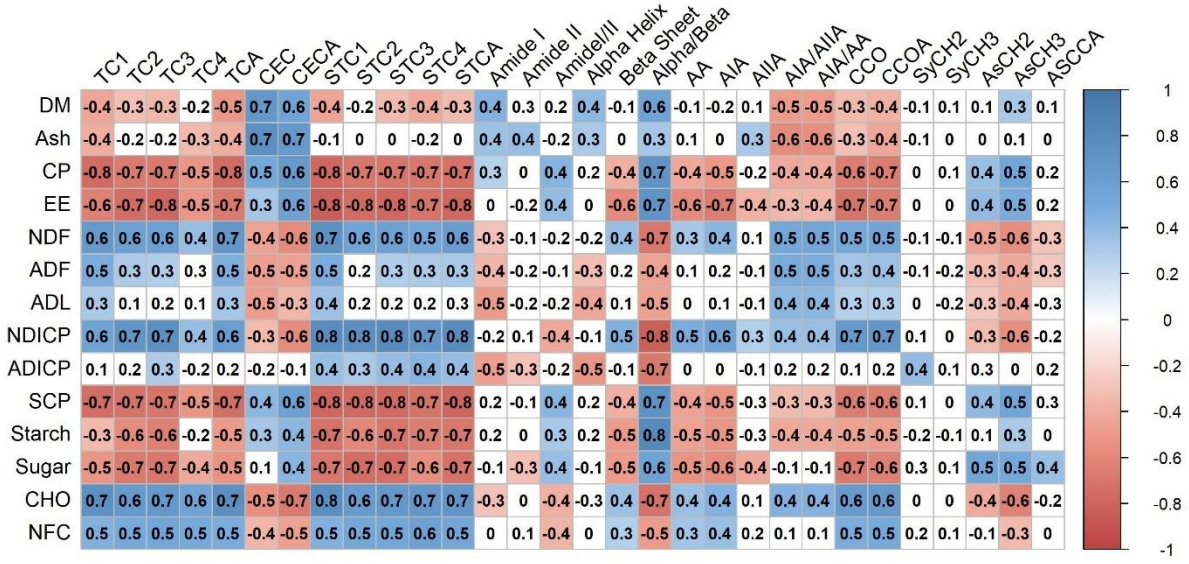

Figure 5.1.1 Correlation plot between molecular structure parameters and chemical composition of alfalfa forage.

Notes: Blue color means positive correlation, while red means negative correlation. Colorless cells contain correlation coefficients that are not significant at $P<0.05$. Values in the plot are correlation coefficients, and the deeper the color, the higher the absolute coefficient value.

Spectral parameters: TC1-TC4, four major peaks in total carbohydrate (TC) region; TCA, peak area of TC region; CEC, cellulosic compounds; CECA, peak area of CEC region; STC1-STC4, four major peaks in structural carbohydrate (STC) region; STCA, peak area of STC region; AA, total amide area; AIA, amide I area; AIIA, amide II area; CCO, carbonyl C=O (CCO) peak; CCOA, CCO peak area. SyCH2, symmetric CH_2; SyCH3, symmetric CH_3; AsCH2, asymmetric CH_2; AsCH3, asymmetric CH_3; ASCCA, peak area of asymmetric and symmetric CH_2 and CH_3 (ASCC) region;

Chemical compositions: DM, dry matter; CP, crude protein; EE, ether extract; NDF, neutral detergent fiber; ADF, acid detergent fiber; ADL, acid detergent lignin; NDICP, neutral detergent insoluble CP; ADICP, acid detergent insoluble CP; SCP, soluble CP; CHO, carbohydrate; NFC, non-fiber carbohydrate;

In the current study, TC, STC and CCO parameters had similar correlations with chemical composition, while CEC parameters, alpha/beta ratio, AsCH2 and AsCH3 were opposite to them in their correlations with chemical composition. Previous studies on correlations between molecular structure and nutritional profiles of alfalfa did not include all molecular structures (Yari et al. 2013, 2017; Li et al. 2015). Instead, either only several spectral parameters were selected, or correlations were only determined between chemical compositions and their corresponding empirical spectral parameters. Yari et al. (2013, 2017) determined the effects of stage of maturity and harvest time on molecular structures and nutritional profiles of alfalfa and also reported correlations between nutritional profiles and molecular parameters of alfalfa.

For carbohydrate molecular parameters, Yari et al. (2017) found that nonstructural carbohydrate area (NSTCA) to TCA ratio and NSTCA to STCA ratio were negatively correlated with ADL, NDF, ADF and CHO but positively correlated with NFC. These two ratios of carbohydrate peak area were similar to CEC parameters, alpha/beta ratio, AsCH2 and AsCH3 in this study in terms of their correlations with carbohydrate chemical profiles. However, Li et al. (2015) studied with *TT8*- and *HB12*-silenced alfalfa reported these two carbohydrate area ratios were positively correlated with CHO , NDF and ADF. In the current study, nonstructural carbohydrate (NSTC) parameters were not characterized due to the inconsistent spectra between samples in terms of NSTC peaks. Also, ratios between carbohydrate areas were not included in the correlations study. For protein spectral parameters, Yari et al. (2013) reported amide I/II ratio was negatively correlated with CP and tended to be negatively correlated with SCP, but positively correlated with NDICP. This was not consistent with the current study, as amide I/II ratio was found positively correlated with CP, SCP, but negatively correlated with NDICP, although correlations were weak ($|r|=0.4$). In contrast, alpha/beta ratio was positively correlated with CP

and SCP, but tended to be negatively correlated with ADICP (Yari et al. 2013), which was in agreement with the current study.

5.1.3.2 Correlations between spectral parameters and CNCPS fractions and between spectral parameters and CNCPS degradations of alfalfa

Like correlations with chemical composition, carbohydrate parameters also had higher correlation coefficients compared with amide and lipid-related parameters (Figure 5.1.2). Parameters of TC, STC, beta-sheet, AA, AIA, CCO and CCOA were negatively correlated with CA4, CB1, PA2 and PB, but positively correlated with CB2, CB3, PB2 and PC. Similarly, ratios of AIA/AIIA and AIA/AA were also negatively correlated with CB1 and PB1, but positively correlated with CB3, PB2 and PC.

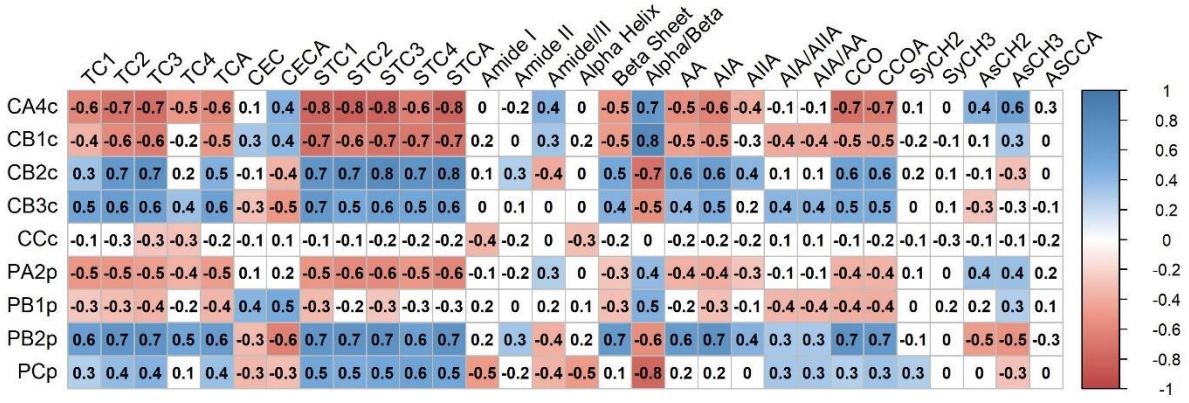

Figure 5.1.2 Correlation plot between molecular structure and CNCPS fractions of alfalfa forage.

Notes: Blue color means positive correlation, while red means negative correlation. Colorless cells contain correlation coefficients that are not significant at $P<0.05$. Values in the plot are correlation coefficients, and the deeper the color, the higher the absolute coefficient value.

Spectral parameters: TC1-TC4, four major peaks in total carbohydrate (TC) region; TCA, peak area of TC region; CEC, cellulosic compounds; CECA, peak area of CEC region; STC1-STC4, four major peaks in structural carbohydrate (STC) region; STCA, peak area of STC region; AA, total amide area; AIA, amide I area; AIIA, amide II area; CCO, carbonyl C=O (CCO) peak; CCOA, CCO peak area. SyCH2, symmetric CH_2; SyCH3, symmetric CH_3; AsCH2, asymmetric CH_2; AsCH3, asymmetric CH_3; ASCCA, peak area of asymmetric and symmetric CH_2 and CH_3 (ASCC) region;

CNCPS fractions: CA4, water-soluble carbohydrate, sugar; CB1, starch; CB2, soluble fiber; CB3, digestible fiber; PA2, soluble true protein; PB1, insoluble true protein; PB2, fiber-bound protein; PC, indigestible protein; The letter "c" and "p" after each fraction mean as percentage of CHO and CP, respectively;

To the contrary, CECA, alpha/beta ratio and AsCH3 were positively correlated with CA4, CB1, PA2 and PB1, but negatively correlated with CB2, CB3, PB2 and PC. In addition, Amide I/II ratio was also positively correlated with CA4, CB1 and PA2, but negatively correlated with CB2, PB2 and PC. Apart from this, there were only insignificant or weak correlations between CNCPS fractions and other spectral parameters. These results suggested that TC, STC, amide and CCO parameters were negatively correlated with rapidly degradable CNCPS fractions, but positively correlated with slowly degradable fractions. In contrast, CECA, alpha/beta ratio and AsCH3 were positively correlated with rapidly degradable fractions and negatively correlated with slowly degradable fractions.

Correlations between spectral parameters and rumen degradations of CNCPS fractions are shown in Figure 5.1.3. Rumen degradable CNCPS fractions had similar correlations with spectral parameters as their undegradable counterparts, which was in line with previous publication (Lei et al. 2018c). Therefore, to make the correlation plot concise, only RDCHO and RDCP were selected along with rumen undegradable CNCPS fractions in the correlation plot. TC, STC, beta sheet, AA, AIA, AIA/AIIA, AIA/AA, CCO and CCOA were positively correlated with RDCHO, RUCB2, RUCB3 and RUPB2, but negatively correlated with RDCP, RUCA4, RUCB1, RUPA2, RUPB1 and RUCP. Also, TC, STC, AIA/AIIA, AIA/AA, CCO and CCOA parameters were positively correlated RUCHO and STC parameters was positively correlated with RUPC. In contrast, CEC, CECA, alpha/beta, AsCH2 and AsCH3 were negatively correlated with RDCHO, RUCB2, RUCB3, RUCC, RUCHO and RUPB2, but positively correlated RDCP, RUCA4, RUCB1, RUPA2, RUPB1 and RUCP. Once again, amide peaks and symmetric CH_2 and CH_3 were only weakly or insignificantly correlated with CNCPS degradations.

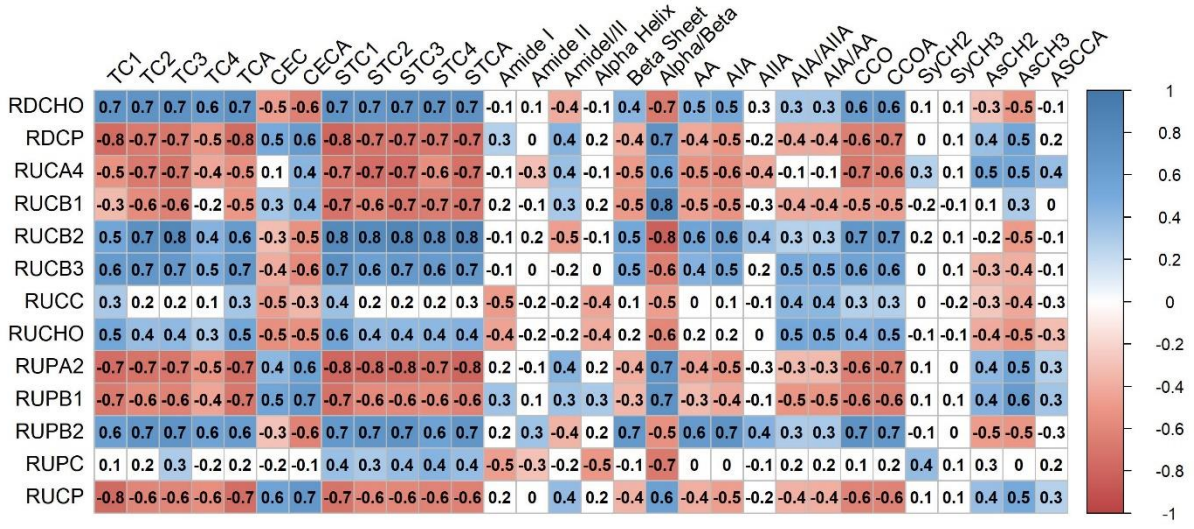

Figure 5.1.3 Correlation plot between molecular structure and degradational profiles of CNCPS fractions of alfalfa forage.

Notes: Blue color means positive correlation, while red means negative correlation. Colorless cells contain correlation coefficients that are not significant at $P<0.05$. Values in the plot are correlation coefficients, and the darker the color, the higher the absolute coefficient value.
Spectral parameters: TC1-TC4, four major peaks in total carbohydrate (TC) region; TCA, peak area of TC region; CEC, cellulosic compounds; CECA, peak area of CEC region; STC1-STC4, four major peaks in structural carbohydrate (STC) region; STCA, peak area of STC region; AA, total amide area; AIA, amide I area; AIIA, amide II area; CCO, carbonyl C=O (CCO) peak; CCOA, CCO peak area. SyCH2, symmetric CH_2; SyCH3, symmetric CH_3; AsCH2, asymmetric CH_2; AsCH3, asymmetric CH_3; ASCCA, peak area of asymmetric and symmetric CH_2 and CH_3 (ASCC) region;
Degradational profiles of CNCPS fractions: RU**, rumen undegradable CNCPS fractions; CA4, water-soluble carbohydrate, sugar; CB1, starch; CB2, soluble fiber; CB3, digestible fiber; PA2, soluble true protein; PB1, insoluble true protein; PB2, fiber-bound protein; PC, indigestible protein; The letter c and p mean as percentage of CHO and CP, respectively;

Same as correlations with chemical composition, TC, STC and CCO parameters had opposite correlations with CNCPS fractions and degradations to CEC parameters, alpha/beta ratio, AsCH2 and AsCH3. TC, STC and CCO parameters were negatively correlated with rapidly degradable CNCPS fractions and positively correlated with slowly or non-degradable fractions. To the contrary, CEC parameters, alpha/beta ratio, AsCH2 and AsCH3 were positively correlated with rapidly degradable fractions, and negatively correlated with slowly or non-degradable fractions. Li et al. (2015) reported correlations between carbohydrate spectral parameters and rumen degradations of carbohydrate CNCPS fractions of alfalfa and found TC and STC parameters

were positively correlated with RDCB1 and RUCB1, which was not in line with the current study. Yari et al. (2013) reported correlations between protein profiles and protein secondary spectral parameters and found a positive correlation between alpha/beta ratio and PB1, which is consistent with the current study. However, amide I/II ratio was found negatively correlated with PB1 and no other significant correlations were found between protein secondary spectral parameters and protein CNCPS fractions (Yari et al. 2013). This was conflict to the current study. The amide I/II ratio was positively correlated with RUPB1, which had similar correlations with spectral parameters (data not shown). Other studies also found conflicting correlations between PB1 and protein spectral parameters (Doiron et al. 2009; Yu and Nuez-Ortín 2010; Theodoridou and Yu 2013a; Li et al. 2016b), which might be partially due to the lack of normalization during spectral processing. Normalization in spectral processing could eliminate the influences of sample depth during spectral collection (Prates et al. 2018a). Moreover, this conflict also indicates that different types of samples might differ in their relationships between spectral parameters and nutritional parameters.

5.1.3.3 Correlations between spectral parameters and truly digestive nutrients and between spectral parameters and energy values of alfalfa

Correlations between spectral parameters and energetic values of alfalfa were illustrated in Figure 5.1.4. Once again, TC, STC, beta sheet, AA, AIA, CCO and CCOA had similar correlation patterns and were positively correlated with tdNFC, tdNDF, but negatively correlated with tdCP, tdFA, TDN and all energetic values. In addition, AIA/AIIA and AIA/AA were also positively correlated with tdNDF, but negatively correlated with tdCP, tdFA, TDN and all energetic values. To the contrast, CEC, CECA, amide I/I, alpha/beta, AsCH2 and AsCH3 had opposite correlation

patters, and were negatively correlated with tdNFC and tdNDF, but positively correlated with tdCP, tdFA, TDN and all energetic values.

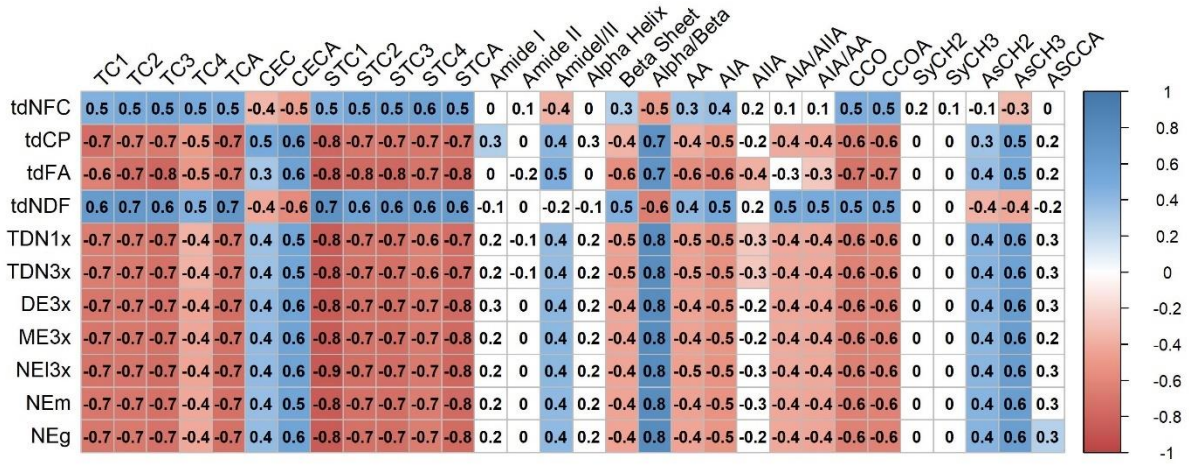

Figure 5.1.4 Correlation plot between molecular structure and energetic values of alfalfa forage.

Notes: Blue color means positive correlation, while red means negative correlation. Colorless cells contain correlation coefficients that are not significant at $P<0.05$. Values in the plot are correlation coefficients, and the darker the color, the higher the absolute coefficient value.
Spectral parameters: TC1-TC4, four major peaks in total carbohydrate (TC) region; TCA, peak area of TC region; CEC, cellulosic compounds; CECA, peak area of CEC region; STC1-STC4, four major peaks in structural carbohydrate (STC) region; STCA, peak area of STC region; AA, total amide area; AIA, amide I area; AIIA, amide II area; CCO, carbonyl C=O (CCO) peak; CCOA, CCO peak area. SyCH2, symmetric CH_2; SyCH3, symmetric CH_3; AsCH2, asymmetric CH_2; AsCH3, asymmetric CH_3; ASCCA, peak area of asymmetric and symmetric CH_2 and CH_3 (ASCC) region;
Truly digestive nutrients and energetic values: tdNFC, truly digestive non-fiber carbohydrate; tdCP, truly digestive crude protein; tdFA, truly digestive fatty acid; tdNDF, truly digestive neutral detergent fiber; TDN1x, total digestible nutrients at one time of maintenance level, and 3x means at three times of maintenance level; DE3x, digestible energy at three times maintenance level; ME3x, metabolizable energy at three times maintenance level; NEL3x, net energy for lactation at three times maintenance level; NEm, net energy for maintenance; NEg, net energy for growth.

Li et al. (2016a) reported correlations between carbohydrate spectral parameters and truly digestive nutrients of alfalfa and found CEC parameters were negatively correlated with tdFA and TC and STC parameters were negatively correlated with tdNDF, which was opposite to the current study. In Li's study, there were no significant correlations found between TDN, which is an index for energy values (NRC Dairy 2001), and carbohydrate spectral parameters (Li et al. 2016a). However, there were only six alfalfa samples in Li's study, which limited its explanation power.

To our knowledge, there were no other studies on correlations between spectral parameters and energetic values of alfalfa. A previous study on canola (*Brassica napus*) seed found that alpha/beta ratio were negatively correlated with TDN and energy values, which contradicts our results (Theodoridou et al. 2013). Same as correlations with CNCPS fractions, correlations between alpha/beta ratio and energy values were not consistent in previous studies (Zhang and Yu 2012, 2014; Theodoridou et al. 2013; Xin and Yu 2013b). This conflict in correlations between spectral parameters and nutritive profiles might be attributed to differences in sample features, population sizes and spectral processing methods. Refat et al. (2017b) reported that NSTCA was negatively correlated with TDN and energy values for corn and barley silage, but not significant correlations found between other carbohydrate spectral parameters and energy values.

One should note that correlations between spectral parameters and nutritional profiles of feed ingredients were only conducted in relatively small scales. Only few spectral parameters were selected for correlations studies and correlations were only determined between spectral parameters and corresponding nutritional profiles (Yu and Nuez-Ortín 2010; Theodoridou et al. 2013; Xin et al. 2014; Li et al. 2016a; Refat et al. 2017b). However, spectral parameters are directly correlated with chemical bonds, not chemical components (Stuart 2004). One chemical compound has more than one type of chemical bonds and one type chemical bond exists in different chemical compounds. This means spectral parameters are not limited to their empirical chemical components, and it could indicates different chemicals depending on the type of samples (Baker et al. 2014). Therefore, in the current study, all spectral parameters within mid-IR range (4000-700 cm^{-1}) were selected for correlation studies, and correlations were not restrained to their empirically corresponding chemical components and related nutritional profiles.

5.1.3.4 Regression of predicting chemical composition, CNCPS fractions, truly digestive nutrients and energetic values from spectral parameters of alfalfa

Table 5.1.1 represents regression equations of predicting chemical composition and CNCPS fractions from spectral parameters of alfalfa. Only equations with an R^2 greater than 0.7 were selected to report. For chemical composition, CHO, CP and NDICP could be predicted with great estimation power (R^2>0.8), while NDF, starch, SCP and EE could be predicted with good estimation power (R^2>0.7). For CNCPS fractions on DM basis and rumen degradable fractions had similar regression equations and estimation power as rumen undegradable fractions. Thus, only equations for fractions on carbohydrate or protein basis and rumen undegradable fractions were reported in this chapter. For CNCPS fractions, RUCB2, RUPB2 and RDCP could be predicted great estimation powers (R^2>0.8), while CA4 (%CHO), RUCB1, RUPA2, RUPB1 and RUCP could be also be well predicted (R^2>0.7).

Regression equations of predicting truly digestive nutrients and energy values were shown in Table 5.1.2. For truly digestive nutrients, tdCP and TDN could be predicted great estimation powers (R^2>0.8), while tdFA and tdNDF could be predicted with reasonable estimation power (R^2>0.7). The tdFA could be predicted from Amide I, alpha/beta and CCOA with an R^2 of 0.737, and tdCP could be predicted from TC4, Amide I, Amide I/II, alpha/beta, SyCH2 and SyCH3 with an R^2 of 0.808. For tdNDF, it could be well predicted from CEC, alpha/beta, SyCH2 and SyCH3 with an R^2 of 0.701. In addition, TDN and all energetic values could be predicted from Amide I, Amide I/II, alpha/beta, SyCH2 and SyCH3 with great estimation powers (R^2>0.8). Regressions of predicting nutritional profiles from spectral parameters have been achieved in other feedstuffs with good estimation power (Peng et al. 2014; Xin et al. 2014; Refat et al. 2017b; Prates et al. 2018b). However, same as correlation studies, only corresponding spectral parameters were used in regression models for previous studies.

Table 5.1.1 Regression equations of predicting chemical composition and CNCPS fractions from molecular structure for alfalfa forage

Items [1]	Prediction Equations [2]	RSE [3]	Adjusted R^2	P value
Chemical composition (%DM)				
CHO	Y = 125.86 - 231.98 CEC - 9.65 Amide I/II - 39.2 alpha/beta - 116.07 SyCH2 + 595.59 SyCH3 - 229.81 AsCH3	2.104	0.827	<0.001
NDF	Y = 83.11 - 28.93 Amide I - 55.34 alpha/beta - 179.06 SyCH2 + 515.4 SyCH3	2.417	0.737	<0.001
Starch	Y = -32.89 + 68.41 TC4 - 15.32 Amide I + 33.88 alpha/beta	1.329	0.735	<0.001
CP	Y = -7.57 - 90.84 TC4 + 34.45 Amide I + 9.68 Amide I/II + 28.99 alpha/beta + 89.12 SyCH2 - 300.36 SyCH3	1.493	0.811	<0.001
NDICP	Y = 4.66 + 30.15 CEC - 4.88 alpha/beta + 0.48 CCOA - 17.83 AsCH3	0.238	0.875	<0.001
SCP	Y = -6.81 - 49.1 TC4 + 18.38 Amide I + 6.94 Amide I/II + 16.19 alpha/beta + 73.27 SyCH2 - 254.78 SyCH3	1.133	0.706	<0.001
EE	Y = -3.9 - 8.08 Amide I + 10.85 alpha/beta - 0.91 CCOA	0.77	0.735	<0.001
CNCPS fractions and degradations (%DM)				
CA4c (%CHO)	Y = 12.52 - 151.37 CEC + 11.83 alpha/beta - 2.55 CCOA	1.100	0.786	<0.001
RUCB1	Y = -4.28 + 8.86 TC4 - 1.99 Amide I + 4.41 alpha/beta	0.173	0.735	<0.001
RUCB2	Y = 5.65 + 19.34 CEC - 4.68 alpha/beta + 0.29 CCOA	0.217	0.812	<0.001
RUPA2	Y = -1.1 - 7.97 TC4 + 2.95 Amide I + 1.12 Amide I/II + 2.61 alpha/beta + 11.8 SyCH2 - 40.95 SyCH3	0.183	0.705	<0.001
RUPB1	Y = -3.85 + 11.91 CEC + 4.77 alpha/beta + 20.96 AsCH3	0.247	0.780	<0.001
RUPB2	Y = 0.74 + 8.78 CEC + 1.06 Amide I - 1.08 alpha/beta + 0.22 CCOA - 8.55 AsCH3	0.099	0.840	<0.001
RDCP	Y = -9.38 - 71.05 TC4 + 28.25 Amide I + 8.11 Amide I/II + 25.06 alpha/beta + 74.27 SyCH2 - 250.52 SyCH3	1.230	0.818	<0.001
RUCP	Y = -1.61 - 21.61 TC4 + 22.63 CEC + 6.1 Amide I + 2.32 Amide I/II + 5.28 alpha/beta + 0.33 CCOA + 27.62 SyCH2 - 86.46 SyCH3	0.282	0.762	<0.001

[1] CHO, carbohydrate; NDF, neutral detergent fiber; CP, crude protein; NDICP, neutral detergent insoluble protein; SCP, soluble crude protein; EE, ether extract; CA4c, water soluble carbohydrate, sugar in the percentage of CHO; RUCB2, rumen undegradable soluble fiber; RUPA2, rumen undegradable soluble true

protein; RUPB1, rumen undegradable insoluble true protein; RUPB2, rumen undegradable fiber-bound protein; RDCP, rumen degradable crude protein; RUCP, rumen undegradable crude protein;
[2] TC4, the fourth major peak in total carbohydrate (TC) region; CEC, cellulosic compounds peak; Amide I, the first peak in amide region; Amide I/II, peak ratio of amide I to amide II; alpha/beta, peak ratio of alpha helix to beta sheet; CCOA, carbonyl C=O peak area. SyCH2, symmetric CH_2; SyCH3, symmetric CH_3; AsCH3, asymmetric CH_3;
[3] RSE, residual standard error; Only regressions with the adjusted R^2 larger than 0.7 were selected.

Table 5.1.2 Regression equations of predicting truly digestive nutrients and energetic values from molecular structure for alfalfa forage

Items [1]	Prediction Equations [2]	RSE [3]	Adjusted R^2	P value
Truly digestive nutrients (%DM)				
tdFA	Y = -4.17 - 8.3 Amide I + 10.21 alpha/beta - 0.9 CCOA	0.740	0.737	<0.001
tdCP	Y = -10.77 - 86.12 TC4 + 36 Amide I + 9.8 Amide I/II + 30.5 alpha/beta + 86.48 SyCH2 - 300.47 SyCH3	1.552	0.808	<0.001
tdNDF	Y = 31.19 - 58.66 CEC - 22.88 alpha/beta - 92.57 SyCH2 + 295.07 SyCH3	1.156	0.701	<0.001
TDN3x	Y = 34.5 + 9.67 Amide I + 4.59 Amide I/II + 25.27 alpha/beta + 81.42 SyCH2 - 236.06 SyCH3	0.965	0.803	<0.001
Energetic values (Mcal/Kg DM)				
DE3x	Y = 1.2 + 0.76 Amide I + 0.32 Amide I/II + 1.48 alpha/beta + 4.93 SyCH2 - 15.11 SyCH3	0.053	0.830	<0.001
Me3x	Y = 0.72 + 0.76 Amide I + 0.33 Amide I/II + 1.53 alpha/beta + 5.07 SyCH2 - 15.43 SyCH3	0.054	0.833	<0.001
NE_{L3x}	Y = 0.32 + 0.53 Amide I + 0.23 Amide I/II + 1.09 alpha/beta + 3.6 SyCH2 - 11.05 SyCH3	0.038	0.835	<0.001
NEm	Y = -0.17 + 0.75 Amide I + 0.32 Amide I/II + 1.55 alpha/beta + 5.12 SyCH2 - 15.51 SyCH3	0.056	0.828	<0.001
NEg	Y = -0.58 + 0.68 Amide I + 0.29 Amide I/II + 1.36 alpha/beta + 4.54 SyCH2 - 13.54 SyCH3	0.048	0.837	<0.001

[1] tdFA, truly digestive fatty acids; tdCP, truly digestive crude protein; tdNDF, truly digestive neutral detergent fiber; TDN3x, total digestible nutrient at three times of maintenance level; DE3x, digestible energy at three times maintenance level; ME3x, metabolizable energy at three times maintenance level; NEL3x, net energy for lactation at three times maintenance level; NEm, net energy for maintenance; NEg, net energy for growth.
[2] TC4, the fourth major peak in total carbohydrate (TC) region; CEC, cellulosic compounds peak; Amide I, the first amide peak; Amide I/II, peak ratio of amide I to amide II; alpha/beta, peak ratio of alpha helix to beta sheet; CCOA, carbonyl C=O peak area. SyCH2, symmetric CH_2; SyCH3, symmetric CH_3.
[3] RSE, residual standard error; Only regressions with the adjusted R^2 larger than 0.7 were selected.

5.1.4 Conclusion

In conclusion, molecular structures of alfalfa were closely correlated with its chemical composition, CNCPS fractions and degradation and energy profiles. Spectral parameters of TC, STC and CCO regions were negatively correlated with readily degradable nutrients and energy, but positively correlated with slowly or non-degradable nutrients. In contrast, CEC parameters, alpha/beta ratio, AsCH2 and AsCH3 had opposite correlations with nutritional profiles of alfalfa. Moreover, CHO, CP, NDICP, CB2, PB2, RDCP, tdCP, TDN and all energy profiles could be predicted from ATR-FTIR spectral parameters with great explanation powers.

5.2 Relationship between molecular structure and fermentation features and between molecular structure and protein metabolic characteristics of alfalfa

Abstract: The objectives of this study were to explore the correlation between molecular structure and nutritional profiles of *in vitro* fermentation and protein metabolic characteristics of alfalfa. Moreover, regression models of predicting some of these nutritive profiles, at least some, from molecular structure parameters were also expected. Molecular structural, terminational and metabolic data were obtained from the previous two projects. Results showed that TC, STC and CCO profiles were positively correlated with undegraded fraction of DM and CP, N^{15} enrichment of LAMN and FAMN and ENDP, but negatively correlated with ruminal degradations of DM, NDF and CP, gas and propionate production, LAMN, MCP profiles and degraded protein balance. However, CEC profiles, alpha/beta ratio, AsCH2 and AsCH3 had opposite correlations with those profiles. Regression equations of predicting DM degradation, EDCP, LAMN, MCP and degraded protein balance were successfully obtained with good estimation power. In conclusion, molecular structures of alfalfa were closely correlated with rumen fermentation and protein metabolic characteristics of alfalfa. Among these nutritional profiles, DM and CP degradation, MCP and degraded protein balance could be well predicted from spectral parameters with attenuated total reflectance-Fourier transform infrared (ATR-FTIR) spectroscopy.

5.2.1 Introduction

Protein availability of feed ingredients is not only related to protein content and amino acid compositions, but also correlated with protein structures (Yu et al. 2009). Protein secondary structures have different degradation patterns with beta-sheet being more resistant to enzymatic digestion (Yu 2005a). Therefore, feed ingredients with higher percentage of beta-sheet structure have low rumen degradation and low protein value to animals (Yari et al. 2013). Traditional evaluation of protein nutritional profiles in ruminant nutrition relies on chemical analysis and degradation and digestion studies, such as NRC and DVE/OEB systems (Theodoridou and Yu 2013b). These nutritional systems require *in vitro/in situ* degradation and digestion studies to assess protein degradation and digestion patters, thereby estimating rumen microbial protein production, rumen bypass protein and endogenous protein pools to total available protein (Theodoridou and Yu 2013b). In contrast, molecular structural studies rely on infrared spectroscopy to reveal the inherent molecular structure of protein, which is rapid, non-destructive and has been used on many feedstuffs (Yu 2012; Xin and Yu 2013a; Yari et al. 2013; Peng et al. 2014). However, spectral analysis only provides structural parameters and its implementation relies on structural-nutritional relationships. Previous studies showed conflict correlations between molecular structures and nutritional profiles for different feed ingredients, implying the structural-nutritional relationship might be unique for different types of feeds depending on their unique chemical profiles.

Alfalfa (*Medicago sativa*) is the most cultivated legume forage crop in the world due to it favorable nutritive values and good adaptability (Lei et al. 2017). Alfalfa hay contains high protein content and low fiber content, therefore it is widely used in ruminant rations, especially for high production dairy cows (Berthiaume et al. 2010). Recently, genetic modifications in alfalfa have been conducted for alfalfa improvement, including traits of stress resistant (Tang et al. 2014), yield

increase (Aung et al. 2015a) and lignin reduction (Guo et al. 2001a). Genetic transformations induced molecular changes in alfalfa inherent structures, and thereby affecting forage degradation and nutrients availability (Wang et al. 2006; Jonker et al. 2010, 2012a; Heendeniya and Yu 2017; Heendeniya et al. 2019). As spectral analysis is rapid and requires much less samples compared with traditional approaches on nutritional values, a comprehensive study on relationships between nutritional values and molecular structure of alfalfa will further benefit alfalfa breeding with genetic techniques. However, studies on relationships between molecular structures and nutritional profiles for alfalfa forage are still limited. Therefore, this study aimed to explore the relationship between molecular structure and protein ruminal degradation and intestinal digestion, microbial nitrogen fractions and protein metabolic characteristics of alfalfa. Linear regressions for predicting protein nutritional profiles from spectral parameters with ATR-FTIR spectroscopy were also conducted in this study.

5.2.2 Materials and Methods

5.2.2.1 Data of spectral parameters

Spectral data of alfalfa were obtained from first two projects. Spectral parameters included peak heights and peak areas of alfalfa samples. Detailed descriptions of spectral parameters could be found in Chapter 3.2, Chapter 4.2, and Chapter 5.1.

5.2.2.2 Data of rumen fermentation, intestinal digestion and microbial nitrogen

Fermentation data included production of gas, ammonia and volatile fatty acids (VFA) and nutrient degradations of dry matter (DM) and neutral detergent fiber (NDF) from *in vitro* gas fermentation and crude protein (CP) degradation and microbial nitrogen (MN) fractions from Daisy II incubation. Intestinal degradation of rumen undegradable protein (IDRUP) from three-step study was also included as part of protein degradation profiles. For end products, production

kinetics of asymptotic production (a), production rate (c), lag time (T0) and average production (AP) were selected for gas, ammonia, acetate, propionate and total VFA productions. For nutrient degradations, degradational kinetics of undegradable fraction (U), degradable fraction (D), soluble fraction (S), effective degradation (ED) were selected for representing degradational data. The MN fractions included liquid associated MN (LMN), loosely attached MN (LAMN) and firmly attached MN (FAMN). In addition, N^{15} enrichment (APE) of LMN, LAMN and residue nitrogen (RN) were also included.

5.2.2.3 Data of protein metabolic characteristics and feed milk value

Protein metabolic characteristics from two nutritional systems, DVE/OEB and NRC-2001 system, were included in relationship study. Protein metabolic characteristics from DVE/OEB system were fermentable organic matter (FOM), microbial protein based on available energy (MCP_FOM), microbial protein based on available nitrogen (MCP_N), absorbable microbial protein (AMCP), endogenous protein (ENDP), bypass protein (BCP), absorbable bypass protein (ABCP), truly absorbable protein (DVE) and degradable protein balance (OEB). Feed milk value (FMV) based DVE value (FMV_DVE) was also calculated. Protein metabolic profiles from NRC-2001 system were microbial protein based on total digestible nutrients (MCP_TDN), microbial protein based on rumen degradable protein (MCP_RDP), absorbable microbial protein (AMCP_NRC), rumen undegradable protein (RUP_NRC), absorbable rumen undegradable protein (ARUP_NRC), endogenous protein (ECP), absorbable endogenous protein (AECP_NRC), metabolizable protein (MP_NRC) and degradable protein balance (DPB). Feed milk value based on MP value (FMV_NRC) were also included.

5.2.2.2 Correlations and Regressions

Correlation and regressions were conducted with R software under RStudio environment (R Core Team 2017). Detailed procedures were previously described in Chapter 5.1.

5.2.3 Results and Discussion

5.2.3.1 Correlations between spectral parameters and nutrients degradational profiles of alfalfa

Figure 5.2.1 shows correlations between spectral parameters and nutrients degradational profiles of alfalfa forage. Spectral parameters of TC, STC, beta sheet, AA, AIA, AIA/AIIA, AIA/AA, CCO and CCOA were positively correlated with degradation rate of DM (DM_Kd), undegradable fraction of DM (DM_U), soluble fraction of DM (DM_S) and undegradable fraction of CP (CP_U), but negatively correlated with degradable fraction of DM (DM_D), effective degradation of DM (DM_ED), degradation rate of NDF (NDF_Kd), effective degradation of NDF (NDF_ED), degradable fraction of CP (CP_D) and effective degradation of CP (CP_ED). On the contrary, parameters of CEC, CECA, Amide I/II, alpha/beta, AsCH2 and AsCH3 were negatively correlated with DM_Kd, DM_U, DM_S and CP_U, but positively correlated with DM_D, DM_ED, NDF_ED, CP_D and CP_ED. Moreover, ASCC parameters were positively correlated with NDF_Kd and alpha/beta was positively correlated with IDRUP. There were no significant or weak correlation relationships for degradational profiles of NDF_U, NDF_D, CP_S and IDRUP, and for spectral parameters of amide I, amide II, alpha helix, SyCH2, SyCH3 and ASCCA.

Yari et al. (2013, 2017) studied the correlations between spectral parameters and nutrients degradation for alfalfa samples harvested after early-bud stage. Nonstructural carbohydrate area (NSTCA) to TCA ratio and NSTCA to STCA ratio were negatively correlated with effective degradations of NDF and NFC; however, correlation coefficients were not significant (Yari et al. 2017). In contrast, NSTCA/TCA and NSTCA/STCA tended to be positively correlated with

effective degradation of total carbohydrate of alfalfa (Yari et al. 2017). However, nonstructural carbohydrates (NSTC) are readily degraded in the rumen. Therefore, a higher ratio of NSTC to TC and STC should be favorable for rumen degradation. In the current study, carbohydrate area ratios were not determined for their correlations with nutrients degradations.

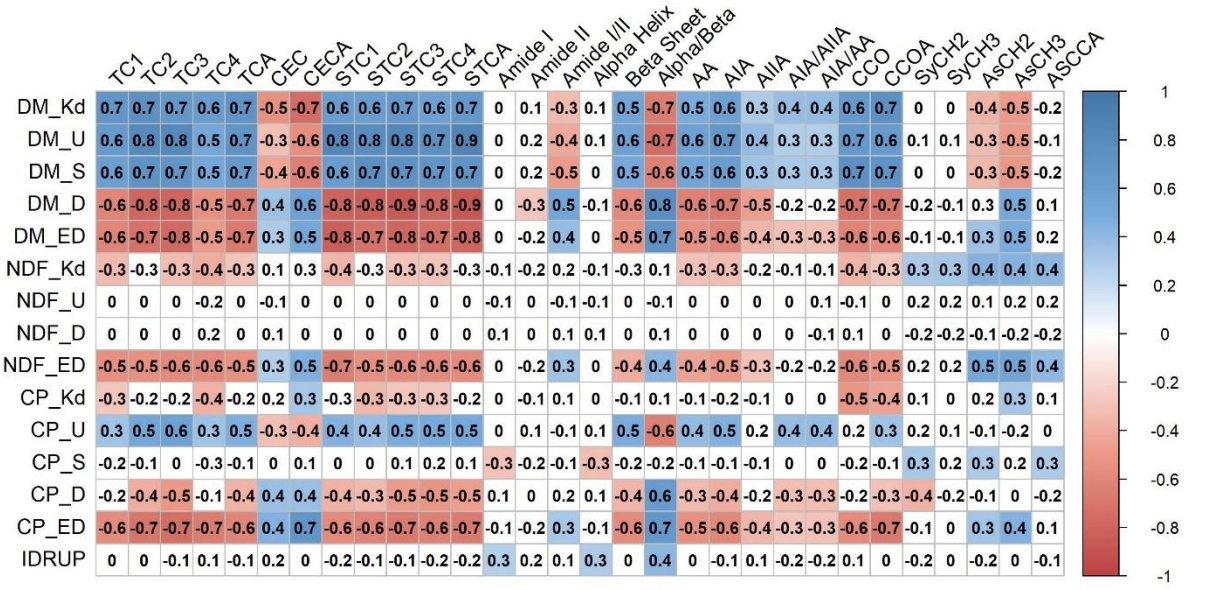

Figure 5.2.1 Correlation plot between molecular structure and nutrients degradational profiles of alfalfa forage.

Notes: Blue color means positive correlation, while red means negative correlation. Colorless cells contain correlation coefficients that are not significant at $P<0.05$. Values in the plot are correlation coefficients, and the deeper the color, the higher the absolute coefficient value.
Spectral parameters: TC1-TC4, four major peaks in total carbohydrate (TC) region; TCA, peak area of TC region; CEC, cellulosic compounds; CECA, peak area of CEC region; STC1-STC4, four major peaks in structural carbohydrate (STC) region; STCA, peak area of STC region; AA, total amide area; AIA, amide I area; AIIA, amide II area; CCO, carbonyl C=O (CCO) peak; CCOA, CCO peak area. SyCH2, symmetric CH_2; SyCH3, symmetric CH_3; AsCH2, asymmetric CH_2; AsCH3, asymmetric CH_3; ASCCA, peak area of asymmetric and symmetric CH_2 and CH_3 (ASCC) region;
Nutrients degradational profiles: U, undegradable fraction; S, soluble fraction; D, degradable fraction; K_d, degradation rate; ED, effective degradation; IDRUP, intestinal digestion of rumen undegraded protein.

Refat et al. (2017b) reported a negative correlation between TCA and effective NDF degradation for barley and corn silages, which was consistent with this study. Instead of just selecting area ratios, all spectral parameters were selected in correlation studies in the current study to illustrate all possible correlations. Chemical correlations showed that TC, STC and CCO

parameters were negatively correlated with DM, CP and rapid degradable nutrients, but positively correlated with carbohydrate and fiber contents of alfalfa (Chapter 5.1). STC region is ca. 1484-1178 cm^{-1}, and was reported more likely to be cellulose, polysaccharides and lignin (Fahey et al. 2017). Expect for soluble carbohydrates, most polysaccharides are slowly degraded in the rumen, which explains the negative correlations between STC parameters and nutrients degradations. As for protein spectral parameters, Yari et al. reported that (2013) amide I/II ratio was positively correlated with RUP, but negatively correlated with RDP, whereas alpha/beta ratio was positively correlated with RDP, but negatively correlated with RUP. In the current study, amide I/II and alpha/beta ratios had similar correlations with protein degradation and were both positively correlated with effective degradation of protein. Study reported that beta sheet structure of protein is resistant enzymatic digestion and rumen degradation (Yu et al. 2015a), indicating that a high beta sheet ratio in protein structure is detrimental to protein degradation.

5.2.3.2 Correlations between spectral parameters and productional kinetics of fermentation end products of alfalfa

There were weak correlations between spectral parameters and productional kinetics of fermentation end products of alfalfa (Figure 5.2.2). Parameters of TC, STC, beta-sheet, AA, AIA, CCO and CCOA were negatively correlated with productions of gas and propionate. In contrast, CEC, CECA and alpha/beta ratio were positively correlated with those productional kinetics. For amide parameters, Amide I, Amide II and alpha helix had weak negative correlations with acetate production and lag time of acetate, propionate and total VFA production. In addition, AA and AIA also had negative correlations with propionate and total VFA productions. As for ASCC profiles, AsCH2, AsCH3 and ASCCA had weak positive correlations with gas production.

A previous study on *HB12* and *TT8*-silenced alfalfa (Chapter 3) reported that TC, STC parameters, beta sheet, amide areas, SyCH2, AsCH2 and ASCCA were negatively correlated with gas production of alfalfa (Lei et al. 2018c). Except for ASCC parameters, other spectral parameters were found similar correlations with gas production. The previous study was conducted with 20 alfalfa samples, whereas there were 56 alfalfa samples in the current study including those 20 samples in this previous study.

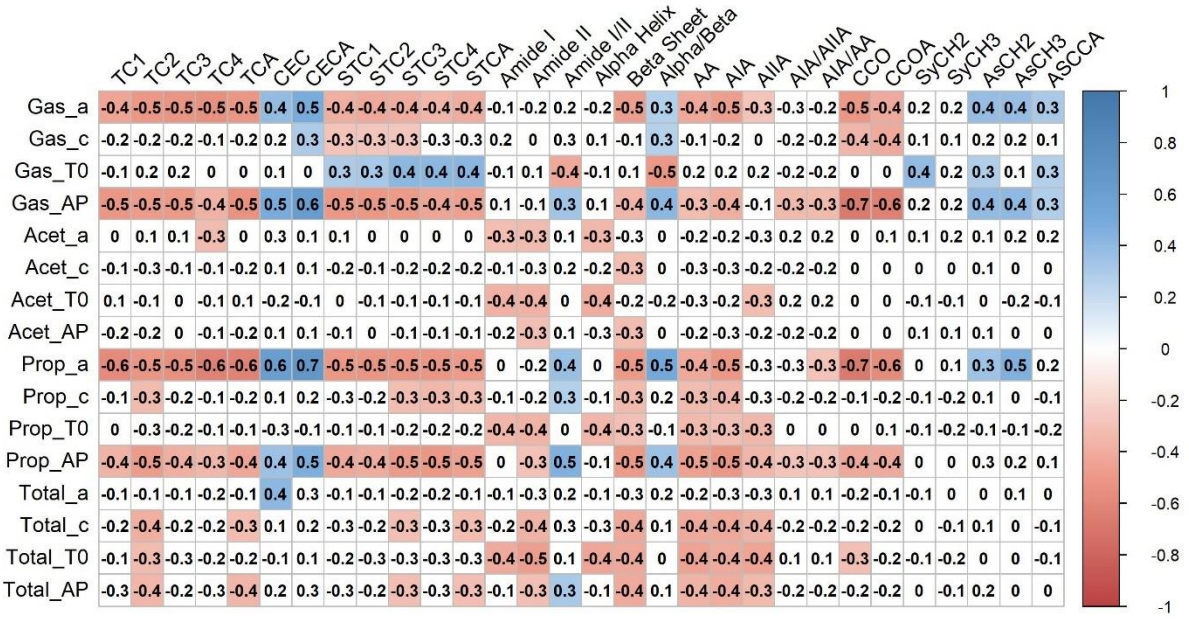

Figure 5.2.2 Correlation plot between molecular structure and *in vitro* fermentation end products of alfalfa forage.

Notes: Blue color means positive correlation, while red means negative correlation. Colorless cells contain correlation coefficients that are not significant at P<0.05. Values in the plot are correlation coefficients, and the deeper the color, the higher the absolute coefficient value.
Spectral parameters: TC1-TC4, four major peaks in total carbohydrate (TC) region; TCA, peak area of TC region; CEC, cellulosic compounds; CECA, peak area of CEC region; STC1-STC4, four major peaks in structural carbohydrate (STC) region; STCA, peak area of STC region; AA, total amide area; AIA, amide I area; AIIA, amide II area; CCO, carbonyl C=O (CCO) peak; CCOA, CCO peak area. SyCH2, symmetric CH_2; SyCH3, symmetric CH_3; AsCH2, asymmetric CH_2; AsCH3, asymmetric CH_3; ASCCA, peak area of asymmetric and symmetric CH_2 and CH_3 (ASCC) region;
Fermentation end products: *a*, asymptotic production (gas mL/g DM, VFA mmol/g DM); *c*, production fractional rate (%/h); To (h), initial delay of production onset; AP, average production at half of asymptotic production (gas ML, VFA mmol), which was calculated as $AP = a \times c \div (2 \times (ln2 + c \times lag))$.

Jonker et al. (2012b, 2012a) reported that *Lc*-transformed alfalfa that accumulates anthocyanin in leaves and stems had lower gas production but had higher peaks of amide I, amide II, alpha helix and beta sheet, compared with non-transformed parental alfalfa. Except for beta sheet that was negatively correlated with gas production, other amide peaks were not significantly correlated with gas production of alfalfa in the current study. In addition, there were no significant differences in VFA production kinetics between *Lc*-transformed and non-transformed alfalfa (Jonker et al. 2012b). A previous study from Wang et al. (2006) found lower gas production for *Lc*-alfalfa at 24 h of fermentation and had higher acetate, propionate and total VFA production at 4 h of fermentation. Correlation study with alfalfa samples just from the first project showed that amide I/II and alpha/beta ratios were positively, whereas STC parameters and amide areas were negatively correlated with VFA production kinetics (data not shown), which was consistent with this study. To our knowledge, there were no other studies have been published on correlations between spectral parameters and fermentation end products of feed ingredients.

5.2.3.3 Correlations between spectral parameters and microbial nitrogen profiles of alfalfa

Correlations between spectral parameters and microbial nitrogen profiles of alfalfa are presented in Figure 5.2.3. Spectral parameters of TC, STC, CCO and CCOA were positively correlated with APE of MN fractions and RN, but negatively correlated with LAMN production. To the contrary, CEC, CECA, alpha/beta ratio and AsCH3 were negatively correlated with APE but positively correlated with LAMN production. Notably, higher correlation coefficients were found at 12 h and 24 h compared with 4 h of fermentation. Moreover, AA and AIA also had weak correlations with APE of LAMN and RN at 12 and 24 h of fermentation. There were weak or insignificant correlations between FAMN, FAMN/RN ratio and spectral parameters of alfalfa. Jonker et al. (2012a) reported that *Lc*-alfalfa had higher amide peaks and protein secondary

structure peaks compared with non-transformed parental alfalfa. In another publication, Jonker et al. (2012b) reported that LAMN production was lower for *Lc*-alfalfa whereas no differences were found in LMN and FAMN fractions. This indicated negative correlations between LAMN and amide peaks for alfalfa. However, except for beta sheet, which was negatively correlated with LAMN production, other amide peaks were not significantly correlated with microbial N fractions. Wang et al. reported that *Lc*-alfalfa had higher APE in RN at 4 h of fermentation and lower FAMN at 12 h of fermentation compared with WT.

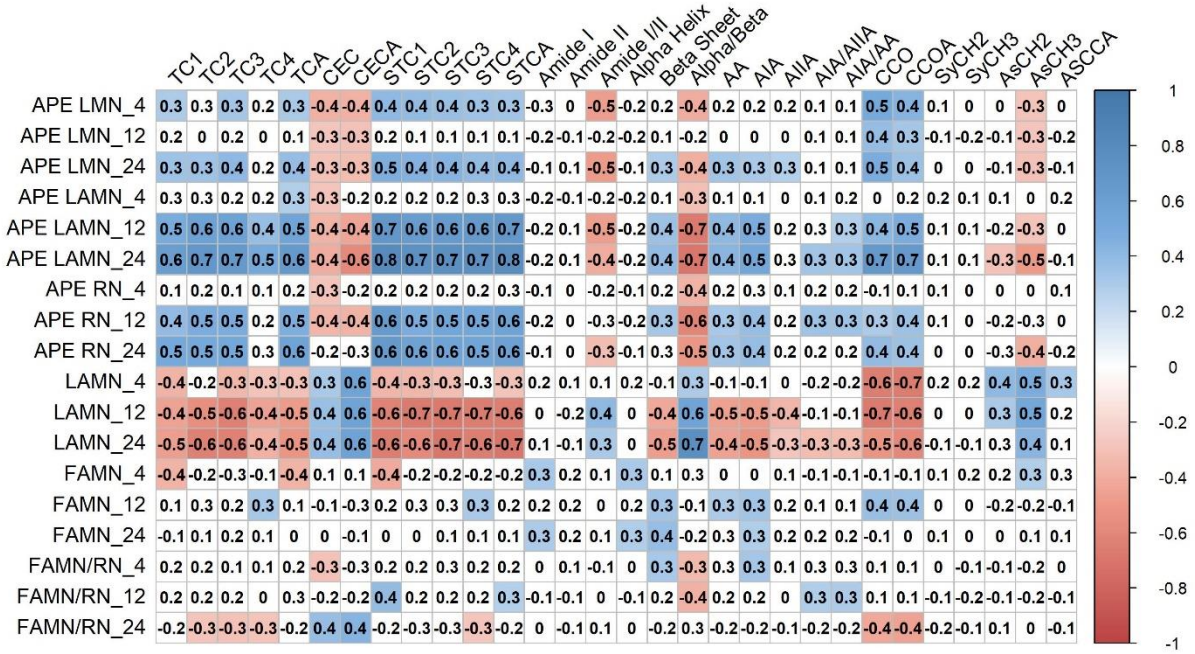

Figure 5.2.3 Correlation plot between molecular structure and microbial nitrogen profiles of alfalfa forage.

Notes: Blue color means positive correlation, while red means negative correlation. Colorless cells contain correlation coefficients that are not significant at $P<0.05$. Values in the plot are correlation coefficients, and the deeper the color, the higher the absolute coefficient value.
Spectral parameters: TC1-TC4, four major peaks in total carbohydrate (TC) region; TCA, peak area of TC region; CEC, cellulosic compounds; CECA, peak area of CEC region; STC1-STC4, four major peaks in structural carbohydrate (STC) region; STCA, peak area of STC region; AA, total amide area; AIA, amide I area; AIIA, amide II area; CCO, carbonyl C=O (CCO) peak; CCOA, CCO peak area. SyCH2, symmetric CH_2; SyCH3, symmetric CH_3; AsCH2, asymmetric CH_2; AsCH3, asymmetric CH_3; ASCCA, peak area of asymmetric and symmetric CH_2 and CH_3 (ASCC) region;
Microbial nitrogen profiles: APE, N^{15} enrichment in microbial nitrogen fractions; LMN, liquid associated microbial nitrogen; LAMN, loosely attached microbial nitrogen; FAMN, firmly attached microbial

nitrogen. Letter "r" followed by MN fractions means the fractions were residue based (mg/g residue). Numbers in the end of each items means the fermentation hour.

Interestingly, parameters of TC, STC and CCO regions were found positively correlated with APE for all MN fractions, especially for LAMN and FAMN. In previous study (Chapter 5.1), these parameters were found negatively correlated with CP and readily digestive nutrients but positively correlated with fiber and non-degradable fractions. The reason behind this might due to the lack of nitrogen from those sample with higher TC, STC and CCO parameters, which lead to a higher assimilation of N^{15} from added ammonium sulfate. Notably, these correlations were determined between MN fractions during *in vitro* fermentation and spectral parameters of alfalfa original samples, not the microbial N residue samples. Therefore, the results of this study should be interpreted carefully when comparing with other studies.

5.2.3.4 Correlations between spectral parameters and protein metabolic characteristics and feed milk value of alfalfa

Correlations between spectral parameters and protein metabolic characteristics and feed milk value of alfalfa are illustrated in Figure 5.2.4. TC, STC, beta sheet, AA, AIA, AIIA, CCO and CCOA parameters were negatively correlated with microbial protein (MCP) and degraded protein balance (OEB or DPB), but positively correlated with BCP, RUP and ENDP. Also, TC and STC parameters were negatively correlated with FOM, DVE and FMV_DVE from DVE/OEB system and ECP from NRC-2001 system. In contrast, CECA, Amide I/II and alpha/beta were negatively correlated with ENDP from DVE/OEB system, but positively correlated with MCP and degraded protein balance (OEB or DPB) from both systems and ECP from NRC-2001 system. Moreover, CECA and Amide I/II also negatively correlated with RUP from both systems. As for ASCC profiles, AsCH2 and AsCH3 were positively correlated with MCP from NRC-2001 systems and degradable protein balance (DPB or OEB) from both nutritional systems.

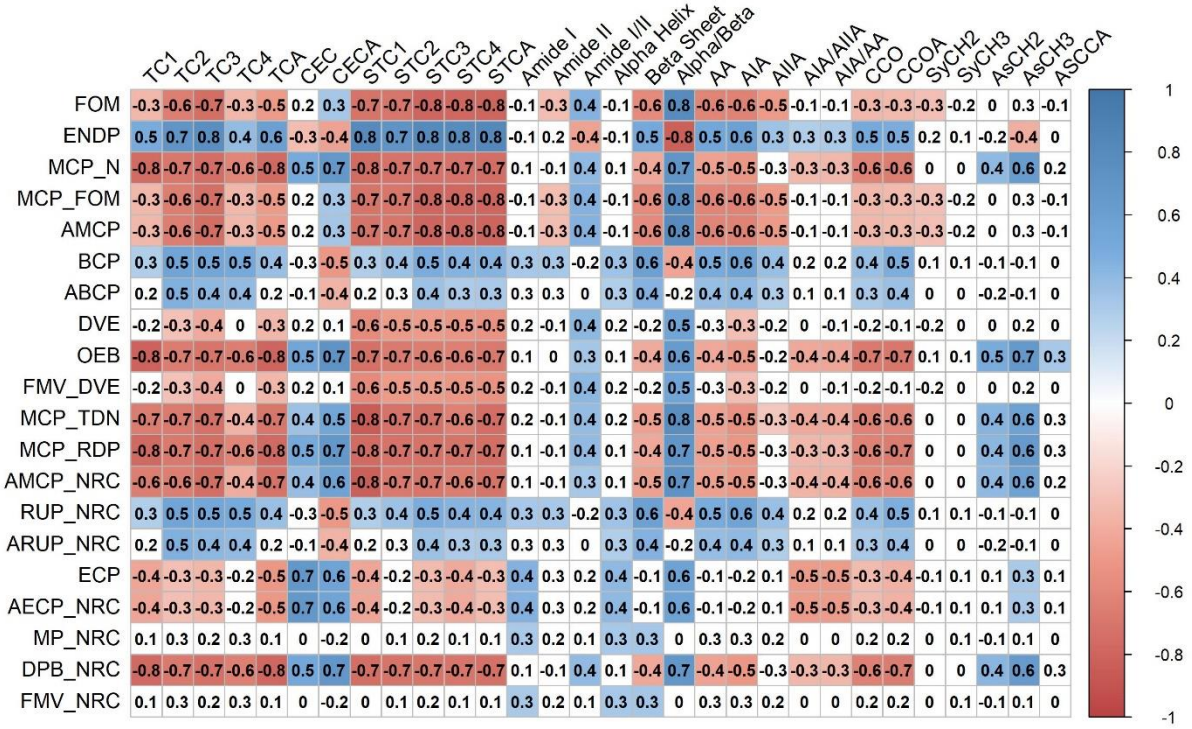

Figure 5.2.4 Correlation plot between molecular structure and protein metabolic characteristics of alfalfa forage with DVE/OEB and NRC-2001 system.

Notes: Blue color means positive correlation, while red means negative correlation. Colorless cells contain correlation coefficients that are not significant at $P<0.05$. Values in the plot are correlation coefficients, and the deeper the color, the higher the absolute coefficient value.
Spectral parameters: TC1-TC4, four major peaks in total carbohydrate (TC) region; TCA, peak area of TC region; CEC, cellulosic compounds; CECA, peak area of CEC region; STC1-STC4, four major peaks in structural carbohydrate (STC) region; STCA, peak area of STC region; AA, total amide area; AIA, amide I area; AIIA, amide II area; CCO, carbonyl C=O (CCO) peak; CCOA, CCO peak area. SyCH2, symmetric CH_2; SyCH3, symmetric CH_3; AsCH2, asymmetric CH_2; AsCH3, asymmetric CH_3; ASCCA, peak area of asymmetric and symmetric CH_2 and CH_3 (ASCC) region;
Protein metabolic profiles: FOM, fermentable organic matter; ENDP and ECP, endogenous protein; MCP_N and MCP_RDP, predicted microbial protein from rumen degradable protein; MCP_FOM and MCP_TDN, predicted microbial protein synthesized based on energy (FOM or TDN); Letter "A" in front of each protein fractions means absorbable fraction; BCP and RUP, rumen undegradable protein; DVE, truly absorbed protein; OEB and DPB, degraded protein balance; FMV, feed milk value.

Yari et al. (2017) reported that NSTCA/TCA and NSTCA/STCA ratios were negatively correlated with ENDP, but positively correlated with AMCP, ARUP, DVE and OEB values of alfalfa. In contrast, SyCH3/SyCH2 ratio was positively correlated with ENDP, but negatively correlated with AMCP, ARUP, DVE and OEB values (Yari et al. 2017). The NSTC is readily degraded in the rumen to provide nutrients for microbial growth, which might explain the positive

correlations between NSTCA ratios and protein availability of alfalfa. However, there was no comparison could be made because of the lack of carbohydrate area ratio in this study.

In terms of protein spectral parameters, Yari et al. (2013) reported that amide I/II ratio was negatively correlated with AMCP, ARUP, DVE and OEB values, but positively correlated with ENDP. In contrast, alpha/beta ratio was positively correlated with AMCP, ARUP, DVE and OEB, but negatively correlated with ENDP of alfalfa. The correlations between alpha/beta ratio and protein metabolic features were consistent with the current study. Jonker et al. (2011, 2012a) studied anthocyanin-accumulating *Lc*-transformed alfalfa which had higher peaks of amide I, amide II, alpha helix and beta sheet also had higher undegradable DM and ENDP, indicating an positive correlation between ENDP and protein spectral peaks. However, in the current study, only beta sheet was positively correlated with ENDP. Doiron et al. (2009) reported that alpha/beta ratio was negatively correlated with ENDP and OEB, but positively correlated with ARUP and DVE for flaxseed. Zhang and Yu (2012) reported alpha helix and beta sheet were positively, while alpha/beta ratio was negatively correlated with DVE, MP, OEB and DPB, although correlation coefficients were not significant. Yu and Nuez-Ortín (2010) reported that amide I/II ratio was positively correlated with OEB but negatively correlated with AMCP_NRC for DDGS samples. The discrepancies in correlation studies might largely reside in the differences in spectral processing methods and types of feed ingredients.

5.2.3.5 Regression of predicting nutrient degradational kinetics, microbial nitrogen and protein metabolic profiles from spectral parameters of alfalfa

Regression equations of predicting nutrient degradational kinetics and microbial nitrogen profiles from spectral parameters of alfalfa are shown in Table 5.2.1. For nutrients degradational kinetics, DM_K_d, DM_S, DM_U, DM_D and CP_ED could be obtained with good estimation

power (R^2>0.7). The DM_K_d could be predicted from CEC, Amide I, alpha/beta, CCOA and AsCH3 with an R^2 of 0.875, and DM_S could be predicted from Amide I/II, alpha/beta and CCOA with an R^2 of 0.709. In addition, DM_U and DM_D could be predicted from Amide I, alpha/beta, CCO and AsCH3 with great estimation power (R^2>0.9). As for CP_ED, it could be predicted with just TC4 and alpha/beta ratio with an R^2 of 0.79. For microbial nitrogen profiles, only APE of LAMN and LAMN production at 24 h of incubation could be well predicted (R^2>0.7). For APE LAMN at 24 h of incubation, it could be predicted from Amide I, Amide I/II, alpha/beta, SyCH2 and SyCH3 with an R^2 of 0.76. And for LAMN at 24 h of incubation, alpha/beta and CCOA were selected in the prediction equation with an R^2 of 0.758.

Regression of predicting protein metabolic characteristics with DVE/OEB and NRC-2001 systems from spectral parameters of alfalfa are shown in Table 5.2.2. Good predictions for microbial protein profiles, degradable protein balance for both systems and endogenous protein for DVE/OEB system could be obtained with R^2 greater than 0.7. For microbial protein with DVE/OEB system, FOM, MCP_FOM and AMCP_DVE could be predicted from CEC, Amide I/II and alpha/beta with R^2 of 0.754, while MCP_N could be predicted from TC4, Amide I, Amide I/II, alpha/beta, SyCH2 and SyCH3 with R^2 of 0.867. As for ENDP, it could be predicted from Amide I/II and alpha/beta ratio with an R^2 of 0.8. In addition, OEB value could be predicted from TC4, Amide I, Amide I/II, alpha/beta and SyCH2 with reasonable estimation power (R^2=0.827). For protein metabolic characteristics with NRC-2001 system, MCP_RDP could be predicted from same spectral parameters for MCP_N with R^2 of 0.864. Prediction of MCP_TDN could be obtained from Amide I, Amide I/II, alpha/beta, SyCH2 and SyCH3 (R^2=0.803) and prediction of AMCP_NRC could be obtained from alpha/beta and SyCH2 (R^2=0.739). Moreover, DPB_NRC could be predicted from TC4, Amide I, Amide I/II and alpha/beta (R^2=0.841).

Table 5.2.1 Regression equations of predicting nutrients degradation and microbial nitrogen (MN) from molecular structure for alfalfa forage.

Dependent Variables [1]	Prediction Equations [2]	RSE [3]	Adjusted R^2	P value
DM degradational kinetics (%)				
DM_K_d	Y = 77.3 - 330.87 CEC + 101.54 Amide I - 64.69 alpha/beta + 6.55 CCOA - 190.34 AsCH3	3.866	0.875	<0.001
DM_S	Y = 62.03 - 10.72 Amide I/II - 14.47 alpha/beta + 3.13 CCOA	2.176	0.709	<0.001
DM_U	Y = 90.56 + 76.93 Amide I - 82.26 alpha/beta + 7.82 CCOA - 232.88 AsCH3	3.681	0.903	<0.001
DM_D	Y = -41.29 - 95.82 Amide I + 100.6 alpha/beta - 10.88 CCOA + 318.19 AsCH3	3.380	0.950	<0.001
Effective degradation of CP (%)				
CP_ED	Y = 57.27 - 159.25 TC4 + 46.43 alpha/beta	2.169	0.792	<0.001
N^{15} enrichment (% atom excess) in loosely attached MN (LAMN) at 24 h incubation				
LAMN	Y = 16.35 - 5.36 Amide I - 2.6 Amide I/II - 9.74 alpha/beta - 38.52 SyCH2 + 139.62 SyCH3	0.402	0.760	<0.001
loosely attached MN fractions (LAMN) at 24 h incubation (mg/g residue)				
LAMN	Y = -31.51 + 47.77 alpha/beta - 1.69 CCOA	2.416	0.758	<0.001

1. U, undegradable fraction; S, soluble fraction; D, degradable fraction; K_d, degradation rate; ED, effective degradation.
2. TC4, the fourth major peak in total carbohydrate (TC) region; CEC, cellulosic compounds peak; Amide I, the first peak in amide region; Amide I/II, peak ratio of amide I to amide II; alpha/beta, peak ration of alpha helix to beta sheet; CCOA, carbonyl C=O peak area. SyCH2, symmetric CH2; SyCH3, symmetric CH3; AsCH3, asymmetric CH3;
3. RSE, residual standard error; 4. adjusted R square. Only regressions with the adjusted R2 larger than 0.7 were selected in this table.

Table 5.2.2 Regression equations of predicting protein metabolic characteristics with DVE/OEB and NRC-2001 systems from molecular structure for alfalfa forage

Dependent Variables [1]	Prediction Equations [2]	RSE [3]	Adjusted R^2	P value
Absorbable microbial protein from DVE/OEB system (g/Kg DM)				
FOM	Y = 47.57 - 1534.87 CEC + 130.9 Amide I/II + 523.2 alpha/beta	21.607	0.754	<0.001
MCP_N	Y = -151.1 - 1050.61 TC4 + 233.49 Amide I + 89.29 Amide I/II + 342.51 alpha/beta + 800.51 SyCH2 - 2225.41 SyCH3	12.670	0.867	<0.001
MCP_FOM	Y = 7.14 - 230.23 CEC + 19.63 Amide I/II + 78.48 alpha/beta	3.241	0.754	<0.001
AMCP_DVE	Y = 4.55 - 146.77 CEC + 12.52 Amide I/II + 50.03 alpha/beta	2.066	0.754	<0.001
Endogenous protein from DVE/OEB system (g/Kg DM)				
ENDP	Y = 74.71 - 10.78 Amide I/II - 43.36 alpha/beta	1.795	0.800	<0.001
Degraded protein balance (OEB) from DVE/OEB system (g/Kg DM)				
OEB	Y = -147.9 - 1211.45 TC4 + 202.78 Amide I + 53.53 Amide I/II + 250.43 alpha/beta + 318.3 SyCH2	12.515	0.827	<0.001
Absorbable microbial protein from NRC-2001 system (g/Kg DM)				
MCP_RDP	Y = -124.07 - 874.06 TC4 + 205.29 Amide I + 77.12 Amide I/II + 286.72 alpha/beta + 699.08 SyCH2 - 1963.98 SyCH3	10.794	0.864	<0.001
MCP_TDN	Y = 44.86 + 12.59 Amide I + 5.97 Amide I/II + 32.85 alpha/beta + 105.85 SyCH2 - 306.97 SyCH3	1.254	0.803	<0.001
AMCP_NRC	Y = 29.87 + 20.42 alpha/beta + 31.22 SyCH2	0.826	0.739	<0.001
Degraded protein balance (DPB) from NRC-2001 system (g/Kg DM)				
DPB_NRC	Y = -122.15 - 1314.95 TC4 + 194.87 Amide I + 70.55 Amide I/II + 258.79 alpha/beta	12.656	0.841	<0.001

1. FOM, fermentable organic matter; MCP_RDP and MCP_N, predicted microbial protein from rumen degradable protein; MCP_FOM and MCP_TDN, predicted microbial protein synthesized based on energy (FOM or TDN); AMCP, absorbable microbial protein; OEB and DPB, degraded protein balance;
2. TC4, the fourth major peak in total carbohydrate (TC) region; CEC, cellulosic compounds peak; Amide I/II, peak ratio of amide I to amide II; alpha/beta, peak ration of alpha helix to beta sheet; CCOA, carbonyl C=O peak area. SyCH2, symmetric CH_2; SyCH3, symmetric CH_3; AsCH3, asymmetric CH_3; AIA/AIIA, ratio of amide I area to amide II area; 3. RSE, residual standard error; Only regressions with the adjusted R^2 larger than 0.7 were selected in this table.

Same as previous study (Chapter 5.1), alpha/beta ratio was the most frequently selected spectral parameters in regression equations for nutrients degradations and microbial N fractions. For protein metabolic profiles. amide I/II was the second most selected predictor after alpha/beta ratio followed by other spectral parameters. Our results showed that DM degradation kinetics could be predicted with more estimation power compared with NDF and CP degradation kinetics, whereas only effective degradation of CP was predictable with high estimation power. In general, it was not practical to predict microbial nitrogen fractions from sample spectral parameters. For microbial fractions, it might be more practical to predict total nitrogen and N^{15} enrichment of MN fractions with residue spectra, as shown in a study of predicting protein content in wheat samples (Shi et al. 2019). Previous studies reported regression equations of predicting nutrients degradation and protein metabolic profiles from spectral parameters (Yu and Nuez-Ortín 2010; Theodoridou and Yu 2013a; Peng et al. 2014; Refat et al. 2017b; Prates et al. 2018a). However, comparisons could not be made between this study and previous studies due to the differences in variable selections. Only empirical spectral parameters were selected to predict corresponding nutritional profiles in previous studies; however, all available spectral parameters were included in regression models in this study.

5.2.4 Conclusion

In conclusion, molecular structures of alfalfa were closely correlated with nutrient degradation, fermentation characteristics and protein metabolic characteristics. In general, TC, STC and CCO structural profiles were negatively, whereas CEC, alpha/beta ratio, AsCH2 and AsCH3 profiles were positively correlated with the nutritive values of alfalfa. Moreover, DM degradation, MCP synthesis and protein degradation balance could be predicted with spectral parameters with good estimation power.

CHAPTER 6
GENERAL DISCUSSION

Alfalfa (*Medicago sativa*) is one of the most important leguminous forage crops and is widely cultivated around the world (Lei et al. 2017). Alfalfa contains high protein and low fiber that is very suitable for ruminant ration, especially for high production dairy cows (Berthiaume et al. 2010). In addition, alfalfa has a robust and deep root system that enables it to flourish in arid and semiarid regions (Radović et al. 2009). Moreover, as a legume forage, alfalfa has symbiotic relationship with *Rhizobium* which could fix nitrogen from the air (Zhang et al. 2016). However, alfalfa is not without drawbacks, which limit its utilization in animal husbandry, such as high contents of lignin and rapid-degradable protein.

Compared with traditional breeding, genetic engineering is more direct and accurate and less time-consuming (Lei et al. 2018c). Therefore, genetic engineering has been used for alfalfa improvement for decades, not only for nutritional improvement, but also for stress resistance and biomass yield increases (Lei et al. 2017). However, most studies were focused on gene expression and agronomic traits, with little emphasis on nutritional value. For studies involving nutritional value, there were reports on only a few nutrients (Aung et al. 2015a). Therefore, the objective of this research was to evaluate the nutritive values and molecular structures of newly developed alfalfa genotypes through genetic modification and transformations. This research included genetically modified alfalfa from two separate projects. The first project studied the effects of silencing *TT8* and *HB12* genes on nutritional values and molecular structures of alfalfa. The second project studied comparative effects of miR156 overexpressing with silencing *SPL6* and *SPL13* genes on molecular structures and nutritional values of alfalfa.

Chapter 3.1 and Chapter 4.1explored such genetic modifications on bioactive compounds, chemical composition, CNCPS fractions and degradations, truly digestive nutrients and energetic values of alfalfa. Results showed that silencing of *TT8* and *HB12* genes increased fiber content, CB3, PC and tdNDF and decreased protein, PB1 and tdFA of alfalfa. As for the second project, overexpression of miR156 resulted in lower fiber, CB3 and tdNDF but higher insoluble true protein (PB1), TDN and energy values. Although both SPL RNAi alfalfa were not significantly different from WT, SPL6 RNAi was more similar to miR156 OE alfalfa.

Studies showed that there was an increase in NDF, ADF and PC while CP and net energy decrease in alfalfa plants approaching maturity; i.e. from early-bud stage to early-flower stage, (Yu et al. 2003b; Yari et al. 2012a). This is confirmed with the chemical differences between alfalfa samples in the first two projects. Alfalfa samples in the second project (miR156 OE and SPL RNAi alfalfa) had higher protein and energy values, but lower fiber compared with the findings in first project (TT8i and HB12i alfalfa). Alfalfa samples were harvested at an earlier age in the second project compared with those in the first project. The higher fiber and lower protein contents of *TT8i* and *HB12i* transgenic alfalfa compared with WT suggests that silencing *TT8* and *HB12* genes had similar effects as maturity, which might promote alfalfa growth. To the contrary, the higher CP and lower fiber of miR156 OE alfalfa indicated that it was at an earlier growth stage compared with WT. This is because miR156 OE affects plant transition both from juvenile stage to adult stage and from adult stage to reproductive stage (Wu and Poethig 2006; Wu et al. 2009; Wang and Wang 2015). Overexpression of miR156 could prolong vegetative growth of alfalfa, resulting in younger alfalfa at harvest compared with WT.

Moreover, silencing of *TT8* resulted in higher phenolic compounds, whereas silencing of *HB12* led to higher lignin of alfalfa. TT8 controls anthocyanins and proanthocyanins syntheses via

its regulations on lateral genes' expression in the phenylpropanoid pathway (Nesi et al. 2000). Silencing of *TT8* gene might lead to a redistribution of intermediates in this pathway which might be responsible for the increase of total phenolic compounds in TT8i transgenic alfalfa. HB12, on the other hand, is a family member in of Homeodomain-Leucine Zipper protein and its expression is inducible by drought stress and abscisic acid (Olsson et al. 2004; Park et al. 2011). The increased lignin content of HB12i might be attributed to the stress reaction of transgenic alfalfa. Research showed that lignin biosynthesis is also enhanced by abiotic stresses (Vanholme et al. 2010), which might explain the increase in lignin content by silencing *HB12* genes in alfalfa. Although TT8i alfalfa had higher fiber and lower protein content than WT, there were no significant differences in tdCP between TT8i and WT alfalfa. In addition, both TT8i and HB12i genotypes had higher tdNDF compared with WT alfalfa, which led to equal energy values between TT8i and WT alfalfa. In the second project, miR156 OE also had higher insoluble protein fraction, which is the PB1 fraction in CNCPS protein pool (Higgs et al. 2015), compared with other genotypes. This implies a higher supply of moderate degradable protein from miR156 OE compared with WT, which could slow down the protein degradation in the rumen to reduce the possibility of rumen bloat. This implication is confirmed with *in vitro* fermentation study in Chapter 4.5, where a lower initial CP degradation of miR156 OE was found compared with other genotypes.

Chapter 3.2 and Chapter 4.2 focused on the effects of genetic modifications on inherent molecular structures of alfalfa with attenuated total reflection-Fourier transform infrared (ATR-FTIR) spectroscopy. In the first project, silencing of *TT8* and *HB12* genes increased TC and STC parameters, but decreased CEC parameters in carbohydrate spectral regions. In addition, HB12i had even higher STC parameters compared with TT8i alfalfa. In amide spectral region, TT8i had higher amide I/II ratio and both transformed alfalfa genotypes had higher beta sheet and lower

alpha/beta ratio. Moreover, HB12i had higher amide areas compared with other genotypes. In lipid-related regions, both TT8i and HB12i alfalfa had higher ASCC parameters. Multivariate analyses showed that WT was clearly separated from transgenic alfalfa genotypes in all carbohydrate regions and ASCC region with both HCA and PCA methods. In addition, alfalfa genotypes were distinguishable from each other in amide region. As for the second project, overexpression of miR156 and silencing of *SPL6* and *SPL13* genes resulted in lower TC and CEC parameters in carbohydrate region, whereas silencing of *SPL6* and *SPL13* genes also reduced STC parameters in alfalfa. In amide region, all transformed alfalfa genotypes had lower amide peak heights, protein second structure heights and amide areas compared with WT alfalfa. In addition, both SPL6 and SPL13 RNAi had higher amide I/II ratio compared with miR156 OE alfalfa, and higher AIA/AIIA and AIA/AA ratios than WT alfalfa. In lipid-related regions, transformed alfalfa had higher CCOA, AsCH3 and ASCCA, whereas WT had lower SyCH2 compared with miR156 OE alfalfa. Multivariate analyses showed that WT was separable from transformed alfalfa with both PCA and HCA analyses. However, in other regions, all alfalfa genotypes were overlapped with each other in both multivariate analyses.

FTIR spectroscopy is a non-destructive analytical tool that enables researcher to obtain structural information of a sample in a short time and with a small amount (Stuart 2004). It is not only applicable to pure molecules but also complex compounds such as feed samples (Ami et al. 2013). Previous studies used this technique on molecular studies of different feed ingredients and different feed processing methods (Theodoridou and Yu 2013a; Xin and Yu 2013a; Peng et al. 2014; Refat et al. 2017b; Prates et al. 2018b). In the current studies, there were four peaks measured both in TC and STC regions, compared with three peaks in previous studies (Yang et al. 2014; Li et al. 2015; Heendeniya and Yu 2017; Ban et al. 2017; Refat et al. 2017b). This could be due to a

possible overlap of two peaks, that were detectable only with second derivatives in our study. Previous studies also used this analytical tool to explore the molecular structures of alfalfa induced by genetic transformation. Jonker et al. (2012a) reported that transformation of alfalfa with *Lc* gene resulted in higher peaks of amide I, amide II, alpha helix and beta sheet. However, Yu et al. (2009) reported that *Lc*-alfalfa had lower alpha helix and beta sheet heights compared with untransformed alfalfa, which implies that molecular structures were different between alfalfa genotypes. Heendeniya and Yu (2017) reported that alfalfa with *Lc* and *C1* genes co-expression had lower peak heights of STC2, CEC, TC1 and TC4, and higher ratios of amide I/II and alpha/beta compared with non-transformed alfalfa.

Correlations studies showed TC, STC and CCO parameters were correlated positively with fiber content but negatively with protein content; however, CEC parameters and alpha/beta ratio were negatively correlated with fiber content but positively with protein content (Chapter 5.1). Chemically, TT8i and HB12i alfalfa had higher fiber and lower CP, which explains their higher TC and STC parameters, but lower alpha/beta ratio. Moreover, TC and STC samples in the second project were lower, while CEC parameters were higher than those in the first project. This is because samples in the second project had higher protein and lower fiber compared with those in the first project. For the second project, miR156 OE had higher insoluble true protein, but lower fiber compared with other genotypes, whereas SPL RNAi alfalfa genotypes were not significantly different from WT alfalfa (Chapter 4.1). In addition, contrast results indicated that transformed alfalfa had lower NDF and ADF content, and SPL RNAi alfalfa tended to have lower ADF compared with WT. These chemical features might explain the lower TC for miR156 OE and lower STC parameters for SPL RNAi alfalfa. However, such correlations failed to explain the lower CEC parameters of transformed alfalfa in the second project, as CEC parameters were

negatively correlated with fiber content. This might be because that TC and STC parameters had higher closer relationship with chemical composition than CEC parameters. As shown in the correlation study (Chapter 5.1), the absolute values of correlation coefficients between CEC and chemical composition were lower than TC and STC parameters.

Multivariate analyses are commonly used on datasets with large numbers of variables, for example spectral data (Chevallier et al. 2006). Hierarchical cluster analysis (HCA) and principle component analysis (PCA) were performed in this research for ATR-FTIR spectral data. The HCA calculates the distance matrix between spectra and then cluster similar spectra into one group. The PCA, on the other hand, transform the original high dimensional dataset into a new uncorrelated dataset with the first few components account for over 95 % of population variance (Yu 2005b). Previous studies utilized these two multivariate analyses to distinguish samples with spectral data with many feed ingredients (Yu 2005b, 2008; Skrobot et al. 2007; Li et al. 2015; Heendeniya and Yu 2017). Li et al. (2015) reported that PCA and HCA failed to distinguish TT8i, HB12i and WT alfalfa samples in carbohydrate spectral regions, whereas distinguishes were successively obtained between alfalfa genotypes in the first project. This discrepancy might be caused by population size as there were only two replicates for alfalfa genotypes in Li's study. Heendeniya and Yu (2017) studied molecular structures of *C1* and *Lc* genes single and double transformed alfalfa and found that alfalfa genotypes transformed with both *C1* and *Lc* genes were distinguishable from non-transformed alfalfa in carbohydrate region.

Chapter 3.3 and Chapter 4.3 explored the molecular structures of alfalfa leaves and the chemical localization in alfalfa leaves with synchrotron based FTIR microspectroscopy (SR-IMS). In the first project, TT8i and HB12i alfalfa had higher CCO parameters compared with WT, whereas there were no significant differences in other spectral regions. Chemical mapping showed

that HB12i had TC and STC functional groups in both mesophyll and epidermises, whereas they were only distributed in epidermises in TT8i and WT alfalfa leaves. In addition, HB12i had higher CCO area and lower lignin intensities compared with other genotypes. The second project showed that miR156 OE alfalfa had higher TC parameters and lower CEC and amide parameters compared with SPL6 RNAi. All transformed alfalfa had lower lignin peak compared with WT and SPL13 RNAi had lower CCO parameters compared with WT and SPL6 RNAi alfalfa. Chemical mapping showed that SPL13 RNAi had TC and STC functional groups evenly distributed in leaf tissues, while they were largely present in the epidemical area in other alfalfa genotypes. In addition, SPL6 RNAi had lower intensities of STC and CCO functional groups, while SPL13 RNAi had lower CEC and amide groups. Moreover, SPL13 RNAi had the highest lignin intensity, followed by WT and both SPL6 RNAi and miR156 OE were equally lower.

Different molecular structures were found between homogenously ground alfalfa samples (stems and leaves) and alfalfa leaves in both projects. Alfalfa leaves had lower TC and STC parameters compared with homogenously ground samples. Correlations studies revealed that TC and STC parameters are positively correlated with fiber content and negatively correlated with protein content. This indicates that alfalfa leaves had higher protein content and lower fiber content compared with homogenous samples. This is confirmed with the fact that half of alfalfa biomass is from stems at vegetative growth stage (Orloff and Putnam 2004; McCaslin et al. 2015) and alfalfa stems were reported to have lower protein and higher fiber compared with leaves (Marković et al. 2012). Different molecular structures were also found in amide and lipid-related regions between ground samples and alfalfa leaves.

Our correlations study (Chapter 5) showed that CCO parameters had similar correlations patterns with TC and STC parameters and were positively correlated with fiber content. Therefore,

the higher CCO parameters of TT8i and HB12i alfalfa indicates higher fiber content in leaves of these transformed alfalfa genotypes. Lignin peak centers at ca. 1515 cm^{-1} and was more obvious in spectra of alfalfa leaves compared with homogenous samples. Therefore, lignin peak was measured in this study. In the second project, transformed alfalfa were found to have lower lignin peak height compared with WT and miR156 OE was even lower than SPL RNAi alfalfa. Chemical mapping also showed lower intensity of lignin area in miR156 OE and SPL6 RNAi. This indicated that transformed alfalfa might have lower lignin content in their leaves, especially for miR156 OE, which is consistent with the lower lignin content in some miR156 subgenotypes (Aung et al. 2015a). In addition, SPL RNAi alfalfa had higher amide I, alpha helix, beta sheet, AA and AIA compared with miR156 OE. Also, SPL6 RNAi had higher amide II and AIIA compared with miR156 OE. Chapter 5 showed beta sheet and amide areas were strongly and negatively correlated with protein content, which indicates that SPL RNAi alfalfa had lower protein content in their leaves compared with miR156 OE alfalfa.

Synchrotron based FTIR microspectroscopy utilizes synchrotron light, which is 1000 times brighter than global light source (Miller and Dumas 2006). Because of this bright light, SR-IMS is able to provide structural information at cellular level with high accuracy and small effective source size (Liu and Yu 2016; Yang and Yu 2017). Therefore, it is possible to evaluate molecular chemistry of samples and localize chemical components in samples (Yu et al. 2004a). Previous studies used this technique to reveal chemical distribution of barley (Yu et al. 2003c), corn (Yu et al. 2004b), feather (Yu et al. 2004a) and alfalfa leaves (Yu et al. 2019). To our knowledge, there were no previous studies on effects of genetic modifications on distributions of chemical components in alfalfa. In the current study, amide area had the highest intensity followed by ASCC area with both mainly located in mesophyll area of alfalfa leaves. In contrast, carbohydrate areas

had lower intensities and TC and STC functional groups are mainly located in epidermises of alfalfa leaves.

Chapter 3.4 and Chapter 4.4 evaluated the effects of such genetic modifications on *in vitro* fermentation features of alfalfa, including gas, VFA and ammonia production and DM and NDF degradation. In the first projects, HB12i had lower gas, VFA and ammonia production and both transformed alfalfa genotypes had lower DM degradation. In addition, TT8i had higher ammonia production at 48 h of fermentation compared with other genotypes. Moreover, transformed alfalfa had lower propionate, butyrate and long-chain VFA compared with WT. The second project showed that miR156 OE had higher DM degradation compared with WT and SPL13 RNAi. In addition, SPL13 RNAi had higher ammonia production at 12 h of fermentation than WT and miR156 OE, higher total VFA production than WT and higher acetate than miR156 OE. Moreover, both SPL RNAi had higher long-chain VFA production compared with WT and miR156 OE.

Gas is produced mainly from carbohydrate hydrolysis and consists of carbon dioxide and methane with little contribution from ammonia (Russell and Rychlik 2001; Getachew et al. 2004; Spanghero et al. 2018). Gas production implies nutrients degradation in the rumen, especially for carbohydrates. Previous studies showed that gas production during *in vitro* fermentation was negatively correlated with NDF and ADF contents (Ndlovu and Nherera 1997; Larbi et al. 1998), which might explain the lower gas production of HB12i alfalfa in the first project. Moreover, gas production was higher in the second project compared with the first project, which might also be explained with the lower NDF and ADF content of alfalfa samples from the second project. However, Getachew et al. (2004) reported that gas production was negatively correlated with CP content, but was not significantly correlated with NDF based on studies on 12 feedstuffs. This discrepancy might be attributed to sample types. Jonker et al. (2012b) studied on fermentation

features of *Lc*-alfalfa and also found that alfalfa samples with lower CP and higher NDF and ADF also had lower gas production, which is consistent with the current research. According to these correlation studies, higher gas production was expected from miR156 OE; however, this was not observed. This indicates NDF content has little effect on gas production when its level is low, which is in line with Getachew et al (2004). The study by Getachew et al. also reported that gas production was positively correlated with ammonia production (Getachew et al. 2004), which might explain the lower ammonia production from HB12i alfalfa. Ammonia concentration increased along with fermentation time in this study. This is because in *in vivo* condition when ammonia production exceeds the utilization of bacteria, the excessive ammonia will be absorbed via rumen epithelium; however, under *in vitro* condition ammonia was accumulated in the fermentation bottle with a small amount released with gas during gas measurement. Interestingly, both HB12i and SPL6 RNAi had lower ammonia production at the end of fermentation, which were coupled with higher N^{15} enrichment (APE) in liquid associate microbial N (LMN) fractions. This might be due to the higher utilization of ammonia from bacteria for these two alfalfa genotypes compared with their counterparts.

In the current research, acetate and propionate accounted for more than 80% of total VFA production during alfalfa fermentation, while butyrate and long-chain VFA only accounted for less than 20%, which is consisted with Jonker et al. (2012b). Acetate to propionate (C2:C3) ratio was about 2.2 in the current study, which is slightly lower than previous studies (Getachew et al. 2004; Jonker et al. 2012b). Berthiaume et al. (2010) reported that alfalfa samples with higher NFC content had lower C2:C3 ratio, and NFC content was higher in the current study compared with previous studies. Moreover, research showed that acetate production is promoted by cellulose, while propionate is promoted by starch and protein (Bannink et al. 2006). Getachew et al. (2004)

also reported positively correlation between gas and VFA productions, which might explain the lower VFA from HB12i alfalfa.

Genetic modifications significantly affected DM degradation of alfalfa in the current study but had no influences on NDF degradation. TT8i and HB12i in the first project and miR156 OE in the second project had higher DM degradation compared with their counterparts. Moreover, alfalfa samples in the second project had higher DM and NDF degradations compared with those in the first project. These differences in nutrient degradations could be attributed to differences in chemical compositions that affected by either genetic modification or harvest time. Transformed alfalfa had lower protein and higher fiber compared with WT in the first project (Chapter 3.1), whereas miR156 OE had higher insoluble protein and lower fiber compared with other genotypes in the second project (Chapter 4.1). Similarly, alfalfa samples were harvested earlier in the second project and thereby contained higher protein and lower fiber compared with those in the first project. Jonker et al. (2012b) also reported that *Lc*-alfalfa contained lower protein and higher fiber and had lower effective degradation of DM compared with WT. Silencing of *TT8* and *HB12* genes in the first project might promote alfalfa growth, thereby resulting more matured chemical composition. In contrast, overexpression of miR156 in the second project prolonged vegetative growth of alfalfa and resulted in younger alfalfa at harvest (Aung et al. 2015a). Alfalfa samples were harvested at vegetative stages in the current study due to biosafety regulations on transgenic plants, which is earlier than commercial harvest. Therefore, more different chemical compositions between transgenic alfalfa and WT control is expected if samples were harvested at commercial bud stage. It is especially true for miR156 OE alfalfa that is highly possible to have higher protein content than WT control at a more advanced growth stage, as indicated by the differences in protein pool of CNCPS fractions.

Chapter 3.5 and Chapter 4.5 focused on effects of genetic modifications on protein degradation and digestion, microbial nitrogen fractions and protein metabolic characteristics of alfalfa with DVE/OEB and NRC-2001 systems. In the first project, transgenic alfalfa genotypes had lower CP degradation at the end of fermentation, while HB12i alfalfa had lower effective CP degradation compared with other genotypes. HB12i had higher APE in microbial N fractions compared with other genotypes. At 24 h of fermentation, WT had higher LAMN, followed by TT8i with HB12i being the lowest. In contrast, HB12i had higher FAMN at 24 h of fermentation compared with WT alfalfa and both transgenic alfalfa genotypes had higher FAMN/RN ratio at 4 and 12 h of fermentation compared with WT. Protein metabolic parameters showed that transgenic alfalfa had lower MCP compared with WT and HB12i was even lower than TT8i alfalfa. In contrast, HB12i had the highest ENDP (lowest ECP), followed by TT8i and WT was the lowest (highest for ECP). Compared with other genotypes, HB12i also had lower available protein and feed milk value according to DVE/OEB system, which were no seen with NRC system.

In the second project, miR156 OE had lower degradation rate and initial CP degradation compared with other genotypes. There were no significant differences in CP degradation between alfalfa genotypes at 24 h of fermentation. SPL6 RNAi had higher APE in LMN at 4 h followed by miR156 OE and WT with SPL13 RNAi being the lowest. Both SPL RNAi alfalfa genotypes had higher LAMN compared with miR156 OE at 12 h of fermentation. In contrast, miR156 OE had higher FAMN at 4 h of fermentation compared with WT and SPL6 RNAi, but lower FAMN/RN ratio compared with WT at 24 h of fermentation. Both nutritional systems showed that all transformed alfalfa tended to have higher degraded protein balance (OEB and DPB) compared with WT. Moreover, the DVE/OEB system showed all transformed alfalfa had higher AMCP compared with WT and miR156 OE had lower ENDP compared with WT and SPL13 RNAi. In

contrast, NRC-2001 system showed miR156 OE had higher AMCP compared with other genotypes. There were no significant differences in total truly absorbable protein (DVE/MP) between alfalfa genotypes.

CP degradation of alfalfa samples (except for miR156 OE) in the second project was higher than those in the first project at 12 h of fermentation and about 80% of protein was degraded at this time point. This is largely due to the differences in chemical composition caused by different harvest times. Alfalfa samples in the second project were harvested at an earlier age compared with those in the first project, therefore they had higher protein content and lower NDICP content. The higher NDICP and lower protein for TT8i and HB12i alfalfa were also to blame for their lower CP degradation. Jonker et al. (2012b) reported that *Lc*-alfalfa had lower protein content and lower effective degradation of protein compared with WT alfalfa. However, all alfalfa genotypes from the second project and WT from the first project had similar CP degradation at 24 h of fermentation, which was around 90%. This indicated that younger alfalfa had higher CP degradations in the beginning of fermentation. The lower initial protein degradation of miR156 OE suggested a better N/CHO balance of this genotypes, and it is less likely to cause rumen bloat, which is largely due to the high initial protein degradation (Jonker et al. 2012a). Both projects showed that genetic modification had no influences on the intestinal digestion of rumen undegradable protein (IDRUP) of alfalfa with three-step *in vitro* digestion trial.

Ammonia is the primary nitrogen source for most ruminal bacteria (Yang et al. 2010). Therefore, by introducing N^{15} labeled ammonium sulfate, we could trace and measure microbial protein syntheses during ruminal fermentation. In this study, N^{15} enrichment (APE) in LMN was higher than those in LAMN, which is consistent with previous study on *Lc*-alfalfa (Wang et al. 2006). This might be attributed to the higher nutrient supply for attached microbes, which resulted

in higher incorporation of N^{15} in microbial protein. Similarly, the higher APE of LMN for HB12i in the first project and SPL6 RNAi in the second project implies higher incorporation of N^{15} in liquid microbial protein. In addition, FAMN of alfalfa samples was also higher than LAMN, which is in agreement with Jonker et al (2012b). The higher FAMN for HB12i and TT8i alfalfa might be due to their higher residue content, which provided more attaching area for microbes. Notably, FAMN to RN ratio were higher than 30% in this project, which is in line with previous study (Wang et al. 2006). This means microbial nitrogen accounts for more than 30% of residue nitrogen for alfalfa *in vitro* study, which could lead to underestimation of protein degradation of alfalfa.

Microbial growth relies on both energy and protein supplies (Clark et al. 1992). Therefore, microbial protein is estimated with both available energy and available protein in the rumen for both DVE/OEB (Tamminga et al. 1994) and NRC-2001 systems (NRC Dairy 2001). A previous study reported that the optimum N/energy ratio for microbial growth should be 32 g N/Kg CHO or 25 g N/Kg OM (Yari et al. 2012a). However, the high positive value of OEB or DPB for alfalfa forages indicated that nitrogen supply of alfalfa is far beyond energy supply for microbial growth, which is consistent with previous studies (Yu et al. 2003b; Yari et al. 2012a, 2012b). Therefore, the final absorbable microbial protein (AMCP) was estimated with available energy supply for alfalfa samples. Different energy values resulted in different AMCP values of alfalfa genotypes, including the lower AMCP for transformed alfalfa in the first project and the higher AMCP for miR156 OE in the second project. The DVE/OEB and NRC-2001 systems had different concepts for endogenous protein with DVE/OEB considering it as a loss while NRC-2001 regarding it as a part of total available protein (Theodoridou and Yu 2013b). In DVE/OEB system, endogenous protein (ENDP) is positively related to undigested DM (Tamminga et al. 1994), which explains the higher value for transgenic alfalfa in the first project and lower value for miR156 OE in the

second project. In contrast, NRC-2001 system calculated endogenous protein (ECP) as part of metabolizable protein (MP) and is related to DM content (NRC Dairy 2001).

Overall, AMCP had highest contribution to total available protein (DVE and MP), followed by RUP and ECP. In the first project, DVE value was lower for HB12i due to lower AMCP and higher loss of ENDP compared with other. But HB12i had similar MP value compared with other genotypes in NRC-2001 system. Previous studies showed that DVE value is lower than MP and the difference was greater when CP content is low (Yu et al. 2003b; Yari et al. 2012b). The FMV was estimated with total available protein of alfalfa samples in the current study. Due to the lower DVE values of HB12i alfalfa with DVE/OEB system, the FMV of HB12i was lower than other genotypes, which was not seen with NRC-2001 system. Meanwhile, there were no significant differences between alfalfa genotypes in the second project. However, like microbial protein production in the rumen, feed milk production also depends on both energy supply and protein supply. According to NRC-2001 system, 0.698 Mcal of NE_L is needed to produce 1 Kg of milk assuming 3.5% milk fat, 3.3% milk protein and 4.85% milk lactose (NRC Dairy 2001). Based on this calculation, feed milk values of HB12i alfalfa in the first project would be lower than other genotypes due to its lower NE_L value. Similarly, miR156 OE alfalfa in the second project would have higher FMV (based on energy) than WT and SPL13 RNAi because of its higher NE_L value. However, FMV of alfalfa samples based on net energy is higher than that based on truly available protein. For example, FMV of WT based on NE_L in the first project was 2.34 Kg milk/Kg feed, which was much higher than its FMV based on DVE and MP (1.72 and 1.91, respectively). Therefore, truly absorbable protein was the limiting factor for milk production of alfalfa samples in the current study. One should be aware of that feed milk values were estimated with nutritional models under the assumption feeding dairy cows with pure alfalfa, which is not practical. Alfalfa

forage is used with other fodders in dairy rations to balance and meet animal nutrients requirement. The second project showed that miR156 OE provided more available energy and microbial protein in the rumen, which could be beneficial on dairy ration. As for TT8i transgenic alfalfa that had comparable energy and total absorbable protein, lower protein and higher fiber compared with WT, it might be possible to use it as a grazing variety to prevent rumen bloat.

Chapter 5 utilized spectral and nutritional data from the previous two projects to explore relationships between molecular structure and nutritional values of alfalfa. Inherent molecular structures of feed samples are closely correlated with their chemical composition and nutritional characteristics. Previous studies reported correlations between molecular structures and nutritional profiles for feedstuffs, including barley (Prates et al. 2018b, 2018a), canola (Xin and Yu 2013a), *Brassica carinata* (Xin and Yu 2013a, 2014), alfalfa (Yari et al. 2013; Li et al. 2015) and other feed ingredients (Peng et al. 2014). However, correlations between spectral parameters and nutritional profiles of samples were not consistent in previous studies (Doiron et al. 2009; Yu and Nuez-Ortín 2010; Zhang and Yu 2012; Theodoridou and Yu 2013b; Xin and Yu 2013b; Refat et al. 2017b; Prates et al. 2018b). This might be attributed to the differences in sample types, as spectral regions might indicate different chemical compounds for different types of sample (Baker et al. 2014).

In the current study, TC, STC and CCO parameters were negatively correlated with rapidly degraded nutrients, energy values, gas production and nutrients degradation, but positively correlated with slowly degraded or undegradable nutrients and N^{15} enrichment of microbial nitrogen. In contrast, CEC parameters, alpha/beta ratio, AsCH2 and AsCH3 had opposite correlations with nutritional profiles compared with TC, STC and CCO parameters. Compared with previous studies discussed above, in which only empirical parameters were selected for

correlation study, this study included all available spectral parameters within mid-IR range. This is because the relationship between spectral parameters and chemical compositions depends on the light absorption of chemical bonds (Prates and Yu 2017) and one chemical component has more than one type of chemical bonds.

The close correlations between spectral parameters and nutritional profiles of alfalfa made it possible to predict nutritional profiles from spectra parameters. In the current study, regression equations could be obtained with good estimation power (R^2>0.7) for chemical composition of CHO, NDF, starch, CP, NDICP, SCP and EE; CNCPS fractions and degradations of CB1, CB2, PA2, PB2, PB2 and rumen degradable and undegradable protein fractions; truly digestive nutrients of tdFA, tdCP and tdNDF; TDN and all energetic values; DM degradational kinetics and effective degradation of CP; APE of LAMN and LAMN production at 24 h; FOM from DVE/OEB system; microbial protein and degraded protein balance with both DVE/OEB and NRC-2001 systems. Among spectral parameters, alpha/beta ratio was the most frequently selected variable in regression equations, followed by amide I/II ratio. Overall, spectral parameters remained in regression equations were TC4, CEC, Amide I, Amide I/II, alpha/beta, CCOA, SyCH2, SyCH3, AsCH3 and AIA/AIIA. Previous studies reported regressions of predicting nutritional profiles from spectral parameters for other feedstuffs (Peng et al. 2014; Xin et al. 2014; Refat et al. 2017b; Prates et al. 2018b). However, same as their correlation studies, only corresponding spectral parameters were used in regression models of previous studies.

In summary, nutritional evaluation of TT8i transgenic alfalfa suggested its potential usage in grazing condition for its improved nutrient balance without compromising energy and protein supply. Future studies should focus on its bloating characteristics, such as foam stability, and nutritional evaluation under field condition. As for miR156 OE alfalfa, future study should aim to

explore its growth performance in the field. Previous study showed that miR156 OE had enhanced branching and thinner stem (Aung et al. 2015a), which might make it more vulnerable to wind damage. Moreover, it is implied that there are other *SPL* genes involved in miR156 OE event, which suggests future researches on identification of other miR156 targeting *SPL* genes in alfalfa. One should be aware of that the nutritional evaluation of transgenic alfalfa in the current study was based on chemical analysis and modeling estimation. The lack of feeding trail of this study might limit the implication of current findings. Applications of growing transgenic TT8i and miR156 OE alfalfa genotypes in the field could enable their nutritional evaluation at commercial cutting stage and with animal feeding trails. These studies could provide more insights on the nutritional profiles of these transgenic alfalfa genotypes and benefit alfalfa producers in the future. For relationship studies between molecular structure and nutritional profiles of alfalfa, the current study provided some preliminary information for the utilization of ATR-FTIR spectroscopy on alfalfa structural and nutritional study. However, the application of current predictions is limited by the population size (n=56) and the nutritional and structural similarities between alfalfa samples (especially for samples in the second project). To further extend the utilization of ATR-FTIR spectroscopy in alfalfa nutritional analysis, a larger sample size of alfalfa forage is needed with more diversity in nutritional and structural profiles.

CHAPTER 7
GENERAL CONCLUSION

7.1 Effects of silencing *TT8* and *HB12* genes on molecular structures and nutritive values of alfalfa in ruminant system

Silencing of *TT8* and *HB12* genes in alfalfa increased total carbohydrate, fiber and ADICP, but decreased DM, CP and starch of alfalfa. Moreover, silencing of *HB12* gene resulted in higher lignin, sugar, NDICP but lower EE, tdCP, tdFA, TDN and energy, while silencing of *TT8* led to higher phenolics.

Silencing of *TT8* and *HB12* genes in alfalfa increased TC, STC and ASCC parameters and beta sheet height, but decreased CEC parameters and alpha/beta ratio. Moreover, silencing of *HB12* gene resulted in higher AA, AIA, while silencing of *TT8* led to amide I/II. Both PCA and HCA could separate WT from transgenic genotypes in all carbohydrate regions and ASCC region and PCA could distinguish every alfalfa genotype in amide region. Silencing of *HB12* gene in alfalfa increased carbonyl compound in leaf tissues, which implies higher lipid deposition in the leaf. Moreover, HB12i had higher intensities of TC, STC and CCO areas, but lower lignin area in leaf tissues compared with TT8i and WT alfalfa. Overall, amide and ASCC chemical groups are mainly located in leaf mesophyll area, whereas TC and STC chemical groups were largely stored in the epidermis tissue.

Silencing *HB12* gene in alfalfa significantly decreased ruminal DM and CP degradation, gas, ammonia and VFA productions, MCP, DVE and FMV of alfalfa, but increased protein solubility, initially CP degradation and N^{15} enrichment of MN fractions. In contrast, silencing *TT8*

gene decreased DM degradation and long-chain VFA production. Although CP degradation of TT8i was lower than WT, there were no significant differences in effective CP degradation.

Taken together, our findings suggest that TT8i might be a better transgenic genotype than HB12i as it provides equivalent of energy and protein to animals with improved nutrient balance.

7.2 Comparative effects of overexpression of mir156 and silencing of *SPL6* and *SPL13* genes on molecular structures and nutritive value of alfalfa in ruminant system

Overexpression of miR156 decreased fiber content of alfalfa and provided more insoluble true protein and energy to animals. There were no significant differences in chemical composition between SPL RNAi and WT alfalfa.

Overexpression of miR156 had similar effects on molecular structure of alfalfa as silencing of *SPL6* and *SPL13* genes. All genetic transformations resulted in lower carbohydrate and amide parameters and higher lipid parameters. Moreover, multivariate analyses showed there were huge differences in lipid region between transformed and WT alfalfa. Overexpression of miR156 and silencing of *SPL6* and *SPL13* decreased lignin peak height in alfalfa leaves. MiR156 OE had higher TC parameters and lower CEC and amide parameters compared with SPL6 RNAi. Moreover, such genetic modifications affected localizations of chemical groups in alfalfa leaves.

Overexpression of miR156 increased DM degradation of alfalfa but had no other influences on rumen fermentation. In contrast, silencing of *SPL6* and *SPL13* genes, especially silencing of *SPL13* gene, had more pronounced effects on fermentation features. Overexpression of miR156 reduced initial degradation and degradation rate of CP but did not affect overall CP degradation, which could improve nutrient synchronization of alfalfa in the rumen.

Overall, overexpression of miR156 in alfalfa improved nutrients content and degradation. Moreover, SPL6 RNAi was more similar to miR156 OE than SPL13 RNAi, indicating *SPL6* gene played a more important role in miR156 overexpression event.

7.3 Relationship between molecular structure parameters and nutritional profiles of alfalfa

TC, STC and CCO parameters were negatively correlated with rapidly degraded nutrients, energy values, gas production and nutrients degradation, but positively correlated with slowly degraded or undegradable nutrients and N^{15} enrichment of microbial nitrogen. In contrast, CEC parameters, alpha/beta ratio, AsCH2 and AsCH3 had opposite correlations with nutritional profiles compared with TC, STC and CCO parameters.

Regression equations could be obtained with good estimation power (R^2>0.7) for chemical composition of CHO, NDF, starch, CP, NDICP, SCP and EE; CNCPS fractions and degradations of CB1, CB2, PA2, PB2, PB2 and rumen degradable and undegradable protein fractions; truly digestive nutrients of tdFA, tdCP and tdNDF; TDN and all energetic values; DM degradational kinetics and effective degradation of CP; APE of LAMN and LAMN production at 24 h; FOM from DVE/OEB system; microbial protein and degraded protein balance with both DVE/OEB and NRC-2001 systems.

LITERATURE CITED

Abeysekara, S., Damiran, D., and Yu, P. 2013. Univariate and multivariate molecular spectral analyses of lipid related molecular structural components in relation to nutrient profile in feed and food mixtures. Spectrochim. Acta. A. Mol. Biomol. Spectrosc. **102**: 432–442. doi:10.1016/j.saa.2012.09.064.

Aerts, R.J., Barry, T.N., and McNabb, W.C. 1999. Polyphenols and agriculture: beneficial effects of proanthocyanidins in forages. Agric. Ecosyst. Environ. **75**: 1–12. doi:10.1016/S0167-8809(99)00062-6.

Aguirreburualde, M.S.P., Gómez, M.C., Ostachuk, A., Wolman, F., Albanesi, G., Pecora, A., Odeon, A., Ardila, F., Escribano, J.M., Santos, M.J.D., and Wigdorovitz, A. 2013. Efficacy of a BVDV subunit vaccine produced in alfalfa transgenic plants. Vet. Immunol. Immunopathol. **151**: 315–324. doi:10.1016/j.vetimm.2012.12.004.

Ainsworth, E.A., and Gillespie, K.M. 2007. Estimation of total phenolic content and other oxidation substrates in plant tissues using Folin–Ciocalteu reagent. Nat. Protoc. **2**: 875–877. doi:10.1038/nprot.2007.102.

Ali, M.B., and McNear, D.H. 2014. Induced transcriptional profiling of phenylpropanoid pathway genes increased flavonoid and lignin content in Arabidopsisleaves in response to microbial products. BMC Plant Biol. **14**: 84. doi:10.1186/1471-2229-14-84.

Allen, M.S., and Piantoni, P. 2013. Metabolic control of feed intake. Vet. Clin. North Am. Food Anim. Pract. **29**: 279–297. doi:10.1016/j.cvfa.2013.04.001.

Ami, D., Mereghetti, P., and Maria, S. 2013. Multivariate analysis for Fourier transform infrared spectra of complex biological systems and processes. Page *in* L. Freitas, ed. Multivariate Analysis in Management, Engineering and the Sciences. InTech. doi:10.5772/53850.

An, Y., Guo, Y., Liu, C., and An, H. 2015. BdVIL4 regulates flowering time and branching through repressing miR156 in ambient temperature dependent way in Brachypodium distachyon. Plant Physiol. Biochem. **89**: 92–99. doi:10.1016/j.plaphy.2015.02.013.

ANKOM Technology 2014.September 3. Fiber analyzer A2000. Analytical methods. [Online] Available: https://www.ankom.com/analytical-methods-support/fiber-analyzer-a2000 [2017 Oct. 6].

Arshad, M., Feyissa, B.A., Amyot, L., Aung, B., and Hannoufa, A. 2017a. MicroRNA156 improves drought stress tolerance in alfalfa (Medicago sativa) by silencing SPL13. Plant Sci. doi:10.1016/j.plantsci.2017.01.018.

Arshad, M., Feyissa, B.A., Amyot, L., Aung, B., and Hannoufa, A. 2017b. MicroRNA156 improves drought stress tolerance in alfalfa (Medicago sativa) by silencing SPL13. Plant Sci. **258**: 122–136. doi:10.1016/j.plantsci.2017.01.018.

Aung, B. 2014.April 15. Effects of MicroRNA156 on flowering time and plant architecture in Medicago sativa. The University of Western Ontario, London, Ontario, Canada. [Online] Available: http://ir.lib.uwo.ca/etd/1956/ [2016 Sep. 27].

Aung, B., Gruber, M.Y., Amyot, L., Omari, K., Bertrand, A., and Hannoufa, A. 2015a. MicroRNA156 as a promising tool for alfalfa improvement. Plant Biotechnol. J. **13**: 779–790. doi:10.1111/pbi.12308.

Aung, B., Gruber, M.Y., Amyot, L., Omari, K., Bertrand, A., and Hannoufa, A. 2015b. Ectopic expression of LjmiR156 delays flowering, enhances shoot branching, and improves forage quality in alfalfa. Plant Biotechnol. Rep. **9**: 379–393. doi:10.1007/s11816-015-0375-2.

Aung, B., Gruber, M.Y., and Hannoufa, A. 2015c. The MicroRNA156 system: A tool in plant biotechnology. Biocatal. Agric. Biotechnol. **4**: 432–442. doi:10.1016/j.bcab.2015.08.002.

Badhan, A., Jin, L., Wang, Y., Han, S., Kowalczys, K., Brown, D.C., Ayala, C.J., Latoszek-Green, M., Miki, B., Tsang, A., and McAllister, T. 2014. Expression of a fungal ferulic acid esterase in alfalfa modifies cell wall digestibility. Biotechnol. Biofuels **7**: 39. doi:10.1186/1754-6834-7-39.

Baker, M.J., Trevisan, J., Bassan, P., Bhargava, R., Butler, H.J., Dorling, K.M., Fielden, P.R., Fogarty, S.W., Fullwood, N.J., Heys, K.A., Hughes, C., Lasch, P., Martin-Hirsch, P.L., Obinaju, B., Sockalingum, G.D., Sulé-Suso, J., Strong, R.J., Walsh, M.J., Wood, B.R., Gardner, P., and Martin, F.L. 2014. Using Fourier transform IR spectroscopy to analyze biological materials. Nat. Protoc. **9**: 1771–1791. doi:10.1038/nprot.2014.110.

Ban, Y., L. Prates, L., and Yu, P. 2017. Investigating molecular structures of bio-fuel and bio-oil seeds as predictors to estimate protein bioavailability for ruminants by advanced nondestructive vibrational molecular spectroscopy. J. Agric. Food Chem. **65**: 9147–9157. doi:10.1021/acs.jafc.7b02239.

Bannink, A., Kogut, J., Dijkstra, J., France, J., Kebreab, E., Van Vuuren, A.M., and Tamminga, S. 2006. Estimation of the stoichiometry of volatile fatty acid production in the rumen of lactating cows. J. Theor. Biol. **238**: 36–51. doi:10.1016/j.jtbi.2005.05.026.

Bassbasi, M., De Luca, M., Ioele, G., Oussama, A., and Ragno, G. 2014. Prediction of the geographical origin of butters by partial least square discriminant analysis (PLS-DA) applied to infrared spectroscopy (FTIR) data. J. Food Compos. Anal. **33**: 210–215. doi:10.1016/j.jfca.2013.11.010.

Baucher, M., Bernard-vailhé, M.A., Chabbert, B., Besle, J.-M., Opsomer, C., Montagu, M.V., and Botterman, J. 1999. Down-regulation of cinnamyl alcohol dehydrogenase in transgenic alfalfa (*Medicago sativa L.*) and the effect on lignin composition and digestibility. Plant Mol. Biol. **39**: 437–447. doi:10.1023/A:1006182925584.

Baudry, A., Caboche, M., and Lepiniec, L. 2006. TT8 controls its own expression in a feedback regulation involving TTG1 and homologous MYB and bHLH factors, allowing a strong and cell-specific accumulation of flavonoids in Arabidopsis thaliana. Plant J. **46**: 768–779. doi:10.1111/j.1365-313X.2006.02733.x.

Baudry, A., Heim, M.A., Dubreucq, B., Caboche, M., Weisshaar, B., and Lepiniec, L. 2004. TT2, TT8, and TTG1 synergistically specify the expression of BANYULS and proanthocyanidin biosynthesis in Arabidopsis thaliana. Plant J. **39**: 366–380. doi:10.1111/j.1365-313X.2004.02138.x.

Bekiaris, G., Bruun, S., Peltre, C., Houot, S., and Jensen, L.S. 2015. FTIR–PAS: A powerful tool for characterising the chemical composition and predicting the labile C fraction of various organic waste products. Waste Manag. **39**: 45–56. doi:10.1016/j.wasman.2015.02.029.

Belyea, R., Restrepo, R., Martz, F., and Ellersieck, M. 1999. Effect of year and cutting on equations for estimating net energy of alfalfa forage. J. Dairy Sci. **82**: 1943–1949. doi:10.3168/jds.S0022-0302(99)75430-5.

Bengera, I., and Norris, K. 1968. Determination of moisture content in soybeans by direct spectrophotometry. Isr. J. Agric. Res. **18**: 125-.

Berthiaume, R., Benchaar, C., Chaves, A.V., Tremblay, G.F., Castonguay, Y., Bertrand, A., Bélanger, G., Michaud, R., Lafrenière, C., McAllister, T.A., and Brito, A.F. 2010. Effects of nonstructural carbohydrate concentration in alfalfa on fermentation and microbial protein synthesis in continuous culture. J. Dairy Sci. **93**: 693–700. doi:10.3168/jds.2009-2399.

Beveridge, C.A., and Kyozuka, J. 2010. New genes in the strigolactone-related shoot branching pathway. Curr. Opin. Plant Biol. **13**: 34–39. doi:10.1016/j.pbi.2009.10.003.

Bhogale, S., Mahajan, A.S., Natarajan, B., Rajabhoj, M., Thulasiram, H.V., and Banerjee, A.K. 2014. MicroRNA156: a potential graft-transmissible microRNA that modulates plant architecture and tuberization in solanum tuberosum ssp. andigena. Plant Physiol. **164**: 1011–1027. doi:10.1104/pp.113.230714.

Birkenbihl, R.P., Jach, G., Saedler, H., and Huijser, P. 2005. Functional dissection of the plant-specific SBP-domain: overlap of the DNA-binding and nuclear localization domains. J. Mol. Biol. **352**: 585–596. doi:10.1016/j.jmb.2005.07.013.

Boerjan, W., Ralph, J., and Baucher, M. 2003. Lignin biosynthesis. Annu. Rev. Plant Biol. **54**: 519–546. doi:10.1146/annurev.arplant.54.031902.134938.

Bonawitz, N.D., and Chapple, C. 2013. Can genetic engineering of lignin deposition be accomplished without an unacceptable yield penalty? Curr. Opin. Biotechnol. **24**: 336–343. doi:10.1016/j.copbio.2012.11.004.

Brinkmann, K., Blaschke, L., and Polle, A. 2002. Comparison of different methods for lignin determination as a basis for calibration of near-infrared reflectance spectroscopy and implications of lignoproteins. J. Chem. Ecol. **28**: 2483–2501.

Brown, M.E., and Chang, M.C. 2014. Exploring bacterial lignin degradation. Curr. Opin. Chem. Biol. **19**: 1–7. doi:10.1016/j.cbpa.2013.11.015.

Budak, H., and Spangenberg, G. (eds.) 2015. Molecular breeding of forage and turf. Springer International Publishing, Cham. [Online] Available: http://link.springer.com/10.1007/978-3-319-08714-6 [2016 Nov. 4].

Canada, H. 2015.June 4. Novel food information - reduced lignin alfalfa KK179. assessments;notices. [Online] Available: https://www.canada.ca/en/health-canada/services/food-nutrition/genetically-modified-foods-other-novel-foods/approved-products/novel-food-information-reduced-lignin-alfalfa-kk179.html [2019 Mar. 26].

Cash, D., and Hu, Y. 2009. Chapter 1. Global status and development trends of alfalfa. Pages 1–14 *in* Alfalfa management guide for Ningxia. United Nations Food and Agriculture Organization. [Online] Available: http://www.fao.org/ag/agp/agpc/doc/ningxia_guide/ningxia_guide.htm [2016 Nov. 5].

Chen, L., Tian, Y., Sun, B., Cai, C., Ma, R., and Jin, Z. 2018. Measurement and characterization of external oil in the fried waxy maize starch granules using ATR-FTIR and XRD. Food Chem. **242**: 131–138. doi:10.1016/j.foodchem.2017.09.016.

Chen, L., Zhang, X., and Yu, P. 2014a. Impact of ethanol bioprocessing on association of protein structures at a molecular level to protein nutrient utilization and availability of different co-products from cereal grains as energy feedstocks. Biomass Bioenergy **69**: 47–57. doi:10.1016/j.biombioe.2014.06.014.

Chen, M., Xuan, L., Wang, Z., Zhou, L., Li, Z., Du, X., Ali, E., Zhang, G., and Jiang, L. 2014b. Transparent Testa8 inhibits seed fatty acid accumulation by targeting several seed development regulators in arabidopsis. Plant Physiol. **165**: 905–916. doi:10.1104/pp.114.235507.

Chen, X., Zhang, Z., Liu, D., Zhang, K., Li, A., and Mao, L. 2010. Squamosa promoter-binding protein-like transcription factors: star players for plant growth and development. J. Integr. Plant Biol. **52**: 946–951. doi:10.1111/j.1744-7909.2010.00987.x.

Chevallier, S., Bertrand, D., Kohler, A., and Courcoux, P. 2006. Application of PLS-DA in multivariate image analysis. J. Chemom. **20**: 221–229. doi:10.1002/cem.994.

Chuck, G., Cigan, A.M., Saeteurn, K., and Hake, S. 2007. The heterochronic maize mutant Corngrass1 results from overexpression of a tandem microRNA. Nat. Genet. **39**: 544–549. doi:10.1038/ng2001.

Clark, J.H., Klusmeyer, T.H., and Cameron, M.R. 1992. Microbial protein synthesis and flows of nitrogen fractions to the duodenum of dairy cows. J. Dairy Sci. **75**: 2304–2323. doi:10.3168/jds.S0022-0302(92)77992-2.

Coates, J. 2006. Interpretation of infrared spectra, a practical approach. Page *in* Encyclopedia of Analytical Chemistry. American Cancer Society. doi:10.1002/9780470027318.a5606.

Corson, D., Waghorn, G.C., Ulyatt, M.J., and Lee, J. 1999. NIRS: Forage analysis and livestock feeding. Pages 127–132 *in* PROCEEDINGS OF THE CONFERENCE-NEW ZEALAND GRASSLAND ASSOCIATION. [Online] Available: http://www.grassland.org.nz/publications/nzgrassland_publication_507.pdf [2017 Jan. 12].

Damiran, D., and Yu, P. 2010. Structural makeup, biopolymer conformation, and biodegradation characteristics of a newly developed super genotype of oats (CDC SO-I versus conventional varieties): A novel approach. J. Agric. Food Chem. **58**: 2377–2387. doi:10.1021/jf903514t.

Dave, L.A., Montoya, C.A., Rutherfurd, S.M., and Moughan, P.J. 2014. Gastrointestinal endogenous proteins as a source of bioactive peptides - An in silico study. PLoS ONE **9**. doi:10.1371/journal.pone.0098922.

Dewanto, V., Wu, X., Adom, K.K., and Liu, R.H. 2002. Thermal processing enhances the nutritional value of tomatoes by increasing total antioxidant activity. J. Agric. Food Chem. **50**: 3010–3014. doi:10.1021/jf0115589.

Dien, B.S., Miller, D.J., Hector, R.E., Dixon, R.A., Chen, F., McCaslin, M., Reisen, P., Sarath, G., and Cotta, M.A. 2011. Enhancing alfalfa conversion efficiencies for sugar recovery and ethanol production by altering lignin composition. Bioresour. Technol. **102**: 6479–6486. doi:10.1016/j.biortech.2011.03.022.

Dixon, R.M., and Coates, D.B. 2015. Application of faecal near infrared spectroscopy to manage the nutrition and productivity of grazing ruminants. Page 207 *in* Forages in Warm Climates. Lavras, Brazil. [Online] Available: http://www.neforufla.com.br/upimg/ck/files/Proceedings_CONFOR_2015.pdf#page=207 [2016 Oct. 4].

Doiron, K., Yu, P., McKinnon, J.J., and Christensen, D.A. 2009. Heat-induced protein structure and subfractions in relation to protein degradation kinetics and intestinal availability in dairy cattle. J. Dairy Sci. **92**: 3319–3330. doi:10.3168/jds.2008-1946.

Doiron, K.J., and Yu, P. 2017. Recent research in flaxseed (oil seed) on molecular structure and metabolic characteristics of protein, heat processing-induced effect and nutrition with advanced synchrotron-based molecular techniques. Crit. Rev. Food Sci. Nutr. **57**: 8–17. doi:10.1080/10408398.2013.764513.

Dong, J.-L., Liang, B.-G., Jin, Y.-S., Zhang, W.-J., and Wang, T. 2005. Oral immunization with pBsVP6-transgenic alfalfa protects mice against rotavirus infection. Virology **339**: 153–163. doi:10.1016/j.virol.2005.06.004.

DuBois, M., Gilles, K.A., Hamilton, J.K., Rebers, P. t, and Smith, F. 1956. Colorimetric method for determination of sugars and related substances. Anal. Chem. **28**: 350–356.

Duinkerken, G.V., Blok, M.C., Bannink, A., Cone, J.W., Dijkstra, J., Vuuren, A.M.V., and Tamminga, S. 2011. Update of the Dutch protein evaluation system for ruminants: the DVE/OEB2010 system. J. Agric. Sci. **149**: 351–367. doi:10.1017/S0021859610000912.

Escaray, F.J., Passeri, V., Perea-García, A., Antonelli, C.J., Damiani, F., Ruiz, O.A., and Paolocci, F. 2017. The R2R3-MYB TT2b and the bHLH TT8 genes are the major regulators of proanthocyanidin biosynthesis in the leaves of Lotus species. Planta **246**: 243–261. doi:10.1007/s00425-017-2696-6.

Fahey, L.M., Nieuwoudt, M.K., and Harris, P.J. 2017. Predicting the cell-wall compositions of Pinus radiata (radiata pine) wood using ATR and transmission FTIR spectroscopies. Cellulose **24**: 5275–5293. doi:10.1007/s10570-017-1506-4.

FAO 2014. Food safety and quality: Commodity details. [Online] Available: http://www.fao.org/food/food-safety-quality/gm-foods-platform/browse-information-by/commodity/commodity-details/en/?com=38946 [2019 Mar. 26].

Ferradini, N., Iannacone, R., Capomaccio, S., Metelli, A., Armentano, N., Semeraro, L., Cellini, F., Veronesi, F., and Rosellini, D. 2015. Assessment of heat shock protein 70 induction by heat in alfalfa varieties and constitutive overexpression in transgenic plants. PLOS ONE **10**: e0126051. doi:10.1371/journal.pone.0126051.

Ferreira, M.A., Waltenberg, F.P.D.C., Pinto, E.R.D.C., and SÁ, M.F.G.D. 2013.October 3. Use of the coffee homeobox gene cahb12 to produce transgenic plants with greater tolerance to water scarcity and salt stress. [Online] Available: https://patents.google.com/patent/WO2012061911A9/en [2019 May 27].

Fiorentini, R., and Galoppini, C. 1983. The proteins from leaves. Plant Foods Hum. Nutr. **32**: 335–350. doi:10.1007/BF01091193.

Foo, L.Y., Lu, Y., McNabb, W.C., Waghorn, G., and Ulyatt, M.J. 1997. Proanthocyanidins from Lotus pedunculatus. Phytochemistry **45**: 1689–1696. doi:10.1016/S0031-9422(97)00198-2.

Fu, C., Xiao, X., Xi, Y., Ge, Y., Chen, F., Bouton, J., Dixon, R.A., and Wang, Z.-Y. 2011. Downregulation of cinnamyl alcohol dehydrogenase (CAD) leads to improved saccharification efficiency in switchgrass. BioEnergy Res. **4**: 153–164. doi:10.1007/s12155-010-9109-z.

Galbraith, H. 2000. Protein and sulphur amino acid nutrition of hair fibre-producing Angora and Cashmere goats. Livest. Prod. Sci. **64**: 81–93. doi:10.1016/S0301-6226(00)00177-9.

Gandikota, M., Birkenbihl, R.P., Höhmann, S., Cardon, G.H., Saedler, H., and Huijser, P. 2007. The miRNA156/157 recognition element in the 3′ UTR of the Arabidopsis SBP box gene SPL3 prevents early flowering by translational inhibition in seedlings. Plant J. **49**: 683–693. doi:10.1111/j.1365-313X.2006.02983.x.

Gao, R., Austin, R.S., Amyot, L., and Hannoufa, A. 2016. Comparative transcriptome investigation of global gene expression changes caused by miR156 overexpression in Medicago sativa. BMC Genomics **17**: 658. doi:10.1186/s12864-016-3014-6.

Gebril, S., Seger, M., Villanueva, F.M., Ortega, J.L., Bagga, S., and Sengupta-Gopalan, C. 2015. Transgenic alfalfa (Medicago sativa) with increased sucrose phosphate synthase activity shows enhanced growth when grown under N2-fixing conditions. Planta **242**: 1009–1024. doi:10.1007/s00425-015-2342-0.

Getachew, G., Ibáñez, A.M., Pittroff, W., Dandekar, A.M., McCaslin, M., Goyal, S., Reisen, P., DePeters, E.J., and Putnam, D.H. 2011. A comparative study between lignin down regulated alfalfa lines and their respective unmodified controls on the nutritional characteristics of hay. Anim. Feed Sci. Technol. **170**: 192–200. doi:10.1016/j.anifeedsci.2011.09.009.

Getachew, G., Robinson, P.H., DePeters, E.J., and Taylor, S.J. 2004. Relationships between chemical composition, dry matter degradation and in vitro gas production of several ruminant feeds. Anim. Feed Sci. Technol. **111**: 57–71. doi:10.1016/S0377-8401(03)00217-7.

Gold, H. 1964. General application of near-infrared moisture analysis to fruit + vegetable materials. Food Technol. **18**: 586-.

Goplen, B., Howarth, R., Sarkar, S., and Lesins, K. 1980. A search for condensed tannins in annual and perennial species of medicago, trigonella, and onobrychis. Crop Sci. **20**: 801–804.

Goplen, B.P., Howarth, R.E., and Lees, G.L. 1993. Selection of alfalfa for a lower initial rate of digestion and corresponding changes in epidermal and mesophyll cell wall thickness. Can. J. Plant Sci. **73**: 111–122. doi:10.4141/cjps93-014.

Gou, J.-Y., Felippes, F.F., Liu, C.-J., Weigel, D., and Wang, J.-W. 2011. Negative regulation of anthocyanin biosynthesis in arabidopsis by a miR156-targeted SPL transcription factor. Plant Cell **23**: 1512–1522. doi:10.1105/tpc.111.084525.

Government of Canada, C.F.I.A. 2012.March 5. The biology of Medicago sativa l. (alfalfa). [Online] Available: http://www.inspection.gc.ca/plants/plants-with-novel-traits/applicants/directive-94-08/biology-documents/medicago-sativa-l-/eng/1330981151254/1330981232360 [2019 Mar. 26].

Government of Canada, S.C. 2016.June 3. Census of Agriculture, hay and field crops. [Online] Available: http://www5.statcan.gc.ca/cansim/pick-choisir?lang=eng&p2=33&id=0040213 [2016 Nov. 4].

Grabber, J.H. 2005. How do lignin composition, structure, and cross-linking affect degradability? A review of cell wall model studies. Crop Sci. **45**: 820–831. doi:10.2135/cropsci2004.0191.

Guo, D., Chen, F., Inoue, K., Blount, J.W., and Dixon, R.A. 2001a. Downregulation of caffeic acid 3-o-methyltransferase and caffeoyl CoA 3-o-methyltransferase in transgenic alfalfa: impacts on lignin structure and implications for the biosynthesis of G and S lignin. Plant Cell **13**: 73–88. doi:10.1105/tpc.13.1.73.

Guo, D., Chen, F., Wheeler, J., Winder, J., Selman, S., Peterson, M., and Dixon, R.A. 2001b. Improvement of in-rumen digestibility of alfalfa forage by genetic manipulation of lignin O-methyltransferases. Transgenic Res. **10**: 457–464.

Halgerson, J.L., Sheaffer, C.C., Martin, N.P., Peterson, P.R., and Weston, S.J. 2004. Near-infrared reflectance spectroscopy prediction of leaf and mineral concentrations in alfalfa. Agron. J. **96**: 344–351.

Hall, M.H., Smiles, W.S., and Dickerson, R.A. 2000. Morphological development of alfalfa cultivars selected for higher quality. Agron. J. **92**: 1077–1080. doi:10.2134/agronj2000.9261077x.

Han, H., Li, Y., and Zhou, S. 2008. Overexpression of phytoene synthase gene from Salicornia europaea alters response to reactive oxygen species under salt stress in transgenic Arabidopsis. Biotechnol. Lett. **30**: 1501–1507.

Hancock, K., Collette, V., Chapman, E., Hanson, K., Temple, S., Moraga, R., and Caradus, J. 2014. Progress towards developing bloat-safe legumes for the farming industry. Crop Pasture Sci. **65**: 1107. doi:10.1071/CP13308.

Hart, J.R., Norris, K.H., and Golumbic, C. 1962. Determination of the moisture content of seeds by near-infrared spectrophotometry of their methanol extracts. Cereal Chem **39**: 94–99.

He, J., Torres Lechuga, M.E., Lei, Y., Refat, B., Prates, L.L., Zhang, H., and Yu, P. 2019. Protein molecular structural, physicochemical and nutritional characteristics of warm-season adapted genotypes of sorghum grain: Impact of heat-related processing. J. Cereal Sci. **85**: 182–191. doi:10.1016/j.jcs.2018.11.015.

Heendeniya, R.G., Gruber, M.Y., Lei, Y., and Yu, P. 2019. Biodegradation profiles of proanthocyanidin-accumulating alfalfa plants coexpressing Lc-bHLH and C1-MYB transcriptive flavanoid regulatory genes. J. Agric. Food Chem. **67**: 4793–4799. doi:10.1021/acs.jafc.9b00495.

Heendeniya, R.G., and Yu, P. 2017. Gene-transformation-induced changes in chemical functional group features and molecular structure conformation in alfalfa plants co-expressing Lc-bHLH and C1-MYB transcriptive flavanoid regulatory genes: effects of single-gene and two-gene insertion. Int. J. Mol. Sci. **18**: 664. doi:10.3390/ijms18030664.

Henriksson, E., Olsson, A.S.B., Johannesson, H., Johansson, H., Hanson, J., Engström, P., and Söderman, E. 2005. Homeodomain leucine zipper class I genes in arabidopsis. expression patterns and phylogenetic relationships. Plant Physiol. **139**: 509–518. doi:10.1104/pp.105.063461.

Higgs, R.J., Chase, L.E., Ross, D.A., and Van Amburgh, M.E. 2015. Updating the Cornell Net Carbohydrate and Protein System feed library and analyzing model sensitivity to feed inputs. J. Dairy Sci. **98**: 6340–6360. doi:10.3168/jds.2015-9379.

Horwitz, W., and Latimer, G.W. (eds.) 2005. Official methods of analysis of AOAC International. 18th edition. AOAC International, Gaithersburg, Md.

Hur, Y.-S., Um, J.-H., Kim, S., Kim, K., Park, H.-J., Lim, J.-S., Kim, W.-Y., Jun, S.E., Yoon, E.K., Lim, J., Ohme-Takagi, M., Kim, D., Park, J., Kim, G.-T., and Cheon, C.-I. 2014. Arabidopsis thaliana homeobox 12 (ATHB12), a homeodomain-leucine zipper protein, regulates leaf growth by promoting cell expansion and endoreduplication. New Phytol. **1**: 316–328. doi:10.1111/nph.12998.

Jackson, M., and Mantsch, H.H. 1995. The use and misuse of FTIR spectroscopy in the determination of protein structure. Crit. Rev. Biochem. Mol. Biol. **30**: 95–120. doi:10.3109/10409239509085140.

Jonker, A. 2011.May. Characterization of anthocyanidin-accumulating Lc-alfalfa for ruminants: nutritional profiles, digestibility, availability and molecular structures, and bloat characteristics. University of Saskatchewan, Saskatoon. [Online] Available: https://ecommons.usask.ca/handle/10388/etd-05312011-144135 [2016 Sep. 30].

Jonker, A., Gruber, M.Y., McCaslin, M., Wang, Y., Coulman, B., McKinnon, J.J., Christensen, D.A., and Yu, P. 2010. Nutrient composition and degradation profiles of anthocyanidin-accumulating Lc-alfalfa populations. Can. J. Anim. Sci. **90**: 401–412. doi:10.4141/CJAS09110.

Jonker, A., Gruber, M.Y., Wang, Y., Coulman, B., Azarfar, A., McKinnon, J.J., Christensen, D.A., and Yu, P. 2011. Modeling degradation ratios and nutrient availability of anthocyanidin-accumulating Lc-alfalfa populations in dairy cows. J. Dairy Sci. **94**: 1430–1444. doi:10.3168/jds.2010-3604.

Jonker, A., Gruber, M.Y., Wang, Y., Coulman, B., McKinnon, J.J., Christensen, D.A., and Yu, P. 2012a. Foam stability of leaves from anthocyanidin-accumulating Lc-alfalfa and relation to molecular structures detected by fourier-transformed infrared-vibration spectroscopy. Grass Forage Sci. **67**: 369–381. doi:10.1111/j.1365-2494.2012.00853.x.

Jonker, A., Gruber, M.Y., Wang, Y., Narvaez, N., Coulman, B., McKinnon, J.J., Christensen, D.A., Azarfar, A., and Yu, P. 2012b. Fermentation, degradation and microbial nitrogen partitioning for three forage colour phenotypes within anthocyanidin-accumulating Lc-alfalfa progeny. J. Sci. Food Agric. **92**: 2265–2273. doi:10.1002/jsfa.5619.

Jonker, A., and Yu, P. 2016. The role of proanthocyanidins complex in structure and nutrition interaction in alfalfa forage. Int. J. Mol. Sci. **17**: 793. doi:10.3390/ijms17050793.

Kamalak, A., Canbolat, Ö., Özkan, Ç.Ö., and Atalay, A.İ. 2009. Effect of thymol on in vitro gas production, digestibility and metabolizable energy content of alfalfa hay. Kafkas Univ. Vet. Fak. Derg. doi:10.9775/kvfd.2010.2854.

Kebrom, T.H., Spielmeyer, W., and Finnegan, E.J. 2013. Grasses provide new insights into regulation of shoot branching. Trends Plant Sci. **18**: 41–48. doi:10.1016/j.tplants.2012.07.001.

Kim, J.B., Kim, S.H., Roh, K.H., Kim, H.U., Lee, K.R., Lee, E.Y., Kim, W.Y., Park, J.H., and Chung, I.S. 2014. Transgenic expression of rotavirus capsid protein (VP7) in alfalfa for edible vaccine. J. Biotechnol. **Supplement**: S112. doi:10.1016/j.jbiotec.2014.07.381.

Kumar, D., Pannu, R., Kumar, S., and Arya, R.K. 2013. A review: Recent advances in forage crop improvement through biotechnology. Biomirror **4**: 97–101.

Kumar, S. 2011. Biotechnological advancements in alfalfa improvement. J. Appl. Genet. **52**: 111–124. doi:10.1007/s13353-011-0028-2.

Larbi, A., Smith, J.W., Kurdi, I.O., Adekunle, I.O., Raji, A.M., and Ladipo, D.O. 1998. Chemical composition, rumen degradation, and gas production characteristics of some multipurpose fodder trees and shrubs during wet and dry seasons in the humid tropics. Anim. Feed Sci. Technol. **72**: 81–96. doi:10.1016/S0377-8401(97)00170-3.

Lee, R.C., Feinbaum, R.L., and Ambros, V. 1993. The C. elegans heterochronic gene lin-4 encodes small RNAs with antisense complementarity to lin-14. Cell **75**: 843–854. doi:10.1016/0092-8674(93)90529-Y.

Lee, Y.-H., and Chun, J.-Y. 1998. A new homeodomain-leucine zipper gene from Arabidopsis thaliana induced by water stress and abscisic acid treatment. Plant Mol. Biol. **37**: 377–384. doi:10.1023/A:1006084305012.

Lee, Y.-H., Oh, H.-S., Cheon, C.-I., Hwang, I.-T., Kim, Y.-J., and Chun, J.-Y. 2001. Structure and expression of the arabidopsis thaliana homeobox gene Athb-12. Biochem. Biophys. Res. Commun. **284**: 133–141. doi:10.1006/bbrc.2001.4904.

Lei, Y., Hannoufa, A., Christensen, D., Shi, H., Prates, L.L., and Yu, P. 2018a. Molecular structural changes in alfalfa detected by ATR-FTIR spectroscopy in response to silencing of TT8 and HB12 genes. Int. J. Mol. Sci. **19**: 1046. doi:10.3390/ijms19041046.

Lei, Y., Hannoufa, A., Louzada Prates, L., Shi, H., Wang, Y., Biligetu, B., Christensen, D., and Yu, P. 2018b. Silencing of TT8 and HB12 Affects Nutritional Profiles and in vitro gas

production Relating to Molecular Structures of Alfalfa (Medicago sativa) Plants. J. Agric. Food Chem. doi:10.1021/acs.jafc.8b01573.

Lei, Y., Hannoufa, A., Prates, L.L., Shi, H., Wang, Y., Biligetu, B., Christensen, D., and Yu, P. 2018c. Effects of TT8 and HB12 silencing on the relations between the molecular structures of alfalfa (Medicago sativa) plants and their nutritional profiles and in vitro gas production. J. Agric. Food Chem. **66**: 5602–5611. doi:10.1021/acs.jafc.8b01573.

Lei, Y., Hannoufa, A., and Yu, P. 2017. The use of gene modification and advanced molecular structure analyses towards improving alfalfa forage. Int. J. Mol. Sci. **18**: 298. doi:10.3390/ijms18020298.

Li, X., and Brummer, E.C. 2012. Applied genetics and genomics in alfalfa breeding. Agronomy **2**: 40–61. doi:10.3390/agronomy2010040.

Li, X., Chen, L., Hong, M., Zhang, Y., Zu, F., Wen, J., Yi, B., Ma, C., Shen, J., Tu, J., and Fu, T. 2012. A large insertion in bHLH transcription factor BrTT8 resulting in yellow seed coat in Brassica rapa. PLOS ONE **7**: e44145. doi:10.1371/journal.pone.0044145.

Li, X., Hannoufa, A., Zhang, Y., and Yu, P. 2016a. Gene-silencing-induced changes in carbohydrate conformation in relation to bioenergy value and carbohydrate subfractions in modeled plant (Medicago sativa) with down-regulation of HB12 and TT8 transcription factors. Int. J. Mol. Sci. **17**: 720. doi:10.3390/ijms17050720.

Li, X., Zhang, Y., Hannoufa, A., and Yu, P. 2015. Transformation with TT8 and HB12 RNAi constructs in model forage (Medicago sativa, alfalfa) affects carbohydrate structure and metabolic characteristics in ruminant livestock systems. J. Agric. Food Chem. **63**: 9590–9600. doi:10.1021/acs.jafc.5b03717.

Li, X., Zhang, Y., and Yu, P. 2016b. Association of bio-energy processing-induced protein molecular structure changes with CNCPS-based protein degradation and digestion of co-products in dairy cows. J. Agric. Food Chem. **64**: 4086–4094. doi:10.1021/acs.jafc.6b00688.

Licitra, G., Hernandez, T.M., and Van Soest, P.J. 1996. Standardization of procedures for nitrogen fractionation of ruminant feeds. Anim. Feed Sci. Technol. **57**: 347–358. doi:10.1016/0377-8401(95)00837-3.

Liu, N., and Yu, P. 2016. Recent research and progress in food, feed and nutrition with advanced synchrotron-based SR-IMS and DRIFT molecular spectroscopy. Crit. Rev. Food Sci. Nutr. **56**: 910–918. doi:10.1080/10408398.2012.733895.

Lu, Z., Yu, H., Xiong, G., Wang, J., Jiao, Y., Liu, G., Jing, Y., Meng, X., Hu, X., Qian, Q., Fu, X., Wang, Y., and Li, J. 2013. Genome-wide binding analysis of the transcription activator IDEAL PLANT ARCHITECTURE1 reveals a complex network regulating rice plant architecture. Plant Cell Online: tpc.113.113639. doi:10.1105/tpc.113.113639.

Ma, L., Wang, Y., Liu, W., and Liu, Z. 2014. Overexpression of an alfalfa GDP-mannose 3, 5-epimerase gene enhances acid, drought and salt tolerance in transgenic Arabidopsis by increasing ascorbate accumulation. Biotechnol. Lett. **36**: 2331–2341. doi:10.1007/s10529-014-1598-y.

Ma, X.-F., Tudor, S., Butler, T., Ge, Y., Xi, Y., Bouton, J., Harrison, M., and Wang, Z.-Y. 2011. Transgenic expression of phytase and acid phosphatase genes in alfalfa (Medicagosativa) leads to improved phosphate uptake in natural soils. Mol. Breed. **30**: 377–391. doi:10.1007/s11032-011-9628-0.

Mahanna, B. 2015. Advancement in developing reduced-lignin alfalfa made. [Online] Available: http://feedstuffs.com/story-advancement-developing-reducedlignin-alfalfa-made-54-132931 [2016 Nov. 4].

Marita, J.M., Ralph, J., Hatfield, R.D., Guo, D., Chen, F., and Dixon, R.A. 2003. Structural and compositional modifications in lignin of transgenic alfalfa down-regulated in caffeic acid 3-O-methyltransferase and caffeoyl coenzyme A 3-O-methyltransferase. Phytochemistry **62**: 53–65. doi:10.1016/S0031-9422(02)00434-X.

Marković, J.P., Scaron, R.T., trbanović, Terzić, D.V., Djokić, D.J., Aleks, Simić, ar S., Vrvić, M.M., and Živković, S.P. 2012. Changes in lignin structure with maturation of alfalfa leaf and stem in relation to ruminants nutrition. Afr. J. Agric. Res. **7**: 257–264. doi:10.5897/AJAR11.1485.

Martin, A., Adam, H., Díaz-Mendoza, M., Żurczak, M., González-Schain, N.D., and Suárez-López, P. 2009. Graft-transmissible induction of potato tuberization by the microRNA miR172. Development **136**: 2873–2881. doi:10.1242/dev.031658.

Mathieu, J., Yant, L.J., Mürdter, F., Küttner, F., and Schmid, M. 2009. Repression of flowering by the miR172 target SMZ. PLOS Biol. **7**: e1000148. doi:10.1371/journal.pbio.1000148.

Maureira, I.J., and Osborn, T.C. 2004. Molecular markers in genetics and breeding: Improvement of alfalfa (Medicago sativa L.). Pages 139–154 *in* Molecular Marker Systems in Plant Breeding and Crop Improvement. Springer. [Online] Available: http://link.springer.com/chapter/10.1007/3-540-26538-4_8 [2017 Jan. 3].

McCaslin, M., Weakley, D., Temple, S., and Reisen, P. 2015. New technologies in alfalfa. Pages 215–222 *in* Advances in Dairy Technology. Western Canadian Dairy Seminar. Red Deer, Canada. [Online] Available: http://www.wcds.ca/proc/2015/Manuscripts/Chapt%2015%20-%20Reisen.pdf.

McCleary, B., Gibson, and C. Mugford, D. 1997. Measurement of total starch in cereal products by amyloglucosidase-α-amylase method: Collaborative study. J. AOAC Int. **80**: 571–579.

Miller, L.M., and Dumas, P. 2006. Chemical imaging of biological tissue with synchrotron infrared light. Biochim. Biophys. Acta BBA - Biomembr. **1758**: 846–857. doi:10.1016/j.bbamem.2006.04.010.

miRBase (n.d.). [Online] Available: http://www.mirbase.org/ [2017 Mar. 15].

Miura, K., Ikeda, M., Matsubara, A., Song, X.-J., Ito, M., Asano, K., Matsuoka, M., Kitano, H., and Ashikari, M. 2010. OsSPL14 promotes panicle branching and higher grain productivity in rice. Nat. Genet. **42**: 545–549. doi:10.1038/ng.592.

Mueller, D., Ferrão, M.F., Marder, L., da Costa, A.B., and de Cássia de Souza Schneider, R. 2013. Fourier transform infrared spectroscopy (FTIR) and multivariate analysis for identification of different vegetable oils used in biodiesel production. Sensors **13**: 4258–4271. doi:10.3390/s130404258.

Mueller, S.C., and Orloff, S.B. 1994. Environmental factors affecting forage quality. Pages 8–9 *in* University of CA Cooperative Extension.

Nakashima, J., Chen, F., Jackson, L., Shadle, G., and Dixon, R.A. 2008. Multi-site genetic modification of monolignol biosynthesis in alfalfa (*Medicago sativa*): effects on lignin composition in specific cell types. New Phytol. **179**: 738–750. doi:10.1111/j.1469-8137.2008.02502.x.

Ndlovu, L.R., and Nherera, F.V. 1997. Chemical composition and relationship to in vitro gas production of Zimbabwean browsable indigenous tree species. Anim. Feed Sci. Technol. **69**: 121–129. doi:10.1016/S0377-8401(97)81627-6.

Nesi, N., Debeaujon, I., Jond, C., Pelletier, G., Caboche, M., and Lepiniec, L. 2000. The TT8 gene encodes a basic helix-loop-helix domain protein required for expression of DFR and BAN genes in Arabidopsis siliques. Plant Cell **12**: 1863–1878.

Nie, L., Liu, H., Sun, J., Yi, J., and Liu, Y. 2015. A study on cold tolerance transgenic alfalfa (Medicago sativa L.) with the AmDHN gene. Pages 173–181 *in* Molecular Breeding of Forage and Turf. Springer. [Online] Available: http://link.springer.com/chapter/10.1007/978-3-319-08714-6_15 [2016 Nov. 4].

Nie, Z., Tremblay, G.F., Bélanger, G., Berthiaume, R., Castonguay, Y., Bertrand, A., Michaud, R., Allard, G., and Han, J. 2009. Near-infrared reflectance spectroscopy prediction of neutral detergent-soluble carbohydrates in timothy and alfalfa. J. Dairy Sci. **92**: 1702–1711. doi:10.3168/jds.2008-1599.

Nobres, P., Patreze, C.M., Waltenberg, F.P., Correa, M.F., Tavano, E.C. da R., Mendes, B.M.J., and Alves-Ferreira, M. 2016. Characterization of the promoter of the Homeobox gene CaHB12 in Coffea arabica. Trop. Plant Biol. **9**: 50–62. doi:10.1007/s12042-016-9159-2.

NRC Dairy 2001. Nutrient requirements of dairy cattle: seventh revised edition. National Academies Press, Washington, D.C. [Online] Available: http://www.nap.edu/catalog/9825 [2016 Sep. 26].

Olsson, A., Engström, P., and Söderman, E. 2004. The homeobox genes ATHB12 and ATHB7encode potential regulators of growth in response to water deficit in Arabidopsis. Plant Mol. Biol. **55**: 663–677.

Orloff, S., and Putnam, D. 2004. Balancing yield, quality and persistence. Page 12 *in*. San Diego, CA.

Padmaja, L.K., Agarwal, P., Gupta, V., Mukhopadhyay, A., Sodhi, Y.S., Pental, D., and Pradhan, A.K. 2014. Natural mutations in two homoeologous TT8 genes control yellow seed coat trait in allotetraploid Brassica juncea (AABB). Theor. Appl. Genet. **127**: 339–347. doi:10.1007/s00122-013-2222-6.

Park, J., Lee, H.-J., Cheon, C.-I., Kim, S.-H., Hur, Y.-S., Auh, C.-K., Im, K.-H., Yun, D.-J., Lee, S., and Davis, K.R. 2011. The arabidopsis thaliana homeobox gene ATHB12 is involved in symptom development caused by geminivirus infection. PLoS ONE **6**: e20054. doi:10.1371/journal.pone.0020054.

Peng, Q., Khan, N.A., Wang, Z., and Yu, P. 2014. Relationship of feeds protein structural makeup in common Prairie feeds with protein solubility, in situ ruminal degradation and intestinal digestibility. Anim. Feed Sci. Technol. **194**: 58–70. doi:10.1016/j.anifeedsci.2014.05.004.

Pirone, C.L., Alexander, L.C., and Lamp, W.O. 2005. Patterns of starch accumulation in alfalfa subsequent to potato leafhopper (homoptera: cicadellidae) injury. Environ. Entomol. **34**: 199–204. doi:10.1603/0046-225X-34.1.199.

Plans, M., Simó, J., Casañas, F., and Sabaté, J. 2012. Near-infrared spectroscopy analysis of seed coats of common beans (Phaseolus vulgaris l.): a potential tool for breeding and quality evaluation. J. Agric. Food Chem. **60**: 706–712. doi:10.1021/jf204110k.

Poethig, R.S. 2013. Vegetative phase change and shoot maturation in plants. Curr. Top. Dev. Biol. **105**: 125–152. doi:10.1016/B978-0-12-396968-2.00005-1.

Prates, L.L., Lei, Y., Refat, B., Zhang, W., and Yu, P. 2018a. Effects of heat processing methods on protein subfractions and protein degradation kinetics in dairy cattle in relation to protein molecular structure of barley grain using advanced molecular spectroscopy. J. Cereal Sci. **80**: 212–220. doi:10.1016/j.jcs.2018.01.008.

Prates, L.L., Refat, B., Lei, Y., Louzada-Prates, M., and Yu, P. 2018b. Relationship of carbohydrates and lignin molecular structure spectral profiles to nutrient profile in newly developed oats cultivars and barley grain. Spectrochim. Acta. A. Mol. Biomol. Spectrosc. **188**: 495–506. doi:10.1016/j.saa.2017.07.042.

Prates, L.L., and Yu, P. 2017. Recent research on inherent molecular structure, physiochemical properties, and bio-functions of food and feed-type Avena sativa oats and processing-induced changes revealed with molecular microspectroscopic techniques. Appl. Spectrosc. Rev. **52**: 850–867. doi:10.1080/05704928.2017.1331447.

Preston, J.C., Wang, H., Kursel, L., Doebley, J., and Kellogg, E.A. 2012. The role of teosinte glume architecture (tga1) in coordinated regulation and evolution of grass glumes and inflorescence axes. New Phytol. **193**: 204–215. doi:10.1111/j.1469-8137.2011.03908.x.

Pu, Y., Chen, F., Ziebell, A., Davison, B.H., and Ragauskas, A.J. 2009. NMR characterization of C3H and HCT down-regulated alfalfa lignin. BioEnergy Res. **2**: 198. doi:10.1007/s12155-009-9056-8.

Pumure, I., Ford, S., Shannon, J., Kohen, C., Mulcahy, A., Frank, K., Sisco, S., and Chaukura, N. 2015. Analysis of ATR-FTIR absorption-reflection data from 13 polymeric fabric materials using chemometrics. Am. J. Anal. Chem. **06**: 305–312. doi:10.4236/ajac.2015.64029.

Putnam, D.H., and Orloff, S. 2016. Agronomic factors affecting forage quality in alfalfa. Page 14 *in*. Reno, NV.

Putnam, D.H., Orloff, S., and Teuber, L.R. 2005. Strategies for balancing quality and yield in alfalfa using cutting schedules and varieties. Page 15 *in*. Visalia, CA.

Qi, S., Liu, K., Gao, C., Li, D., Jin, C., Duan, S., Ma, H., Hai, J., and Chen, M. 2017. The effect of BnTT8 on accumulation of seed storage reserves and tolerance to abiotic stresses during Arabidopsis seedling establishment. Plant Growth Regul. **82**: 271–280. doi:10.1007/s10725-017-0257-4.

R Core Team 2017. R: A language and environment for statistical computing. R Foundation for Statistical Computing, Vienna, Austria. [Online] Available: https://www.R-project.org/.

Radović, J., Sokolović, D., and Marković, J. 2009. Alfalfa-most important perennial forage legume in animal husbandry. Biotechnol. Anim. Husb. **25**: 465–475.

Rai, A., Umashankar, S., Rai, M., Kiat, L.B., Bing, J.A.S., and Swarup, S. 2016. Coordinate regulation of metabolite glycosylation and stress hormone biosynthesis by TT8 in arabidopsis. Plant Physiol. **171**: 2499–2515. doi:10.1104/pp.16.00421.

Rai, V., Mukherjee, R., Routray, A., Ghosh, A.K., Roy, S., Ghosh, B.P., Mandal, P.B., Bose, S., and Chakraborty, C. 2018. Serum-based diagnostic prediction of oral submucous fibrosis using FTIR spectrometry. Spectrochim. Acta. A. Mol. Biomol. Spectrosc. **189**: 322–329. doi:10.1016/j.saa.2017.08.018.

Ray, H., Yu, M., Auser, P., Blahut-Beatty, L., McKersie, B., Bowley, S., Westcott, N., Coulman, B., Lloyd, A., and Gruber, M.Y. 2003. Expression of anthocyanins and proanthocyanidins after transformation of alfalfa with maize Lc. Plant Physiol. **132**: 1448–1463.

Ré, D.A., Capella, M., Bonaventure, G., and Chan, R.L. 2014. Arabidopsis AtHB7 and AtHB12 evolved divergently to fine tune processes associated with growth and responses to water stress. BMC Plant Biol. **14**: 150.

Reddy, M.S., Chen, F., Shadle, G., Jackson, L., Aljoe, H., and Dixon, R.A. 2005. Targeted down-regulation of cytochrome P450 enzymes for forage quality improvement in alfalfa (Medicago sativa L.). Proc. Natl. Acad. Sci. U. S. A. **102**: 16573–16578.

Refat, B., Christensen, D.A., Mckinnon, J.J., Prates, L.L., Nair, J., Beattie, A.D., Yang, W., McAllister, T.A., and Yu, P. 2017a. Evaluation of barley silage with varying ruminal in vitro fiber digestibility on lactation performance and chewing activity of lactating dairy cows in comparison with corn silage. Can. J. Anim. Sci. **98**: 177–186. doi:10.1139/cjas-2016-0191.

Refat, B., Prates, L.L., Khan, N.A., Lei, Y., Christensen, D.A., McKinnon, J.J., and Yu, P. 2017b. Physiochemical characteristics and molecular structures for digestible carbohydrates of silages. J. Agric. Food Chem. **65**: 8979–8991. doi:10.1021/acs.jafc.7b01032.

Resende, S., Maria, R., Casler, M.D., Resende, V. de, and Deon, M. 2014. Genomic selection in forage breeding: accuracy and methods. Crop Sci. **54**: 143–156. doi:10.2135/cropsci2013.05.0353.

Rhoades, M.W., Reinhart, B.J., Lim, L.P., Burge, C.B., Bartel, B., and Bartel, D.P. 2002. Prediction of plant microrna targets. Cell **110**: 513–520. doi:10.1016/S0092-8674(02)00863-2.

Roe, M.B., Sniffen, C.J., and Chase, L.E. 1990. Techniques for measuring protein fractions in feedstuffs. Pages 81–88 *in* Proceedings - Cornell Nutrition Conference for Feed Manufacturers (USA). Ithaca, NY, USA. [Online] Available: http://agris.fao.org/agris-search/search.do?recordID=US9322404 [2017 Oct. 6].

Ruan, Y.-L., Patrick, J.W., Bouzayen, M., Osorio, S., and Fernie, A.R. 2012. Molecular regulation of seed and fruit set. Trends Plant Sci. **17**: 656–665. doi:10.1016/j.tplants.2012.06.005.

Russell, J.B., and Rychlik, J.L. 2001. Factors that alter rumen microbial ecology. Science **292**: 1119–1122. doi:10.1126/science.1058830.

Russelle, M.P. 2001. Alfalfa: After an 8,000-year journey, the "Queen of Forages" stands poised to enjoy renewed popularity. Am. Sci. **89**: 252–261.

Sánchez-Duarte, J.I., and García, A. 2017. Ammonia-N concentration in alfalfa silage and its effects on dairy cow performance: a meta-analysis. Rev. Colomb. Cienc. Pecu. Medellín **30**: 175–184.

Saxton, A.M. 1998. A macro for converting mean separation output to letter groupings in Proc Mixed. Pages 1243–1246 *in*. SAS Institute, Cary, NC. [Online] Available: http://ci.nii.ac.jp/naid/20000872853/.

Schaart, J.G., Dubos, C., Romero De La Fuente, I., van Houwelingen, A.M.M.L., de Vos, R.C.H., Jonker, H.H., Xu, W., Routaboul, J.-M., Lepiniec, L., and Bovy, A.G. 2013. Identification and characterization of MYB-bHLH-WD40 regulatory complexes controlling proanthocyanidin biosynthesis in strawberry (Fragaria × ananassa) fruits. New Phytol. **197**: 454–467. doi:10.1111/nph.12017.

Sewalt, V.J.H., Glasser, W.G., and Beauchemin, K.A. 1997a. Lignin impact on fiber degradation. 3. reversal of inhibition of enzymatic hydrolysis by chemical modification of lignin and by additives. J. Agric. Food Chem. **45**: 1823–1828. doi:10.1021/jf9608074.

Sewalt, V.J.H., Ni, W., Jung, H.G., and Dixon, R.A. 1997b. Lignin impact on fiber degradation: Increased enzymatic digestibility of genetically engineered tobacco (Nicotiana tabacum) stems reduced in lignin content. J. Agric. Food Chem. **45**: 1977–1983. doi:10.1021/jf9609690.

Shadle, G., Chen, F., Srinivasa Reddy, M.S., Jackson, L., Nakashima, J., and Dixon, R.A. 2007. Down-regulation of hydroxycinnamoyl CoA: Shikimate hydroxycinnamoyl transferase in transgenic alfalfa affects lignification, development and forage quality. Phytochemistry **68**: 1521–1529. doi:10.1016/j.phytochem.2007.03.022.

Shenk, J.S., and Westerhaus, M.O. 1985. Accuracy of NIRS instruments to analyze forage and grain. Crop Sci. **25**: 1120. doi:10.2135/cropsci1985.0011183X002500060054x.

Shi, H., Lei, Y., Louzada Prates, L., and Yu, P. 2019. Evaluation of near-infrared (NIR) and Fourier transform mid-infrared (ATR-FT/MIR) spectroscopy techniques combined with chemometrics for the determination of crude protein and intestinal protein digestibility of wheat. Food Chem. **272**: 507–513. doi:10.1016/j.foodchem.2018.08.075.

Shi, H., and Yu, P. 2017. Advanced synchrotron-based and globar-sourced molecular (micro) spectroscopy contributions to advances in food and feed research on molecular structure, mycotoxin determination, and molecular nutrition. Crit. Rev. Food Sci. Nutr. **0**: 1–12. doi:10.1080/10408398.2017.1303769.

Shikata, M., Koyama, T., Mitsuda, N., and Ohme-Takagi, M. 2009. Arabidopsis SBP-box genes SPL10, SPL11 and SPL2 control morphological change in association with shoot maturation in the reproductive phase. Plant Cell Physiol. **50**: 2133–2145. doi:10.1093/pcp/pcp148.

Shin, D., Koo, Y.D., Lee, J., Lee, H., Baek, D., Lee, S., Cheon, C.-I., Kwak, S.-S., Lee, S.Y., and Yun, D.-J. 2004. Athb-12, a homeobox-leucine zipper domain protein from Arabidopsis thaliana, increases salt tolerance in yeast by regulating sodium exclusion. Biochem. Biophys. Res. Commun. **323**: 534–540. doi:10.1016/j.bbrc.2004.08.127.

Skrobot, V.L., Castro, E.V.R., Pereira, R.C.C., Pasa, V.M.D., and Fortes, I.C.P. 2007. Use of principal component analysis (PCA) and linear discriminant analysis (LDA) in gas chromatographic (GC) data in the investigation of gasoline adulteration. Energy Fuels **21**: 3394–3400. doi:10.1021/ef0701337.

Sniffen, C.J., O'connor, J.D., Van Soest, P.J., Fox, D.G., and Russell, J.B. 1992. A net carbohydrate and protein system for evaluating cattle diets: II. Carbohydrate and protein availability. J. Anim. Sci. **70**: 3562–3577.

Soest, P.J.V. 1994. Nutritional ecology of the ruminant. 2 edition. Comstock Publishing Associates, Ithaca.

Son, O., Hur, Y.-S., Kim, Y.-K., Lee, H.-J., Kim, S., Kim, M.-R., Nam, K.H., Lee, M.-S., Kim, B.-Y., Park, J., Park, J., Lee, S.-C., Hanada, A., Yamaguchi, S., Lee, I.-J., Kim, S.-K., Yun, D.-J., Söderman, E., and Cheon, C.-I. 2010. ATHB12, an ABA-inducible homeodomain-leucine zipper (HD-zip) protein of arabidopsis, negatively regulates the growth of the inflorescence stem by decreasing the expression of a gibberellin 20-oxidase gene. Plant Cell Physiol. **51**: 1537–1547. doi:10.1093/pcp/pcq108.

Spanghero, M., Nikulina, A., and Mason, F. 2018. Use of an in vitro gas production procedure to evaluate rumen slow-release urea products. Anim. Feed Sci. Technol. **237**: 19–26. doi:10.1016/j.anifeedsci.2017.12.017.

Spanudakis, E., and Jackson, S. 2014. The role of microRNAs in the control of flowering time. J. Exp. Bot. **65**: 365–380. doi:10.1093/jxb/ert453.

Stefanova, G., Slavov, S., Gecheff, K., Vlahova, M., and Atanassov, A. 2013. Expression of recombinant human lactoferrin in transgenic alfalfa plants. Biol. Plant. **57**: 457–464. doi:10.1007/s10535-013-0305-5.

Stief, A., Altmann, S., Hoffmann, K., Pant, B.D., Scheible, W.-R., and Bäurle, I. 2014. Arabidopsis miR156 regulates tolerance to recurring environmental stress through SPL transcription factors. Plant Cell Online: tpc.114.123851. doi:10.1105/tpc.114.123851.

Stuart, B.H. 2004. Infrared spectroscopy: fundamentals and applications. John Wiley & Sons.

Susmel, P., and Stefanon, B. 1993. Aspects of lignin degradation by rumen microorganisms. J. Biotechnol. **30**: 141–148. doi:10.1016/0168-1656(93)90035-L.

Tadege, M., Chen, F., Murray, J., Wen, J., Ratet, P., Udvardi, M.K., Dixon, R.A., and Mysore, K.S. 2015. Control of vegetative to reproductive phase transition improves biomass yield and simultaneously reduces lignin content in Medicago truncatula. BioEnergy Res. **8**: 857–867. doi:10.1007/s12155-014-9565-y.

Tamminga, S., Van Straalen, W.M., Subnel, A.P.J., Meijer, R.G.M., Steg, A., Wever, C.J.G., and Blok, M.C. 1994. The Dutch protein evaluation system: the DVE/OEB-system. Livest. Prod. Sci. **40**: 139–155. doi:10.1016/0301-6226(94)90043-4.

Tanaka, A., and Makino, A. 2009. Photosynthetic Research in Plant Science. Plant Cell Physiol. **50**: 681–683. doi:10.1093/pcp/pcp040.

Tang, L., Cai, H., Zhai, H., Luo, X., Wang, Z., Cui, L., and Bai, X. 2014. Overexpression of Glycine soja WRKY20 enhances both drought and salt tolerance in transgenic alfalfa (Medicago sativa L.). Plant Cell Tissue Organ Cult. PCTOC **118**: 77–86. doi:10.1007/s11240-014-0463-y.

Tang, M., Zhou, C., Meng, L., Mao, D., Peng, C., Zhu, Y., Huang, D., Tan, Z., Chen, C., Liu, C., and Zhang, D. 2016. Overexpression of OsSPL9 enhances accumulation of Cu in rice grain and improves its digestibility and metabolism. J. Genet. Genomics **43**: 673–676. doi:10.1016/j.jgg.2016.09.004.

Tas, B.M., Taweel, H.Z., Smit, H.J., Elgersma, A., Dijkstra, J., and Tamminga, S. 2006. Rumen degradation characteristics of perennial ryegrass cultivars during the growing season. Anim. Feed Sci. Technol. **131**: 103–120. doi:10.1016/j.anifeedsci.2006.02.002.

Tesfaye, M., Silverstein, K.A.T., Bucciarelli, B., Samac, D.A., and Vance, C.P. 2006. The affymetrix medicago genechip array is applicable for transcript analysis of alfalfa (Medicago sativa). Funct. Plant Biol. FPB **33**: 783–788.

Theodoridou, K., and Yu, P. 2013a. Application potential of ATR-FT/IR molecular spectroscopy in animal nutrition: revelation of protein molecular structures of canola meal and presscake, as affected by heat-processing methods, in relationship with their protein digestive behavior and utilization for dairy cattle. J. Agric. Food Chem. **61**: 5449–5458.

Theodoridou, K., and Yu, P. 2013b. Metabolic characteristics of the proteins in yellow-seeded and brown-seeded canola meal and presscake in dairy cattle: comparison of three systems (PDI, DVE, and NRC) in nutrient supply and feed milk value (FMV). J. Agric. Food Chem. **61**: 2820–2830. doi:10.1021/jf305171z.

Theodoridou, K., Yu, P., and others 2013. Detect the sensitivity and response of protein molecular structure of whole canola seed (yellow and brown) to different heat processing methods and relation to protein utilization and availability using ATR-FT/IR molecular spectroscopy with chemometrics. Spectrochim. Acta. A. Mol. Biomol. Spectrosc. **105**: 304–313.

Tong, Z., Li, H., Zhang, R., Ma, L., Dong, J., and Wang, T. 2015. Co-downregulation of the hydroxycinnamoyl-CoA:shikimate hydroxycinnamoyl transferase and coumarate 3-hydroxylase significantly increases cellulose content in transgenic alfalfa (Medicago sativa L.). Plant Sci. **239**: 230–237. doi:10.1016/j.plantsci.2015.08.005.

Tong, Z., Xie, C., Ma, L., Liu, L., Jin, Y., Dong, J., and Wang, T. 2014. Co-expression of bacterial aspartate kinase and adenylylsulfate reductase genes substantially increases sulfur amino acid levels in transgenic alfalfa (Medicago sativa L.). PLOS ONE **9**: e88310. doi:10.1371/journal.pone.0088310.

Tremblay, G.F., Michaud, R., and Bélanger, G. 2003. Protein fractions and ruminal undegradable proteins in alfalfa. Can. J. Plant Sci. **83**: 555–559. doi:10.4141/P02-148.

Undersander, D., Cosgrove, D., Cullen, E., Grau, C., and Rice, M.E. 2011. Alfalfa management guide. American Society of Agronomy, Madison, Wis.

Vahdani, N., Moravej, H., Rezayazdi, K., and Dehghan-Banadki, M. 2014. Evaluation of nutritive value of grass pea hay in sheep nutrition and its palatability as compared with alfalfa. J. Agric. Sci. Technol. **16**: 537–550.

Vail, A.W., Wang, P., Uefuji, H., Samac, D.A., Vance, C.P., Wackett, L.P., and Sadowsky, M.J. 2014. Biodegradation of atrazine by three transgenic grasses and alfalfa expressing a modified bacterial atrazine chlorohydrolase gene. Transgenic Res. **24**: 475–488. doi:10.1007/s11248-014-9851-7.

Valdés, A.E., Övernäs, E., Johansson, H., Rada-Iglesias, A., and Engström, P. 2012. The homeodomain-leucine zipper (HD-Zip) class I transcription factors ATHB7 and ATHB12 modulate abscisic acid signalling by regulating protein phosphatase 2C and abscisic acid receptor gene activities. Plant Mol. Biol. **80**: 405–418. doi:10.1007/s11103-012-9956-4.

Van Amburgh, M.E., Collao-Saenz, E.A., Higgs, R.J., Ross, D.A., Recktenwald, E.B., Raffrenato, E., Chase, L.E., Overton, T.R., Mills, J.K., and Foskolos, A. 2015. The Cornell Net Carbohydrate and Protein System: Updates to the model and evaluation of version 6.5. J. Dairy Sci. **98**: 6361–6380. doi:10.3168/jds.2015-9378.

Vanholme, R., Demedts, B., Morreel, K., Ralph, J., and Boerjan, W. 2010. Lignin biosynthesis and structure. PLANT Physiol. **153**: 895–905. doi:10.1104/pp.110.155119.

Verdier, J., Zhao, J., Torres-Jerez, I., Ge, S., Liu, C., He, X., Mysore, K.S., Dixon, R.A., and Udvardi, M.K. 2012. MtPAR MYB transcription factor acts as an on switch for proanthocyanidin biosynthesis in Medicago truncatula. Proc. Natl. Acad. Sci. **109**: 1766–1771. doi:10.1073/pnas.1120916109.

Vogel, K.P., and Jung, H.-J.G. 2001. Genetic modification of herbaceous plants for feed and fuel. Crit. Rev. Plant Sci. **20**: 15–49. doi:10.1080/20013591099173.

Vogt, T. 2010. Phenylpropanoid biosynthesis. Mol. Plant **3**: 2–20. doi:10.1093/mp/ssp106.

Volenec, J.J., Cunningham, S.M., Haagenson, D.M., Berg, W.K., Joern, B.C., and Wiersma, D.W. 2002. Physiological genetics of alfalfa improvement: past failures, future prospects. Field Crops Res. **75**: 97–110. doi:10.1016/S0378-4290(02)00020-5.

Vu, V. 2018. ggbiplot: A biplot based on ggplot2. R. [Online] Available: https://github.com/vqv/ggbiplot [2018 Mar. 19].

Wang, H., and Wang, H. 2015. The miR156/SPL module, a regulatory hub and versatile toolbox, gears up crops for enhanced agronomic traits. Mol. Plant **8**: 677–688. doi:10.1016/j.molp.2015.01.008.

Wang, J.-W. 2016. Chapter 18 - the multifaceted roles of miR156-targeted spl transcription factors in plant developmental transitions. Pages 281–293 *in* D.H. Gonzalez, ed. Plant Transcription Factors. Academic Press, Boston. doi:10.1016/B978-0-12-800854-6.00018-X.

Wang, J.-W., Czech, B., and Weigel, D. 2009. miR156-regulated SPL transcription factors define an endogenous flowering pathway in Arabidopsis thaliana. Cell **138**: 738–749. doi:10.1016/j.cell.2009.06.014.

Wang, J.-W., Park, M.Y., Wang, L.-J., Koo, Y., Chen, X.-Y., Weigel, D., and Poethig, R.S. 2011. Mirna control of vegetative phase change in trees. PLOS Genet. **7**: e1002012. doi:10.1371/journal.pgen.1002012.

Wang, Y., Frutos, P., Gruber, M.Y., Ray, H., and McAllister, T.A. 2006. In vitro ruminal digestion of anthocyanidin-containing alfalfa transformed with the maize Lc regulatory gene. Can. J. Plant Sci. **86**: 1119–1130. doi:10.4141/P06-001.

Wang, Y., Majak, W., and McAllister, T.A. 2012. Frothy bloat in ruminants: Cause, occurrence, and mitigation strategies. Anim. Feed Sci. Technol. **172**: 103–114. doi:10.1016/j.anifeedsci.2011.12.012.

Wang, Y., McAllister, T.A., and Acharya, S. 2015a. Condensed tannins in sainfoin: composition, concentration, and effects on nutritive and feeding value of sainfoin forage. Crop Sci. **55**: 13–22. doi:10.2135/cropsci2014.07.0489.

Wang, Y., Ren, H., Pan, H., Liu, J., and Zhang, L. 2015b. Enhanced tolerance and remediation to mixed contaminates of PCBs and 2,4-DCP by transgenic alfalfa plants expressing the 2,3-dihydroxybiphenyl-1,2-dioxygenase. J. Hazard. Mater. **286**: 269–275. doi:10.1016/j.jhazmat.2014.12.049.

Wang, Z., Ke, Q., Kim, M.D., Kim, S.H., Ji, C.Y., Jeong, J.C., Lee, H.-S., Park, W.S., Ahn, M.-J., Li, H., Xu, B., Deng, X., Lee, S.-H., Lim, Y.P., and Kwak, S.-S. 2015c. Transgenic alfalfa plants expressing the sweetpotato orange gene exhibit enhanced abiotic stress tolerance. PLoS One **10**. doi:http://dx.doi.org.cyber.usask.ca/10.1371/journal.pone.0126050.

Wu, G., Park, M.Y., Conway, S.R., Wang, J.-W., Weigel, D., and Poethig, R.S. 2009. The sequential action of miR156 and miR172 regulates developmental timing in arabidopsis. Cell **138**: 750–759. doi:10.1016/j.cell.2009.06.031.

Wu, G., and Poethig, R.S. 2006. Temporal regulation of shoot development in Arabidopsis thaliana by miR156 and its target SPL3. Development **133**: 3539–3547. doi:10.1242/dev.02521.

Xiccato, G., Trocino, A., De Boever, J.L., Maertens, L., Carabaño, R., Pascual, J.J., Perez, J.M., Gidenne, T., and Falcao-E-Cunha, L. 2003. Prediction of chemical composition, nutritive value and ingredient composition of European compound feeds for rabbits by near infrared reflectance spectroscopy (NIRS). Anim. Feed Sci. Technol. **104**: 153–168. doi:10.1016/S0377-8401(02)00294-8.

Xie, D.-Y., Sharma, S.B., Wright, E., Wang, Z.-Y., and Dixon, R.A. 2006a. Metabolic engineering of proanthocyanidins through co-expression of anthocyanidin reductase and the PAP1 MYB transcription factor. Plant J. **45**: 895–907.

Xie, K., Shen, J., Hou, X., Yao, J., Li, X., Xiao, J., and Xiong, L. 2012. Gradual Increase of miR156 Regulates Temporal Expression Changes of Numerous Genes during Leaf Development in Rice. Plant Physiol. **158**: 1382–1394. doi:10.1104/pp.111.190488.

Xie, K., Wu, C., and Xiong, L. 2006b. Genomic organization, differential expression, and interaction of Squamosa promoter-binding-like transcription factors and microRNA156 in rice. Plant Physiol. **142**: 280–293. doi:10.1104/pp.106.084475.

Xin, H., Khan, N.A., Falk, K.C., and Yu, P. 2014. Mid-infrared spectral characteristics of lipid molecular structures in brassica carinata seeds: relationship to oil content, fatty acid and glucosinolate profiles, polyphenols, and condensed tannins. J. Agric. Food Chem. **62**: 7977–7988. doi:10.1021/jf502209x.

Xin, H., and Yu, P. 2013a. Detect changes in protein structure of carinata meal during rumen fermentation in relation to basic chemical profile and comparison with canola meal using ATR–FT/IR molecular spectroscopy with chemometrics. Spectrochim. Acta. A. Mol. Biomol. Spectrosc. **112**: 318–325.

Xin, H., and Yu, P. 2013b. Chemical profile, energy values, and protein molecular structure characteristics of biofuel/bio-oil co-products (carinata meal) in comparison with canola meal. J. Agric. Food Chem. **61**: 3926–3933. doi:10.1021/jf400028n.

Xin, H., and Yu, P. 2014. Detect changes in lipid-related structure of brown-and yellow-seeded Brassica Carinata seed during rumen fermentation in relation to basic chemical profile using ATR-FT/IR molecular spectroscopy with chemometrics. Spectrochim. Acta. A. Mol. Biomol. Spectrosc. **133**: 811–817.

Xu, W., Dubos, C., and Lepiniec, L. 2015. Transcriptional control of flavonoid biosynthesis by MYB–bHLH–WDR complexes. Trends Plant Sci. **20**: 176–185. doi:10.1016/j.tplants.2014.12.001.

Xu, W., Grain, D., Gourrierec, J.L., Harscoët, E., Berger, A., Jauvion, V., Scagnelli, A., Berger, N., Bidzinski, P., Kelemen, Z., Salsac, F., Baudry, A., Routaboul, J.-M., Lepiniec, L., and Dubos, C. 2013. Regulation of flavonoid biosynthesis involves an unexpected complex transcriptional regulation of TT8 expression, in Arabidopsis. New Phytol. **198**: 59–70. doi:10.1111/nph.12142.

Yamaguchi, A., and Abe, M. 2012. Regulation of reproductive development by non-coding RNA in Arabidopsis: to flower or not to flower. J. Plant Res. **125**: 693–704. doi:10.1007/s10265-012-0513-7.

Yamaguchi, A., Wu, M.-F., Yang, L., Wu, G., Poethig, R.S., and Wagner, D. 2009. The microRNA regulated SBP-box transcription factor SPL3 is a direct upstream activator of LEAFY, FRUITFULL, and APETALA1. Dev. Cell **17**: 268–278. doi:10.1016/j.devcel.2009.06.007.

Yan, X., Khan, N.A., Zhang, F., Yang, L., and Yu, P. 2014. Microwave irradiation induced changes in protein molecular structures of barley grains: relationship to changes in protein chemical profile, protein subfractions, and digestion in dairy cows. J. Agric. Food Chem. **62**: 6546–6555. doi:10.1021/jf501024j.

Yan, Z., Hossain, M.S., Wang, J., Valdés-López, O., Liang, Y., Libault, M., Qiu, L., and Stacey, G. 2013. miR172 regulates soybean nodulation. Mol. Plant. Microbe Interact. **26**: 1371–1377. doi:10.1094/MPMI-04-13-0111-R.

Yang, J.Y., Seo, J., Kim, H.J., Seo, S., and Ha, J.K. 2010. Nutrient synchrony: Is it a suitable strategy to improve nitrogen utilization and animal performance. Asian-Aust J Anim Sci **23**: 972–979.

Yang, L., McKinnon, J.J., Christensen, D.A., Beattie, A.D., and Yu, P. 2014. Characterizing the molecular structure features of newly developed hulless barley cultivars with altered carbohydrate traits (Hordeum vulgare L.) by globar-sourced infrared spectroscopy in relation to nutrient utilization and availability. J. Cereal Sci. **60**: 48–59. doi:10.1016/j.jcs.2013.12.013.

Yang, L., Xu, M., Koo, Y., He, J., and Poethig, R.S. 2013. Sugar promotes vegetative phase change in Arabidopsis thaliana by repressing the expression of MIR156A and MIR156C. eLife **2**: e00260. doi:10.7554/eLife.00260.

Yang, L., and Yu, P. 2017. Synchrotron-based and globar-sourced molecular (micro)spectroscopy contributions to advances in new hulless barley (with structure alteration) research on molecular structure, molecular nutrition, and nutrient delivery. Crit. Rev. Food Sci. Nutr. **57**: 224–236. doi:10.1080/10408398.2013.876386.

Yari, M., Valizadeh, R., Naserian, A.A., Ghorbani, G.R., Rezvani Moghaddam, P., Jonker, A., and Yu, P. 2012a. Botanical traits, protein and carbohydrate fractions, ruminal degradability

and energy contents of alfalfa hay harvested at three stages of maturity and in the afternoon and morning. Anim. Feed Sci. Technol. **172**: 162–170. doi:10.1016/j.anifeedsci.2012.01.004.

Yari, M., Valizadeh, R., Naserian, A.A., Jonker, A., and Yu, P. 2012b. Modeling nutrient availability of alfalfa hay harvested at three stages of maturity and in the afternoon and morning in dairy cows. Anim. Feed Sci. Technol. **178**: 12–19. doi:10.1016/j.anifeedsci.2012.09.001.

Yari, M., Valizadeh, R., Naserian, A.A., Jonker, A., and Yu, P. 2013. Protein molecular structures in alfalfa hay cut at three stages of maturity and in the afternoon and morning and relationship with nutrient availability in ruminants: FTIR spectroscopy of alfalfa hay protein. J. Sci. Food Agric. **93**: 3072–3080. doi:10.1002/jsfa.6141.

Yari, M., Valizadeh, R., Nnaserian, A.A., Jonker, A., and Yu, P. 2017. Carbohydrate and lipid spectroscopic molecular structures of different alfalfa hay and their relationship with nutrient availability in ruminants. Asian-Australas. J. Anim. Sci. **30**: 1575–1589. doi:10.5713/ajas.16.0756.

Yu, G.Q., Warkentin, T., Niu, Z., Khan, N.A., and Yu, P. 2015a. Molecular basis of processing-induced changes in protein structure in relation to intestinal digestion in yellow and green type pea (Pisum sativum L.): A molecular spectroscopic analysis. Spectrochim. Acta. A. Mol. Biomol. Spectrosc. **151**: 980–988. doi:10.1016/j.saa.2015.06.050.

Yu, N., Cai, W.-J., Wang, S., Shan, C.-M., Wang, L.-J., and Chen, X.-Y. 2010. Temporal control of trichome distribution by microRNA156-targeted SPL genes in Arabidopsis thaliana. Plant Cell **22**: 2322–2335. doi:10.1105/tpc.109.072579.

Yu, N., Niu, Q.-W., Ng, K.-H., and Chua, N.-H. 2015b. The role of miR156/SPLs modules in Arabidopsis lateral root development. Plant J. **83**: 673–685. doi:10.1111/tpj.12919.

Yu, P. 2004. Application of advanced synchrotron radiation-based Fourier transform infrared (SR-FTIR) microspectroscopy to animal nutrition and feed science: a novel approach. Br. J. Nutr. **92**: 869. doi:10.1079/BJN20041298.

Yu, P. 2005a. Protein secondary structures (α-helix and β-sheet) at a cellular level and protein fractions in relation to rumen degradation behaviours of protein: a new approach. Br. J. Nutr. **94**: 655–665.

Yu, P. 2005b. Applications of hierarchical cluster analysis (CLA) and principal component analysis (PCA) in feed structure and feed molecular chemistry research, using synchrotron-based Fourier transform infrared (FTIR) microspectroscopy. J. Agric. Food Chem. **53**: 7115–7127.

Yu, P. 2006. Synchrotron IR microspectroscopy for protein structure analysis: Potential and questions. J. Spectrosc. **20**: 229–251.

Yu, P. 2007. Molecular chemical structure of barley proteins revealed by ultra-spatially resolved synchrotron light sourced FTIR microspectroscopy: Comparison of barley varieties. Biopolymers **85**: 308–317. doi:10.1002/bip.20661.

Yu, P. 2008. Synchrotron-based microspectroscopic analysis of molecular and biopolymer structures using multivariate techniques and advanced multi-components modeling. Can. J. Anal. Sci. Spectrosc. **53**. [Online] Available: http://www.osti.gov/scitech/biblio/980594 [2016 Oct. 4].

Yu, P. 2010. Plant-based food and feed protein structure changes induced by gene-transformation, heating and bio-ethanol processing: A synchrotron-based molecular structure and nutrition research program. Mol. Nutr. Food Res. **54**: 1535–1545. doi:10.1002/mnfr.201000178.

Yu, P. 2012. Study of barley grain molecular structure for ruminants using DRIFT, FTIR-ATR and synchrotron radiation infrared microspectroscopy (SR-IMS): a review. Page 012008 *in* Journal of Physics: Conference Series. IOP Publishing. [Online] Available: http://iopscience.iop.org/article/10.1088/1742-6596/359/1/012008/meta [2016 Oct. 5].

Yu, P., Christensen, D.A., and McKinnon, J.J. 2003a. Comparison of the National Research Council-2001 model with the Dutch system (DVE/OEB) in the prediction of nutrient supply to dairy cows from forages. J. Dairy Sci. **86**: 2178–2192. doi:10.3168/jds.S0022-0302(03)73808-9.

Yu, P., Christensen, D.A., McKinnon, J.J., and Markert, J.D. 2003b. Effect of variety and maturity stage on chemical composition, carbohydrate and protein subfractions, in vitro rumen degradability and energy values of timothy and alfalfa. Can. J. Anim. Sci. **83**: 279–290. doi:10.4141/A02-053.

Yu, P., Jonker, A., and Gruber, M. 2009. Molecular basis of protein structure in proanthocyanidin and anthocyanin-enhanced Lc-transgenic alfalfa in relation to nutritive value using synchrotron-radiation FTIR microspectroscopy: A novel approach. Spectrochim. Acta. A. Mol. Biomol. Spectrosc. **73**: 846–853. doi:10.1016/j.saa.2009.04.006.

Yu, P., Lei, Y., Hu, H., Deng, H., and Zhang, W. 2019. A methodology study on chemical and molecular structure imaging in modified forage leaf tissue with cutting-edge synchrotron-powered technology (SR-IMS) as a potential research tool. Spectrochim. Acta. A. Mol. Biomol. Spectrosc. **213**: 330–336. doi:10.1016/j.saa.2019.01.064.

Yu, P., Mckinnon, J.J., Christensen, C.R., and Christensen, D.A. 2004a. Using synchrotron-based FTIR microspectroscopy to reveal chemical features of feather protein secondary structure: comparison with other feed protein sources. J. Agric. Food Chem. **52**: 7353–7361.

Yu, P., McKinnon, J.J., Christensen, C.R., and Christensen, D.A. 2004b. Imaging molecular chemistry of pioneer corn. J. Agric. Food Chem. **52**: 7345–7352. doi:10.1021/jf049291b.

Yu, P., McKinnon, J.J., Christensen, C.R., Christensen, D.A., Marinkovic, N.S., and Miller, L.M. 2003c. Chemical imaging of microstructures of plant tissues within cellular dimension using synchrotron infrared microspectroscopy. J. Agric. Food Chem. **51**: 6062–6067.

Yu, P., and Nuez-Ortín, W.G. 2010. Relationship of protein molecular structure to metabolisable proteins in different types of dried distillers grains with solubles: a novel approach. Br. J. Nutr. **104**: 1429–1437.

Zabala, G., Zou, J., Tuteja, J., Gonzalez, D.O., Clough, S.J., and Vodkin, L.O. 2006. Transcriptome changes in the phenylpropanoid pathway of Glycine max in response to Pseudomonas syringaeinfection. BMC Plant Biol. **6**: 26. doi:10.1186/1471-2229-6-26.

Zeineldin, M., Barakat, R., Elolimy, A., Salem, A.Z.M., Elghandour, M.M.Y., and Monroy, J.C. 2018. Synergetic action between the rumen microbiota and bovine health. Microb. Pathog. **124**: 106–115. doi:10.1016/j.micpath.2018.08.038.

Zeng, Y., Zhao, S., Yang, S., and Ding, S.-Y. 2014. Lignin plays a negative role in the biochemical process for producing lignocellulosic biofuels. Curr. Opin. Biotechnol. **27**: 38–45. doi:10.1016/j.copbio.2013.09.008.

Zhang, X., and Yu, P. 2014. Using a non-invasive technique in nutrition: synchrotron radiation infrared microspectroscopy spectroscopic characterization of oil seeds treated with different processing conditions on molecular spectral factors influencing nutrient delivery. J. Agric. Food Chem. **62**: 6199–6205. doi:10.1021/jf501553g.

Zhang, X., Zou, Z., Zhang, J., Zhang, Y., Han, Q., Hu, T., Xu, X., Liu, H., Li, H., and Ye, Z. 2011. Over-expression of sly-miR156a in tomato results in multiple vegetative and reproductive

trait alterations and partial phenocopy of the sft mutant. FEBS Lett. **585**: 435–439. doi:10.1016/j.febslet.2010.12.036.

Zhang, X.W., and Yu, P.Q. 2012. Using ATR-FT/IR molecular spectroscopy to detect effects of blend DDGS inclusion level on the molecular structure spectral and metabolic characteristics of the proteins in hulless barley. Spectrochim. Acta Part -Mol. Biomol. Spectrosc. **95**: 53–63. doi:10.1016/j.saa.2012.04.022.

Zhang, Y.-M., Liu, Z.-H., Wen, Z.-Y., Zhang, H.-M., Yang, F., and Guo, X.-L. 2012. The vacuolar Na^+–H^+ antiport gene *TaNHX2* confers salt tolerance on transgenic alfalfa (*Medicago sativa*). Funct. Plant Biol. **39**: 708–716. doi:10.1071/FP12095.

Zhang, Y.-M., Zhang, H.-M., Liu, Z.-H., Li, H.-C., Guo, X.-L., and Li, G.-L. 2014. The wheat NHX antiporter gene TaNHX2 confers salt tolerance in transgenic alfalfa by increasing the retention capacity of intracellular potassium. Plant Mol. Biol. **87**: 317–327. doi:10.1007/s11103-014-0278-6.

Zhang, Z., Shao, L., Chang, L., Cao, Y., Zhang, T., Wang, Y., Liu, Y., Zhang, P., Sun, X., Wu, Y., Hu, T., and Yang, P. 2016. Effect of rhizobia symbiosis on lignin levels and forage quality in alfalfa (Medicago sativa L.). Agric. Ecosyst. Environ. **233**: 55–59. doi:10.1016/j.agee.2016.08.035.

Zhou, J., Lee, C., Zhong, R., and Ye, Z.-H. 2009. MYB58 and MYB63 are transcriptional activators of the lignin biosynthetic pathway during secondary cell wall formation in Arabidopsis. Plant Cell **21**: 248–266. doi:10.1105/tpc.108.063321.

Zhou, L.-L., Shi, M.-Z., and Xie, D.-Y. 2012. Regulation of anthocyanin biosynthesis by nitrogen in TTG1–GL3/TT8–PAP1-programmed red cells of Arabidopsis thaliana. Planta **236**: 825–837. doi:10.1007/s00425-012-1674-2.

APPENDIX

Table 1. Effect of silencing *TT8* and *HB12* gene on protein degradational kinetics of alfalfa with *in vitro* gas fermentation method: Comparison between gene transformed and wild type.

Items [1]	WT	Transformed Alfalfa		SEM [2]	P value	Contrast [3]
		HB12i	TT8i			W vs G
U (%)	8.98b	43.36a	16.32b	2.401	<0.001	<0.001
S (%)	31.68b	37.70a	37.63a	0.794	<0.001	<0.001
D (%)	59.33a	19.11c	46.05b	2.491	<0.001	<0.001
K_d (%/h)	12.98	22.50	14.65	3.670	0.124	0.304
ED_{CP} (g/Kg DM)	75.51a	52.99b	72.79a	1.619	<0.001	<0.001

[1] U, undegradable fraction; S, soluble fraction; D, degradable fraction; K_d, degradation rate; ED, effective degradation.
[2] SEM, standard error of mean. Means with different letters in each row differ significantly at P<0.05.
[3] Contrast between wild type and genetic transformed alfalfa.

Table 2. Regression equations of predicting chemical composition, CNCPS fractions from molecular structure for alfalfa forage (R^2>0.5, appendix to Chapter 5.1)

Dependent Variables [1]	Prediction Equations [2]	RSE [3]	Adjusted R^2	P value
Chemical composition (%DM)				
DM	Y = 85.44 + 35.48 CEC + 2.1 Amide I/II + 2.3 alpha/beta - 1.14 AIA/AIIA + 0.34 CCOA + 18.61 AsCH3	0.306	0.603	<0.001
Ash	Y = 6.04 + 80.96 CEC - 1.55 AIA/AIIA + 0.42 CCOA - 66.09 SyCH3 + 50.13 AsCH3	0.509	0.569	<0.001
ADF	Y = 66.99 - 121.46 CEC - 22.87 Amide I - 30.54 alpha/beta - 1.5 CCOA - 152.79 SyCH2 + 373.68 SyCH3	1.952	0.502	<0.001
ADICP	Y = 1.61 + 10.12 CEC - 2.67 Amide I - 1.38 alpha/beta + 3.71 SyCH2	0.123	0.549	<0.001
Sugar	Y = 11.12 - 96.48 CEC + 3.89 alpha/beta - 1.37 CCOA	0.727	0.651	<0.001
OM	Y = 93.96 - 80.96 CEC + 1.55 AIA/AIIA - 0.42 CCOA + 66.09 SyCH3 - 50.13 AsCH3	0.509	0.569	<0.001
CNCPS fractions and degradations (%DM)				
CA4	Y = 11.12 - 96.48 CEC + 3.89 alpha/beta - 1.37 CCOA	0.727	0.651	<0.001
CB1	Y = -32.89 + 68.41 TC4 - 15.32 Amide I + 33.88 alpha/beta	1.329	0.735	<0.001
CB2	Y = 49.75 + 169.3 CEC - 41.19 alpha/beta + 2.53 CCOA	1.91	0.811	<0.001
CB3	Y = 40.37 - 37.18 alpha/beta - 128.2 SyCH2 + 428.51 SyCH3	1.913	0.651	<0.001
PA2	Y = -6.81 - 49.1 TC4 + 18.38 Amide I + 6.94 Amide I/II + 16.19 alpha/beta + 73.27 SyCH2 - 254.78 SyCH3	1.133	0.706	<0.001
PB1	Y = -15.6 + 48.91 CEC + 19.27 alpha/beta + 84.43 AsCH3	0.998	0.780	<0.001
PB2	Y = 1.92 + 22.73 CEC + 2.67 Amide I - 2.81 alpha/beta + 0.55 CCOA - 21.74 AsCH3	0.253	0.841	<0.001
PC	Y = 1.61 + 10.12 CEC - 2.67 Amide I - 1.38 alpha/beta + 3.71 SyCH2	0.123	0.549	<0.001

[1] DM, dry matter; ADF, acid detergent fiber; ADICP, acid detergent insoluble protein; OM, organic matter; CA4, sugar; CB1, starch; CB2, soluble fiber; CB3, digestible fiber; PA2, soluble true protein; PB1, insoluble true protein; PB2, fiber-bound protein; PC, indigestible protein;

[2] TC4, the fourth major peak in total carbohydrate (TC) region; CEC, cellulosic compounds peak; Amide I, the first amide peak; Amide I/II, peak ratio of amide I to amide II; alpha/beta, peak ratio of alpha helix to beta sheet; AIA/AIIA, amide I area to amide II area ratio; CCOA, carbonyl C=O peak area. SyCH2, symmetric CH_2; SyCH3, symmetric CH_3; AsCH3, asymmetric CH_3.

[3] RSE, residual standard error;

Table 3. Regression equations of predicting CNCPS fractions and rumen degradable CNCPS fractions from molecular structure for alfalfa forage (R^2>0.5, appendix to Chapter 5.1)

Dependent Variables [1]	Prediction Equations [2]	RSE [3]	Adjusted R^2	P value
Rumen degradable CNCPS fractions (%DM)				
RDCB1	Y = -28.61 + 59.55 TC4 - 13.33 Amide I + 29.47 alpha/beta	1.156	0.735	<0.001
RDCB2	Y = 44.1 + 149.96 CEC - 36.51 alpha/beta + 2.24 CCOA	1.693	0.811	<0.001
RDCA4	Y = 9.99 - 86.65 CEC + 3.5 alpha/beta - 1.23 CCOA	0.654	0.650	<0.001
RDCB3	Y = 24.58 - 22.63 alpha/beta - 78.01 SyCH2 + 260.68 SyCH3	1.164	0.651	<0.001
RDCHO	Y = 48.04 + 121.33 TC4 - 25.6 alpha/beta	1.883	0.663	<0.001
RDPA2	Y = -5.71 - 41.13 TC4 + 15.43 Amide I + 5.82 Amide I/II + 13.58 alpha/beta + 61.47 SyCH2 - 213.83 SyCH3	0.95	0.706	<0.001
RDPB1	Y = -11.75 + 37 CEC + 14.5 alpha/beta + 63.47 AsCH3	0.751	0.780	<0.001
RDPB2	Y = 1.18 + 13.95 CEC + 1.61 Amide I - 1.73 alpha/beta + 0.33 CCOA - 13.19 AsCH3	0.154	0.841	<0.001
Rumen undegradable CNCPS fractions (%DM)				
RUCA4	Y = 1.13 - 9.83 CEC + 0.39 alpha/beta - 0.14 CCOA	0.072	0.66	<0.001
RUCB3	Y = 15.79 - 14.55 alpha/beta - 50.18 SyCH2 + 167.83 SyCH3	0.749	0.651	<0.001
RUCHO	Y = 72.74 - 131.31 CEC - 23.36 Amide I - 6.98 Amide I/II - 29.13 alpha/beta - 1.34 CCOA - 142.45 SyCH2 + 400.66 SyCH3	1.641	0.622	<0.001
RUPC	Y = 1.61 + 10.12 CEC - 2.67 Amide I - 1.38 alpha/beta + 3.71 SyCH2	0.123	0.549	<0.001

[1] RD**, rumen degradable fraction; RU**, rumen undegradable fraction; CHO, carbohydrate; CA4, sugar; CB1, starch; CB2, soluble fiber; CB3, digestible fiber; PA2, soluble true protein; PB1, insoluble true protein; PB2, fiber-bound protein; PC, indigestible protein;

[2] TC4, the fourth major peak in total carbohydrate (TC) region; CEC, cellulosic compounds peak; Amide I, the first amide peak; Amide I/II, peak ratio of amide I to amide II; alpha/beta, peak ratio of alpha helix to beta sheet; AIA/AIIA, amide I area to amide II area ratio; CCOA, carbonyl C=O peak area. SyCH2, symmetric CH_2; SyCH3, symmetric CH_3; AsCH3, asymmetric CH_3.

[3] RSE, residual standard error;

Table 4. Regression equations of predicting nutrients degradation, microbial nitrogen, protein metabolic parameters from molecular structure for alfalfa forage (R2>0.5, appendix to Chapter 5.2)

Dependent Variables [1]	Prediction Equations [2]	RSE [3]	Adjusted R^2	P value
Nutrients degradation kinetics (%)				
DM_ED	Y = 6.51 - 36.62 Amide I + 57.15 alpha/beta + 169.53 AsCH3	3.189	0.674	<0.001
CP_U	Y = 76.23 - 63.7 alpha/beta	3.847	0.573	<0.001
CP_D	Y = -25.35 + 82.4 alpha/beta - 303.67 AsCH3	5.323	0.504	<0.001
N^{15} enrichment (APE, atom excess %) of microbial nitrogen at 12 h of fermentation				
LAMN	Y = 17.05 - 7.51 Amide I - 4.12 Amide I/II - 7.88 alpha/beta - 32.13 SyCH2 + 138.08 SyCH3	0.484	0.656	<0.001
FAMN	Y = 4.93 - 2.02 Amide I/II - 3.14 alpha/beta + 0.81 AIA/AIIA - 0.17 CCOA - 10.75 SyCH2 + 31.84 SyCH3	0.189	0.561	<0.001
Loosely attached microbial nitrogen (LAMN) at 12 h of fermentation (mg/g residue)				
LAMN	Y = -4.72 + 4.87 AIA/AIIA - 2.05 CCOA - 83.9 SyCH2 + 212.45 AsCH3	1.73	0.577	<0.001
Endogenous protein (ECP) estimated with NRC-2001 system (g/Kg DM)				
ECP	Y = 10.15 + 4.21 CEC + 0.25 Amide I/II + 0.27 alpha/beta - 0.14 AIA/AIIA + 0.04 CCOA + 2.21 AsCH3	0.036	0.603	<0.001
AECP	Y = 4.06 + 1.68 CEC + 0.1 Amide I/II + 0.11 alpha/beta - 0.05 AIA.AIIA + 0.02 CCOA + 0.88 AsCH3	0.015	0.603	<0.001

[1] DM_ED, effective DM degradation; CP_U, undegradable fraction of protein; CP_D, degradable fraction of protein; LAMN, loosely attached microbial nitrogen; FAMN, firmly attached microbial nitrogen, ECP, endogenous protein; AECP, absorbable endogenous protein.
[2] CEC, cellulosic compounds peak; Amide I, the first amide peak; Amide I/II, peak ratio of amide I to amide II; alpha/beta, peak ratio of alpha helix to beta sheet; AIA/AIIA, amide I area to amide II area ratio; CCOA, carbonyl C=O peak area. SyCH2, symmetric CH_2; SyCH3, symmetric CH_3; AsCH3, asymmetric CH_3.
[3] RSE, residual standard error;

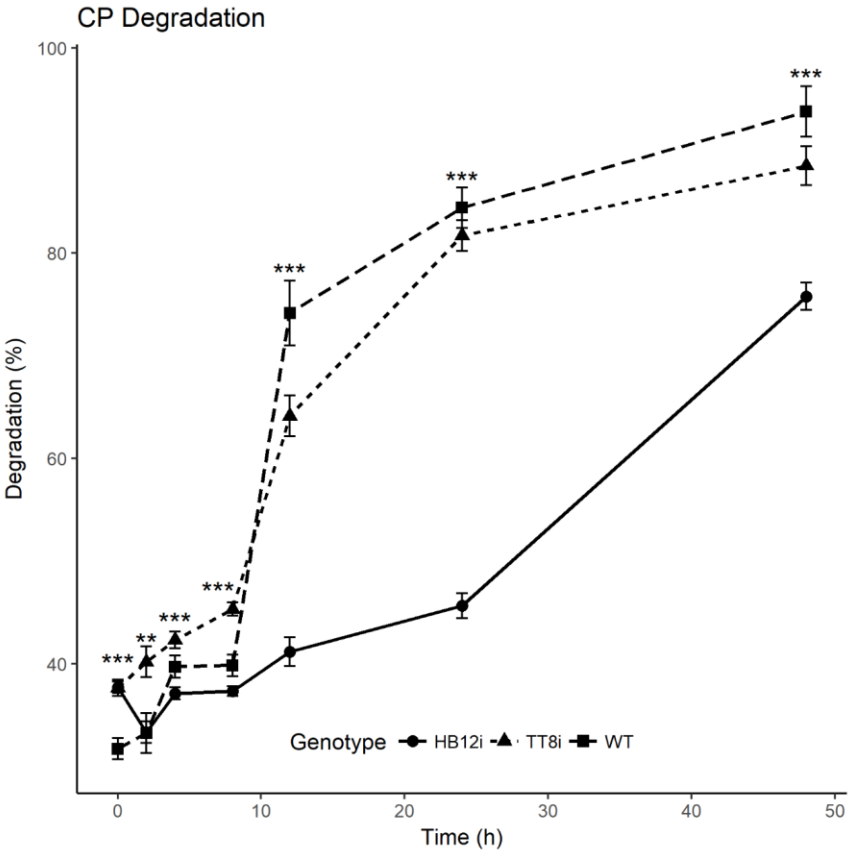

Figure 1. Protein degradation of transformed (HB12i and TT8i) and wild type alfalfa during with *in vitro* gas fermentation. *, P<0.05; **, P<0.01; ***, P<0.001.